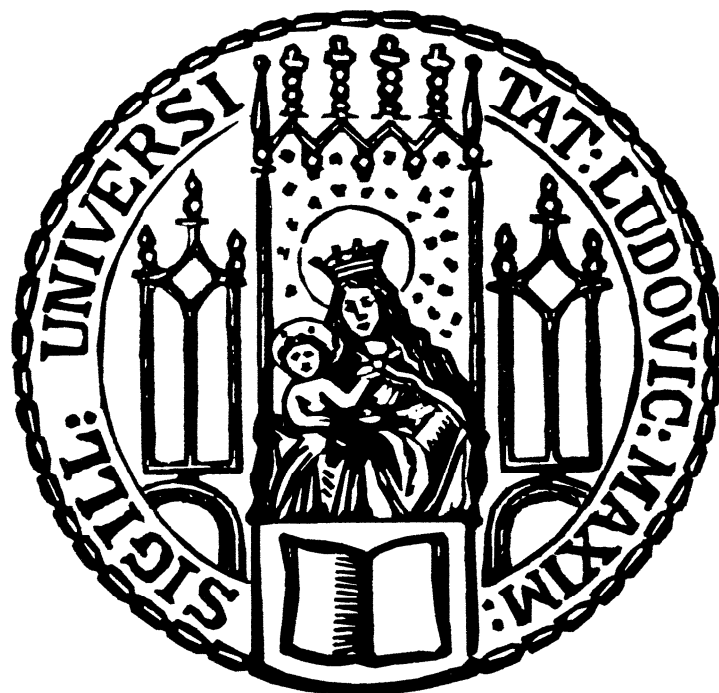


Dissertation zur Erlangung des Doktorgrades der Fakultät für
Chemie und Pharmazie der Ludwig-Maximilians-Universität
München



Method development for the analysis of steroids, steroid acids
and sterol sulfates in biological samples

Julia Christina Junker

aus

Erlangen

2021

Erklärung

Diese Dissertation wurde im Sinne von § 7 der Promotionsordnung vom 28. November 2011 von Herrn Prof. Dr. Franz Bracher betreut.

Eidesstattliche Versicherung

Diese Dissertation wurde selbstständig und ohne unerlaubte Hilfe erarbeitet.

München, den 19.02.2021

Julia Christina Junker

Dissertation eingereicht am: 22.02.2021

1. Gutachter: Prof. Dr. Franz Bracher

2. Gutachter: Prof. Dr. Michael Vogeser

Mündliche Prüfung am: 23.03.2021

Danksagung

Mein Dank gilt zuallererst Herrn Prof. Dr. Franz Bracher dafür, dass er mich als "Analytikerin" in seinen Arbeitskreis aufgenommen hat und meine Arbeit von Anfang an unterstützt und gefördert hat.

Desweiteren gilt mein Dank Prof Dr. Vogeser für die freundliche Übernahme des Koreferats. Ihm und allen anderen Mitgliedern der Prüfungskommission danke ich für Ihre Zeit und Hilfe.

Ganz besonders bedanken möchte ich mich bei Dr. Christoph Müller, der mir immer mit Rat und Tat zur Seite stand, für seine engagierte fachliche Unterstützung und die vielen konstruktiven Gespräche.

Meinen Kooperationspartnern Prof. Dr. Harald Steiner und Dr. Frits Kamp möchte ich für die Unterstützung und Förderung des Projekts danken.

Ebenso möchte ich mich bei allen Mitgliedern des Arbeitskreises ganz herzlich für die schöne gemeinsame Zeit bedanken. Besonders bedanken möchte ich mich bei Kathi, Alex, Bini, Desi und Susi für die hervorragende Zusammenarbeit im 8. Semester. Außerdem danke ich Sonja und Anna für die tolle Arbeitsatmosphäre im Analytiklabor.

Bei meinen Freunden und Simon möchte ich mich für vor allem für die moralische Unterstützung und den starken Rückhalt ganz herzlich bedanken.

Mein größter Dank gebührt meiner Familie und besonders meine Eltern, die mich immer uneingeschränkt und in allem unterstützt haben.

Table of contents

1. Introduction	1
1.1. Significance of natural sterols.....	1
1.2. Steroid biosynthetic pathways	2
1.2.1. Cholesterol	2
1.2.2. Oxysterols	5
1.2.3. Steroid acids.....	6
1.2.4. Neurosteroids	9
1.2.5. Sterol sulfates.....	10
1.3. Steroids and Alzheimer's disease.....	11
1.4. Steroid analysis.....	11
2. Topic	13
3. Sterol sulfate analysis	14
3.1. Summary.....	14
3.2. Personal contribution.....	15
3.3. Article	17
3.4. Supplementary material	37
4. Analysis of neutral steroids, steroid acids and sterol sulfates	39
4.1. Summary.....	39
4.2. Personal contribution.....	40
4.3. Article	41
5. Characterization of inhibitors of cholesterol biosynthesis	80
5.1. Summary.....	80
5.2. Personal contribution.....	81
5.3. Article	82
5.4. Supplementary material	111
6. Traceless isoprenylation.....	152
6.1. Summary.....	152
6.2. Personal contribution.....	153

6.3. Article.....	154
6.4. Supplementary material	164
7. Summary.....	208
8. Abbreviations	210
9. References.....	211

1. Introduction

1.1. Significance of natural sterols

Sterols are omnipresent in living nature, whereby the most abundant sterols are cholesterol in mammals, β -sitosterol in plants and ergosterol in fungi (Figure 1a) [1].

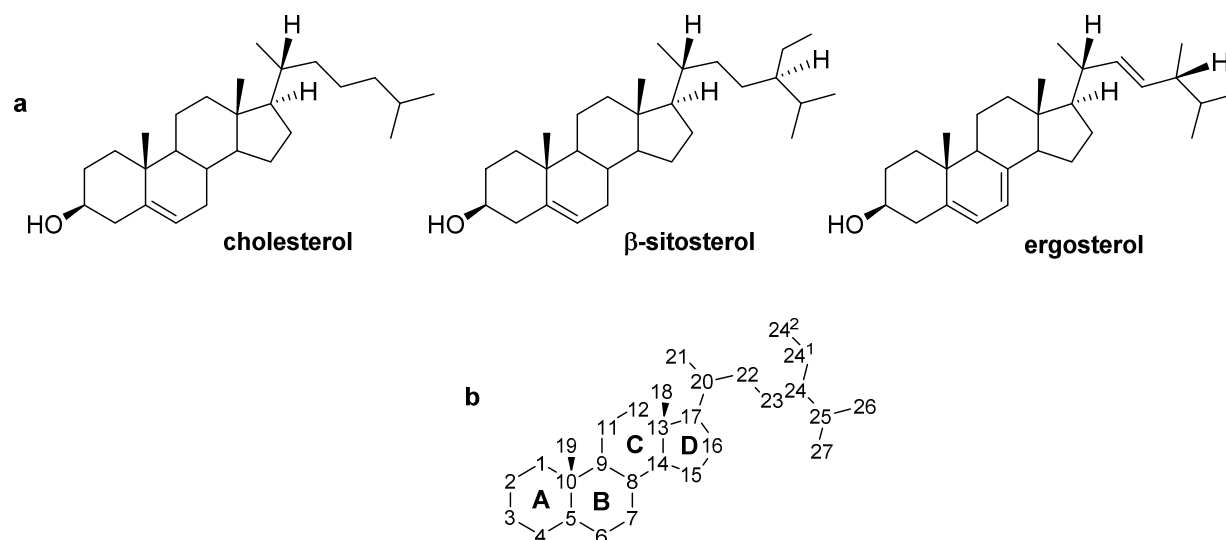


Figure 1 a: Structures of cholesterol, β -sitosterol and ergosterol, **b:** Numbering and ring letters of steroids according to IUPAC [2]

These sterols are synthesized *de novo* in most organisms starting from acetyl-CoA (coenzyme A) and isoprenoids, but they can also be acquired from diet [3]. The latter was shown for invertebrates like insects that lack an own *de novo* biosynthesis, but are able to synthesize the required sterols from dietary precursors [4]. The fact that sterols are vital for so many different species and that the enzyme squalene monooxygenase, which performs the initial step for sterol biosynthesis, has several conserved motifs throughout the different species [5, 6] gives a hint to the importance of sterols for early eukaryotic evolution. It has been suggested, see *e.g.* [6, 7], that sterols played an important role in the evolution from prokaryotes to eukaryotes. This evolutionary step is characterized by the development of cell compartments and the differentiation of cell organelles as well as the endocytosis and exocytosis [5]. All these processes involve rapid deformation of cell membranes, and sterols play a crucial role for membrane fluidity and function [5]. Due to their amphiphilic properties they are stored in between the phospholipids in the cell membranes. Cholesterol, for example, is oriented perpendicular to the membrane plane and causes an increase of the membrane's stability [8]. Hence, sterols are essential building materials and a prerequisite for the function of every cell. Despite of their important physical properties, sterols like cholesterol act as precursors for further essential sterols or bile acids [3, 9]. The focus of this work is the mammalian sterol cholesterol and its biosynthesis and metabolism.

1. Introduction

1.2. Steroid biosynthetic pathways

1.2.1. Cholesterol

Cholesterol *de novo* biosynthesis in mammals generally can take place in every tissue. However, the majority is synthesized in the liver [9, 10]. It is then distributed throughout the body *via* the blood circulation, when bound to specific transport proteins as very low density lipoprotein (VLDL) and low density lipoprotein (LDL) [9-11]. In the form of LDL, cholesterol is taken up into cells by LDL receptor mediated endocytosis, and excess cholesterol can be redistributed to the liver in the form of high density lipoprotein (HDL) [9, 11]. One exception to this cholesterol dissemination is the central nervous system (CNS). Almost all CNS cholesterol is synthesized *de novo* within the brain and it is remarkable that the CNS, which accounts for about 2% of the body mass, accounts for about one quarter of the whole unesterified cholesterol [11]. Cholesterol biosynthesis can be divided into pre- and post-squalene pathway. In Figure 2 the pre-squalene section and the involved enzymes and intermediates are shown. First, HMG-CoA (3-hydroxy-3-methylglutaryl-CoA) (C₆) is synthesized from three acetyl CoA (C₂) building blocks. Following reduction of HMG-CoA leads to mevalonate (C₆). After activation of mevalonate by conjugation with pyrophosphate and subsequent decarboxylation, isopentenyl diphosphate (IPP) (C₅) and its isomer dimethylallyl diphosphate (C₅) are formed. IPP is a central element of terpenoids, a huge group of natural products. Afterwards, farnesyl diphosphate (C₁₅) is synthesized from three IPP building blocks. The final product of this pathway, squalene (C₃₀), is then formed out of two molecules farnesyl diphosphate.

1. Introduction

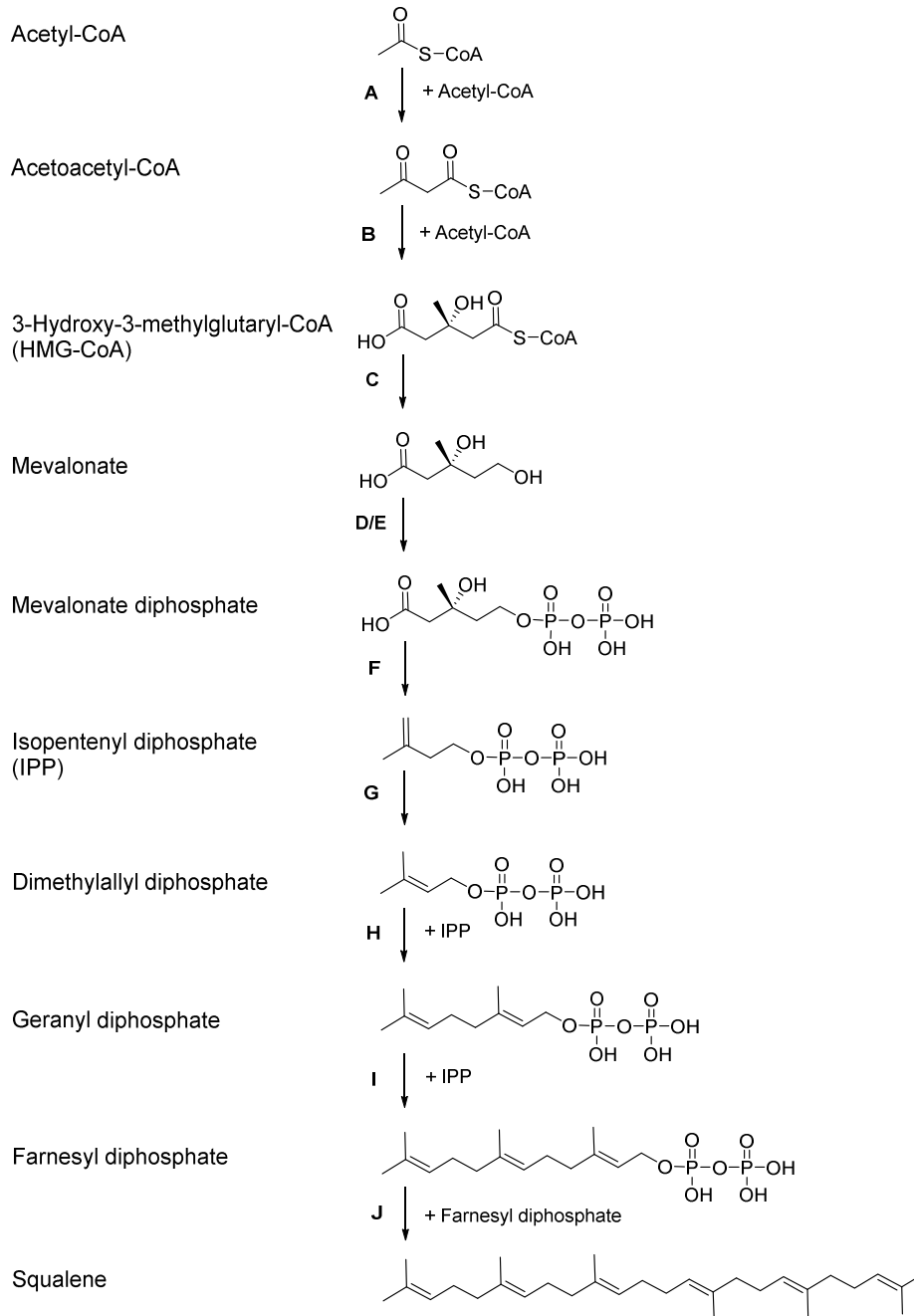


Figure 2 Pre-squalene pathway of cholesterol biosynthesis. Involved enzymes: **A**: acetyl-CoA acetyltransferase **B**: HMG-CoA synthase **C**: HMG-CoA reductase **D**: mevalonate kinase **E**: mevalonate-P kinase **F**: mevalonate-PP decarboxylase **G**: isopentenyl-PP isomerase **H**: geranyl-PP synthase **I**: farnesyl-PP synthase **J**: squalene synthase [12, 13].

The second part of cholesterol biosynthesis starts with the epoxidation and cyclization of squalene to form lanosterol. The core pathway from lanosterol to cholesterol involves nine different enzymes that are integral membrane-bound proteins of the endoplasmic reticulum [13]. These steps can proceed *via* C24–C25 unsaturated intermediates (Bloch pathway), or *via* the corresponding C24–C25 saturated intermediates (Kandutsch-Russell pathway) [13]. Both pathways begin with C14 demethylation followed by elimination of both C3 methyl groups. Final modifications of the double bonds lead to cholesterol (Figure 3).

1. Introduction

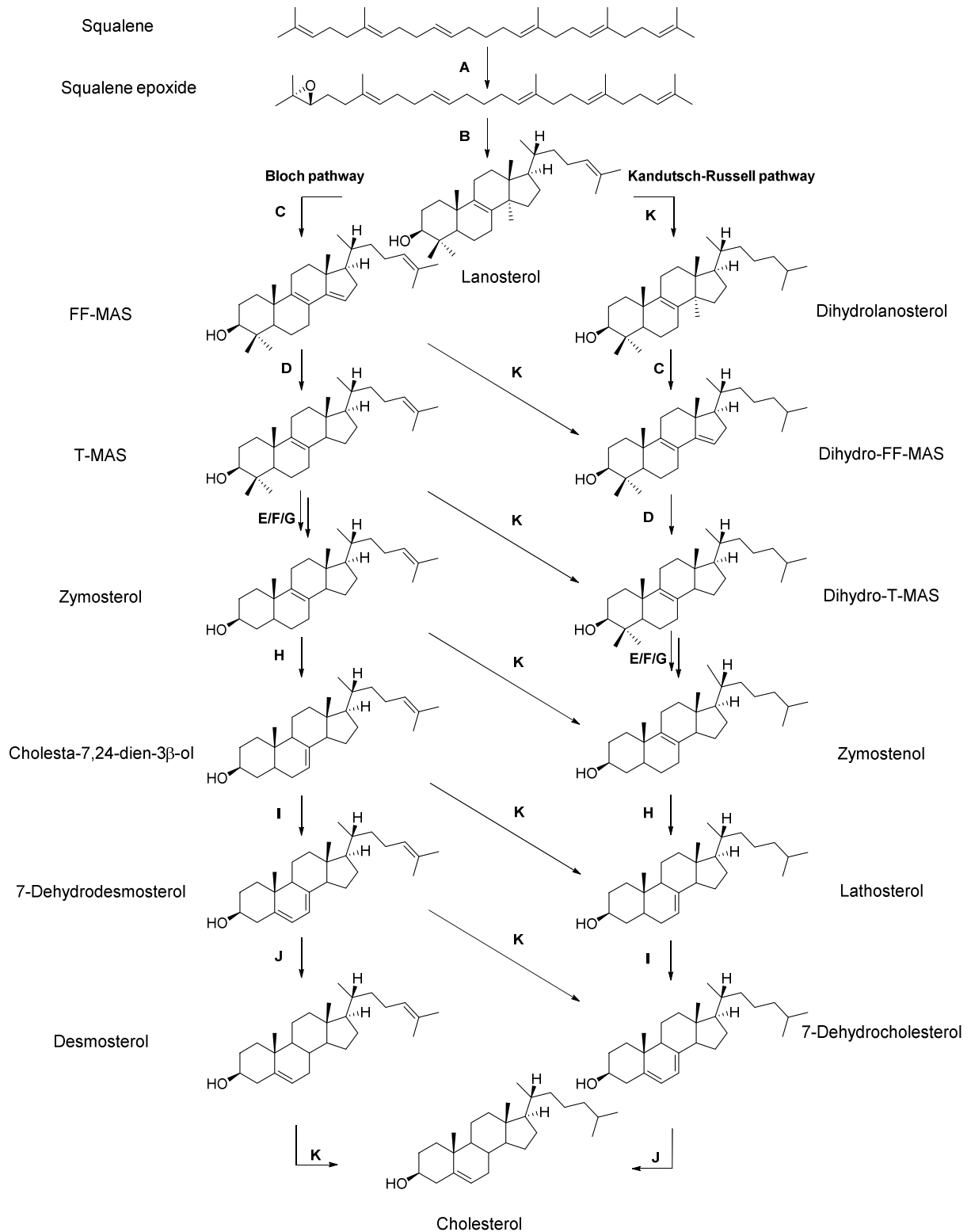


Figure 3 Post-squalene pathway of cholesterol biosynthesis and involved enzymes. **A:** squalene epoxygenase **B:** 2,3-oxidosqualene cyclase **C:** sterol C14-demethylase **D:** sterol C14-reductase **E:** methylsterol monooxygenase **F:** sterol 4 α -carboxylate-3-dehydrogenase **G:** 3-keto steroid reductase **H:** sterol Δ^8 - Δ^7 -isomerase **I:** sterol Δ^5 -desaturase **J:** sterol Δ^7 -reductase **K:** sterol Δ^{24} -reductase [12-15].

1. Introduction

Several congenital diseases are associated with malfunctions in cholesterol biosynthesis or cholesterol distribution. The most common disorder is the Smith-Lemli-Opitz syndrome (SLOS) which is caused by a defect of sterol Δ^7 -reductase (Figure 3, J) [12, 16, 17]. This enzyme catalyzes the reduction of 7-dehydrocholesterol to cholesterol as final step of cholesterol biosynthesis which leads to an accumulation of 7-dehydrocholesterol in the Kandutsch-Russell pathway [12, 16, 17]. This disease is characterized by growth retardation, malformations and intellectual deficiencies [16]. Further examples for cholesterol biosynthesis associated diseases are Antley-Bixler-syndrome, CHILD-syndrome (Congenital Hemidysplasia with Ichthyosiform nevus and Limb Defects) and desmosterolosis [17]. An example for a disease associated with cholesterol distribution is Niemann-Pick type C disease (NPC). NPC is a severe neurodegenerative disease and is characterized by an accumulation of cholesterol and other lipids in endosomes [18]. This is due to a mutation of the NPC protein 1, which is mandatory for the release of the acquired cholesterol from the endosomes to the endoplasmic reticulum [11].

1.2.2. Oxysterols

Oxysterols are phase 1 metabolites of cholesterol which are formed by hydroxylation of the ring structure or the side chain. Oxysterols are products of enzymatic hydroxylation and/or cholesterol autoxidation [19]. For example, 25-hydroxycholesterol is an autoxidation product of cholesterol, as well as a product of enzymatic hydroxylation (Figure 4) [19]. Oxysterols are formed by different CYP enzymes. One exception is cholesterol 25-hydroxylase, which is a member of a small enzyme class that uses diiron cofactors and is not a CYP enzyme [19-21]. The expression of the different enzymes and their corresponding oxysterols depends on the tissue. For example, cholesterol 24-hydroxylase is mainly expressed in neurons and sparsely in liver, while cholesterol 7 α -hydroxylase is only expressed in liver [21]. In contrast cholesterol 25-hydroxylase and cholesterol 27-hydroxylase can be found in many tissues [19, 21]. Especially sterol 27-hydroxylase has a broad substrate specificity and can form different oxysterols and plays a key role in steroid acid formation (Chapter 1.2.3) [19]. The major oxysterols and the respective enzymes of their biosynthesis are shown in Figure 4. Further oxysterols are for example C20-, C22-, or C6-hydroxylated sterols [22, 23].

1. Introduction

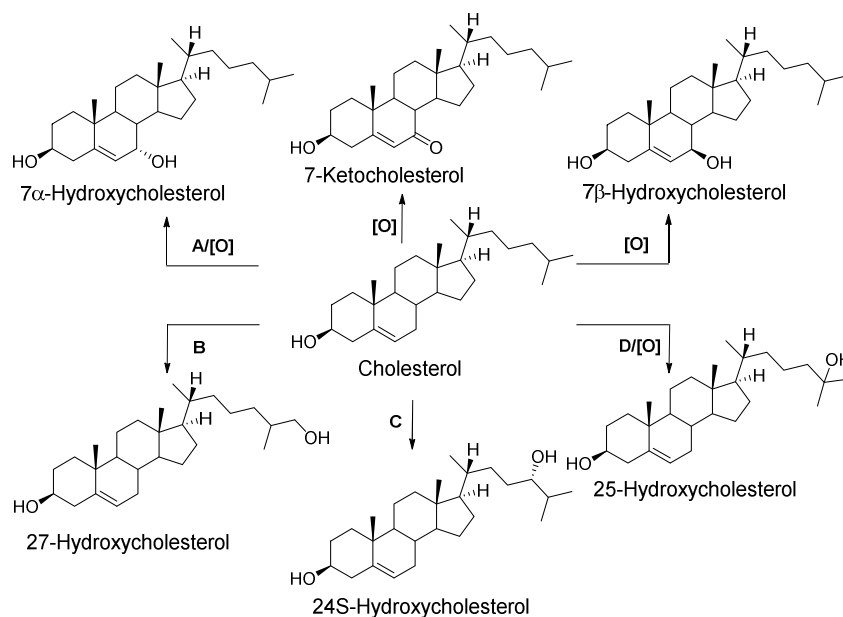


Figure 4 Oxysterol biosynthesis starting from cholesterol and the respective enzymes, **A:** cholesterol 7 α -hydroxylase (CYP 7A1) **B:** sterol 27-hydroxylase (CYP27A1) **C:** cholesterol 24-hydroxylase (CYP46A1) **D:** cholesterol 25-hydroxylase **[O]:** autoxidation [22].

Oxysterols have specific biological functions, like cholesterol, they are localized in the cell membrane but with different orientation and seem to have a destabilizing effect on the membrane [8]. Furthermore, oxysterols are ligands of nuclear receptors like liver X receptor (LXR) [8, 24]. Due to this interaction they affect lipid homeostasis and show immunomodulatory effects [8, 24, 25]. A known malfunction in oxysterol genesis is, for example, 7 α -hydroxylase deficiency, leading to higher cholesterol levels in serum and liver and a decrease of bile acid formation [21]. Sterol 27-hydroxylase deficiency is the cause of cerebrotendinous xanthomatosis (CTX), due to the key role of 27-hydroxylase in bile acid formation. This disease is characterized by a decrease of bile acid formation and elevated cholesterol and cholestanol levels in blood and tissues like the CNS, which can lead to progressive neurological dysfunction [21, 26].

1.2.3. Steroid acids

Oxysterols are further processed to bile acids by hydroxylation of the ring structure and side chain modifications. The involved enzymes have a broad substrate specificity so the order of the different reaction steps may vary [21]. The possible pathways can be roughly divided into acidic, 24-hydroxylase-, 25-hydroxylase- and neutral pathway (Figure 5) [21]. In the acidic pathway, the side chain is first oxidized to form the carboxylic acid, and the ring structure modifications are performed afterwards. In the other pathways, the ring structure is modified first, followed by the side chain oxidation. About 75% of the metabolized cholesterol is processed *via* the neutral pathway, also known as classic pathway, and about 25% are

1. Introduction

processed following the acidic pathway [21]. The first bile acids that are formed along these pathways are known as primary bile acids. Examples are cholic acid and chenodeoxycholic acid [21]. It is remarkable that the structure of the primary bile acids can vary between different mammalian species, like muricholic acid which can only be found in mice, and ursodeoxycholic acid which is characteristic for bears [21]. Bile acids play an important role in digestion. They are excreted by the liver into the gut and can solubilize hydrophobic dietary components like fat-soluble vitamins and enable their absorption [27]. The primary bile acids can be further processed by bacteria in the gut to form the so-called secondary bile acids, for example, lithocholic acid and deoxycholic acid [21, 27]. Most bile acids excreted from the liver are bile acids conjugated to glycine or taurine, which are more amphiphilic [21]. So, the bile acid pool of an organism consists of a variety of diverse bile acids and is noticeably different between the species. A lack of bile acids, for example due to 3β -hydroxy- Δ^5 - C_{27} -steroid oxidoreductase (Figure 5, **D**) deficiency, leads to neonatal jaundice, liver enlargement and malabsorption of lipids and fat-soluble vitamins [21, 27].

1. Introduction

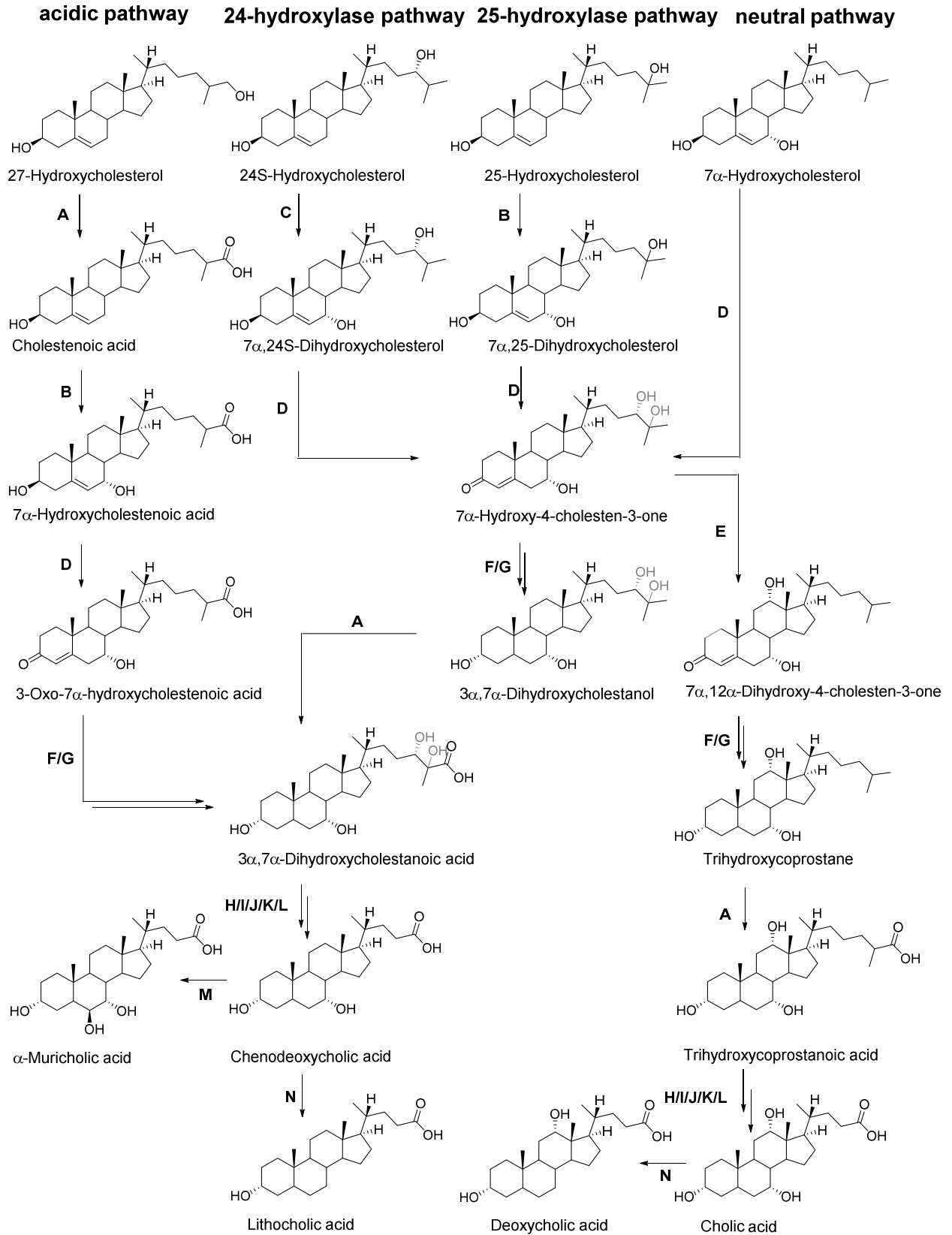


Figure 5 Possible pathways of bile acid synthesis and the involved enzymes. grey: Structure variations arising from 24- or 25-hydroxylase pathway. **A:** sterol 27-hydroxylase **B:** oxysterol 7α-hydroxylase (CYP 7B1) **C:** oxysterol 7α-hydroxylase (CYP 39A1) **D:** 3β-hydroxy-Δ⁵-C₂₇-steroid oxidoreductase **E:** sterol 12α-hydroxylase **F:** Δ⁴-3-oxosteroid-5β-reductase **G:** 3α-hydroxysteroid dehydrogenase **H:** bile acid CoA ligase **I:** 2-methylacyl-CoA racemase **J:** branched-chain acyl-CoA oxidase **K:** D-bifunctional protein **L:** peroxisomal thiolase 2 **M:** 6β-hydroxylase **N:** 7α-dehydroxylase [21, 28-30].

1. Introduction

1.2.4. Neurosteroids

Cholesterol side chain hydroxylation at C20 and C22 by cholesterol monoxygenase leads to side chain cleavage and the formation of the C₂₁ steroid pregnenolone (Figure 6). Pregnenolone is the precursor for several classes of steroid hormones like progestagens, mineralocorticoids, glucocorticoids, androgens and estrogens.

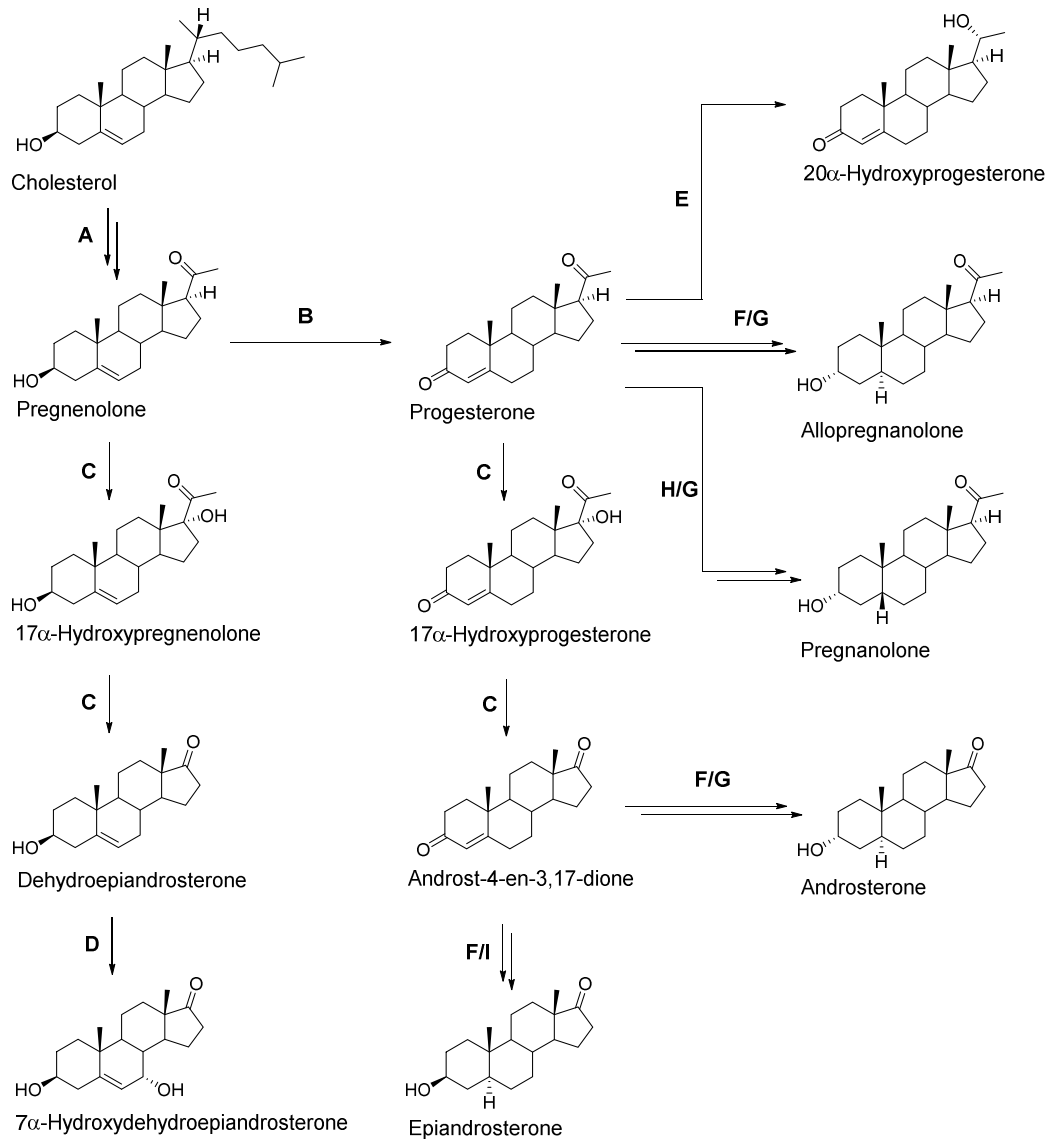


Figure 6 Neurosteroid biosynthesis starting from cholesterol and involved enzymes. **A:** cholesterol monoxygenase **B:** 3 β -hydroxysteroid dehydrogenase **C:** steroid-17 α -hydroxylase-17,20-lyase **D:** oxysterol-7 α -hydroxylase **E:** 20 α -hydroxysteroid dehydrogenase **F:** steroid-5 α -reductase **G:** 3 α -hydroxysteroid dehydrogenase **H:** steroid-5 β -reductase **I:** 3 β -hydroxysteroid dehydrogenase [31-34].

As hormones, these steroids can bind to intracellular steroid hormone receptors and thereby modulate the transcription of distinct genes. In this way they can unfold huge effects even at low endogenous levels. The term “neurosteroids” originally referred to steroids that were synthesized within the nervous system [35, 36]. Later, this term was also used to describe the

1. Introduction

neuromodulatory function of neurosteroids [37] and the additional term “neurosterols” was introduced to describe C₂₇ neurosteroids [38]. In this work, the term “neurosteroids” refers to C₁₉ and C₂₀ steroids with focus on progestagens and androgens. These steroids do not only take effect *via* steroid hormone receptors, but can also bind to neurotransmitter receptors like γ -aminobutyric acid (GABA_A) receptors [22, 35, 37, 39], *N*-methyl-D-aspartate (NMDA) receptors [22, 35] or sigma receptors [35]. They are known to play an important role in brain development, neuronal growth and plasticity [35]. In addition, they show neuroprotective effects, for example, after injuries or ischemia [35] and alterations in neurosteroids genesis are associated with neurodegenerative diseases like Alzheimer’s disease, Parkinson’s disease and multiple sclerosis [40].

1.2.5. Sterol sulfates

The hydroxyl group of sterols can be sulfo-conjugated by sulfotransferases [41]. Two different human hydroxysteroid sulfotransferases, SULT2A1 and SULT2B1, see Figure 7, are known [41]. The most important substrate of SULT2A1 is dehydroepiandrosterone with its 3 β -hydroxyl group, but also steroids with 3 α -, 17 β - or phenolic hydroxyl groups can serve as substrate for SULT2A1 [41]. The enzyme SULT2B1 and especially the subtype SULT2B1b selectively sulfonates C3-hydroxy groups of C₂₇ sterols [41, 42].

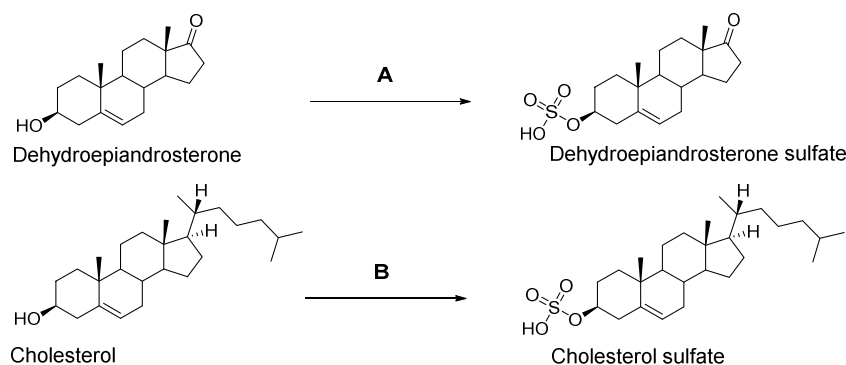


Figure 7 Biosynthesis of sterol sulfates. **A:** sulfotransferase (SULT2A1) **B:** sulfotransferase (SULT2B1b) [31, 41-43].

In general, sterol sulfates cannot bind to intracellular steroid hormone receptors as the respective unconjugated sterols [44], but they still have inherent biological activities [45]. So, the sulfo-conjugates of the aforementioned neurosteroids are known to modulate GABA_A receptors [46], NMDA receptors [46, 47] and melastatin-like transient receptor potential channels (TRPM1 and TRPM3) [46]. Sterol sulfates contribute significantly to reproduction [48] and cognitive performance [49]. Alterations in SULT activities are also associated with Alzheimer’s disease [50]. Cholesterol sulfate as C₂₇ sterol sulfate is, beside dehydroepiandrosterone sulfate, the most abundant sterol sulfate in humans [42]. It modifies cell membrane stability and modulates the function of blood platelets [42, 51].

1. Introduction

1.3. Steroids and Alzheimer's disease

At the “Deutsches Zentrum für neurodegenerative Erkrankungen” (DZNE), the research interest of the group of Prof. Dr. Harald Steiner is the enzyme γ -secretase, an enzyme associated with Alzheimer's disease (AD) [52]. The amyloid precursor protein (APP) is a transmembrane glycoprotein and is amongst others cleaved by β -secretase and γ -secretase to form amyloid β (A β) peptides [52]. Depending on the length of the A β fragment, these peptides could aggregate and form extracellular plaques, which are characteristic for AD. The major species A β 1-40 and some shorter A β fragments aggregate less likely as the longer species A β 42 [53, 54]. So, the specific cleavage site of the γ -secretase is responsible for plaque formation and the factors which modulate the γ -secretase activity are therefore under investigation [53, 55]. In the group of Prof. Dr. Steiner, the impact of different steroids on γ -secretase activity is investigated. They observed that free sterols and their corresponding sulfates can show contrary activities. Also Vaňková et al. [31] showed different concentrations of sterols and sterol sulfates in women with AD compared to healthy women. But not only neurosteroids and sterol sulfates are known to affect the γ -secretase, also steroid acids [29], cholesterol precursors [56, 57] and oxysterols [58] are under investigation. It remains unclear if γ -secretase is modulated *via* direct binding sites for steroids, or if an altered steroid composition in the membrane can influence γ -secretase activity because of the modified microenvironment. Effects of cholesterol binding to APP [59], membrane thickness [60] and the formation of lipid rafts [61] were already demonstrated.

1.4. Steroid analysis

The example of Alzheimer's disease illustrates the multiple ways steroids are involved in the development of diseases. To learn more about these mechanisms a broad view on all the steroid classes in specific tissues or experimental cell lines is necessary. This kind of steroid analysis is hampered by the very similar structures within the single classes, for example pregnanolone and allopregnanolone, and the great differences in concentration which can vary by a factor of about 100,000 like cholesterol ($\sim 10 \mu\text{g}/\text{mg}$) versus pregnenolone ($< 0.1 \text{ ng}/\text{mg}$) in brain tissue (see Chapter 4). Some of the first analytical procedures, that are still used today, are radioimmunoassays (RIA). These play an important role in clinical diagnosis but show limited sensitivity and specificity, as cross-reactivities to similar steroids cannot be excluded [62-64]. In addition, these assays are not capable of giving information about the presence of possibly unexpected accumulating steroids. Such pitfalls can be avoided by mass spectrometry (MS) combined with chromatographic systems like gas chromatography-mass spectrometry (GC-MS) [62], liquid chromatography-mass spectrometry (LC-MS) [62] and even supercritical fluid chromatography-mass spectrometry (SFC-MS) [65]. The most popular

1. Introduction

systems are LC-MS and GC-MS which have their own specific strengths. The “older” technology GC impresses with its huge separation power and, therefore, significant specificity even for isobaric steroids [66]. GC-MS systems usually apply electron ionization which is especially effective for lipophilic analytes and results in characteristic and highly reproducible mass spectra [64, 67]. This enables identification of unexpected compounds using MS-spectra libraries [64, 66]. But not every steroidal compound can be analyzed with GC because they need to be vaporable without decomposition. Thus, steroids are usually derivatized before GC-MS analysis, and conjugated steroids, for example, steroid sulfates, also need to be cleaved before GC-MS analysis [64]. This makes sample preparation time-consuming and fault prone. LC-MS has its strengths in shorter run times and faster sample preparation [62, 64]. However, the shorter run time leads to a limited chromatographic resolution [62], so separation of very similar compounds cannot always be accomplished. In addition, the ionization of the usually applied electro spray procedure is not very effective for lipophilic steroids [64, 67]. Therefore, derivatization is also often used in LC-MS procedures [68]. On the other hand the more polar analytes like steroid acids or sterol sulfates are easily detected with LC-MS and can be analyzed directly without cleavage [64].

2. Topic

Topic of this work was the development of a GC-MS based analytical procedure, to analyze the steroidome in tissue and cell samples. The term steroidome covers the whole set of steroids found in an organism or tissue [69]. Information about the steroidome is necessary to get a better understanding of the underlying pathomechanisms of diseases like, for example, Alzheimer's disease. Hence, a comprehensive analytical method, that gives an as broad as possible view on the steroidome, is needed. Nevertheless, there was a focus on some steroids of special interest. Those steroids were defined by the group of Prof. Dr. Steiner at DZNE, based on their previous experimental results. Consequently, the method ought to include specific neurosteroids, oxysterols, sterol sulfates, steroid acids, but should still provide information about accumulating unexpected steroidal compounds. The method should be applied on biological samples like mouse brain or cultured cells. In order to achieve this goal some problems needed to be solved. As mentioned before the sterol sulfates are not vaporable without decomposition, so for GC-MS analysis a suitable method for deconjugation was required. In addition, the sterol sulfates needed to be separated from unconjugated sterols before deconjugation. But also unconjugated steroids needed some additional sample preparation before GC-MS analysis. To improve the peak shape and the sensitivity, hydrophilic functional hydroxyl groups are frequently derivatized to trimethylsilyl (TMS) ethers using a mixture of *N*-methyl-*N*-trimethylsilyl acetamide (MSTFA) and trimethylsilyl imidazole (TSIM). But this well-established procedure [14, 70, 71] was not sufficient for all steroids of interest, especially those with keto groups were subject to artefact formation [72]. So, an additional derivatization of the keto groups was necessary. For bile acid analysis an appropriate sample preparation procedure including carboxylate derivatization was needed, too. In addition, these different steroid classes had to be extracted from the tissue and separated from each other before derivatization. The main task of this work was the development of a suitable sample preparation procedure which ensured all these requirements. As mentioned before, the endogenous levels of some steroids of interest are very low (*e.g.* pregnenolone < 0.1 ng/mg). The well-established measurement in scan mode on an ion trap- (IT-) MS system [14, 66, 70, 71] could not provide the required sensitivity and therefore, the development of an additional method in dynamic multiple reaction monitoring (dMRM) mode on a triple quadrupole- (QqQ-) MS system was also part of this work.

3. Sterol sulfate analysis

J. Junker, I. Chong, F. Kamp, H. Steiner, M. Giera, C. Müller, F. Bracher, Comparison of strategies for the determination of sterol sulfates via GC-MS leading to a novel deconjugation-derivatization protocol, Molecules, 24 (2019) 2353

3.1. Summary

The impact of steroids and sterol sulfates on the γ -secretase activity is of special interest in the group of Prof. Dr. Steiner at DZNE. In their *in vitro* assays sterol sulfates have shown contrary effects compared to their unconjugated counterparts. These findings, in addition to reports of divergent sulfotransferase activity in AD patients [31, 50], show the necessity of an analytical method which enables the analysis of steroids as well as sterol sulfates in biological samples. As mentioned in Chapter 1.4, GC-MS is the analytical method of choice especially for untargeted “screening” analysis. However, the analysis of sterol sulfates with GC-MS is challenging, because these sterol conjugates are not vaporable without decomposition. For this reason, the sterol sulfates need to be cleaved and the free sterol must be derivatized to achieve sufficient sensitivity and reproducibility. In the following article we compared and discussed different strategies for deconjugation and derivatization of sterol sulfates on the basis of eight exemplary sterol sulfates. Therefore, “older” literature methods [73, 74] for chemical sulfate cleavage were adapted and modified for the analysis of smaller sample amounts. Also, an enzymatic procedure was investigated as a possible alternative to the chemical cleavage. The resulting free sterols were then converted into TMS or MO-TMS (methyloxime-trimethylsilyl) derivatives (Figure 8). Additionally, the direct derivatization using trifluoroacetic anhydride (TFAA) and the resulting trifluoroacetyl (TFA) derivatives were examined. I was also able to identify another direct derivatization procedure that was not previously reported. This novel deconjugation-derivatization protocol utilized the reagent *O*-methylhydroxylamine hydrochloride (2% in pyridine). This reagent is usually used for derivatization of the keto groups and has shown to lead simultaneously to the cleavage of the sulfate esters. This could be explained with the relatively high nucleophilic properties of *O*-methylhydroxylamine due to the so called α -effect. This new method was optimized and compared to the solvolysis and MO-TMS derivatization procedure (both well-established). All these strategies and the associated advantages and limitations were discussed in detail. Especially the discovery of the direct MO-TMS derivatization could simplify future sterol sulfate analysis with GC-MS. This method enables the deconjugation of sterol sulfates regardless of C5-C6 saturation or C3-configuration. Beside this wide application range, the finally resulting MO-TMS derivatives have excellent chromatographic properties and give meaningful mass

3. Sterol sulfate analysis

spectra that are frequently used and therefore can be found in many mass spectral libraries. This new method was an important element of the final sample preparation protocol for simultaneous analysis of neutral steroids, steroid acids and sterol sulfates (Chapter 4).

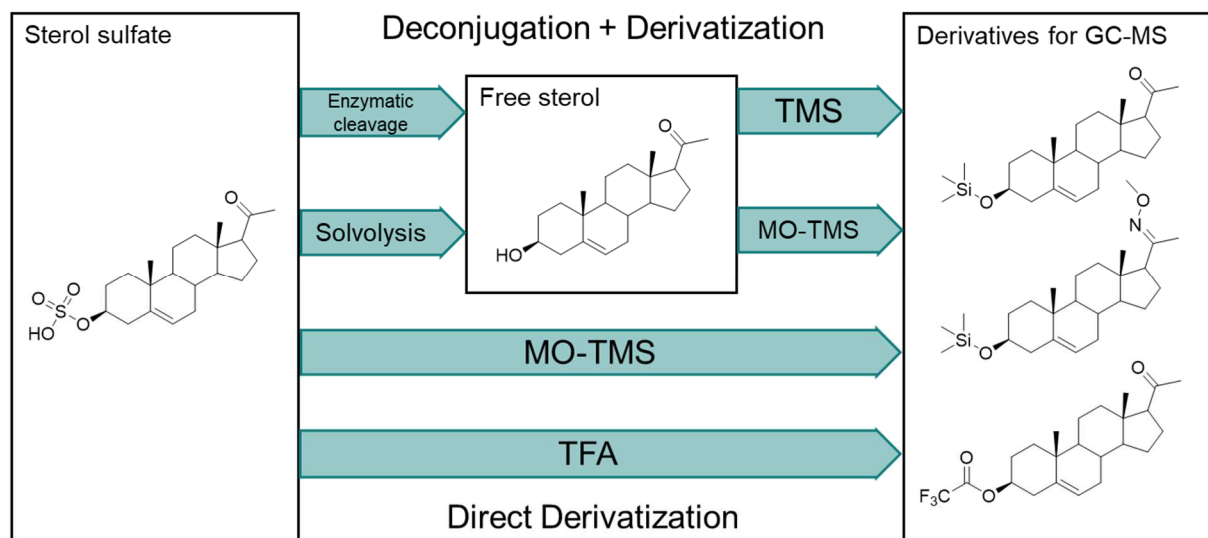


Figure 8 Graphical abstract of the original article: Comparison of strategies for the determination of sterol sulfates via GC-MS leading to a novel deconjugation-derivatization protocol

Some preliminary experiments focusing on the sterol sulfate pregnenolone sulfate have already been part of my diploma thesis [75]. These experiments included TMS derivatization, TFA derivatization, solvolysis with dioxane/acetic acid and enzymatic cleavage. The experiments on the other seven exemplary sterol sulfates and the use of *O*-methyl hydroxylamine hydrochloride for derivatization of the keto groups as well as the described novel direct deconjugation/derivatization procedure were part of my doctoral thesis.

3.2. Personal contribution

My contributions to this article were the previous research and conduction of preliminary experiments. Also, conceptualization, the final methodology and designs for the reported experiments were part of my contribution. The subsequent performance of the experiments, as well as the analysis of the measurement data, formal analysis and data curation was done by me. Finally, visualization of the experimental results, writing of the original draft as well as reviewing and editing were my contribution to this publication.

The experiments were carried out with support of Isabelle Chong (internship in the Master, Pharmaceutical Sciences), who also contributed to the analysis of the measurement data, as well as the formal analysis.

3. Sterol sulfate analysis

Prof. Dr. Harald Steiner and Dr. Frits Kamp were involved in the conceptualization of the project as well as in granting of resources and acquisition of funding. They further contributed in reviewing and editing of the original draft.

Dr. Martin Giera supported this publication regarding the investigation, formal analysis and data curation. He was also involved in reviewing and editing of the original draft.

Dr. Christoph Müller contributed in the planning of the experimental design and in the whole investigation. He was involved in the formal analysis and curation of the experimental data and further supported the visualization of these results. In addition, he contributed in the development of the article structure, writing of the original draft as well as reviewing and editing.

Prof Dr. Franz Bracher supervised this work along with Prof. Dr Harald Steiner and Dr. Martin Giera and was involved in the conceptualization of the project. He also supported the investigation, formal analysis and curation of the experimental data. Additionally, he provided resources and contributed in reviewing and editing of the original draft.

3.3. Article

The following article is printed in the original wording. The formatting may vary slightly compared to the original article.



Article

Comparison of Strategies for the Determination of Sterol Sulfates via GC-MS Leading to a Novel Deconjugation-Derivatization Protocol

Julia Junker ¹, Isabelle Chong ¹, Frits Kamp ², Harald Steiner ^{2,3}, Martin Giera ⁴,
Christoph Müller ¹ and Franz Bracher ¹,

¹ Department of Pharmacy-Center for Drug Research, Ludwig-Maximilians University Munich, Butenandtstraße 5-13, 81377 Munich, Germany

² Biomedical Center (BMC), Metabolic Biochemistry, Ludwig-Maximilians University Munich, Feodor-Lynen-Strasse 17, 81377 Munich, Germany

³ German Center for Neurodegenerative Diseases (DZNE), Feodor-Lynen-Strasse 17, 81377 Munich, Germany

⁴ Leiden University Medical Center, Center for Proteomics and Metabolomics, Albinusdreef 2, 2300 RC Leiden, The Netherlands

* Correspondence: franz.bracher@cup.uni-muenchen.de; Tel.: +49-892-1807-7301

Academic Editor: Yasunori Yaoita

Received: 27 April 2019; Accepted: 21 June 2019; Published: 26 June 2019

Abstract: Sulfoconjugates of sterols play important roles as neurosteroids, neurotransmitters, and ion channel ligands in health and disease. In most cases, sterol conjugate analysis is performed with liquid chromatography-mass spectrometry. This is a valuable tool for routine analytics with the advantage of direct sterol sulfates analysis without previous cleavage and/or derivatization. The complementary technique gas chromatography-mass spectrometry (GC-MS) is a preeminent discovery tool in the field of sterolomics, but the analysis of sterol sulfates is hampered by mandatory deconjugation and derivatization. Despite the difficulties in sample workup, GC-MS is an indispensable tool for untargeted analysis and steroid profiling. There are no general sample preparation protocols for sterol sulfate analysis using GC-MS. In this study we present a reinvestigation and evaluation of different deconjugation and derivatization procedures with a set of representative sterol sulfates. The advantages and disadvantages of trimethylsilyl (TMS), methyloxime-trimethylsilyl (MO-TMS), and trifluoroacetyl (TFA) derivatives were examined. Different published procedures of sterol sulfate deconjugation, including enzymatic and chemical cleavage, were reinvestigated and examined for diverse sterol sulfates. Finally, we present a new protocol for the chemical cleavage of sterol sulfates, allowing for simultaneous deconjugation and derivatization, simplifying GC-MS based sterol sulfate analysis.

3. Sterol sulfate analysis

Keywords: direct derivatization; solvolysis; sterol methoxime-trimethylsilyl ether

1. Introduction

The sulfoconjugates of sterols, also called sterol sulfates, are synthesized *in vivo* by conversion of the respective sterols by specific cytosolic sulfotransferase enzymes (SULT) [1,2]. These sterol sulfates are much more than just terminal stages of steroid metabolism and reservoir of their free analogues [2,3]. Several sterol sulfates are known to activate, modulate and inhibit specific enzymes and ion channels. For example, pregnenolone sulfate (6), dehydroepiandrosterone sulfate (2) and epipregnanolone sulfate are known to modulate neurotransmitter receptors like the γ -aminobutyric acid type A (GABA_A) and the *N*-methyl-d-aspartate (NMDA) receptors [4,5]. Furthermore, epipregnanolone sulfate and pregnenolone sulfate (6) are activators of melastatin-like transient receptor potential (TRPM) ion channels [3,4]. Steroid sulfates can also bind to membrane-associated G-protein coupled receptors (GPCRs) and activate MAP kinase cascade or phospholipase C [6]. Amongst other functions, cholesteryl sulfate (7) interferes with blood coagulation by activating Factor XII and inhibiting the serine proteases thrombin and plasmin [7,8]. The balance between sulfatation and desulfatation is fundamental for the tissue distribution and function of sterols and its dysregulation is involved in many diseases [9]. For instance, pregnenolone sulfate (6) and dehydroepiandrosterone sulfate (2) have been reported to be decreased in the brains of Alzheimer's disease (AD) patients [10]. Altered levels of pregnenolone sulfate (6) and several other sterol conjugates have also been found in the blood female AD patients [11], which might be related to an attenuated activity of SULT2A1 in the adrenal zona reticularis [12].

The analysis of sterol sulfates is hampered by the highly similar chemical structures of the sterol sulfates and their low abundance in biological samples. Several methodically different approaches are being applied in sterol sulfate analysis, the most common being radioimmunoassays (RIA), gas chromatography-mass spectrometry (GC-MS) and liquid chromatography-(tandem)mass spectrometry (LC-MS(/MS)). The major concerns about RIA are the need for using radioactive material as well as the low selectivity and possible cross-reactivity of similar analytes in addition to matrix effects [13]. In the last decade LC-MS(/MS) was the predominantly-used method for sterol conjugate analysis [14]. In contrast to GC-MS, as the gold standard of neutral cholesterol metabolites analysis [15], LC-MS(/MS) provides the possibility to analyze the non-volatile sterol conjugates without prior deconjugation [13,16,17]. Moreover, faster workup without deconjugation and/or derivatization and shorter run times of liquid chromatography makes it a high throughput method for targeted analysis ideally suited for clinical purposes [13,14]. Nevertheless, LC-MS(/MS) also has disadvantages such as limited chromatographic resolution and detection by electrospray ionization (ESI) mass spectra, that contain limited structural information due to low fragmentation rates [13,18]. In these aspects GC-MS cannot be replaced by LC-MS, since its high chromatographic resolution and the option for recording information-rich electron ionization (EI) mass spectra makes GC-MS a powerful tool for untargeted analyses and steroid profiling [13,16–19]. In particular, EI mass spectra of derivatives like sterol trimethylsilyl (TMS) ethers and methyloxime-trimethylsilyl (MO-TMS) ethers provide considerable structural information which can help

3. Sterol sulfate analysis

to identify unknown steroidal analytes and can be used for suspected-target screening [18,20,21].

While these derivatization methods are well established for unconjugated steroids (free sterols including keto sterols, Figure 1) [20,22], there is no general procedure for the analysis of sterol sulfates using GC-MS. There are many different approaches published for deconjugation including enzymatic cleavage using sulfatases or chemical solvolysis, but an universally applicable method is lacking [23,24]. We discuss here in detail the most commonly used methods for deconjugation and derivatization for the GC-MS based analysis of sterol sulfates (Figure 1), and provide a significantly simplified procedure developed in the course of our investigations, allowing for simultaneous deconjugation and derivatization.

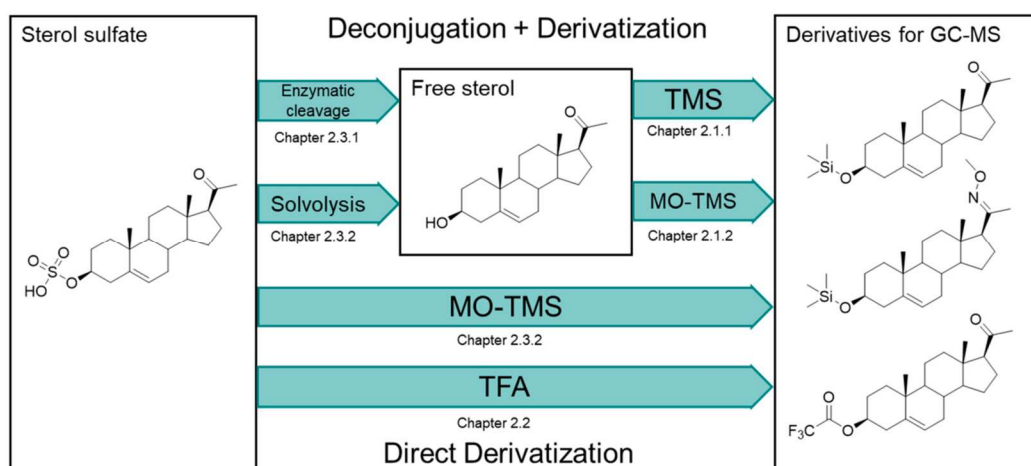


Figure 1. Strategies for sterol sulfate determination utilizing gas chromatography-mass spectrometry (GC-MS). “Two step” methods make use of a prior deconjugation step to form the free (unconjugated) sterol and a subsequent derivatization of the hydroxyl and, for methyloxime-trimethylsilyl (MO-TMS) derivatives, also the keto group. Direct derivatization refers to simultaneous cleavage of the sterol sulfate and derivatization. The deconjugation and derivatization strategies are shown with pregnenolone sulfate (6) here. TMS = derivatization to pregnenolone trimethylsilyl ether, MO-TMS = deconjugation/derivatization to pregnenolone methyloxime-trimethylsilyl ether, TFA = deconjugation/derivatization to pregnenolone trifluoroacetyl ester.

Furthermore, we present a comprehensive re-investigation of published methods demonstrating the scope and limitations of different derivatization procedures including direct acylation and formation of TMS and MO-TMS ethers. Additionally, we present a new protocol which allows the direct formation of MO-TMS derivatives from sterol sulfates, effectively combining sulfate ester cleavage and the formation of methyloximes (MO). The residual free hydroxyl groups can then be selectively silylated in a second step. The experiments were carried out with a representative collection of eight sterol sulfates with and without keto groups including 3α - and 3β -sterol sulfates and Δ^5 -unsaturated and saturated sterols. The structures of the model analytes are shown in Figure 2.

3. Sterol sulfate analysis

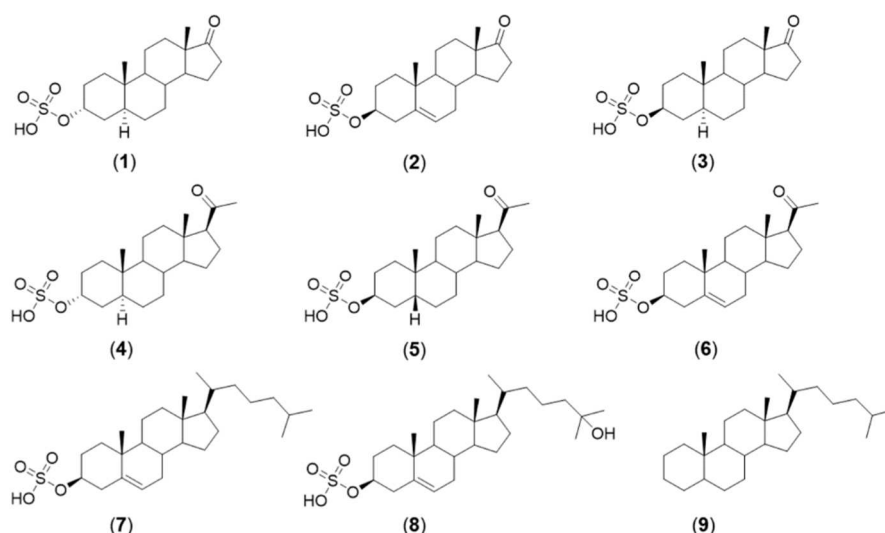


Figure 2. Overview of the model analytes: 1 androsterone sulfate, 2 dehydroepiandrosterone sulfate, 3 epiandrosterone sulfate, 4 allopregnanolone sulfate, 5 pregnanolone sulfate, 6 pregnenolone sulfate, 7 cholesterol sulfate, 8 25-hydroxycholesterol sulfate, and 9 cholestane (internal standard, IS).

2. Results

2.1. Derivatization Strategies for Free Sterols (Deconjugated Sterol Sulfates)

2.1.1. Trimethylsilyl (TMS) Derivatives

The most popular derivatization method for sterols is the formation of sterol TMS ethers [22,25–30]. For this derivatization free hydroxyl groups are required, so in the case of sterol sulfates a prior deconjugation step is mandatory. Available deconjugation procedures are subject of Section 2.3.

For silylation several reagents with different silyl donor abilities are available. To ensure a complete derivatization even of sterically hindered tertiary hydroxyl groups, the addition of a catalyst like *N*-trimethylsilylimidazole (TSIM) and trimethyliodosilane and/or an auxiliary base like pyridine is necessary [25]. An established silylation mixture for complete derivatization of secondary and tertiary hydroxyl groups even at room temperature is *N*-methyl-*N*-trimethylsilyltrifluoroacetamide (MSTFA) with 10% TSIM [20,31]. A known difficulty in TMS derivatization is the presence of keto groups, because the formation of artifacts (identified as enol TMS ethers) can be observed under these conditions [32]. We investigated the extent of the reported artifact formation for the exemplary keto sterol pregnenolone. The observed total ion chromatogram (TIC) in Figure 3 shows one peak (I) for pregnenolone with only one TMS ether (silylated 3-OH) and three (II–IV) artifacts corresponding to pregnenolone derivatives with an additional enol TMS ether. The plausible structures of these derivatives are shown in Figure 3c [33].

One attempt to avoid the formation of mixtures of mono- and bis-silylated products has been the application of a stronger silylating reagent which should enhance the enol TMS formation. For this purpose trimethyliodosilane can be used. This reactive reagent is generated in situ in a mixture of MSTFA and ammonium iodide. A reducing agent such as mercaptoethanol is further added in order to avoid undesired side reactions resulting from accidentally formed iodine [33–38]. This method requires much effort for optimization depending on the analytes of interest [36]. In addition also with this procedure artifacts can be

3. Sterol sulfate analysis

observed, resulting from incorporation of mercaptoethanol [34,35]. In conclusion, silylation of keto sterols is cumbersome in most cases.

2.1.2. Methyloxime-Trimethylsilyl (MO-TMS) Derivatives

The problematic (and frequently inevitable) enol TMS ether formation of keto sterols can be avoided with a two-step derivatization protocol. In this approach the keto groups are converted into methoxylamine (synonym: oxime methyl ether; MO) derivatives first, typically using 2% *O*-methylhydroxylamine hydrochloride (*m/v*) in pyridine (Scheme 1). In a second step the hydroxyl groups can be selectively transformed into TMS ethers using the methods described in Section 2.1.1 [20,32,34,39].

However, with this method two isomeric MO derivatives (*syn*, *anti*) can be formed, which are partially or fully separated by GC giving two peaks with the same fragmentation patterns [32,40,41]. We were able to convert all exemplary keto sterol sulfates into their respective MO-TMS derivatives after solvolysis (see Section 2.3). The acquired chromatogram in Figure 4a shows only one peak for each sterol derivative and no additional peaks or peak shoulders due to *syn*-/*anti*-isomers of the MO residues were observed. With this procedure keto sterols (derived from sulfates 1–6) and sterols without keto groups (derived from 7, 8) can be analyzed likewise.

3. Sterol sulfate analysis

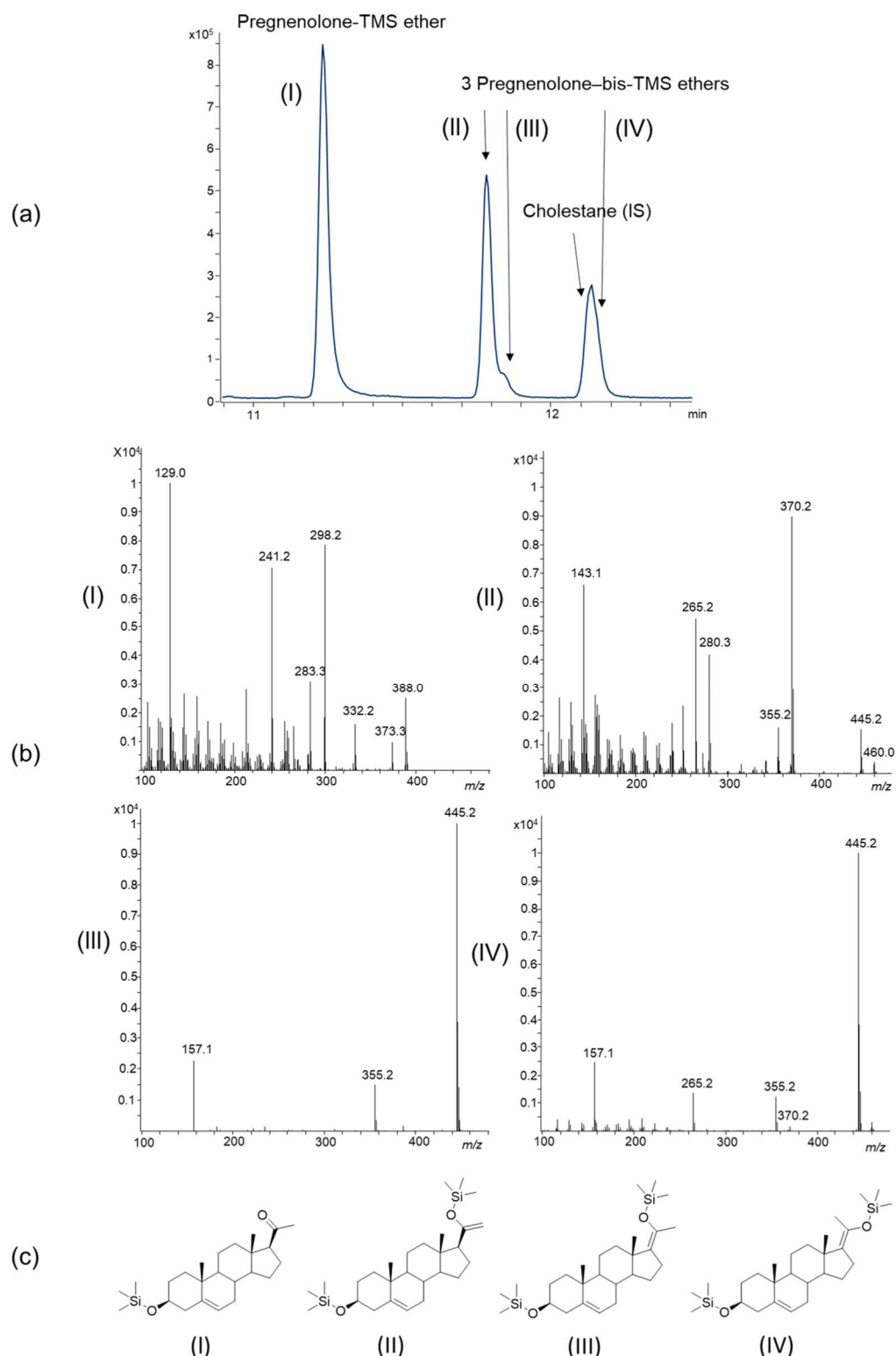
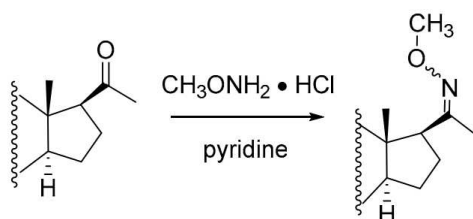


Figure 3. (a) Total ion chromatogram (TIC) of pregnenolone-TMS derivatives (containing cholestane (IS)). (b) Mass spectra of resulting pregnenolone TMS ethers peaks (I)–(IV) after derivatization with *N*-methyl-*N*-trimethylsilyltrifluoroacetamide (MSTFA)/*N*-trimethylsilylimidazole (TSIM) (9:1). (c) Structures of pregnenolone-mono-TMS ether (I) and pregnenolone-bis-TMS ethers (II–IV) [33]; for chromatographic and mass spectral characteristics see Supplementary Table S1.

3. Sterol sulfate analysis



Scheme 1. Example for derivatization of keto groups with *O*-methylhydroxylamine hydrochloride in pyridine [20].

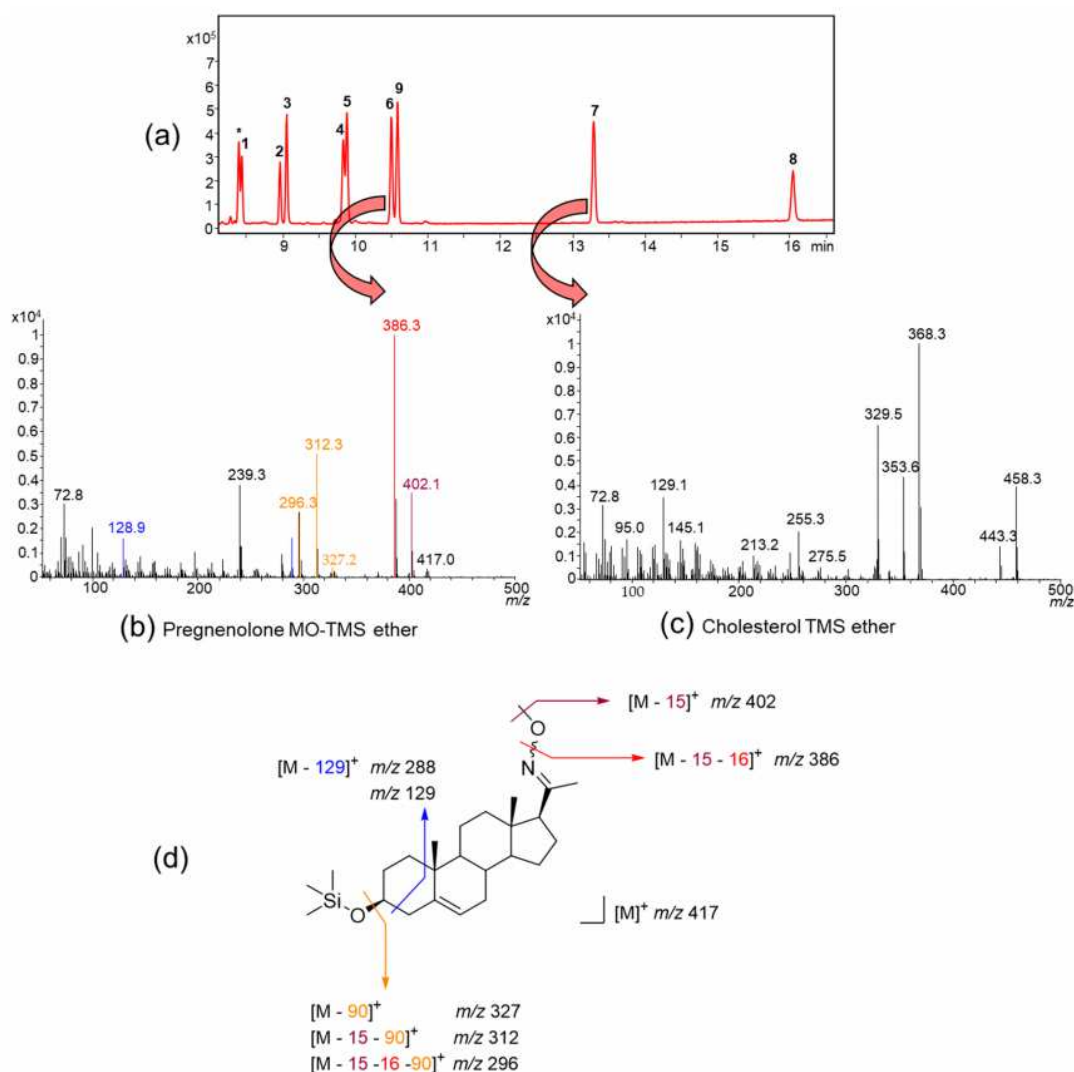


Figure 4. (a) Total ion chromatogram (TIC) of the eight sterol (MO-)TMS ethers and internal standard (IS). Analyzed sterols: 1 androsterone sulfate, 2 dehydroepiandrosterone sulfate, 3 epiandrosterone sulfate, 4 allopregnanolone sulfate, 5 pregnanolone sulfate, 6 pregnenolone sulfate, 7 cholesterol sulfate, 8 25-hydroxycholesterol sulfate, and 9 cholestane (IS). * Impurity of silylating reagent; (b) mass spectrum of pregnenolone MO-TMS ether; (c) mass spectrum of cholesterol-TMS ether; (d) proposed fragmentations of pregnenolone MO-TMS ether according to literature [29]. For chromatographic and mass spectral characteristics see Supplementary Table S1.

The mass spectra of these derivatives provide much structural information. They show the molecular ion peaks and characteristic fragmentations, which can be seen in Figure 4b,c. As

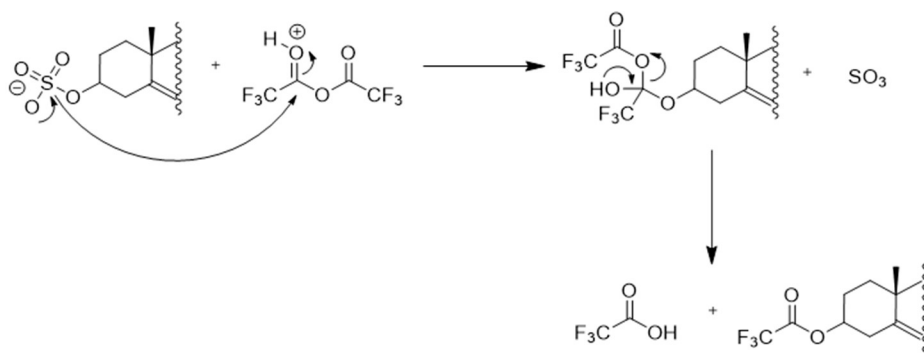
3. Sterol sulfate analysis

exemplarily shown for pregnenolone MO-TMS ether in Figure 4d the molecular ion $[M]^+$ is observable, and the base peak $m/z [M - 15 - 16]^+$ clearly indicates the fragmentation of the MO moiety. The ion $m/z [M - 90]^+$ is typical for the loss of trimethylsilanol and the ions $m/z [M - 129]^+$ as well as $m/z 129$ are characteristic for Δ^5 -sterol TMS ethers referring to the loss of trimethylsilanol from C-3 together with C-1, C-2 and C-3 [42].

2.2. Direct Deconjugation/Derivatization of Sterol Sulfates to Give Trifluoroacetyl (TFA) Derivatives

The problematic deconjugation step of sterol sulfates (for details see Section 2.3) can in certain cases be avoided if *O*-perfluoroacylation is chosen instead of TMS derivatization. The formation of perfluoroacyl derivatives is a fast and easy way to obtain volatile derivatives directly from sterol sulfates in one single operation. This method was first described by Touchstone and Dobbins [43] who used heptafluorobutyric anhydride (HFBA) in benzene to form the 3-*O*-acylated products directly from estriol sulfate and dehydroepiandrosterone sulfate (**2**). Also, Liere et al. [44] and Schumacher et al. [5] used successfully HFBA for the direct derivatization of **2** and **6** without prior sulfate deconjugation in one single step.

Further investigations with different anhydrides, sterol sulfates and reaction conditions were performed by Murray and Baille [45], who observed that this direct derivatization protocol is limited to sulfates derived from Δ^5 -sterols and estrogens. They also showed that there is no need for using additional solvents like benzene, and demonstrated that the supplement of the auxiliary base pyridine, which is normally used to enhance the esterification of free sterols, even inhibits the reaction with sterol sulfates [45]. Complete derivatization of the Δ^5 -sterol sulfate dehydroepiandrosterone sulfate (**2**) was further obtained using trifluoroacetic anhydride (TFAA) without additional solvent reacted at 70 °C for 30 min. The authors [45] proposed an acid-catalyzed reaction which is shown in Scheme 2.



Scheme 2. Mechanism for the acid-catalyzed reaction of Δ^5 -sterol sulfates with trifluoroacetic anhydride according to Murray and Baille [45].

We examined the scope of this direct derivatization protocol with the eight exemplary sterol sulfates shown in Figure 2. The results of this experiment are shown in Figure 5 and confirm the previously claimed limitation of this method to Δ^5 -sterol sulfates. The Δ^5 -unsaturated sterol sulfates **2**, **6**, and **7** showed good results while the saturated sterol sulfates **1**, **3**, **4**, and **5** did not undergo noteworthy conversion. An exception is the Δ^5 -unsaturated 25-hydroxycholesterol sulfate (**8**) whose TFA derivative was detected only in trace amounts (Figure 5a). The peak of analyte **8** in the chromatogram (Figure 5b) shows a peak shoulder and the corresponding mass spectra indicate an incomplete derivatization. The addition of

3. Sterol sulfate analysis

pyridine is not useful in this case because it would inhibit the deconjugation of the sulfated hydroxyl group at C-3 at the same time [45].

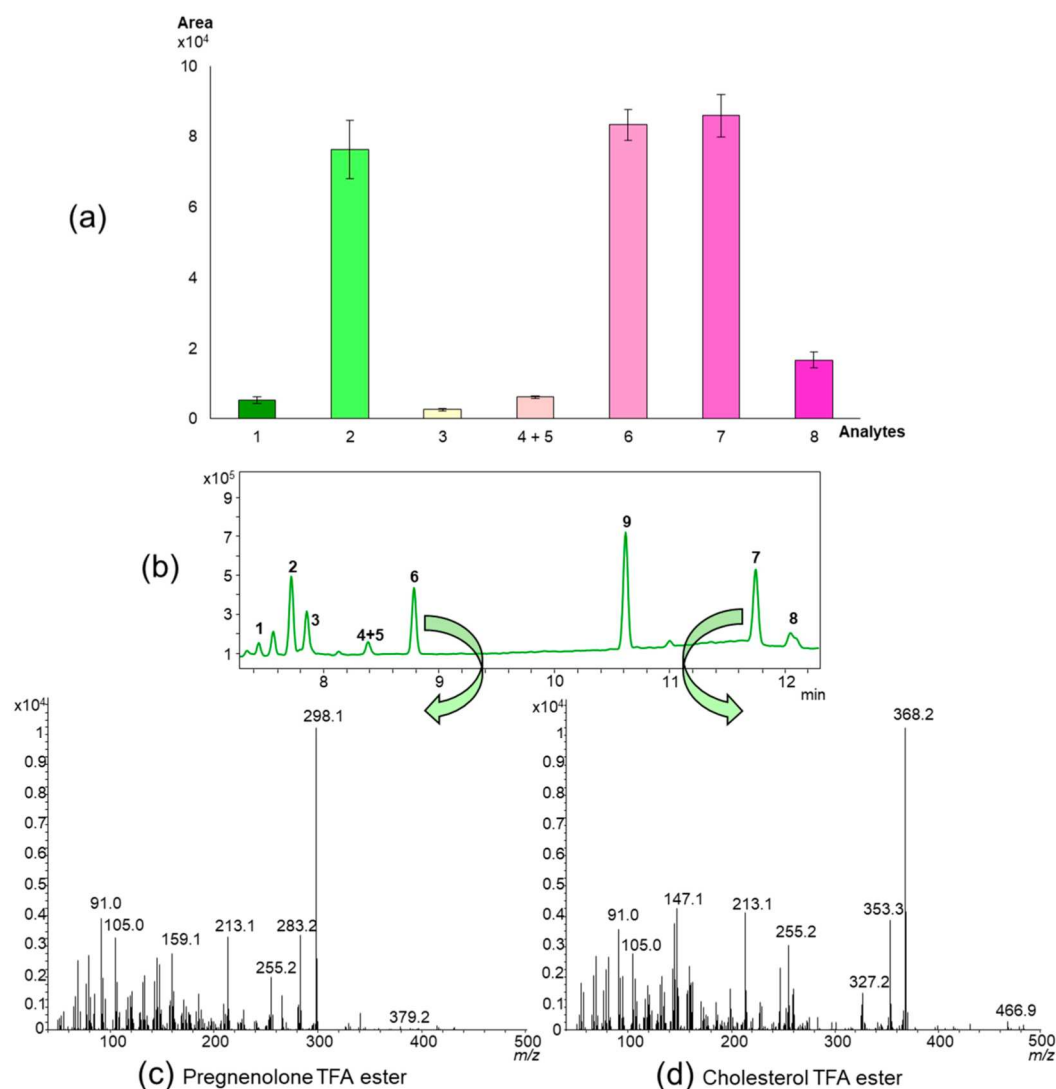


Figure 5. (a) Bar chart with mean base peak areas and standard deviations ($n = 6$) of the sterol TFA esters obtained by treatment of sterol sulfates 1–8 with trifluoroacetic anhydride. (b) Total ion chromatogram (TIC) of the eight sterol TFA esters and the internal standard, derived from: 1 androsterone sulfate, 2 dehydroepiandrosterone sulfate, 3 epiandrosterone sulfate, 4 allopregnanolone sulfate, 5 pregnanolone sulfate, 6 pregnenolone sulfate, 7 cholesterol sulfate, 8 25-hydroxycholesterol sulfate, and 9 cholestane (IS). (c) Mass spectrum of pregnenolone TFA ester ($[M]^+ m/z$ 412). (d) Mass spectrum of cholesterol TFA ester ($[M]^+ m/z$ 482). For chromatographic and mass spectral characteristics see Supplementary Table S1.

Another weakness of this approach is the missing molecular ion of Δ^5 -sterol acyl derivatives [26,42,46,47] which is evident from the mass spectra shown in Figure 5c,d. This fact may lead to difficulties in identification of unknown compounds. Besides the missing molecular ion peak and the incomplete derivatization for some sterols, the residual TFA amounts in the samples lead to column bleeding and a shorter shelf life of the GC capillary column.

3. Sterol sulfate analysis

2.3. Strategies for Sterol Sulfate Deconjugation

2.3.1. Enzymatic Cleavage of Sterol Sulfates

For the analysis of sterol sulfates as their corresponding TMS derivatives by GC-MS free hydroxyl groups of the unconjugated sterols are mandatory. Hence, an additional step for deconjugation is required. The enzymatic cleavage of sterol conjugates is a frequently used procedure especially in analysis of anabolic androgenic steroids in urine samples [23,24,48]. For glucuronides enzymatic cleavage utilizing the highly specific *E. coli* β -glucuronidase is the gold standard for steroid analysis in urine samples [23]. For the cleavage of sterol sulfates enzyme preparations from molluscs are commonly used, because these contain sulfatase activity beside β -glucuronidase activity. The most common preparations are from *Helix pomatia*, but also *Patella vulgata*, *Haliotis* spp. and *Ampullaria* are current sources [24]. These sulfatasases are known to hydrolyze sulfates of 3β -hydroxy- Δ^5 -sterols, 3β -hydroxy- 5α -sterols, and 3α -hydroxy- 5β -sterols, but fail to cleave 3α -hydroxy- 5α -sterol sulfates [39,49]. Another known problem is the conversion and degradation of sterols especially by *Helix pomatia* preparations, which contain additional enzymes with various activities [24,25,28]. Due to these limitations there is no general procedure available for enzymatic cleavage of sterol sulfates. Gomes et al. [24] present several published procedures utilizing different enzymes, buffers and reaction conditions. We adopted the method described by Xu. et al. [50] with the difference that we used an aqueous solution of the sterol sulfates instead of a urinary sample. Under the described conditions (Section 5.3.4) we obtained only partial hydrolysis of dehydroepiandrosterone sulfate (2), a 3β -hydroxy- Δ^5 -sterol sulfate, and epiandrosterone sulfate (3), a 3β -hydroxy- 5α -sterol sulfate, with poor reproducibility. The other sterol sulfates in the experiment did not show any measurable hydrolysis. Variations of the buffer system (acetate buffer pH 7, phosphate buffer pH 5, 7, and 8) and reaction conditions (35 °C for 4 h and 20 h, 55 °C for 4 h and 20 h) did not improve our results. Hence, as optimization of the hydrolysis conditions is rather complex [48] and many sulfate conjugates (e.g., androsterone (1), a 3α -hydroxy- 5α -sterol sulfate) are known to be resistant to enzymatic hydrolysis [39,49], this method seems not to be suitable for the untargeted analysis of sterol sulfates.

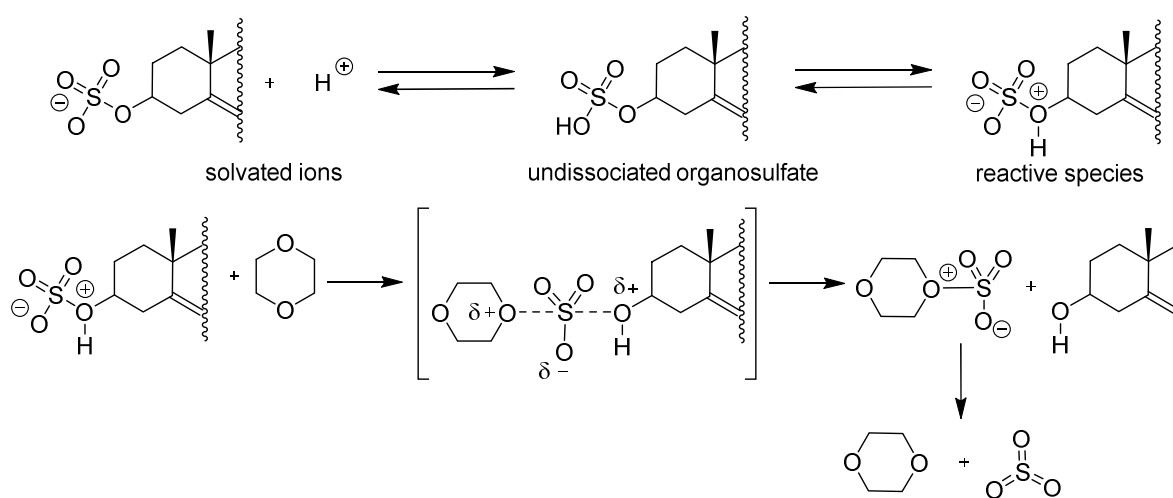
2.3.2. Chemical Cleavage of Sterol Sulfates

An alternative to the enzymatic hydrolysis is the chemical hydrolysis or solvolysis. Traditionally acidic hydrolysis at elevated temperatures was used for deconjugation of sterol sulfates. But the drastic conditions that are required for this hydrolysis including high amounts of mineral acid and refluxing, can lead to degradation or transformation of some sterols [51–53]. In turn, solvolysis under mild conditions is preferred and can be achieved by extracting the sterol sulfates from an acidified (with sulfuric acid) aqueous sample with ethyl acetate and storing this moist organic phase for 24 h at 39 °C [54] or with trimethylchlorosilane in methanol (methanolysis) [30]. The ability of oxygen-containing solvents, especially ethers, to cleave sterol sulfates in presence of minor amounts of water and acid was investigated in 1958 by Burstein and Lieberman [55]. They proposed an acid-catalyzed mechanism for the solvolysis (Scheme 3) in oxygen containing solvents, like 1,4-dioxane [55]. Having examined several published protocols, we found the solvolysis in 1,4-dioxane to be a particularly effective and

3. Sterol sulfate analysis

mild method. It is applicable for both 3 α - and 3 β -sterol sulfates as well as for sulfates derived from saturated and unsaturated sterols [55,56].

To examine the scope of solvolysis we modified a method published by Hutchins and Kaplanis [57] who applied 1% acetic acid in 1,4-dioxane under reflux overnight (here: ≤ 6 h, 100 °C; see Section 5.3.5.1). This solvolysis worked for every sterol sulfate in this experiment regardless of the configuration at C3 and presence of a Δ^5 -double bond. The experiments revealed the best reaction time for solvolysis was 3 h for the entire set of tested sterol sulfates. The optimum reaction times for solvolysis for individual sterol sulfates, shown in Figure 6a and Supplementary Table S2, vary between 3 h and 4 h. The solvolysed sterol sulfates were measured as their MO-TMS derivatives (two-step derivatization as described in Section 2.1.2).



Scheme 3. Mechanism of the acid-catalyzed solvolysis of sterol sulfates in 1,4-dioxane proposed by Burstein and Lieberman [55]

3. Sterol sulfate analysis

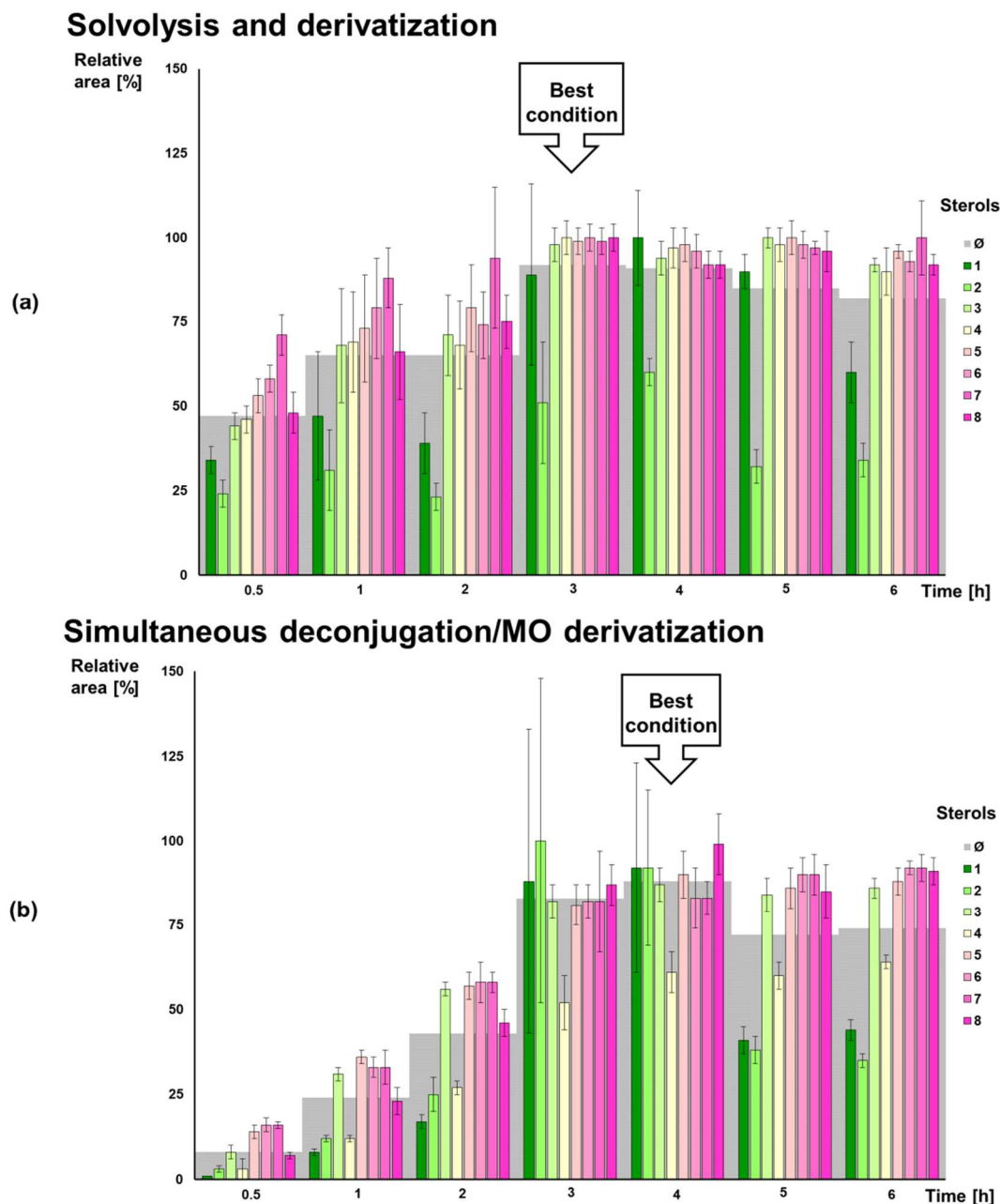


Figure 6. Determination of (keto-)sterol sulfates 1–8 as (MO)-TMS derivatives (a) with and (b) without previous sulfate solvolysis step (with 1% acetic acid in 1,4-dioxane). The indicated time refers to the duration of solvolysis prior to MO-TMS derivatization (for “Solvolysis and derivatization”, (a)) or to the incubation with *O*-methylhydroxylamine solution (for “Simultaneous deconjugation/MO derivatization”, (b)). The results obtained for each individual sterol sulfate under the different conditions are shown as relative peak areas [%] ± standard deviation (n = 6); the mean value of all steroids for every time point is shown in the background (grey), the best conditions for all tested sterol sulfates are marked as “Best condition”. The maximum recorded peak area for each sterol derivative within this experiment was set as 100%. Analyzed sterols: 1 androsterone sulfate, 2 dehydroepiandrosterone sulfate, 3 epiandrosterone sulfate, 4 allopregnanolone sulfate, 5 pregnanolone sulfate, 6 pregnenolone sulfate, 7 cholesterol sulfate, and 8 25-hydroxycholesterol sulfate.

Further experiments surprisingly revealed a possibly new form of chemical cleavage. Sterol sulfate deconjugation was found to be a side effect of the first derivatization step, the

3. Sterol sulfate analysis

methyloxime (MO) formation of the keto groups. We examined scope and efficiency of this new method for simultaneous cleavage and MO derivatization of sterol sulfates in additional experiments. To this end, eight sterol sulfates 1–8 (Figure 2) were incubated with *O*-methylhydroxylamine solution for different times (0.5 h–6 h; see Section 5.3.5.2) without previous solvolysis, then silylated, and the results were compared with the results of the solvolysis approach. This comparison is shown in Figure 6b, and Supplementary Table S2. In conclusion, we found that the acidic solvolysis step is dispensable for all investigated sterol sulfates. Optimal results for all analytes under investigation, using our new simultaneous deconjugation/MO derivatization protocol, were obtained after 4 h incubation with *O*-methylhydroxylamine solution. The optimum conditions of this simultaneous deconjugation/MO derivatization method for each individual sterol sulfate, shown in Figure 6b and Supplementary Table S2, vary between 3 h and 6 h. Two criteria were employed for evaluation of optimal conditions, on the one hand the relative peak area was taken as indicator for the degree of deconjugation, on the other hand the standard deviation (SD) should be as small as possible.

Figure 6a shows that solvolysis is a reliable method which achieves the best results for most of the tested sterol sulfates (100% is the best result achieved for individual sterols, not the recovery). The disadvantage of solvolysis is the additional workup step, because derivatization including methyloxime formation for 0.5 h, if keto sterols are analyzed, and silylation has to be performed in addition to the solvolysis step. This extra deconjugation procedure can be avoided in the approach with simultaneous deconjugation/MO derivatization. In this case, incubation for 4 h achieves the best results for most of the tested sterol sulfates. The peak areas achieved under these conditions are similar to those obtained with solvolysis with the advantage of less workup efforts.

Which method should be preferred is dependent on the target analytes. If sterols without keto groups are analyzed solely, a simplified approach with solvolysis and subsequent silylation is advisable. If keto sterols are determined it depends on the particular sterols, for example for dehydroepiandrosterone sulfate (2) better results can be achieved with the simultaneous deconjugation/MO derivatization protocol, whereas allopregnanolone sulfate (4) can be cleaved with solvolysis more effectively.

3. Discussion

We investigated the scope and limitations of most of the commonly used procedures including direct acylation and formation of TMS and MO-TMS ethers. The advantages and disadvantages of these methods are summarized in Table 1.

Surprisingly, we found that in the course of the methoximation of keto sterol sulfates, originally intended only to protect their keto groups as MO derivatives for avoiding undesired enol silylation in the subsequent silylation of the 3-hydroxy groups (see Section 2.1.2), that sterol sulfates were as well cleaved upon treatment with the *O*-methylhydroxylamine reagent. To the best of our knowledge, this reaction has not yet been utilized in the analysis of sterol sulfates before. Only scarce evidence on this type of organosulfate cleavage has been published before, and previous investigations were performed only with aryl [58] and methyl sulfates [59,60]. Most likely, this exceptional reactivity of methoxylamine is due to the so-called α -effect [59,61], leading to strongly enhanced nucleophilicity of the NH₂ group, even enabling

3. Sterol sulfate analysis

this reagent to cleave organosulfates under uncommon nucleophilic attack at the S-atom. This novel sample pretreatment allows for an unprecedented, short and easy-to-perform derivatization of keto sterol sulfates involving both organosulfate deconjugation and ketone methoximation under relatively mild reaction conditions. Subsequent silylation of liberated hydroxyl groups provides suitable derivatives for GC-MS analysis. Hence, this new deconjugation/derivatization protocol represents a considerable progress in the analysis of keto sterol sulfates. Our present investigations on the chemical behavior of sterol sulfates provided further useful evidence for the analysis of sterol sulfates.

Table 1. Overview of derivatization methods for analysis of sterol sulfates.

Analyzed by GC-MS as	Advantages	Disadvantages
TMS ether (Sections 2.1.1 and 5.3.1)	Fast and easy workup Mass spectra with molecular ion and characteristic fragmentation pattern	Prior deconjugation step afforded (e.g., solvolysis) Artifact formation with keto groups possible
MO-TMS ether (Sections 2.1.2, 2.3.2 and 5.3.2 and Section 5.3.5.2)	Mass spectra with molecular ion and characteristic fragmentation pattern Simultaneous deconjugation/MO-derivatization of sterol sulfates possible No artifacts (apart from possible <i>syn</i> - and <i>anti</i> -isomers of the MO group) in presence of keto groups	Time consuming workup with two step derivatization and additional clean up step
TFA ester (Sections 2.2 and 5.3.3)	Fast and easy workup Direct derivatization of sterol sulfates possible Short GC run times	Direct derivatization is limited to estrogens and Δ^5 -sterol-3-sulfates Derivatization of additional free hydroxyl groups could be problematic (e.g., 25-hydroxycholesterol sulfate) Residual TFA leads to column bleeding Mass spectra do not show a molecular ion

4. Conclusions

The aim of the present work was to find the best deconjugation/derivatization strategy for the analysis of sterol sulfates by GC-MS. As expected, there is no single best method for deconjugation and derivatization of sterol sulfates. Depending on the nature of the analyte of interest, the methods have individual strengths and weaknesses (Section 2.3.2, Table 1). For the targeted determination of known (Δ^5 -)sterol sulfates an especially fast workup employing direct perfluoroacylation can be the method of choice. But one of the biggest advantages of GC-MS is its strength as discovery tool for unexpected sterols. For this untargeted approach workup procedures are necessary, that are not limited to a subset of sterol sulfates. In addition, these workup procedures should form derivatives with characteristic mass spectra. Both our new protocol for simultaneous deconjugation/MO-derivatization followed by TMS derivatization and the protocol for acidic solvolysis followed by MO-TMS derivatization meet these requirements.

5. Materials and Methods

5.1. Materials and Reagents

All consumables were from VWR (Ismaning, Germany). Derivatization reagents trifluoroacetic anhydride (TFAA), 1-(trimethylsilyl)imidazole (TSIM), and *N*-methyl-*N*-trimethylsilyltrifluoroacetamide (MSTFA) were from Macherey-Nagel (Düren, Germany). Deionized water was prepared with an in-house ion-exchanger. 1,4-Dioxane and methyl *tert*-

3. Sterol sulfate analysis

butyl ether (*MtBE*) were distilled before use. β -Glucuronidase/sulfatase from *Helix pomatia* type HP-2, 5 α -cholestane ($\geq 97\%$), pregnenolone ($>98\%$), pregnenolone sulfate sodium salt ($>98\%$), and cholesteryl sulfate sodium salt ($>99\%$) were purchased from Sigma-Aldrich (Schnelldorf, Germany). Dehydroepiandrosterone sulfate sodium salt ($>99\%$) and 25-hydroxycholesteryl sulfate sodium salt ($>99\%$) were from Avanti Polar Lipids (Alabaster, AL, USA). All other sterol sulfate sodium salts were from Steraloids (Newport, RI, USA). All other reagents and solvents were purchased in HPLC grade or in pro analysis quality from Sigma-Aldrich (Schnelldorf, Germany).

5.2. Instruments and Equipment

Gas chromatography (GC) was performed on a Varian 3800 gas chromatograph coupled to a Saturn 2200 ion trap from Varian (Darmstadt, Germany). The autosampler was from CTC Analytics (Zwingen, Switzerland) and the split/splitless injector was a Varian 1177 (Darmstadt, Germany). Instrument control and data analysis were carried out with Varian Workstation 6.9 SP1 software (Darmstadt, Germany) and Agilent MassHunter Workstation Software package B.08.00 (Santa Clara, CA, USA). An Agilent HP-5-ms capillary column (Santa Clara, CA, USA) of 30 m length, 0.25 mm i.d., and 0.25 μm film thickness was used at a constant flow rate of 1.4 mL/min. Carrier gas was helium 99.999% from Air Liquide (Düsseldorf, Germany). The inlet temperature was kept at 300 °C and injection volume was 1 μL with splitless time 1.0 min. The initial column temperature was 50 °C and was held for 1.0 min. Then temperature was ramped up to 250 °C with 50 °C/min. Then the sterols were eluted at a rate of 5 °C/min until 310 °C (hold time 3 min). Total run time was 20 min. Transfer line temperature was 300 °C and the ion trap temperature was 150 °C. The ion trap was operated with electron ionization (EI) at 70 eV in scan mode (m/z 50–650) with a solvent delay of 6.3 min.

5.3. Methods

A stock solution containing androsterone sulfate (**1**), dehydroepiandrosterone sulfate (**2**), epiandrosterone sulfate (**3**), allopregnanolone sulfate (**4**), pregnanolone sulfate (**5**), pregnenolone sulfate (**6**), cholesterol sulfate (**7**), 25-hydroxycholesterol sulfate (**8**), and cholestane (**9**) as internal standard (IS) with a concentration of 10 μM of each analyte in ethyl acetate was prepared. Substance structures are shown in Figure 1.

5.3.1. TMS Derivatives by Direct Silylation

Pregnenolone (2 μg) and cholestane (1 μg , IS) was silylated with 50 μL of a mixture of MSTFA and TSIM (9:1) at room temperature for 30 min. After the addition of 950 μL methyl *tert*-butyl ether (*MtBE*) the sample was analyzed as described above by GC-MS.

5.3.2. Acidic Deconjugation and Formation of MO-TMS Derivatives

An aliquot of the stock solution containing 10 nmol of each sterol sulfate and IS was transferred into an autosampler vial and the solvent (ethyl acetate) was evaporated under a stream of nitrogen. Deconjugation was performed in 1,4-dioxane with 1% acetic acid (*v/v*) for 3 h (see Section 5.3.5.1). Subsequently, the sample was evaporated to dryness under a stream of nitrogen. The dry residue was derivatized with 100 μL 2% *O*-methylhydroxylamine

3. Sterol sulfate analysis

hydrochloride in pyridine (*m/v*) at 80 °C for 30 min. This reaction time is sufficient for a complete derivatization of the keto groups. Then the sample was diluted with 400 µL water and the sterols were extracted with 2 × 1000 µL *MtBE*. The combined organic phases were transferred into a new autosampler vial and evaporated to dryness under a stream of nitrogen. Then the residue was silylated with 50 µL of a mixture of MSTFA and TSIM (9:1) at room temperature for 30 min. After addition of 950 µL *MtBE* the sample was analyzed by GC-MS.

5.3.3. TFA Derivatives by Direct Deconjugation/Derivatization

An aliquot of the stock solution containing 10 nmol of each sterol sulfate and IS was transferred into an autosampler vial (*n* = 6) and evaporated to dryness under a stream of nitrogen. Fifty microliters of trifluoroacetic anhydride (TFAA) was added to the residue. The vial was closed and stored at 70 °C for 30 min, then the volatiles were evaporated under a stream of nitrogen. The residue was dissolved in 1000 µL *MtBE* and analyzed by GC-MS.

5.3.4. Enzymatic Cleavage of Sulfates and Derivatization

An aliquot of the stock solution containing 10 nmol of each sterol sulfate and IS was transferred into an autosampler vial (*n* = 6) and was evaporated to dryness under a stream of nitrogen. The residue was diluted in 0.5 mL water and 0.5 mL buffer containing β-glucuronidase/sulfatase from *Helix pomatia* type HP-2 was added [50]. The closed vial was stored at 37 °C for 20 h. Then the sample was extracted with 2 × 1000 µL *MtBE*. The combined organic phases were transferred into a new autosampler vial and evaporated to dryness under a stream of nitrogen. The residue was silylated with 50 µL of a mixture of MSTFA and TSIM (9:1) at room temperature for 30 min. After addition of 950 µL *MtBE* the sample was analyzed by GC-MS. The acquired peak area for each sterol was compared to the area obtained by solvolysis (see Section 5.3.5.1) followed by TMS derivatization. The obtained data are listed in Table 1.

5.3.5. Chemical Cleavage of Sulfates and Derivatization

5.3.5.1. With Acidic Deconjugation (Solvolysis)

An aliquot of the stock solution containing 10 nmol of each sterol sulfate and IS was transferred into an autosampler vial (*n* = 6) and the solvent (ethyl acetate) was evaporated under a stream of nitrogen. For solvolysis 500 µL of 1,4-dioxane with 1% acetic acid (*v/v*) was added and the vial was closed tightly. The mixture was stored at 100 °C for different periods of time (0.5–6 h, Figure 6 and Supplementary Table S2). Then the sample was evaporated to dryness under a stream of nitrogen. The residue was derivatized with 100 µL 2% *O*-methylhydroxylamine hydrochloride in pyridine (*m/v*) at 80 °C for 30 min. Then the sample was diluted with 400 µL water and the sterols were extracted with 2 × 1000 µL *MtBE*. The combined organic phases were transferred into a new autosampler vial and evaporated to dryness under a stream of nitrogen. Then the residue was silylated with 50 µL of a mixture of MSTFA and TSIM (9:1) at room temperature for 30 min. After addition of 950 µL *MtBE* the sample was analyzed by GC-MS.

3. Sterol sulfate analysis

5.3.5.2. With Deconjugation/Methoximation with *O*-Methylhydroxylamine

An aliquot of the stock solution containing 10 nmol of each sterol sulfate and IS was transferred into an autosampler vial ($n = 6$) and the solvent (ethyl acetate) was evaporated under a stream of nitrogen. Simultaneous deconjugation/MO derivatization was achieved by addition of 100 μL 2% *O*-methylhydroxylamine hydrochloride in pyridine (m/v) directly to the neat sterol sulfates ($n = 6$). The vial was stored at 80 °C for different periods of time (0.5–6 h, Figure 6 and Supplementary Table S2). Then the sample was diluted with 400 μL water and the sterols were extracted with $2 \times 1000 \mu\text{L}$ *Mt*BE. The combined organic phases were transferred into a new autosampler vial and evaporated to dryness under a stream of nitrogen. Then the residue was silylated with 50 μL of a mixture of MSTFA and TSIM (9:1) at room temperature for 30 min. After addition of 950 μL *Mt*BE the sample was analyzed by GC-MS.

Supplementary Materials: Table S1: Gas chromatography-mass spectrometry data for the eight model sterol sulfates. Table S2: Determination of sterol sulfates as MO-TMS derivatives with and without solvolysis.

Author Contributions: Conceptualization, J.J., F.K., H.S., and F.B.; Methodology, J.J. and I.C.; Formal Analysis, J.J., I.C., M.G., C.M., and F.B.; Investigation, J.J., I.C., M.G., C.M., and F.B.; Resources, F.K., H.S., and F.B.; Data Curation, J.J., M.G., C.M., and F.B.; Writing—Original Draft Preparation, J.J. and C.M.; Writing—Review and Editing, J.J., F.K., H.S., M.G., C.M., and F.B.; Visualization, J.J. and C.M.; Supervision, H.S., M.G., and F.B.; Funding Acquisition, F.K. and H.S.

Funding: This work was supported by the Deutsche Forschungsgemeinschaft (DFG) grant STE 847/6–1 (H.S.) and the VERUM Stiftung für Verhalten und Umwelt (F.K.).

Conflicts of Interest: The authors declare no conflict of interest.

References

1. Falany, C.N. Enzymology of human cytosolic sulfotransferases. *FASEB J.* **1997**, *11*, 206–216. [[CrossRef](#)] [[PubMed](#)]
2. Geyer, J.; Bakhaus, K.; Bernhardt, R.; Blaschka, C.; Dezhkam, Y.; Fietz, D.; Grosser, G.; Hartmann, K.; Hartmann, M.F.; Neunzig, J.; et al. The role of sulfated steroid hormones in reproductive processes. *J. Steroid Biochem. Mol. Biol.* **2017**, *172*, 207–221. [[CrossRef](#)] [[PubMed](#)]
3. Harteneck, C. Pregnenolone sulfate: From steroid metabolite to TRP channel ligand. *Molecules* **2013**, *18*, 12012–12028. [[CrossRef](#)] [[PubMed](#)]
4. Smith, C.C.; Gibbs, T.T.; Farb, D.H. Pregnenolone sulfate as a modulator of synaptic plasticity. *Psychopharmacology (Berl.)* **2014**, *231*, 3537–3556. [[CrossRef](#)] [[PubMed](#)]
5. Schumacher, M.; Liere, P.; Akwa, Y.; Rajkowski, K.; Griffiths, W.; Bodin, K.; Sjövall, J.; Baulieu, E.E. Pregnenolone sulfate in the brain: A controversial neurosteroid. *Neurochem. Int.* **2008**, *52*, 522–540. [[CrossRef](#)]
6. Fietz, D. Transporter for sulfated steroid hormones in the testis—Expression pattern, biological significance and implications for fertility in men and rodents. *J. Steroid Biochem. Mol. Biol.* **2018**, *179*, 8–19. [[CrossRef](#)]
7. Strott, C.A.; Higashi, Y. Cholesterol sulfate in human physiology: What's it all about? *J. Lipid Res.* **2003**, *44*, 1268–1278. [[CrossRef](#)]
8. Iwamori, M.; Iwamori, Y.; Ito, N. Regulation of the activities of thrombin and plasmin by cholesterol sulfate as a physiological inhibitor in human plasma. *J. Biochem.* **1999**, *125*, 594–601. [[CrossRef](#)]
9. Mueller, J.W.; Gilligan, L.C.; Idkowiak, J.; Arlt, W.; Foster, P.A. The regulation of steroid action by sulfation and desulfation. *Endocr. Rev.* **2015**, *36*, 526–563. [[CrossRef](#)]
10. Luchetti, S.; Huitinga, I.; Swaab, D.F. Neurosteroid and GABA-A receptor alterations in Alzheimer's disease, Parkinson's disease and multiple sclerosis. *Neuroscience* **2011**, *191*, 6–21. [[CrossRef](#)]

3. Sterol sulfate analysis

11. Vaňková, M.; Hill, M.; Velíková, M.; Včelák, J.; Vacínová, G.; Dvořáková, K.; Lukášová, P.; Rusina, R.; Holmerová, I.; Jarolímová, E.; et al. Preliminary evidence of altered steroidogenesis in women with Alzheimer's disease: Have the patients "OLDER" adrenal zona reticularis? *J. Steroid Biochem. Mol. Biol.* **2016**, *158*, 157–177. [[CrossRef](#)]
12. Vančková, M.; Hill, M.; Velíková, M.; Včelák, J.; Vacínová, G.; Lukášová, P.; Vejražková, D.; Dvořáková, K.; Rusina, R.; Holmerová, I.; et al. Reduced sulfotransferase SULT2A1 activity in patients with Alzheimer's disease. *Physiol. Res.* **2015**, *64* (Suppl. 2), S265–S273.
13. Wudy, S.A.; Schuler, G.; Sánchez-Guijo, A.; Hartmann, M.F. The art of measuring steroids: Principles and practice of current hormonal steroid analysis. *J. Steroid Biochem. Mol. Biol.* **2018**, *179*, 88–103. [[CrossRef](#)] [[PubMed](#)]
14. Shackleton, C. Clinical steroid mass spectrometry: A 45-year history culminating in HPLC–MS/MS becoming an essential tool for patient diagnosis. *J. Steroid Biochem. Mol. Biol.* **2010**, *121*, 481–490. [[CrossRef](#)]
15. Griffiths, W.J.; Abdel-Khalik, J.; Yutuc, E.; Morgan, A.H.; Gilmore, I.; Hearn, T.; Wang, Y. Cholesterolomics: An update. *Anal. Biochem.* **2017**, *524*, 56–67. [[CrossRef](#)] [[PubMed](#)]
16. Krone, N.; Hughes, B.A.; Lavery, G.G.; Stewart, P.M.; Arlt, W.; Shackleton, C.H. Gas chromatography/mass spectrometry (GC/MS) remains a pre-eminent discovery tool in clinical steroid investigations even in the era of fast liquid chromatography tandem mass spectrometry (LC/MS/MS). *J. Steroid Biochem. Mol. Biol.* **2010**, *121*, 496–504. [[CrossRef](#)]
17. Liere, P.; Schumacher, M. Mass spectrometric analysis of steroids: All that glitters is not gold. *Expert Rev. Endocrinol. Metab.* **2015**, *10*, 463–465.
18. Giera, M.; Plössl, F.; Bracher, F. Fast and easy in vitro screening assay for cholesterol biosynthesis inhibitors in the post-squalene pathway. *Steroids* **2007**, *72*, 633–642. [[CrossRef](#)] [[PubMed](#)]
19. Velikanova, L.I.; Strel'nikova, E.G.; Obedkova, E.V.; Krivokhizhina, N.S.; Shafigullina, Z.R.; Grigoryan, K.; Povarov, V.G.; Moskvina, A.L. Generation of urinary steroid profiles in patients with adrenal incidentaloma using gas chromatography–mass spectrometry. *J. Anal. Chem.* **2016**, *71*, 748–754. [[CrossRef](#)]
20. Marcos, J.; Pozo, O.J. Derivatization of steroids in biological samples for GC–MS and LC–MS analyses. *Bioanalysis* **2015**, *7*, 2515–2536. [[CrossRef](#)] [[PubMed](#)]
21. Wang, Y.; Griffiths, W.J. Chapter 3 steroids, sterols and the nervous system. In *Metabolomics, Metabonomics and Metabolite Profiling*, 1st ed.; Griffiths, W.J., Ed.; The Royal Society of Chemistry: Cambridge, UK, 2008; Volume 1, pp. 71–115.
22. Christakoudi, S.; Cowan, D.A.; Taylor, N.F. Steroids excreted in urine by neonates with 21-hydroxylase deficiency. 3. Characterization, using GC–MS and GC–MS/MS, of androstanes and androstenes. *Steroids* **2012**, *77*, 1487–1501. [[CrossRef](#)] [[PubMed](#)]
23. Gomez, C.; Fabregat, A.; Pozo, Ó.J.; Marcos, J.; Segura, J.; Ventura, R. Analytical strategies based on mass spectrometric techniques for the study of steroid metabolism. *Trends Anal. Chem.* **2014**, *53*, 106–116. [[CrossRef](#)]
24. Gomes, R.L.; Meredith, W.; Snape, C.E.; Sephton, M.A. Analysis of conjugated steroid androgens: Deconjugation, derivatisation and associated issues. *J. Pharm. Biomed. Anal.* **2009**, *49*, 1133–1140. [[CrossRef](#)] [[PubMed](#)]
25. Choi, M.H.; Chung, B.C. Bringing GC–MS profiling of steroids into clinical applications. *Mass Spectrom. Rev.* **2015**, *34*, 219–236. [[CrossRef](#)] [[PubMed](#)]
26. Giera, M.; Müller, C.; Bracher, F. Analysis and experimental inhibition of distal cholesterol biosynthesis. *Chromatographia* **2015**, *78*, 343–358. [[CrossRef](#)]
27. Matysik, S.; Schmitz, G. Determination of steroid hormones in human plasma by GC–triple quadrupole MS. *Steroids* **2015**, *99*, 151–154. [[CrossRef](#)]
28. Christakoudi, S.; Cowan, D.A.; Taylor, N.F. Sodium ascorbate improves yield of urinary steroids during hydrolysis with *Helix pomatia* juice. *Steroids* **2008**, *73*, 309–319. [[CrossRef](#)]

3. Sterol sulfate analysis

29. Ebner, M.J.; Corol, D.I.; Havlíková, H.; Honour, J.W.; Fry, J.P. Identification of neuroactive steroids and their precursors and metabolites in adult male rat brain. *Endocrinology* **2006**, *147*, 179–190. [[CrossRef](#)]
30. Dehennin, L.; Lafarge, P.; Dailly, P.; Bailloux, D.; Lafarge, J.P. Combined profile of androgen glucuroand sulfoconjugates in post-competition urine of sportsmen: A simple screening procedure using gas chromatography-mass spectrometry. *J. Chromatogr. B* **1996**, *687*, 85–91. [[CrossRef](#)]
31. Müller, C.; Binder, U.; Bracher, F.; Giera, M. Antifungal drug testing by combining minimal inhibitory concentration testing with target identification by gas chromatography-mass spectrometry. *Nat. Protoc.* **2017**, *12*, 947–963. [[CrossRef](#)]
32. Little, J.L. Artifacts in trimethylsilyl derivatization reactions and ways to avoid them. *J. Chromatogr. A* **1999**, *844*, 1–22. [[CrossRef](#)]
33. Teubel, J.; Wüst, B.; Schipke, C.G.; Peters, O.; Parr, M.K. Methods in endogenous steroid profiling—A comparison of gas chromatography mass spectrometry (GC-MS) with supercritical fluid chromatography tandem mass spectrometry (SFC-MS/MS). *J. Chromatogr. A* **2018**, *1554*, 101–116. [[CrossRef](#)] [[PubMed](#)]
34. Poole, C.F. Alkylsilyl derivatives for gas chromatography. *J. Chromatogr. A* **2013**, *1296*, 2–14. [[CrossRef](#)] [[PubMed](#)]
35. van de Kerkhof, D.H.; van Ooijen, R.D.; de Boer, D.; Fokkens, R.H.; Nibbering, N.M.; Zwicker, J.W.; Thijssen, J.H.; Maes, R.A. Artifact formation due to ethyl thio-incorporation into silylated steroid structures as determined in doping analysis. *J. Chromatogr. A* **2002**, *954*, 199–206. [[CrossRef](#)]
36. Hadeif, Y.; Kaloustian, J.; Portugal, H.; Nicolay, A. Multivariate optimization of a derivatisation procedure for the simultaneous determination of nine anabolic steroids by gas chromatography coupled with mass spectrometry. *J. Chromatogr. A* **2008**, *1190*, 278–285. [[CrossRef](#)] [[PubMed](#)]
37. Fang, K.; Pan, X.; Huang, B.; Liu, J.; Wang, Y.; Gao, J. Simultaneous derivatization of hydroxyl and ketone groups for the analysis of steroid hormones by GC-MS. *Chromatographia* **2010**, *72*, 949–956. [[CrossRef](#)]
38. Meunier-Solère, V.; Maume, D.; André, F.; Le Bizec, B. Pitfalls in trimethylsilylation of anabolic steroids. New derivatisation approach for residue at ultra-trace level. *J. Chromatogr. B* **2005**, *816*, 281–288. [[CrossRef](#)]
39. Shackleton, C.H.L. Profiling steroid hormones and urinary steroids. *J. Chromatogr. B Biomed. Sci. Appl.* **1986**, *379*, 91–156. [[CrossRef](#)]
40. Halket, J.M.; Waterman, D.; Przyborowska, A.M.; Patel, R.K.P.; Fraser, P.D.; Bramley, P.M. Chemical derivatization and mass spectral libraries in metabolic profiling by GC/MS and LC/MS/MS. *J. Exp. Bot.* **2005**, *56*, 219–243. [[CrossRef](#)]
41. Nicholson, J.D. Derivative formation in the quantitative gas-chromatographic analysis of pharmaceuticals. Part II. A review. *The Analyst* **1978**, *103*, 193–222. [[CrossRef](#)]
42. Goad, L.J.; Akihisa, T. Mass spectrometry of sterols. In *Analysis of Sterols*; Springer: Dordrecht, The Netherlands, 1997; pp. 152–196.
43. Touchstone, J.C.; Dobbins, M.F. Direct determination of steroidal sulfates. *J. Steroid Biochem.* **1975**, *6*, 1389–1392. [[CrossRef](#)]
44. Liere, P.; Pianos, A.; Eychenne, B.; Cambourg, A.; Liu, S.; Griffiths, W.; Schumacher, M.; Sjövall, J.; Baulieu, E.-E. Novel lipoidal derivatives of pregnenolone and dehydroepiandrosterone and absence of their sulfated counterparts in rodent brain. *J. Lipid Res.* **2004**, *45*, 2287–2302. [[CrossRef](#)] [[PubMed](#)]
45. Murray, S.; Baillie, T.A. Direct derivatization of sulphate esters for analysis by gas chromatography mass spectrometry. *Biol. Mass Spectrom.* **1979**, *6*, 82–89. [[CrossRef](#)]
46. Galli, G.; Maroni, S. Mass spectrometric investigations of some unsaturated sterols biosynthetically related to cholesterol. *Steroids* **1967**, *10*, 189–197. [[CrossRef](#)]
47. Knights, B.A. Identification of plant sterols using combined GLC/mass spectrometry. *J. Chromatogr. Sci.* **1967**, *5*, 273–282. [[CrossRef](#)]

3. Sterol sulfate analysis

48. Ferchaud, V.; Courcoux, P.; Le Bizec, B.; Monteau, F.; André, F. Enzymatic hydrolysis of conjugated steroid metabolites: Search for optimum conditions using response surface methodology. *The Analyst* **2000**, *125*, 2255–2259. [[CrossRef](#)] [[PubMed](#)]
49. Cawley, L.P.; Faucette, W.; Musser, B.O.; Beckloff, S. Steric hindrance of the sulfatase of *Helix pomatia* on some 17-ketosteroid sulfate conjugates. *Am. J. Clin. Pathol.* **1969**, *52*, 652–655. [[CrossRef](#)]
50. Xu, X.; Keefer, L.K.; Ziegler, R.G.; Veenstra, T.D. A liquid chromatography–mass spectrometry method for the quantitative analysis of urinary endogenous estrogen metabolites. *Nat. Protoc.* **2007**, *2*, 1350–1355. [[CrossRef](#)]
51. Venturelli, E.; Cavalleri, A.; Secreto, G. Methods for urinary testosterone analysis. *J. Chromatogr. B* **1995**, *671*, 363–380. [[CrossRef](#)]
52. Robards, K.; Towers, P. Chromatography as a reference technique for the determination of clinically important steroids. *Biomed. Chromatogr.* **1990**, *4*, 1–19. [[CrossRef](#)] [[PubMed](#)]
53. Muehlbaeher, C.A.; Smith, E.K. Three hydrolysis methods for 17-ketosteroid sulfates compared by colorimetric and gas–liquid chromatographic analyses. *Clin. Chem.* **1970**, *16*, 158–160. [[PubMed](#)]
54. Burstein, S.; Lieberman, S. Hydrolysis of ketosteroid hydrogen sulfates by solvolysis procedures. *J. Biol. Chem.* **1958**, *233*, 331–335. [[PubMed](#)]
55. Burstein, S.; Lieberman, S. Kinetics and mechanism of solvolysis of steroid hydrogen sulfates. *J. Am. Chem. Soc.* **1958**, *80*, 5235–5239. [[CrossRef](#)]
56. Cohen, S.L.; Oneson, I.B. The conjugated steroids. IV. The hydrolysis of ketosteroid sulfates. *J. Biol. Chem.* **1953**, *204*, 245–256. [[PubMed](#)]
57. Hutchins, R.F.N.; Kaplanis, J.N. Sterol sulfates in an insect. *Steroids* **1969**, *13*, 605–614. [[CrossRef](#)]
58. Benkovic, S.J.; Benkovic, P.A. Studies on sulfate Esters. I. Nucleophilic reactions of amines with p-nitrophenyl sulfate. *J. Am. Chem. Soc.* **1966**, *88*, 5504–5511. [[CrossRef](#)]
59. Kirby, A. Reactions of alpha-nucleophiles with a model phosphate diester. *Arkivoc* **2008**, *2009*, 28–38.
60. Wolfenden, R.; Yuan, Y. Monoalkyl sulfates as alkylating agents in water, alkylsulfatase rate enhancements, and the “energy-rich” nature of sulfate half-esters. *PNAS* **2007**, *104*, 83–86. [[CrossRef](#)]
61. Fina, N.J.; Edwards, J.O. The alpha effect. A review. *Int. J. Chem. Kinet.* **1973**, *5*, 1–26. [[CrossRef](#)]

Sample Availability: Samples of the compounds are not available from the authors.



© 2019 by the authors. Licensee MDPI, Basel, Switzerland. This article is an open access article distributed under the terms and conditions of the Creative Commons Attribution (CC BY) license (<http://creativecommons.org/licenses/by/4.0/>).

3. Sterol sulfate analysis

3.4. Supplementary material

Table S1. Gas chromatography-mass spectrometry (GC-MS) data for the derivatives obtained from the eight model sterol sulfates **1 – 8** using different deconjugation/derivatization protocols; chemical formulae of the sterol sulfates; TFA: trifluoroacetyl ester; TMS: trimethylsilyl ether; MO-TMS: methyloxime-trimethylsilyl ether; relative retention times (RRT) related to internal standard cholestane (**9**); bold *m/z* value: base peak; * predominantly ($2 \times$ TFA); ^a analyzed as TMS ether (since no keto group present for MO formation); ^b no derivatization possible.

No.	Compound	Chemical formula	Relative Retention Time (RRT)			Characteristic ions [<i>m/z</i>]		
			TFA	TMS	MO-TMS	TFA	TMS	MO-TMS
1	Androsterone sulfate	C ₁₉ H ₃₀ O ₅ S	0.701	0.759	0.796	386	347	391
						368	272	360
						342	215	270
2	Dehydroepiandrosterone sulfate	C ₁₉ H ₂₈ O ₅ S	0.728	0.804	0.846	270	360	389
						255	270	358
						121	129	268
3	Epiandrosterone sulfate	C ₁₉ H ₃₀ O ₅ S	0.732	0.813	0.855	386	347	391
						368	272	360
						342	215	270
4	Allopregnanolone sulfate	C ₂₁ H ₃₄ O ₅ S	0.790	0.873	0.929	396*	300	404
						267	285	388
						215	215	100
5	Pregnanolone sulfate	C ₂₁ H ₃₄ O ₅ S	0.790	0.882	0.934	396*	375	404
						267	300	388
						215	285	298
6	Pregnenolone sulfate	C ₂₁ H ₃₂ O ₅ S	0.827	0.926	0.992	298	388	402
						283	298	386
						213	129	312
7	Cholesterol sulfate	C ₂₇ H ₄₆ O ₄ S	1.106	1.257	1.257	368	458	458 ^a
						353	368	368
						255	329	329
8	25-Hydroxycholesterol sulfate	C ₂₇ H ₄₆ O ₅ S	1.134	1.516	1.516	366	456	456 ^a
						351	271	271
						245	131	131
9	Cholestane (IS)	C ₂₇ H ₄₈	1.000	1.000	1.000	357 ^b	357 ^b	357 ^b
						262	262	262
						217	217	217

3. Sterol sulfate analysis

Table S2. Determination of (keto-)sterol sulfates **1 - 8** as (MO-)TMS derivatives with and without previous sulfate solvolysis step (with 1% acetic acid in 1,4-dioxane). The indicated time refers to the duration of solvolysis prior to derivatization (MO-TMS) (upper row "Solv. + Deriv.") or to the duration of the simultaneous deconjugation/MO derivatization (lower row "Deconjug./MO"). The results obtained for each individual sterol sulfate under the different conditions are shown as relative peak areas [%] \pm standard deviation (n = 6); optimum conditions for all tested sterol sulfates are shown in the last two rows **Ø 1 - 8**; in bold: the best conditions for each sterol sulfate; in red: optimum method for all tested sterol sulfates. The maximum recorded peak area for each sterol derivative within this experiment was set as 100% (Note: The values presented here are *not* recoveries). Analyzed sterols: **1** androsterone sulfate, **2** dehydroepiandrosterone sulfate, **3** epiandrosterone sulfate, **4** allopregnanolone sulfate, **5** pregnanolone sulfate, **6** pregnenolone sulfate, **7** cholesterol sulfate, **8** 25-hydroxycholesterol sulfate.

Sterol sulfate	Method	Incubation time						
		0.5 h	1 h	2 h	3 h	4 h	5 h	6 h
1	Solv. + Deriv.	34 \pm 4	47 \pm 19	39 \pm 9	89 \pm 27	100 \pm 14	90 \pm 5	60 \pm 9
	Deconjug./MO	0 \pm 0	8 \pm 1	17 \pm 2	88 \pm 45	92 \pm 31	41 \pm 4	44 \pm 3
2	Solv. + Deriv.	24 \pm 4	31 \pm 12	23 \pm 4	51 \pm 18	60 \pm 4	32 \pm 5	34 \pm 5
	Deconjug./MO	3 \pm 1	12 \pm 1	24 \pm 5	100 \pm 48	92 \pm 23	38 \pm 4	35 \pm 2
3	Solv. + Deriv.	44 \pm 4	68 \pm 17	71 \pm 12	98 \pm 5	94 \pm 5	100 \pm 3	92 \pm 2
	Deconjug./MO	8 \pm 2	31 \pm 2	56 \pm 2	82 \pm 5	87 \pm 5	84 \pm 5	86 \pm 3
4	Solv. + Deriv.	46 \pm 4	69 \pm 15	68 \pm 13	100 \pm 5	97 \pm 6	98 \pm 5	90 \pm 7
	Deconjug./MO	3 \pm 1	12 \pm 1	27 \pm 2	52 \pm 8	61 \pm 6	60 \pm 4	64 \pm 2
5	Solv. + Deriv.	53 \pm 5	73 \pm 16	79 \pm 13	99 \pm 4	98 \pm 5	100 \pm 5	96 \pm 2
	Deconjug./MO	14 \pm 2	36 \pm 2	57 \pm 4	81 \pm 6	90 \pm 7	86 \pm 6	88 \pm 4
6	Solv. + Deriv.	58 \pm 4	79 \pm 15	74 \pm 10	100 \pm 4	96 \pm 5	98 \pm 4	93 \pm 3
	Deconjug./MO	13 \pm 2	38 \pm 3	62 \pm 6	92 \pm 5	100 \pm 9	93 \pm 5	95 \pm 2
7	Solv. + Deriv.	71 \pm 6	88 \pm 9	94 \pm 21	99 \pm 4	92 \pm 4	97 \pm 2	100 \pm 11
	Deconjug./MO	16 \pm 1	33 \pm 5	58 \pm 3	82 \pm 15	83 \pm 5	90 \pm 6	92 \pm 4
8	Solv. + Deriv.	48 \pm 6	66 \pm 14	75 \pm 8	100 \pm 4	92 \pm 4	96 \pm 6	92 \pm 3
	Deconjug./MO	7 \pm 1	23 \pm 4	46 \pm 4	87 \pm 6	99 \pm 9	85 \pm 8	91 \pm 4
Ø 1 - 8	Solv. + Deriv.	47 \pm 4	65 \pm 15	65 \pm 11	92 \pm 9	91 \pm 6	85 \pm 4	82 \pm 5
	Deconjug./MO	8 \pm 1	24 \pm 2	43 \pm 3	83 \pm 17	88 \pm 12	72 \pm 5	74 \pm 3

4. Analysis of neutral steroids, steroid acids and sterol sulfates

The article “Effective sample preparation procedure for the analysis of neutral steroids, steroid acids and sterol sulfates in different tissues by GC-MS” was submitted to the Journal of Steroid Biochemistry and Molecular Biology.

A revised version of the manuscript has been submitted to the editor. This manuscript is presented here.

4.1. Summary

The γ -secretase research of the group of Prof. Dr. Steiner does not only focus on neurosteroids and sterol sulfates, but this group is also interested in oxysterols and steroid acids. These analytes were reported by others to affect the γ -secretase [29, 76-78], and the aim of this work was to develop an analytical method for the analysis of these compounds. Also, cholesterol precursors, like desmosterol were reported to play a role in AD [56, 57] and their level is presumably altered in mouse models like the frequently used NPC knockout mice. Hence, an inclusion of this steroid class to the new method was desired and straightforward, as we already had much experience in the analysis of cholesterol precursors from earlier work (Chapter 4). In the end, the method was validated for nine cholesterol precursors, five oxysterols, nine neurosteroids, seven sterol sulfates and seven steroid acids. These analytes were measured using GC-MS/MS (tandem MS) in dMRM mode with high sensitivity and additionally using GC/MS in scan mode in an untargeted approach. With this untargeted screening method further steroids could be identified (*e.g.* phytosterols). Hence, this method enabled the analysis of unexpected occurring steroids as well as the analysis of steroids occurring at trace levels. So, this method provides a broader overview on the sterolome as other published methods and could therefore help to get a better understanding of sterol associated diseases like AD. To accomplish analysis of this wide spectrum of analytes an effective sample preparation procedure was developed. As shown in Figure 9 it consists of the lipid extraction from the tissue, the steroid group separation and subsequent GC-MS(/MS) analysis of each group.

4. Analysis of neutral steroids, steroid acids and sterol sulfates

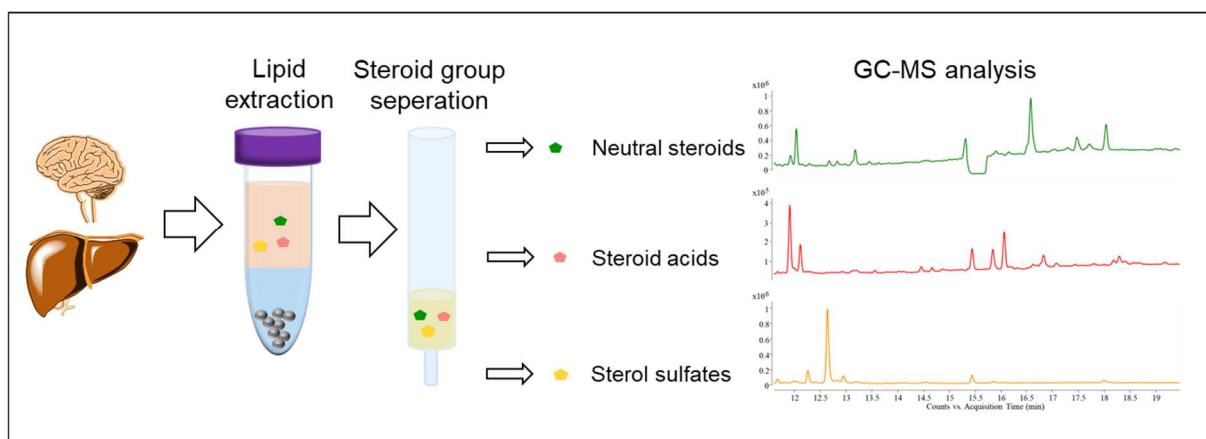


Figure 9 Graphical abstract of the article showing the lipid extraction from liver and brain tissue and the principle of steroid group separation on the SPE cartridge with subsequent GC-MS analysis.

First the samples (brain/liver tissue or cultured cells) were homogenized using a bead mill and subjected to liquid-liquid extraction using an optimized solvent mixture. The organic phase containing the analytes of interest was then further processed on a solid phase extraction (SPE) cartridge containing a weak anion exchange sorbent. This enabled the separation of neutral steroids (neurosteroids, oxysterols and cholesterol precursors) from steroid acids and steroid sulfates using specific eluents. These steroid groups could then be derivatized and measured separately. This method was validated for liver and brain tissue and was applied on different samples (mice 10 months /three weeks old, cultured cells). Overall, 45 steroids were identified and the endogenous concentrations higher than the limit of quantification ($> \text{LOQ}$) were reported.

4.2. Personal contribution

My contribution to this work were the conceptualization, investigation and method development. The latter included optimization of lipid extraction and SPE, concerning the choice of solvents, sorbents and eluents. Also, the implementation of the GC-MS procedure especially optimization of mass transitions and collision energies for dMRM mode was part of the method development. Method validation and application on biological samples were also part of my contribution. This included the planning and execution of necessary experiments as well as the formal analysis and curation of the measurement data. In addition, the visualization of the obtained results as well as writing of the original draft were done by me.

Prof. Dr. Harald Steiner and Dr. Frits Kamp supported this project by providing resources like analytical standards and biological samples. They also designated the steroids of special interest for this project. Additionally, they contributed by acquisition of funding.

4. Analysis of neutral steroids, steroid acids and sterol sulfates

Further biological samples were provided by Edith Winkler, who also performed preliminary experiments to determine steroids of interest for this project.

Prof. Dr. Franz Bracher contributed to this project by providing the necessary resources and acquisition of funding. He was also involved in reviewing and editing of the original draft.

Dr. Christoph Müller was involved in the conceptualization of the project and supported the determination of the final experimental design and methodology. He further contributed in the formal analysis of the obtained data and especially in reviewing and editing of the original draft.

4.3. Article

The following article was submitted to the Journal of Steroid Biochemistry and Molecular Biology. It is printed in the original wording of the revised manuscript, that was submitted to the editor in February 2021.

Effective sample preparation procedure for the analysis of neutral steroids, steroid acids and sterol sulfates in different tissues by GC-MS

Julia Junker¹, Frits Kamp², Edith Winkler², Harald Steiner^{2,3} Franz Bracher¹ and Christoph Müller^{1,*}

¹ Department of Pharmacy-Center for Drug Research, Ludwig-Maximilians University-Munich, Butenandtstraße 5-13, 81377 Munich, Germany

² Biomedical Center (BMC), Metabolic Biochemistry, Ludwig-Maximilians University-Munich, Feodor-Lynen-Straße 17, 81377 Munich, Germany

³ German Center for Neurodegenerative Diseases (DZNE), Feodor-Lynen-Straße 17, 81377 Munich, Germany

* Correspondence: christoph.mueller@cup.uni-muenchen.de; Tel.: +49-89-2180-7250

Abstract

Steroids play an important role in cell regulation and homeostasis. Many diseases like Alzheimer's disease or Smith-Lemli-Opitz syndrome are known to be associated with deviations in the steroid profile. Most published methods only allow the analysis of small subgroups of steroids and cannot give an overview of the total steroid profile. We developed and validated a method that allows the analysis of neutral steroids, including intermediates of cholesterol biosynthesis, oxysterols, C₁₉ and C₂₁ steroids, steroid acids, including bile acids, and sterol sulfates using gas chromatography-mass spectrometry. Samples were analyzed in scan mode for screening purposes and in dynamic multiple reaction monitoring mode for highly sensitive quantitative analysis. The method was validated for mouse brain and liver tissue and consists of sample homogenization, lipid extraction, steroid group separation, deconjugation, derivatization and gas chromatography-mass spectrometry analysis. We applied the method on brain and liver samples of mice (10 months and 3 weeks old) and cultured N2a cells and report the endogenous concentrations of 29 physiological steroids.

Keywords

Screening method, bile acids, group separation, steroid profiling, deconjugation, gas chromatography-mass spectrometry

1. Introduction

Steroids are a very large and versatile class of biomolecules. Versatile by means of structure, occurrence and by means of biological activity. They act as important cell-building material and as signaling molecules on different intracellular and membrane-bound receptors. The set of all steroids of a cell or organism is called steroidome and its qualitative and quantitative analysis is known by the term steroidomics [1]. In the last decades, steroidomics were used to investigate changes of the steroidome in the context of different diseases like congenital adrenal hyperplasia (CAH) [2-5], cerebrotendinous xanthomatosis (CTX) [6], Alzheimer's disease (AD) [7-9], Smith-Lemli-Opitz syndrome (SLOS) [10] and more [11, 12]. A change in steroid metabolism leads to an accumulation or reduction of certain steroids and this change in the steroid pattern can affect the whole organism in various ways. A change of the sterol composition in cell membranes, for example, can alter membrane structure and thickness [13, 14], in turn this can modulate the activity of membrane-bound enzymes like γ -secretase [15], an enzyme involved in AD. Oxysterols like 27-hydroxycholesterol (**23**, Table 2) can take effect *via* nuclear receptors like liver X receptor (LXR) and therefore interfere with cellular lipid homeostasis [16, 17]. Some oxysterols also reveal immunomodulatory actions, like the Epstein-Barr virus-induced G-protein

4. Analysis of neutral steroids, steroid acids and sterol sulfates

coupled receptor 2 (EBI2) ligand $7\alpha,25$ -dihydroxycholesterol (**25**) [18, 19] and other oxysterols, which are involved in neuroinflammation in AD patients [7]. A further important steroid class are neurosteroids, like pregnenolone (**26**), dehydroepiandrosterone (**31**), allopregnanolone (**38**) and their respective sulfates, which are synthesized and/or take action in the central and peripheral nervous system [20-23]. Their biological targets are neurotransmitter receptors like γ -aminobutyric acid type A (GABA_A) and *N*-methyl-D-aspartate (NMDA) receptors in brain, and they effect cognitive performance [20, 24, 25]. In addition, they have all been investigated in context of AD [8, 9, 26-28]. These neurosteroids further interfere with cholesterol biosynthesis, for example pregnenolone (**26**), 17α -hydroxypregnenolone (**28**) and progesterone (**29**) are supposed to be inhibitors of 24-dehydrocholesterol reductase (DHCR24) and lead to an accumulation of desmosterol (**13**) [29]. Desmosterol (**13**), other cholesterol precursors [30-32] and also cholesterol (**10**) [33, 34] itself are known to play a role in AD pathogenesis. Also, the class of steroid acids do not only play an important role in cholesterol homeostasis in liver as bile acids, they also occur in brain and are connected to neurodegenerative disorders like AD as well [35-37]. All these different steroidal compounds play their own important roles in cell development and homeostasis and are connected to each other by biosynthesis.

In order to understand the mechanism behind pathological changes in the steroidome, all these different steroids need to be analyzed qualitatively and quantitatively. A universal method covering all possible steroidal compounds and their conjugates is still far away, but there are already methods published covering large numbers of analytes (Table 1). Neurosteroids and conjugates can be analyzed using gas chromatography-(tandem) mass spectrometry (GC-MS(/MS)) [2-5, 38-41], liquid chromatography-tandem mass spectrometry (LC-MS/MS) [42-46], supercritical fluid chromatography-(tandem) mass spectrometry (SFC-MS(/MS)) [47] and also with radioimmunoassays (RIA) [48, 49]. Other methods cover oxysterols [50-52] and steroid acids [52-58]. Representative validated analytical methods are shown in Table 1. However, for most published methods no validation data are provided. The challenge in method validation often is a lack of authentic standards or appropriate blank matrix. Hence, most methods are qualitative or semi-quantitative, which seems sufficient for most biological studies, in which solely variations between different experimental groups are examined.

4. Analysis of neutral steroids, steroid acids and sterol sulfates

Table 1 Available validated methods for steroid analysis in biological samples

References	Analytical system	Number analytes	Type of analytes	Biological matrix	Additional information
Dzeletovic et al. 1995 [59]	GC-MS	9	oxysterols	plasma	
Liere et al. 2000 [41]	GC-MS	6	C ₁₉ /C ₂₁ steroids + conjugates	brain	
Acimovic et al. 2009 [60]	GC-MS	11	cholesterol precursors + plant sterols	cultured cells	
Hill et al. 2010 [38]	GC-MS	44	C ₁₉ /C ₂₀ /C ₂₁ steroids	serum/amniotic fluid	6 separate runs
Kumar et al. 2011 [57]	GC-MS	16	oxysterols/ steroid acids	urine	
Tsai et al 2011 [61]	GC-MS	8	steroid acids	liver/ kidney	
Schött et al. 2015 [50]	GC-MS	13	oxysterols	serum	
Matysik et al. 2015 [62]	GC-MS	4	C ₁₉ /C ₂₁ steroids	plasma	
Hill et al. 2019 [40]	GC-MS	100	C ₁₉ /C ₂₀ /C ₂₁ steroids + conjugates	serum	3 separate runs
Müller et al. 2019 [63]	GC-MS	12	cholesterol precursors	cultured cells	
Liu et al. 2003 [43]	Nano LC-MS	7	C ₁₉ /C ₂₁ steroids + conjugates	brain	runtime 155 min
Honda et al. 2009 [45]	LC-MS	7	oxysterols	serum/ liver microsomes	
Rustichelli et al. 2013 [46]	LC-MS	3	C ₁₉ /C ₂₁ steroids + conjugates	brain	
Sánchez-Guijo et al. 2015 [64]	LC-MS	11	C ₁₉ /C ₂₁ sterol sulfates + cholesterol sulfate	serum	
Crick et al. 2015 [65]	LC-MS	27	oxysterols/steroid acids	plasma	
Matysik et al. 2017 [66]	LC-MS	8	C ₁₉ /C ₂₁ steroids	serum	
Yang et al. 2017 [67]	LC-MS	19	steroid acids	plasma/liver/intestinal section contents	
Gomez-Gomez et al. 2020 [68]	LC-MS	28/15/12	C ₁₉ /C ₂₁ steroids + glucuronides	amniotic fluid/ saliva/ breast milk	free and conjugated steroids are not distinguished

As shown in Table 1, most methods which enable the analysis of multiple compounds are GC-MS-based. This is due to the higher separation efficiencies for the highly similar steroidal compounds compared to LC-MS methods [69]. An often-named advantage of LC-MS is the simple sample work up without need for derivatization, as it is mandatory for GC-MS analysis. Even though derivatization with Girard's P reagent (1-(hydrazinocarbonylmethyl)pyridinium chloride) or similar reagents is common in LC-MS analysis of oxosteroids and of 3 β -hydroxysteroids after enzymatic oxidation, in order to enhance sensitivity and improve identification [44, 56]. Careful sample preparation is also important to reduce matrix effects, which play a role in both analytical systems, although LC-MS is more susceptible to matrix effects [69, 70]. The main disadvantage of GC-MS is the tedious determination of steroid conjugates (*e.g.* glucuronides, sulfates) which must be separated completely from their unconjugated counterparts first and cleaved afterwards. A direct measurement of these conjugates can be achieved by LC-MS and mistaken identification can therefore be avoided [64]. The same applies to the analysis of the even more complex conjugated steroid acids and bile acids. Although GC-MS is the recommended method for the analysis of complex mixtures of unconjugated bile acids [71] the analysis of the conjugated bile acids is cumbersome. Various groups of different conjugated bile acids are known, including but not limited to taurine-, glycine- and sulfo-conjugates [71]. Procedures for bile acid extraction and group separation have been discussed in detail by Sjövall and Setchell [72]. Using a combination of different reverse phase and ion exchange columns, for example, allowed the separation and detailed analysis of the bile acid profile in faeces [73, 74]. Nevertheless, for most conjugated bile acids deconjugation before GC-MS analysis is mandatory [72], similar to the process for sterol sulfates. This deconjugation is rather difficult as acid hydrolysis leads to a deconstruction of the nuclear structure, while alkaline hydrolysis does not work for all bile acids [72]. For example, C₂₇ bile acids need more harsh conditions than C₂₄ bile acids and a quantitative cleavage and prevention of artifact formation is

4. Analysis of neutral steroids, steroid acids and sterol sulfates

not guaranteed [72]. For this reason, the direct analysis without deconjugation using LC-MS after group separation, as demonstrated by Yang et al. [75], seems to be a more promising approach for the analysis of conjugated bile acids. For this reason, the scope of our method was limited to unconjugated steroid acids.

Based on these previously published methods, a method was developed and validated which enables the analysis of differed groups of steroidal compounds including cholesterol precursors, oxysterols, neurosteroids, unconjugated steroid acids and sterol sulfates. We used GC-MS with its high separation efficiency as analytical system. The samples were first analyzed on a gas chromatograph-ion trap-mass spectrometer (GC-IT-MS) system in scan mode for untargeted analysis of unexpected compounds (screening method). Additionally, for targeted analysis a gas chromatograph-tandem mass spectrometer (GC-MS/MS) was used to obtain higher sensitivity. Most of the methods shown in Table 1 were developed for one specific biological matrix, mainly serum or brain. Especially for neutral steroids only one method for liver microsomes [45] and one for cultured hepatocytes [60] were published, but no method for neutral steroids or sterol sulfates is described in literature for liver tissue. Therefore, the steroid content in liver had to be measured until now with methods for serum or brain that were applied to liver tissue [76, 77]. In this work we present our validated and optimized sample preparation procedure consisting of lipid extraction from murine brain and liver tissues, steroid group separation on a solid-phase extraction (SPE) cartridge, deconjugation, derivatization and GC-MS(/MS) analysis.

2. Experimental

2.1 Chemicals, reagents and materials

C₁₉/C₂₁ steroids: Pregnenolone (>98%), progesterone (>99%), allopregnanolone (>98%) and pregnanolone (>98%) were purchased from Sigma-Aldrich (Schnelldorf, Germany). Dehydroepiandrosterone (>99%) was from Avanti Polar Lipids (Alabaster, AL, USA). Etiocholanolone, epietiocholanolone, 17-hydroxyprogesterone, 20-hydroxyprogesterone and 17-hydroxypregnenolone were acquired from Steraloids (Newport, RI, USA). Epipregnenolone was synthesized by us and will be published elsewhere. **Neutral steroids and precursors:** Cholesterol (>99%), cholestanol (>99%), squalene (>98%), squalene epoxide (>92%), 8-dehydrocholesterol (>99%), and 7-dehydrocholesterol (>99%) were purchased from Sigma-Aldrich (Schnelldorf, Germany). Zymosterol (>99%), lathosterol (>99%), lanosterol (>99%), dihydrolanosterol (>99%), cholesta-8,14-dien-3 β -ol (>99%), 4,4-dimethylcholesta-5,7-dien-3 β -ol (>99%), and 4,4-dimethylcholesta-8,14-dien-3 β -ol (>99%) were from Avanti Polar Lipids (Alabaster, AL, USA). Desmosterol was purchased from Santa Cruz Biotechnology (Dallas, TX, USA) and 4,4-dimethylcholest-8-en-3 β -ol was synthesized according to literature [78]. **Oxysterols:** 24(*S*)-Hydroxycholesterol (>99%), 7 α -hydroxycholesterol (>99%), 7 β -hydroxycholesterol (>99%) and (25*R*)-27-hydroxycholesterol (>99%) were from Avanti Polar Lipids (Alabaster, AL, USA). 7 α ,25-Dihydroxycholesterol was purchased from Santa Cruz Biotechnology (Dallas, TX, USA). 7-Ketocholesterol and trihydroxycoprostanone were acquired from Steraloids (Newport, RI, USA). **Sterol sulfates:** Cholesterol sulfate sodium salt (>99%) and pregnenolone sulfate sodium salt (>98%) were purchased from Sigma-Aldrich (Schnelldorf, Germany). Dehydroepiandrosterone sulfate sodium salt (>99%) and 25-hydroxycholesterol sulfate sodium salt (>99%) were from Avanti Polar Lipids (Alabaster, AL, USA). Allopregnanolone sulfate sodium salt, pregnanolone sulfate sodium salt, androsterone sulfate sodium salt and epiandrosterone sulfate sodium salt were acquired from Steraloids (Newport, RI, USA). **Steroid acids:** 5 β -Cholanic acid (>99%), cholic acid (>98%), deoxycholic acid (>98%) and lithocholic acid (>98%) were purchased from Sigma-Aldrich (Schnelldorf, Germany). Cholestenoic acid (>99%), 7 α -hydroxycholestenoic acid (>99%) and 3 α ,7 α ,12 α -trihydroxycholestanoic acid (>99%) were from Avanti Polar Lipids (Alabaster, AL, USA). Chenodeoxycholic acid was from Santa Cruz Biotechnology (Dallas, TX, USA). **Standards:** 5 α -Cholestane (>97%), pregnenolone-20,21-¹³C₂-16,16-*d*₂ (>98%), and pregnenolone-20,21-¹³C₂-16,16-*d*₂ sulfate sodium salt (>98%) were purchased from Sigma-Aldrich (Schnelldorf, Germany). Cholesterol-25,26,26,26,27,27,27-*d*₇ (>99%)

4. Analysis of neutral steroids, steroid acids and sterol sulfates

and desmosterol-26,26,26,27,27,27-*d*₆ (>99%) was purchased from Avanti Polar Lipids (Alabaster, AL, USA). Fernholtz acid was acquired from Steraloids (Newport, RI, USA).

Derivatization reagents *N*-methyl-*N*-trimethylsilyltrifluoroacetamide (MSTFA) and 1-(trimethylsilyl)imidazole (TSIM) were from Macherey-Nagel (Düren, Germany). Deionized water was prepared with an in-house ion-exchanger. *Iso*-hexane and methyl *tert*-butyl ether (MtBE) were distilled before use. All other reagents and solvents were purchased in HPLC grade or in *pro analysis* quality from Sigma-Aldrich (Schnelldorf, Germany). All solvent mixtures were mixed by (*v/v*). We used the following solid-phase extraction cartridges: Chromabond HR-XAW 45 µm, 3 mL/200 mg from Macherey-Nagel (Düren, Germany) and Bond Elut C₁₈ 40 µm, 1 mL/100 mg from Agilent Technologies (Santa Clara, CA, USA). For tissue homogenization we used an IKA (Staufen, Germany) Ultra Turrax Tube Drive with BMT-20S Tubes for grinding with stainless steel beads (5.0 mm) or a vortexer equipped with a bead tube holder from a Macherey-Nagel (Düren, Germany) and 2 mL microcentrifuge tubes containing glass beads (2.0 mm and 3.0 mm). All other consumables were from VWR (Ismaning, Germany).

2.2 Stock solutions

Stock solutions of each analyte (1 mg/mL) were prepared in ethanol (EtOH) or ethyl acetate (EtOAc) and stored at 4 °C. Mixtures for each experiment were prepared right before use in the necessary concentration.

2.3 Biological samples

For method development, optimization and validation pig brain and bovine liver from local markets were used. For the data presented, whole brains and livers were taken from wild-type mice (C57BL/6J, 3 male mice were sacrificed after 3 weeks and 3 female mice were sacrificed at 10 months of age). Additionally, mouse neuroblastoma (N2a) cells were taken for analysis. These tissues were stored at -20 °C before analysis.

2.4 Gas chromatography - mass spectrometry

Samples were analyzed with two different gas chromatography - mass spectrometry (GC-MS) systems. An ion trap-mass spectrometer (IT-MS) was used for the screening method (non-targeted screening) and a tandem mass spectrometer (MS/MS) was used for highly sensitive and selective analysis (targeted screening).

2.4.1 GC-IT-MS (screening method)

Gas chromatography (GC) was performed on a Varian 3800 gas chromatograph coupled to a Saturn 2200 ion trap from Varian (Darmstadt, Germany). The autosampler was from CTC Analytics (Zwingen, Switzerland) and the split/splitless injector was a Varian 1177 (Darmstadt, Germany). Instrument control and data analysis were carried out with Varian Workstation 6.9 SP1 software (Darmstadt, Germany) and Agilent MassHunter Workstation Software package B.08.00 (Santa Clara, CA, USA). An Agilent VF-5ms capillary column of 30 m length with 10 m EZ-Guard, 0.25 mm i.d. and 0.25 µm film thickness was used at a constant flow rate of 1.4 mL/min. Carrier gas was helium 99.999% from Air Liquide (Düsseldorf, Germany). The inlet temperature was kept at 300 °C and injection volume was 1 µL. The different steroid groups were analyzed with different split ratios. Neutral steroids (cholesterol biosynthesis intermediates, oxysterols and C₁₉/C₂₁ steroids) were measured with split 1:5, steroid acids with split 1:2 and sterol sulfates were measured splitless. The initial column temperature was 50 °C and was held for 1.0 min. Then the temperature was ramped up to 250 °C with 50 °C/min. The steroids were eluted at a rate of 5 °C/min until 310 °C (hold time 3 min). The total run time was 20 min. The transfer

4. Analysis of neutral steroids, steroid acids and sterol sulfates

line temperature was 300 °C and the ion trap temperature was 150 °C. The ion trap was operated with electron ionization (EI) at 70 eV in scan mode (m/z 50–650) with a solvent delay of 9.0 min. For measurement of neutral steroids (except cholesterol) an additional time segment (15.35 min -15.70 min) without ionization was added.

The analysis of cholesterol was performed on the above-mentioned chromatographic system with a shorter run time (15.4 min). The inlet temperature was kept at 300 °C and injection volume was 1 μ L. Cholesterol was measured splitless for liver tissue or with split (1:10) for brain tissue. The initial column temperature was 50 °C and was held for 1.0 min. Then the temperature was ramped up to 270 °C with 50 °C/min. Then cholesterol was eluted at a rate of 5 °C/min until 310 °C (hold time 2 min).

2.4.2 GC-MS/MS (targeted analysis)

An Agilent Technologies 7890B gas chromatograph (Santa Clara, CA, USA) with an Agilent Technologies Multimode Inlet (MMI) was coupled to an Agilent Technologies 7010B triple quadrupole detector with a high efficiency source (HES) and a Pal3 RSI autosampler from CTC Analytics (Zwingen, Switzerland). Two connected 15 m Agilent J&W HP-5ms ultra inert capillary columns with 0.25 mm i.d. and 0.25 μ m film thickness were used at a flow rate of 1.0 mL/min on the first column and 1.2 mL/min on the second column. Carrier gas was helium 99.999% from Air Liquide (Düsseldorf, Germany). The inlet was utilized in solvent vent mode with a start temperature of 70 °C and vent flow of 100 mL/min for 0.01 min, then temperature was raised at a rate of 600 °C/min to 300 °C and was held for 5.0 min. During post run and backflush the inlet temperature was elevated to 310 °C. The injection volume was 5 μ L. Initial oven temperature was 50 °C and was held for 5.0 min. Then temperature was ramped up to 250 °C with 50 °C/min. Then the steroids were eluted at a rate of 5 °C/min until 310 °C (hold time 3 min). Total runtime was 20 min and additional 4 min post run with backflush of the first column at 310 °C. Instrument control and data analysis were carried out with Agilent MassHunter Workstation Software package B.08.00 (Santa Clara, CA, USA). The triple quadrupole (MS/MS) was operated with electron ionization (EI) at 70 eV in dynamic multiple reaction monitoring mode (dMRM) with collision gas argon 99.995% from Air Liquide (Düsseldorf, Germany) with a flow rate of 0.9 mL/min. Source temperature was 230 °C. The multiplier operated with gain factor 10. Solvent delay was 8.0 min. The transitions and collision energies were optimized using MassHunter MRM optimizations software and authentic standards and are given in Table 2.

4. Analysis of neutral steroids, steroid acids and sterol sulfates

Table 2 Analytical details of the analyzed steroidal compounds. dMRM transitions were only determined for compounds of interest that were available in sufficient purity. Some compounds were identified by comparison with literature data: ¹ [79], ² [80], ³ [63], ⁴ [81], ⁵ [82]. *: Relative retention time (RRT) is referring to the highest peak in case of double peaks; n.d.: not determined. The unknown muricholic acids **52** and **53** are likely β - and ω -muricholic acid. In bold: quantifier ions/transitions. In brackets: collision energy. Sterol sulfates were measured as their unconjugated counterpart and are marked in the text with an additional “S” to the compound number.

No.	Analytes		Scan (IT-MS system)		dMRM (MS/MS system)	
	Trivial name	Systematic name	Characteristic ions [m/z]	RRT	Transitions [m/z] (CE [V])	RRT
1	Squalene	6 <i>E</i> ,10 <i>E</i> ,14 <i>E</i> ,18 <i>E</i> -2,6,10,15,19,23-Hexamethyltetracos-2,6,10,14,18,22-hexaene	121, 81, 69	0.943	163→107(5), 121→93(5) , 121→51(40)	0.958
2	Squalene epoxide	2,2-Dimethyl-3-[(3 <i>E</i> ,7 <i>E</i> ,11 <i>E</i> ,15 <i>E</i>)-3,7,12,16,20-pentamethylhenicosa-3,7,11,15,19-pentaenyl]oxirane	143, 107 , 69	1.085	n.d.	n.d.
3	Lanosterol	Lanosta-8,24-dien-3 β -ol	498, 393 , 241	1.385	498→393(5), 483→393(0) , 393→95(20)	1.401
4	Dihydrolanosterol	5 α -Lanost-8-en-3 β -ol	485, 395 , 229	1.350	500→395(5), 485→395(0) , 395→55(45)	1.362
5	4,4-Dimethylcholesta-8,14-dienol	4,4-Dimethylcholesta-8,14-dien-3 β -ol	484, 379 , 351	1.361	484→379(10) , 379→251(20), 379→223(20)	1.380
6	4,4-Dimethylcholest-8-enol	4,4-Dimethyl-5 α -cholest-8-en-3 β -ol	486 , 396, 381	1.375	n.d.	n.d.
7	Zymostenol	5 α -Cholest-8-en-3 β -ol	458 , 353, 213	1.247	458→213(10) , 458→81(35), 443→353(5)	1.257
8	Lathosterol	Cholest-7-en-3 β -ol	458 , 353, 255	1.279	458→229(5), 458→213(15) , 458→147(5)	1.290
9	7-Dehydrocholesterol	Cholesta-5,7-dien-3 β -ol	366, 351 , 325	1.269	456→143(35), 351→143(15) , 325→119(15)	1.273
10	Cholesterol	Cholest-5-en-3 β -ol	458, 368 , 329	1.226	458→145(2), 368→145(20), 329→91(45)	1.239
10d	Cholesterol- <i>d</i> ₇	Cholesterol-25,26,26,26,27,27,27- <i>d</i> ₇	465, 375 , 336	1.208	n.d.	n.d.
11	Cholestanol	5 α -Cholestan-3 β -ol	455, 355, 215	1.232	460→215(10), 445→75(25), 215→91(35)	1.239
12	Zymosterol	5 α -Cholesta-8,24-dien-3 β -ol	441, 351 , 213	1.284	456→105(45) , 372→357(5)	1.290
13	Desmosterol	Cholesta-5,24-dien-3 β -ol	456, 351 , 253	1.267	456→366(0), 456→351(10) , 351→91(35)	1.274
13d	Desmosterol- <i>d</i> ₆	Cholesta-5,24-dien-3 β -ol-26,26,26,27,27,27- <i>d</i> ₆	462, 372, 357	1.255	462→372(5) , 462→357(10)	1.263
14	Cholesta-8,14-dienol	Cholesta-8,14-dien-3 β -ol	456, 351 , 182	1.240	456→351(10), 351→238(10) , 182→45(35)	1.250
15	4,4-Dimethylcholesta-5,7-dienol	4,4-Dimethylcholesta-5,7-dien-3 β -ol	379 , 353, 325	1.381	379→171(15) , 379→156(35), 172→157(5)	1.386
16	8-Dehydrocholesterol	Cholesta-5,8-dien-3 β -ol	456, 351 , 325	1.234	456→325(10), 351→143(15), 351→128(45)	1.246
17	4,4-Dimethylcholest-8(14)-enol	4,4-Dimethyl-5 α -cholest-8(14)-en-3 β -ol	486 , 396, 381	1.357	n.d.	n.d.
18	7-Ketocholesterol	7-Oxocholest-5-en-3 β -ol	486, 470 , 380	1.427	501→197(25), 501→95(40), 486→81(30)	1.455
19	7 β -Hydroxycholesterol	Cholest-5-en-3 β ,7 β -diol	456 , (442, 351)	1.300	456→233(15), 456→73(40)	1.318
20	7 α -Hydroxycholesterol	Cholest-5-en-3 β ,7 α -diol	456 , (443, 129)	1.185	456→233(15), 456→73(45)	1.212

4. Analysis of neutral steroids, steroid acids and sterol sulfates

21	Trihydroxycoprostan	5 β -Cholestane-3 α ,7 α ,12 α -triol	456, 366 , 253	1.193	366 → 281(5) , 343→253(5), 253→128(40)	1.228
22	24S-Hydroxycholesterol	Cholest-5-en-3 β ,24(S)-diol	456, 413, 323	1.440	413 → 323(0) , 413→159(5), 323→91(45)	1.463
23	27-Hydroxycholesterol	Cholest-(25R)-5-en-3 β ,26-diol	546, 456 , 417	1.514	456→145(25), 456 → 105(45)	1.536
24	25-Hydroxycholesterol	Cholest-5-en-3 β ,25-diol	546, 456, 131	1.458	131 → 73(5) , 131→58(30)	1.479
25	7 α ,25-Dihydroxycholesterol	Cholest-5-en-3 β ,7 α ,25-triol	544 , 454, 131	1.392	544→73(45), 454→73(45), 131 → 73(5)	1.440
26	Pregnenolone	3 β -Hydroxypregn-5-en-20-one	402, 386 , 312	0.969	402 → 239(5) , 386→70(25), 100→54(15)	0.990
26d	Pregnenolone-20,21- ¹³ C ₂ -16,16- <i>d</i> ₂	3 β -Hydroxypregn-5-en-20-one-20,21- ¹³ C ₂ -16,16- <i>d</i> ₂	406, 390 , 316	0.967	406 → 316(0) , 406→241(5)	0.989
27	Epipregnenolone	3 α -Hydroxypregn-5-en-20-one	402 , 386, 312	0.799	n.d.	n.d.
28	17-Hydroxypregnenolone	3 β ,17 α -Dihydroxypregn-5-en-20-one	505, 474 , 384	1.012	474→105(40), 474→73(40), 474 → 384(5)	1.032
29	Progesterone	Pregn-4-ene-3,20-dione	372, 341 , 386	1.067	372 → 341(5) , 286→126(15), 153→95(10)	1.067*
30	17-Hydroxyprogesterone	17-Hydroxypregn-4-ene-3,20-dione	460, 429 , 339	1.095	460 → 429(5) , 429→370(10), 429→73(45)	1.107*
31	Dehydroepiandrosterone	3 β -Hydroxyandrost-5-en-17-one	374, 358, 268	0.827	358 → 84(10) , 358→268(5)	0.849
32	7 α -Hydroxydehydroepiandrosterone	3 β ,7 α -Dihydroxyandrost-5-en-17-one	387 , 357, 266	0.826	387→356(5), 387 → 73(40)	0.858
33	Androsterone	3 α -Hydroxy-5 α -androstan-17-one	376, 360, 270	0.784	360 → 270(5) , 270→213(5), 270→91(35)	0.798
34	Epiandrosterone	3 β -Hydroxy-5 α -androstan-17-one	376, 360 , 270	0.837	360 → 270(5) , 270→91(35), 270→84(10)	0.857
35	Etiocolanolone	3 α -Hydroxy-5 β -androstan-17-one	376, 360, 270	0.794	360 → 270(5) , 270→105(25), 270→91(35)	0.802
36	Epietiocolanolone	3 β -Hydroxy-5 β -androstan-17-one	376, 360, 270	0.774	360→270(5), 270→213(15), 270 → 84(5)	0.794
37	20-Hydroxyprogesterone	20-Hydroxypregn-4-en-3-one	417, 286, 117	1.069	417 → 117(10) , 417→73(35), 117→73(5)	1.086*
38	Allopregnanolone	3 α -Hydroxy-5 α -pregnane-20-one	388 , 298, 100	0.915	388 → 70(25) , 100→68(5), 100→54(20)	0.929
39	Pregnanolone	3 α -Hydroxy-5 β -pregnan-20-one	388 , 298, 100	0.925	388 → 70(25) , 100→68(5), 100→54(15)	0.933
40	Cholestenoic acid	3 β -Hydroxycholest-5-en-26-oic acid	502, 412 , 373	1.514	412 → 145(20) , 412→105(45), 255→159(10)	1.540
41	3 β ,7 α -Dihydroxycholestenoic acid	3 β ,7 α -Dihydroxycholest-5-en-26-oic acid	410, 211 , 158	1.420	410→211(5), 158 → 143(10) , 158→128(20)	1.413
42	7 α -Hydroxy-3-oxo-4-cholestenoic acid	7 α -Hydroxy-3-oxocholest-4-en-26-oic acid	498 , 483, 470	1.573	269 → 133(10) , 269→105(30), 133→105(10)	1.706
43	Trihydroxycoprostanoic acid	3 α ,7 α ,12 α -Trihydroxy-5 β -cholestan-26-oic acid	410 , 343, 253	1.458	410→281(10), 253 → 143(15) , 253→128(40)	1.511
44	Cholic acid	3 α ,7 α ,12 α -Trihydroxy-5 β -cholan-24-oic acid	458, 368 , 252	1.272	458→368(5), 368→253(5), 253 → 143(15)	1.313
45	Chenodeoxycholic acid	3 α ,7 α -Dihydroxy-5 β -cholan-24-oic acid	370 , 355, 255	1.284	370 → 105(45) , 370→91(45), 213→157(10)	1.306
46	Deoxycholic acid	3 α ,12 α -Dihydroxy-5 β -cholan-24-oic acid	535, 370, 255	1.251	370→255(5), 255 → 105(25) , 255→91(40)	1.288
47	Lithocholic acid	3 α -Hydroxy-5 β -cholan-24-oic acid	372, 357, 215	1.242	372 → 215(5) , 215→105(20), 215→91(35)	1.241
48	Cholestane	5 α -Cholestane	372, 357, 217	1.000	372→217(5), 217→121(5), 217→67(25)	1.000

4. Analysis of neutral steroids, steroid acids and sterol sulfates

49	5 β -Cholanic acid	5 β -Cholan-24-oic acid	374, 359, 217	1.043	n.d.	n.d.
50	Fernholtz acid	23,24-Bisnor-5-cholenic acid-3 β -ol	342 , 303, 215	1.069	342 → 105(40) , 215→159(10), 215→91(35)	1.087
51	α -Murcholic acid	3 α ,6 α ,7 β -Trihydroxy-5 β -cholan-24-oic acid	458 , 443, 195 ^{1,2}	1.254		
52	unknown-Muricholic acid 1	unknown-Muricholic acid 1	195 , 285, 369 ^{1,2}	1.453		
53	unknown-Muricholic acid 2	unknown-Muricholic acid 2	195, 285, 361 ^{1,2}	1.462		
54	T-MAS	4,4-Dimethylcholesta-8,24-dien-3 β -ol	394, 379 , 135 ³	1.407		
55	Sitosterol	24S-Stigmast-5-en-3 β -ol	486, 396 , 357 ⁴	1.387		
56	Campesterol	Ergost-5-en-3 β -ol	382 , 343, 129 ⁵	1.316		
57	Cholesta-7,24-dienol	Cholesta-7,24-dien-3 β -ol	456, 441, 343 ³	1.315		
58	Lophenol	4 α -Methylcholest-7-en-3 β -ol	472 , 382, 367 ³	1.320		
59	4-Methylcholesta-7,24-dienol	4 α -Methylcholesta-7,24-dien-3 β -ol	470, 455, 365 ³	1.352		

4. Analysis of neutral steroids, steroid acids and sterol sulfates

2.5 Sample preparation

2.5.1 Lipid extraction procedure

Lipid extraction was performed in 15 mL grinding tubes or 2 mL microcentrifuge tubes depending on the available sample amount.

Mouse brain and liver tissues of 250 - 1,500 mg were homogenized in grinding tubes containing 10 steel beads. The samples were homogenized without additional solvent at 6,000 rpm for 2 min. Then 2 mL EtOH containing 5 mg/mL butylated hydroxytoluene (BHT) as antioxidant and 8 mL EtOAc containing internal standards as described in Chapter 2.8.1 were added. The samples were mixed one more time at 6,000 rpm for 2 min. Then 4 mL of 0.2 M HCl with 25% (*m/v*) aqueous KCl solution and 4 mL EtOAc were added to the mixture. The samples were homogenized for another 2 min. Then the whole content of the grinding tubes was transferred into 50 mL centrifuge tubes and the samples were centrifuged for 5 min at 3,300 g. The organic layer was collected, and the aqueous phase was extracted two more times by addition of 10 mL EtOAc, shaking for 1 min and subsequent centrifugation. The organic phases were combined.

Smaller amounts (50 mg – 250 mg) of tissue or cell samples were extracted in 2 mL microcentrifuge tubes containing 3 big and 3 small glass beads on a tube shaker (see Chapter 2.1). The samples were homogenized without additional solvent at 3,200 rpm for 10 min. Then 200 μ L EtOH containing 5 mg/mL BHT and 800 μ L EtOAc containing internal standards as described in Chapter 2.8.1 were added. The samples were mixed one more time at 3,200 rpm for 10 min. Then 400 μ L of 0.2 M HCl with 25% (*m/v*) aqueous KCl solution and 400 μ L EtOAc were added to the microcentrifuge tubes. The samples were homogenized for another 10 min at maximum speed. Then the samples were centrifuged for 5 min at 12,000 g. The organic layer was collected, and the aqueous phase was extracted two more times by addition of 1000 μ L EtOAc, mixed for 1 min and centrifuged for 5 min at 12,000 g. The organic phases were combined.

Aliquots ($n=3$) of these lipid extracts corresponding to 1 mg liver tissue or 0.4 mg brain tissue were used for cholesterol determination. For solid-phase extraction and determination of the other steroids, aliquots ($n=3$) corresponding to 250 mg liver tissue or 100 mg brain tissue were used. The aliquots were transferred into glass vials (5 mL) and concentrated to dryness under a gentle stream of nitrogen.

2.5.2 Steroid group separation

After extraction the lipids were separated in different groups: neutral steroids, steroid acids and sterol sulfates. Therefore, a mixed mode solid-phase extraction (SPE) cartridge with reversed-phase (RP) and weak anion exchange abilities was used. All steps were carried out without additional pressure or vacuum, exceptions are mentioned explicitly. First, possible lipophilic contaminations from manufacturing were removed from the column by washing with 2 mL *Mt*BE. Then the sorbent was conditioned with 4 mL MeOH and 4 mL of MeOH/H₂O (3:7). Care was taken that the sorbent was always wetted. The dried lipid extracts were reconstituted in 600 μ L MeOH and then diluted with 1400 μ L H₂O. The final pH was spot-checked and ranged between 5 and 7. The sample solution was loaded on the column. After the whole solvent had run through, the cartridge was dried by through-flow of nitrogen for 1 h. Steroid groups were eluted in the following order: neutral steroids, steroid acids, and sterol sulfates. After every elution step, the cartridges were dried for 5 min by through-flow of nitrogen. Each eluate was evaporated to dryness under a stream of nitrogen (exception sterol sulfates, see below) and was stored at -20 °C prior to further analysis. Different solvents were tested for elutions to find the most suitable mixture for every single steroid group. For this purpose, lipid extracts of 50 mg brain tissue were spiked with several representative steroidal compounds at concentrations of 1 μ g/50 mg tissue each, which exceeds the unneglectable endogenous concentration of most steroidal compounds. In case of desmosterol, which occurs in a higher concentration in brain, we used desmosterol-*d*₆ (**13d**).

4. Analysis of neutral steroids, steroid acids and sterol sulfates

Optimization was performed in separate experiments for each steroid group and each experiment was performed in triplicate.

Starting with neutral steroids, desmosterol-*d*₆ (**13d**), pregnenolone (**26**), 17-hydroxypregnenolone (**28**), 17-hydroxyprogesterone (**30**), androsterone (**33**), 20-hydroxyprogesterone (**37**), allopregnanolone (**38**) and pregnanolone (**39**) were used as model analytes. The steroid acid lithocholic acid (**47**) was used as negative control here, and the following solvents were tested: MeOH, *iso*-hexane/*iso*-propanol (7:3), CHCl₃/M*t*BE (9:1) and dichloromethane (DCM)/M*t*BE (9:1). Neutral steroids were eluted with 3 × 3 mL solvent and the internal standard (IS) cholestane (**48**) (10 μL of 100 μg/mL stock solution) was added to each eluate. The eluates were evaporated under a stream of nitrogen and the dry residue of each sample was derivatized following the protocol for neutral and sulfated steroids (Chapter 2.6.2). After derivatization the samples were analyzed with GC-IT-MS (Chapter 2.4.1). In the case of CHCl₃/M*t*BE (9:1) additional fractions of 2 × 3 mL were analyzed to monitor the elution of the huge amount of cholesterol occurring in the brain extracts. Recovery was calculated by comparison to the spiked steroids measured without SPE in solvent.

The solvent for elution of steroid acids was optimized using the model compounds cholic acid (**44**), chenodeoxycholic acid (**45**), lithocholic acid (**47**), cholanic acid (**49**), and Fernholtz acid (**50**). After elution of neutral steroids with 3 × 3 mL CHCl₃/M*t*BE (9:1), steroid acids were eluted using the following solvents, each with addition of 5% trifluoroacetic acid (TFA): MeOH, *iso*-hexane/*iso*-propanol (7:3), CHCl₃/M*t*BE (9:1), EtOH/EtOAc (2:8) and CH₃CN/acetone (2.5:7.5). Analytes were eluted with 2 × 1.5 mL solvent and cholestane (1 μg, IS) was added to each eluate. The eluates were evaporated under a stream of nitrogen and the dry residue of each sample was derivatized following the protocol for steroid acids (Chapter 2.6.3). The derivatized samples were analyzed with GC-IT-MS (Chapter 2.4.1). Recovery was calculated by comparison to the spiked steroids measured without SPE in solvent.

Optimization of sterol sulfate elution was performed using cholesterol sulfate (**10S**), 25-hydroxycholesterol sulfate (**24S**), pregnenolone sulfate (**26S**), dehydroepiandrosterone sulfate (**31S**), androsterone sulfate (**33S**), epiandrosterone sulfate (**34S**), allopregnanolone sulfate (**38S**), and pregnanolone sulfate (**39S**) as model sterol sulfates. Elution of sterol sulfates was investigated after elution of neutral steroids (with 3 × 3 mL CHCl₃/M*t*BE (9:1) and steroid acids (with 2 × 1.5 mL EtOH/EtOAc (2:8) + 5% TFA) with 2 × 1.5 mL of the following solvents CHCl₃/MeOH (1:1), MeOH/H₂O (1:1), MeOH/H₂O (8:2), MeOH/H₂O (9:1) and acetone. To each solvent mixture 5% triethylamine (TEA) was added for mixed mode SPE. The consecutive use of TFA and TEA leads to the formation of small amounts of TEA-TFA salt in the fractions of sterol sulfates. For the removal of this contamination an additional C₁₈ SPE was necessary. For this purpose, the sterol sulfate eluate of mixed mode SPE was evaporated to almost dryness under a stream of nitrogen and the residue dissolved in 1 mL of 0.1 M HCl/MeOH (7:3). Cholesterol-*d*₇ (**10d**) (10 μL of 100 μg/mL stock solution) was added to each sample to examine the behavior of probably co-eluting traces of cholesterol (cross-contamination). The C₁₈ sorbent was conditioned with 2 mL M*t*BE, then 2 mL MeOH and 2 mL of 0.1 M HCl/MeOH (7:3) and was kept wetted for the whole time. Samples were loaded on the conditioned SPE cartridge and contaminants of TEA-TFA salt were removed by washing with 1 mL H₂O/MeOH (7:3). Sterol sulfates were subsequently eluted with 1 mL of the same solvent as used before for mixed mode SPE, but this time without the addition of TEA. Cholestane (10 μL of 100 μg/mL stock solution) was added to each eluate. Solvents were removed under a stream of nitrogen at 50 °C and the dry residue of each sample was derivatized following the protocol for neutral and sulfated steroids (Chapter 2.6.2). The derivatized samples were analyzed with GC-IT-MS (Chapter 2.4.1). Recovery was calculated by comparison to the spiked steroids measured without SPE in solvent.

4. Analysis of neutral steroids, steroid acids and sterol sulfates

2.6 Deconjugation and derivatization

2.6.1 Cholesterol

Cholesterol was measured as trimethylsilyl ether (TMS ether). Fifty microliters of MSTFA/TSIM (10:1) was added and the sample was kept for 30 min at RT. Finally, 950 μL of *Mt*BE was added and the sample was ready for GC-IT-MS analysis (Chapter 2.4.1).

2.6.2 Neutral steroids and sterol sulfates

Neutral steroids and sterol sulfates were measured as their respective *O*-methyloxime-trimethylsilyl ethers (MO-TMS). Sterol sulfates were deconjugated and derivatized in the same step as described previously [83]. For this purpose, 200 μL of a solution of *O*-methylhydroxylamine hydrochloride in pyridine 2% (*m/v*) was added to the dry lipids and kept for 4 h at 80 °C in a 4 mL glass vial. Then the sample was transferred into a 2 mL microcentrifuge tube and 400 μl H₂O and 1000 μL *Mt*BE were added. Liquid-liquid extraction (LLE) was performed by shaking manually for 1 min and centrifugation at 10,000 g for 5 min. The organic layer was separated and transferred into an autosampler vial and the aqueous phase was extracted one more time with 1000 μL *Mt*BE. The organic phases were combined and evaporated to dryness under a stream of nitrogen. Then 50 μL of MSTFA/TSIM (10:1) was added and the sample was kept for 30 min at RT. Finally, 940 μL of *Mt*BE and 10 μL internal standard (IS) cholestane (**48**, 1 $\mu\text{g}/\text{mL}$ in *Mt*BE) were added before analysis.

2.6.3 Steroid acids

Steroid acids were measured as methyl ester-trimethylsilyl ethers (Me-TMS). To the dry lipids 200 μL MeOH and 50 μL HCl conc. were added and the mixture was kept at 80 °C for 30 min. The sample was then brought to dryness under a stream of nitrogen at 50 °C. Then 50 μL of MSTFA/TSIM (10:1) was added and the sample was kept at RT for 30 min. Finally, 940 μL of *Mt*BE and 10 μL internal standard (IS) cholestane (**48**, 1 $\mu\text{g}/\text{mL}$ in *Mt*BE) were added before analysis.

2.7 Investigation of matrix effects

Matrix effects were determined by comparison of the measured peak areas analyzed with and without addition of matrix. Therefore, mouse brain samples (50 mg, n=3) were extracted and group separation with optimized solvents was performed (see Chapter 2.8.1). The eluates of each class of analytes (neutral sterols, steroid acids, and sterol sulfates) were used as matrix. Steroid standards were added to matrix in a concentration of 1 $\mu\text{g}/50$ mg brain tissue, which exceeds the neglectable endogenous concentrations of most steroidal compounds in the brain extracts. In case of desmosterol (**13**) we used desmosterol-*d*₆ (**13d**). Solvent samples were prepared with the same steroid standards and concentration. Samples were derivatized as described in Chapters 2.6.2 and 2.6.3 and were analyzed with GC-IT-MS (Chapter 2.4.1). The ratios of the obtained peak areas with and without matrix were determined for 11 neutral steroids (**23**, **24**, **26d**, **28**, **29-32**, and **37-39**), 6 steroid acids (**40**, **44-47**, and **50**) and 8 sterol sulfates (**10S**, **24S**, **26S**, **31S**, **33S**, **34S**, **38S** and **39S**).

2.8 Final method and validation

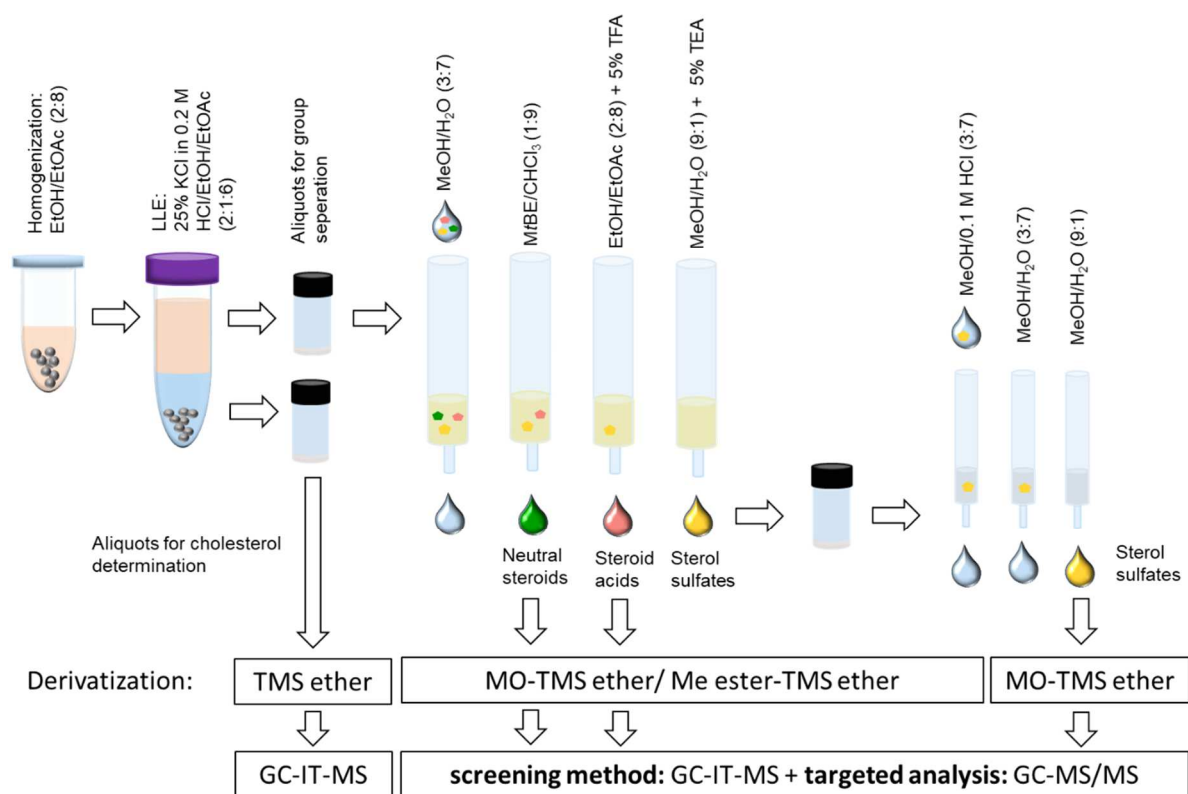
2.8.1 Final sample preparation protocol

The optimized sample preparation procedure is shown in Figure 1. Tissues (250 -1,500 mg) were extracted in grinding tubes, smaller amounts of tissues were extracted in 2 mL microcentrifuge tubes as described in 2.5.1. The internal standards were added. For cholesterol precursors desmosterol-*d*₆ (**13d**) (100 ng/250 mg liver; 1000 ng/100 mg brain) was used as internal standard. Pregnenolone-20,21-¹³C₂-

4. Analysis of neutral steroids, steroid acids and sterol sulfates

16,16- d_2 (**26d**) (10 ng/250 mg liver; 10 ng/ 100 mg brain) was used as internal standard for the other neutral steroids. Pregnenolone-20,21- $^{13}C_2$ -16,16- d_2 sulfate (**26Sd**) (10 ng/250 mg liver; 10 ng/100 mg brain) was used as internal standard for sterol sulfates. Fernholtz acid (**50**) (500 ng/250 mg liver; 50 ng/100 mg brain) was used as internal standard for steroid acids. After addition of these standards, a small aliquot of the extract corresponding to 1 mg liver or 0.4 mg brain tissue was diverted for cholesterol analysis. For cholesterol analysis cholestane (**48**) (10 μ L of 100 μ g/mL stock solution) was added to the aliquot and solvent was evaporated to dryness under a stream of nitrogen. Derivatization was performed as described in Chapter 2.6.1. and cholesterol samples were analyzed with GC-IT-MS (Chapter 2.4.1.). Aliquots for group separation referring to 100 mg brain tissue or 250 mg liver tissue were used for SPE. The extracts were dried under a stream of nitrogen and stored at -20 °C before analysis. Conditioning and loading of the weak anion exchange cartridge was performed as described in Chapter 2.5.2. The best elution solvent for neutral steroids was $CHCl_3$ /M β BE (9:1) 3 \times 3 mL, for steroid acids EtOH/EtOAc (2:8) + 5% TFA 2 \times 1.5 mL and for sterol sulfates MeOH/H $_2$ O (9:1) + 5% TEA 2 \times 1.5 mL and MeOH/H $_2$ O (9:1) 1 mL. Every sample was derivatized (Chapters 2.6.2 an 2.6.3) and analyzed with GC-IT-MS and/or GC-MS/MS (Chapters 2.4.1 and 2.4.2).

Figure 10 Final Sample preparation protocol



2.8.2 Identification of steroids

Steroidal compounds were identified using their respective relative retention time (RRT) relating to the internal standard cholestane (**48**) and, in the case of scan data, on basis of the obtained mass spectra. The spectra were compared to those obtained for authentic standards or mass spectra previously published by us and others [63, 79, 81, 82] (Table 2). In case of dMRM data steroidal compounds were identified using their respective relative retention time (RRT) relating to the internal standard cholestane (**48**) and on basis of one or two qualifier and one quantifier transitions (Table 2) [84]. The transitions for each compound were chosen under consideration of co-eluting similar compounds and matrix

4. Analysis of neutral steroids, steroid acids and sterol sulfates

components. Collision energies were optimized using MassHunter MRM optimizations software and are shown in Table 2.

2.8.3 Quantification

Quantification was performed using an external calibration. The calibration standards were measured in 6 different concentrations with a consistent concentration of internal standard. This concentration was 100 ng/mL for liver and 1000 ng/mL for brain samples desmosterol-*d*₆ (**13d**) for cholesterol precursors and 10 ng/mL pregnenolone-20,21-¹³C₂-16,16-*d*₂ (**26d**) for the other neutral steroids. For the steroid acids Fernholtz acid (**50**) was used as internal standard in a concentration of 500 ng/mL for liver samples and 50 ng/mL for brain samples. For sterol sulfates pregnenolone-20,21-¹³C₂-16,16-*d*₂ sulfate (**26dS**, 10 ng/mL) was used. For cholesterol (**10**) determination the internal standard was cholestane (**48**, 1 μg/mL). The calibrators were measured in triplicates using a bracketing procedure and peak area ratios from quantifier ions/transitions of the analytes and internal standards were plotted against the corresponding concentration. The individual calibration ranges and results of linear regression are given in Tables 7 and 8.

2.8.4 Determination of LOD and LOQ

Limit of detection (LOD) and limit of quantification (LOQ) were determined using linear regression according to DIN 32645 [85]. Authentic standards (**3-5**, **8-10**, **12**, **13**, **15**, **18**, **19**, **22-24**, **24S**, **26**, **26S**, **28-32**, **31S**, **33S**, **34S**, **37-41**, **38S**, **39S** and **43-47**) were measured in solvent because no steroid-free brain or liver matrix was available and matrix effects have shown to be limited (Chapter 3.2). LOD and LOQ values were calculated individually for liver and brain tissue with regards to the different amounts of tissue which could be used for analysis (250 mg liver tissue; 100 mg brain tissue). LOD and LOQ for the analyzed steroids are given in Tables 7 and 8.

2.8.5 Precision and recovery

Precision and recovery were determined as described by Rustichelli et al. [46], who used three different sets of quality control (QCa, QCb and QCc) samples. QCa samples were prepared from 400 mg brain (n=3) and 1,000 mg liver (n=3). For this purpose, the respective concentrations of internal standards were added, and the samples were prepared as described in Chapter 2.8.1. QCb samples were prepared from 400 mg brain (n=6) and 1000 mg liver (n=6). In addition to the respective concentrations of internal standards the samples were spiked with authentic standards (**3-5**, **8**, **9**, **12**, **13**, **15**, **18**, **19**, **22-24**, **24S**, **26**, **26S**, **28-32**, **31S**, **33S**, **34S**, **37-41**, **38S**, **39**, **39S** and **43-47**) at two different concentrations (LOQ: n=6; 50 × LOQ: n=6). Then the samples were prepared as described in chapter 2.8.1. QCc samples were prepared in the same manner as the QCb samples but were spiked with authentic standards (LOQ: n=3; 50 × LOQ: n=3) after sample preparation, just before the deconjugation/derivatization step. Precision was calculated as relative standard deviation (RSD) of the spiked authentic standards in QCb samples (n=6). Recovery was calculated by comparing the mean values obtained from QCc-QCa samples with those of QCb-QCa.

2.9 Application on biological samples

The method was applied on brain and liver samples of 10 months old female mice and on brain of 3 weeks old male mice. The whole brains and livers were extracted in grinding tubes and further sample preparation and analysis was done in technical triplicates. Furthermore, the method was also applied to cultured N2a cells which were extracted using microcentrifuge tubes. Per sample ~ 3 × 10⁷ cells corresponding to ~ 200 μg cell mass were used (n = 6).

4. Analysis of neutral steroids, steroid acids and sterol sulfates

3. Results and discussion

3.1 Sample preparation

3.1.1 Lipid extraction

There are various methods published for lipid extraction from biological samples. The most popular methods were published by Folch et al. [86] and Bligh and Dyer [87]. Their methods work with varying amounts of MeOH, CHCl₃ and H₂O. These solvents are still frequently used for lipid extraction even if the exact procedure may vary [31, 39]. In recent publications some authors tried to substitute these solvents by less toxic EtOH and EtOAc [88, 89]. Another possible procedure is saponification with hot aqueous NaOH or KOH and then extraction in an organic solvent like diethyl ether, *Mt*BE or hexane [63, 90]. Preliminary experiments revealed that a mixture of EtOAc, EtOH and H₂O was as effective as CHCl₃/MeOH mixtures or saponification with hot aqueous NaOH solution for neutral steroid extraction, and even superior for steroid acids extraction. The extraction procedure with EtOAc has some more advantages, as unlike to CHCl₃ the organic phase is the upper layer and can easily be collected without contaminations with the aqueous phase. And in contrast to the saponification protocol we do not need harsh conditions and elevated temperatures, which is one main reason for cholesterol autoxidation that could lead to the formation of artefacts like 7-hydroxy- or 7-oxocholesterol [91]. Without saponification free cholesterol can also be distinguished from cholesterol fatty acid esters. Hence, in the final extraction protocol the solvent system EtOH, EtOAc and H₂O was used. In addition, the antioxidant butylhydroxytoluene (BHT) was used to avoid cholesterol autoxidation and hydrochloric acid was used for acidification of the aqueous phase to increase extraction of steroidal acids and sterol sulfates. Additionally, a high concentration of KCl improved phase separation and lipid recovery.

3.1.2 Steroid group separation

After extraction the lipids were separated into different groups: neutral steroids, steroid acids and sterol sulfates. This separation is necessary to differentiate between sterols and the respective sterol sulfates, which were finally also measured in their deconjugated form. Another reason is the derivatization procedure for the steroid acids which varies from neutral or sulfated steroids. A separation just basing on the polarity of the analytes, as liquid-liquid-extraction (LLE) [40], column chromatography [92] or reversed phase SPE [41] was only successful for a smaller group of steroids, for example C₁₉ and C₂₁ steroids and their corresponding sulfates. Including C₂₇ steroids (cholesterol precursors), whose corresponding sulfates could be more lipophilic than unconjugated smaller steroids, the analysis requires another separation mechanism. This could be achieved by SPE with an anion exchange sorbent. Griffiths et al. [93] presented a universal extraction scheme employing subsequent solid phase extractions on C₁₈, cation exchange and anion exchange sorbents. Following this principle including three to five separation steps Liu et al. [43] measured neurosteroids (*e.g.* progesterone, dehydroepiandrosterone and pregnenolone) and sterol sulfates in rat brain. Their sample preparation also gave a fraction of weak acids that was not further analyzed. We followed this principle using reversed phase (RP) SPE in combination with ion exchange sorbents, but instead of subsequent extraction steps on different cartridges, we used a mixed mode sorbent with RP and weak anion exchange properties. So, we could reduce the number of extraction steps and achieve a robust method with high reproducibility. In the first elution step neutral steroids were eluted from the cartridge. Subsequently, steroid acids were eluted in their uncharged form from the sorbent under acidic conditions. The more acidic sterol sulfates remained on the column under these conditions and were eluted in a last step under alkaline conditions.

3.1.3 Neutral steroids

The results of the optimization experiments for elution of neutral steroids are shown in Table 3. The best results were obtained for CHCl₃/*Mt*BE (9:1). Under these conditions the highest recoveries for most tested steroids were achieved and the relative standard deviations (RSD) were within an acceptable

4. Analysis of neutral steroids, steroid acids and sterol sulfates

range. Steroids were eluted with a final volume of 9 mL (3×3 mL). Further experiments with larger volumes of $\text{CHCl}_3/\text{M}t\text{BE}$ (9:1) were performed and it was determined that 99.9% of the endogenous cholesterol is eluted with the first 9 mL. Moreover, lithocholic acid (**47**) started to elute from the solid phase after 15 mL of $\text{CHCl}_3/\text{M}t\text{BE}$ (9:1). So, a final volume of 9 mL was chosen for extraction of neutral steroids.

Table 3

Mean recovery for various neutral steroids using different solvents (n=3) and respective average relative standard deviations (RSD). Log P values (calculated) of analyzed neutral steroids are shown. The final extraction mixture is given in bold letters.

No.	Trivial name	Log P	MeOH [%]	<i>iso</i> -hexane/ <i>iso</i> -propanol (7:3) [%]	$\text{CHCl}_3/\text{M}t\text{BE}$ (9:1) [%]	$\text{M}t\text{BE}/\text{DCM}$ (9:1) [%]
13d	Desmosterol- <i>d</i> ₆	6.7	84	54	90	80
26	Pregnenolone	3.6	87	79	100	61
28	17-Hydroxypregnenolone	2.8	28	20	67	84
30	17-Hydroxyprogesterone	3.4	29	20	72	57
33	Androsterone	3.8	76	76	100	59
37	20 α -Hydroxyprogesterone	3.9	80	84	100	47
38	Allopregnanolone	4.0	78	73	95	62
39	Pregnanolone	4.0	80	74	98	62
Average recovery [%]			68	60	90	64
Average RSD [%]			19	23	19	16

3.1.4 Steroid acids

The results of the optimization experiment for elution of steroid acids are shown in Table 4. The best recoveries for most steroid acids were obtained with *iso*-hexane/*iso*-propanol (7:3) + 5% TFA and EtOH/EtOAc (2:8) + 5% TFA. The recovery of the EtOH/EtOAc (2:8) + 5% TFA protocol was better and with lower RSD for the more lipophilic steroid acids. With consideration of further steroid acids that are even more lipophilic than lithocholic acid (**47**), *e.g.* 3 β -hydroxycholestenic acid (**40**), and are expected to be found only in trace amounts, the mixture of EtOH/EtOAc (2:8) + 5% TFA was chosen. The example of **49** shows the limitation of this separation step. This very lipophilic steroidal acid was eluted to a great extent in the fraction of neutral steroids. For that reason, we performed an additional experiment for cholestenic acid (**40**) because it has similar lipophilic properties (Log P 6.1) and confirmed that this steroidal acid was indeed eluting in the steroid acid fraction.

4. Analysis of neutral steroids, steroid acids and sterol sulfates

Table 4

Mean recovery in % for various steroid acids using different solvents (n=3) and respective average RSD. Log P values (calculated) of analyzed steroid acids are shown. The final extraction mixture is given in bold letters.

No.	Trivial name	Log P	MeOH + 5% TFA [%]	iso-hexane/iso- propanol (7:3) + 5% TFA [%]	MBE/CHCl₃ (9:1) +5% TFA [%]	EtO/EtOAc (2:8) + 5% TFA [%]	CH₃CN/acetone (2.5:7.5) + 5% TFA [%]
44	Cholic acid	2.5	133	123	15	118	75
45	Chenodeoxycholic acid	3.7	100	107	113	104	86
47	Lithocholic acid	5.0	75	89	115	93	75
49	Cholanic acid	6.5	21	5	4	5	6
50	Fernholtz acid	4.0	21	106	113	88	93
Average recovery [%]			70	86	72	82	67
Average RSD [%]			39	10	28	6	33

3.1.5 Sterol sulfates

The results of the optimization experiment for elution of sterol sulfates are shown in Table 5. The best results were obtained for MeOH/H₂O (9:1) + 5% TEA. Sterol sulfates were eluted under alkaline conditions from the SPE sorbent. For this reason, the Log D value (calculated) for the sterol sulfate anion is specified. The elution of sterol sulfates from the weak anion exchange sorbent was followed by an additional purification step on a C₁₈ SPE cartridge. This is necessary to remove the TFA-TEA salt, originating from reaction of TFA from the previous elution step with TEA from the present elution, which had shown to disturb the following deconjugation and derivatization steps. In this experiment the same mixture was used for both SPEs, but in case of the C₁₈ SPE without the addition of TEA. Furthermore, cholesterol-*d*₇ (**10d**) was added right before C₁₈ SPE to monitor the elution of unconjugated cholesterol, which could still be retained in small amounts in the sample and would cause wrong results for cholesterol sulfate (**10S**) measurement. For this reason, solvents which were able to elute **10d** were excluded. This was the case for acetone and CHCl₃/MeOH (1:1). In both cases large amounts of detected cholesterol sulfate could be co-eluting with residual free cholesterol.

4. Analysis of neutral steroids, steroid acids and sterol sulfates

Table 5

Mean recovery in % for various sterol sulfates using different solvents (n=3) and respective average RSD. Log D values (calculated) of analyzed sterol sulfate anions are shown. *: Solvents which also elute unconjugated cholesterol-*d*₇. The final extraction mixture is given in bold letters.

No.	Trivial Name	Log D	CHCl₃/MeOH (1:1)* + 5% TEA [%]	MeOH/H₂O (1:1) + 5% TEA [%]	MeOH/H₂O (8:2) + 5% TEA [%]	MeOH/H₂O (9:1) + 5% TEA [%]	Acetone* + 5% TEA [%]
10S	Cholesterol sulfate	4.8	223	3	6	6	162
24S	25-Hydroxycholesterol sulfate	3.4	76	0	52	79	29
26S	Pregnenolone sulfate	1.3	93	0	96	107	27
31S	Dehydroepiandrosterone sulfate	1.0	96	24	104	111	30
33S	Androsterone sulfate	1.5	87	18	105	106	31
34S	Epiandrosterone sulfate	1.5	100	19	107	116	22
38S	Allopregnanolone sulfate	1.7	83	0	95	105	29
39S	Pregnanolone sulfate	1.7	90	0	94	104	27
Average recovery [%]			106*	8	82	92	45*
Average RSD [%]			15	37	27	13	29

3.2 Investigation of matrix effects

Compared to LC-MS/MS matrix effects in GC-MS are known to be minimal [69], even so it is recommended to prepare calibration standards in blank matrix [94]. As no steroid-free matrix for brain or liver tissue was available the calibration standards had to be prepared in solvent. For this reason, matrix effects for all three groups of steroidal compounds were investigated before method validation. Brain tissue was chosen for the experiments due to its large amounts of lipids, which are likely to be co-extracted with the steroids. The matrix effects for neutral steroids (**23**, **24**, **28**, **29**, **30**, **31**, **32**, **37**, **38** and **39**), steroid acids (**40**, **44**, **45**, **46**, and **47**) and sterol sulfates (**10S**, **24S**, **31S**, **33S**, **34S**, **38S** and **39S**) were investigated using several representative compounds (1 µg/50 mg brain tissue) from each steroid group. The matrix effects were determined by comparing the peak areas obtained in matrix with those obtained in solvent. The mean value for every steroid group is shown in the first row of Table 6. In the second row the effect is given after correction with the respective internal standards. The internal standards were isotope-labelled pregnenolone (**26d**) for neutral steroids, Fernholtz acid (**50**) for steroid acids and isotope-labelled pregnenolone sulfate (**26dS**) for the sterol sulfates.

Table 6

Mean ratio of peak areas of steroidal compounds measured in spiked matrix compared to pure solvent.

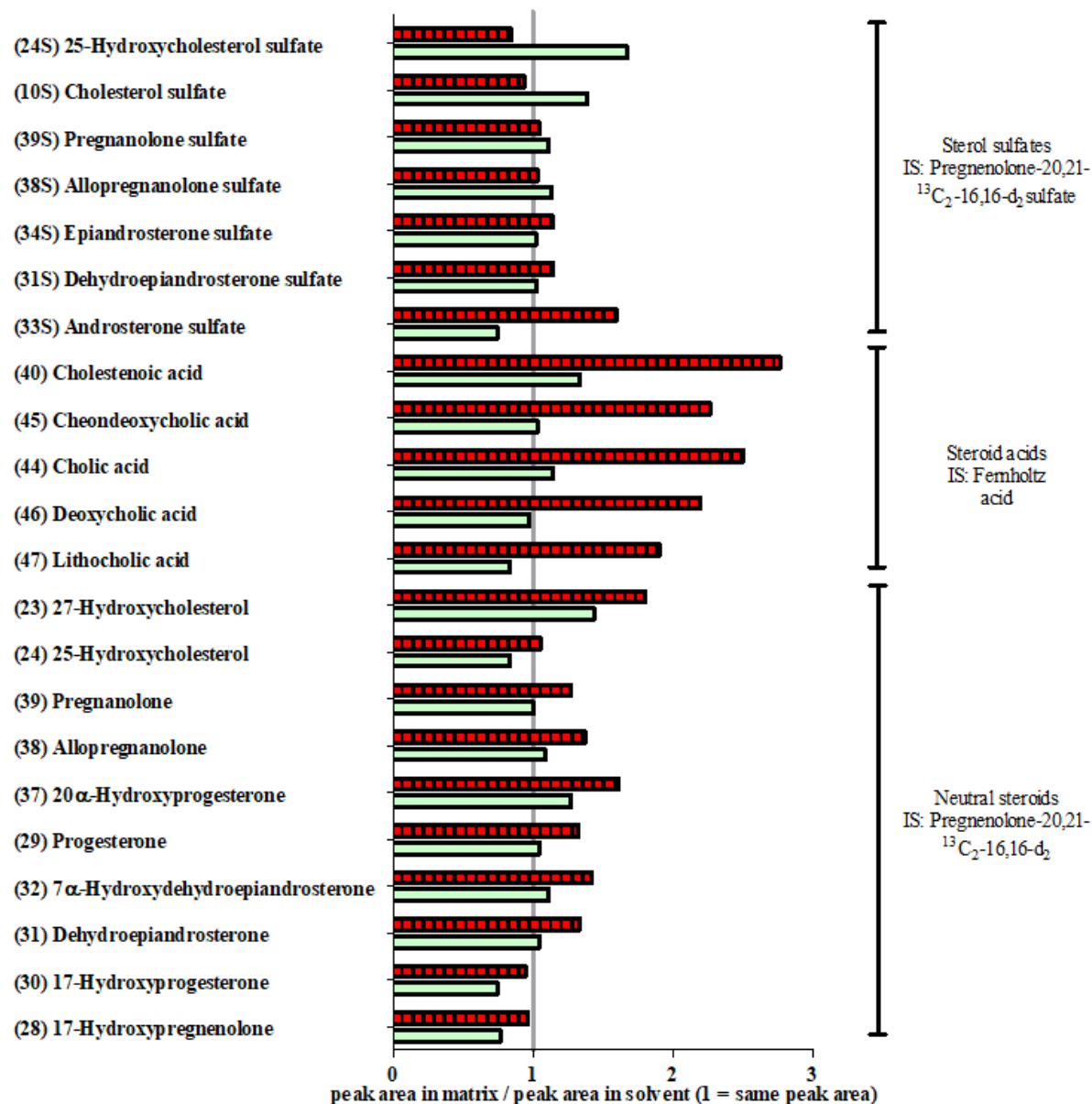
	Neutral steroids	Steroid acids	Sterol sulfates
Peak area ratio without correction with IS	1.30	2.32	1.11
Peak area ratio after correction with IS	1.03	1.06	1.15

There was a trend to higher areas with matrix matched standards compared to standards analyzed in solvent. This matrix enhancement effect [95] seems to take effect especially on the steroid acids. However, this effect was successfully compensated by the used of appropriate internal standards. The

4. Analysis of neutral steroids, steroid acids and sterol sulfates

enhancing effect on sterol sulfates is not as high as for other groups, this is most likely due to the matrix composition of this group. In this case the effect of the internal standard is small and does not improve the result. Despite of that the internal standard for the sterol sulfates is important regarding the whole sample preparation procedure because it compensates losses and variations in sample preparation, which includes two critical solid phase extraction steps. The chosen internal standards are acceptable for a huge number of steroids in the particular groups (individual values for every tested compound are given in Figure 2). Anyway the best internal standard for every analyte would be its isotope-labeled counterpart, but these labeled compounds are often not commercially available or very expensive.

Figure 2 Matrix effects for individual compounds with (green) and without (red) correction using the respective internal standards



3.3 Method performance

The method performance was investigated for 23 neutral steroids (3-5, 8-10, 12, 13, 15, 18, 19, 22-24, 26, 28- 32 and 37-39) 7 steroid acids (40, 41 and 43-47) and 7 sterol sulfates (24S, 26S, 31S, 33S, 34S, 38S and 39S). We determined the selectivity, linearity, precision, recovery, limit of detection (LOD), and limit of quantification (LOQ) for each individual analyte in brain and in liver tissue. As no great differences between those two matrices were noticed, no further validation experiments for cultured cell matrix were necessary.

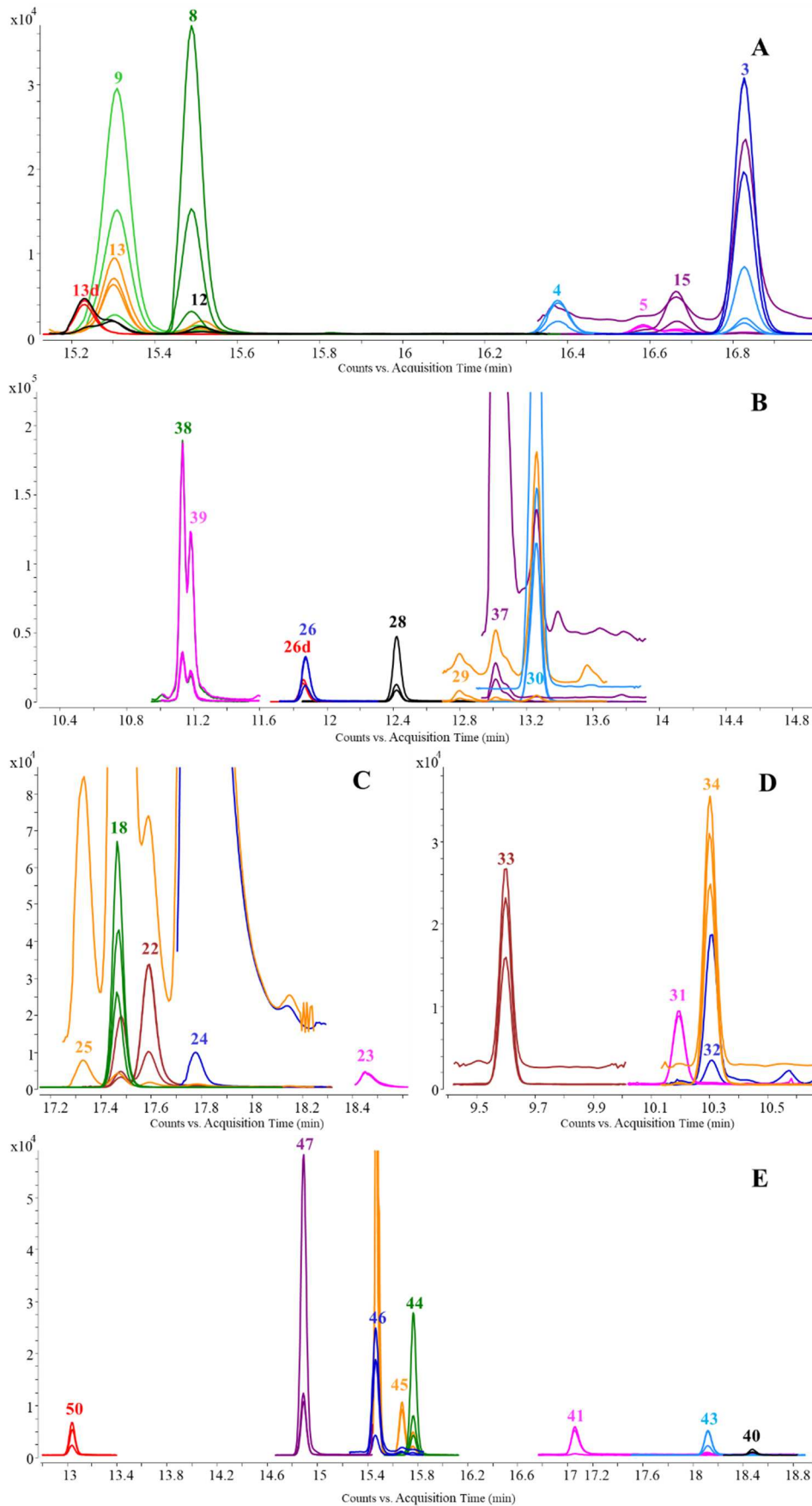
4. Analysis of neutral steroids, steroid acids and sterol sulfates

3.3.1 Selectivity

Compounds were identified using the RRT relative to cholestane (**48**) and full scan mass spectra or dynamic MRM transitions. In Figure 3 chromatograms of dynamic MRM measurements are shown. The chosen transitions were sufficiently distinctive even for compounds with identical retention times, as for example 7 α -hydroxydehydroepiandrosterone (**32**) and epiandrosterone (**34**) (Figure 3D). Other compounds could be distinguished because of their different retention times although they have identical mass transitions, as for example allopregnanolone (**38**) and pregnanolone (**39**) (Figure 3B). It should be mentioned that progesterone (**29**) and its hydroxylated metabolites have asymmetrical peak shapes (**29**, **37**, and **30**) (Figure 3B). This is due to *endo*- and *exo*-isomeric MO derivatives. These peaks were processed as one single peak.

4. Analysis of neutral steroids, steroid acids and sterol sulfates

Figure 3 dMRM chromatograms with selected transitions for several steroidal compounds. Transitions referring to one compound are marked in the same color. Numbers in the diagram represent the detected steroids as are given in Table 2. A: cholesterol precursors (C₂₇ – C₃₀ steroids); B: C₂₁ steroids C: oxysterols; D: C₁₉ steroids; E: steroid acids.



4. Analysis of neutral steroids, steroid acids and sterol sulfates

Cholesterol is, because of its high concentration in most biological samples, not analyzed in the same run as the other neutral steroids. But its huge amount, especially in brain samples, could still be problematic for the analysis of the other neutral steroids. The high on column concentration on the GC-MS/MS system and the thereof resulting tailing of the cholesterol peak can lead to an overlap with the next eluting steroids like lathosterol (**8**) or desmosterol (**13**). In this case these steroids could be measured alternatively on the GC-IT-MS system with lower on column cholesterol concentration due to the lower injection volume (1 μ L instead of 5 μ L; see Chapter 2.4).

3.3.2 LOD, LOQ, linearity, precision and recovery

LOD and LOQ were calculated according to DIN 32645 [85]. This method considered slope, intercept and residual standard deviation of a calibration curve over a limited concentration range. The advantage of this method is that it reveals the individual values for each compound even if they have large differences in their LOD and LOQ (see Tables 7 and 8). The achieved limits enable the measurement of most endogenous steroids. Only the 17-hydroxylated compounds **28** and **30** had relatively high LOD and LOQ. For verification the method precision (RSD of QCb samples, n=6) was measured at LOQ or at the lower end of the working range (e.g. 25 ng lanosterol/100 mg brain tissue). One exception was cholesterol that was only analyzed at the endogenous level. In this case the precision was calculated as RSD of all QC samples. The obtained precision was <20% for 31 compounds in liver tissue and for 20 compounds in brain tissue and <30% for 34 (liver) and 30 (brain) compounds. Method precision was measured also at a medium level corresponding to the middle concentration of working range (e.g. 1,250 ng lanosterol/100mg brain tissue) and was <20% for 34 (liver) and 31 (brain) compounds and <30% for 35 (liver) and 32 (brain) compounds. So, no great differences could be determined between the different matrices. Measurement of technical replicates would be useful if a sufficient amount of sample is available. Higher concentrations were not tested, because this concentration in combination with the endogenous amount would exceed the working range by far for some compounds (e.g. cholesterol precursors). Determination of recovery is challenging due to the necessary subtraction of the endogenous concentration which can lead to inaccuracies because no steroid-free matrix is available for brain and liver tissue. So, the recovery was only estimated at medium concentration because endogenous concentration did not affect these values that much. For 30 (liver) and 23 (brain) compounds the recovery was >50%. Linearity was measured in a bracketing process and was >0.980 for 26 (liver) and 19 (brain) compounds. Some compounds showed just sufficient linearity, for example 7-ketocholesterol (**18**, R^2 0.932), this problem was already described by other authors [65]. Other compounds show difficulties at higher concentrations, like desmosterol (**13**) or lathosterol (**8**) measured in dMRM in case of liver samples. The steroid acids in general showed a smaller linear range compared to the other compounds. Linearity and recovery could be improved when using the respective isotope-labelled internal standard, which is recommended if a specific steroid of interest should be quantitated with higher accuracy.

4. Analysis of neutral steroids, steroid acids and sterol sulfates

Table 7 Validation data for brain samples. *: Desmosterol-*d*₆ as IS instead of isotope labeled pregnenolone. ^{IT}: measured with GC-IT-MS; * precision calculated by the analytical data obtained at the endogenous level.

No.	Trivial name	LOD [ng/mg]	LOQ [ng/mg]	Range [ng/mL]	R ²	Precision [%] Medium level	Recovery [%] Medium level
3	Lanosterol	0.049	0.247	25 - 2500	0.924	8	27
4	Dihydrolanosterol	0.016	0.028	1.6 - 160	0.958	8	36
5	4,4-Dimethyl-5 α -cholesta-8,14-dienol	0.006	0.016	0.6 - 60	0.960	8	42
8	Lathosterol	0.006	0.039	50 – 5000 ^{IT}	0.997 ^{IT}	15 ^{IT}	162 ^{IT}
10	Cholesterol	0.850	4.700	10 - 100 ^{IT}	0.999 ^{IT}	9 ^{IT*}	n.d.
13	Desmosterol	0.009	0.025	200 – 20000 ^{IT}	0.998 ^{IT}	16 ^{IT}	112 ^{IT}
15	4,4-Dimethylcholesta-5,7-dienol	0.018	0.018	1.8 - 180	0.916	7	49
18	7-Ketocholesterol	0.159	0.251	25 - 2500	0.932	20	42
22	24S-Hydroxycholesterol	0.013	0.040	50 – 5000 ^{IT*}	0.968 ^{IT*}	42 ^{IT*}	59 ^{IT*}
23	27-Hydroxycholesterol	0.004	0.006	10 - 1000	0.905	10	35
24	25-Hydroxycholesterol	0.008	0.032	0.80 – 80	0.998	8	50
24S	25-Hydroxycholesterol sulfate	0.004	0.004	0.41 - 41	0.985	8	35
26	Pregnenolone	0.002	0.004	0.40 - 40	0.999	26	79
26S	Pregnenolone sulfate	0.004	0.010	1.0 - 100	0.997	4	49
28	17-Hydroxypregnenolone	0.134	0.383	38 - 3800	0.997	67	102
29	Progesterone	0.001	0.002	0.08 – 8.0	0.982	4	78
30	17-Hydroxyprogesterone	0.162	0.487	49 - 4900	0.993	8	75
31	Dehydroepiandrosterone	0.003	0.005	0.33 - 33	0.999	3	68
31S	Dehydroepiandrosterone sulfate	0.006	0.006	0.63 - 63	0.993	5	75
32	7 α -Hydroxydehydroepiandrosterone	0.001	0.002	0.04 – 4.0	0.971	16	31
33S	Androsterone sulfate	0.004	0.010	0.99 - 99	0.995	6	65
34S	Epiandrosterone sulfate	0.014	0.030	3.0 - 300	0.988	8	55
37	20 α -Hydroxyprogesterone	0.002	0.002	0.16 - 16	0.983	7	81
38	Allopregnanolone	0.002	0.002	0.24 - 24	0.972	6	58
38S	Allopregnanolone sulfate	0.001	0.002	0.22 - 22	0.998	13	61
39	Pregnanolone	0.002	0.010	0.20 - 20	0.987	6	68
39S	Pregnanolone sulfate	0.001	0.002	0.16 - 16	0.998	13	50
40	Cholestenic acid	0.016	0.035	3.5 - 350	0.858	8	94
41	3 β ,7 α -Dihydroxycholestenic acid	0.006	0.269	26 - 2600	0.923	15	19
43	Trihydroxycoprostanic acid	0.006	0.031	3.0 - 300	0.979	5	83
44	Cholic acid	0.017	0.171	17 - 1700	0.968	13	118
45	Chenodeoxycholic acid	0.012	0.033	3.3 - 330	0.975	5	96
46	Deoxycholic acid	0.009	0.028	2.8 - 280	0.994	18	81
47	Lithocholic acid	0.003	0.013	1.3 - 130	0.961	1	82

4. Analysis of neutral steroids, steroid acids and sterol sulfates

Table 8 Validation data for liver samples. ^{IT}: measured with GC-IT-MS; * precision calculated by the analytical data obtained at the endogenous level.

No.	Trivial name	LOD [ng/mg]	LOQ [ng/mg]	Range [ng/mL]	Linearity	Precision [%] Medium level	Recovery [%] Medium level
3	Lanosterol	0.020	0.099	25 - 2500	0.987	5	68
4	Dihydrolanosterol	0.006	0.011	1.60 - 160	0.995	4	62
5	4,4-Dimethyl-5 α -cholesta-8,14-dienol	0.002	0.007	0.6 - 60	0.989	7	62
8	Lathosterol	0.002	0.016	0.6 - 60	0.902	4	58
9	7-Dehydrocholesterol	0.008	0.009	15 - 1500	0.916	5	73
10	Cholesterol	0.340 ^{IT}	1.880 ^{IT}	1.0 - 10 ^{IT}	0.999 ^{IT}	9 ^{IT*}	n.d.
12	Zymosterol	0.009	0.009	2.2 - 220	0.917	14	97
13	Desmosterol	0.003	0.010	10 - 1000	0.912	5	68
15	4,4-Dimethylcholesta-5,7-dienol	0.007	0.007	1.8 - 180	0.989	8	64
18	7-Ketocholesterol	0.064	0.100	25 - 2500	0.930	7	63
19	7 β -Hydroxycholesterol	0.001	0.001	0.14 - 14	0.996	11	91
22	24S-Hydroxycholesterol	0.005	0.016	1.3 - 130	0.999	11	61
23	27-Hydroxycholesterol	0.002	0.003	0.37 - 37	0.979	4	51
24	25-Hydroxycholesterol	0.003	0.013	0.8 - 80	0.970	7	66
24S	25-Hydroxycholesterol sulfate	0.002	0.002	0.41 - 41	0.998	18	35
26	Pregnenolone	0.001	0.002	0.40 - 40	0.989	7	78
26S	Pregnenolone sulfate	0.001	0.004	1.00 - 100	0.999	10	55
28	17-Hydroxypregnenolone	0.054	0.153	38 - 3800	0.990	9	74
29	Progesterone	0.001	0.001	0.08 - 8.0	0.984	7	80
30	17-Hydroxyprogesterone	0.065	0.195	49 - 4900	0.989	12	76
31	Dehydroepiandrosterone	0.001	0.002	0.33 - 33	0.993	23	22
31S	Dehydroepiandrosterone sulfate	0.003	0.003	0.63 - 63	0.994	8	72
32	7 α -Hydroxydehydroepiandrosterone	0.001	0.001	0.04 - 4.0	0.993	9	26
33S	Androsterone sulfate	0.001	0.004	0.99 - 99	0.992	4	56
34S	Epiandrosterone sulfate	0.005	0.012	3.0 - 300	0.994	6	52
37	20 α -Hydroxyprogesterone	0.001	0.001	0.16 - 16	0.997	4	78
38	Allopregnanolone	0.001	0.002	0.24 - 24	0.988	11	71
38S	Allopregnanolone sulfate	0.001	0.001	0.22 - 22	0.990	50	30
39	Pregnanolone	0.001	0.004	0.20 - 20	0.985	11	70
39S	Pregnanolone sulfate	0.001	0.001	0.16 - 16	0.999	46	37
40	Cholestenoic acid	0.006	0.014	3.5 - 350	0.921	8	68
41	3 β ,7 α -Dihydroxycholestenoic acid	0.002	0.108	26 - 2600	0.975	14	64
43	Trihydroxycoprostanoic acid	0.002	0.012	3.1 - 310	0.983	8	80
44	Cholic acid	0.007	0.068	17 - 850	0.992	8	19
45	Chenodeoxycholic acid	0.005	0.013	15 - 750	0.976	7	61
46	Deoxycholic acid	0.004	0.011	30 - 1500	0.964	9	68
47	Lithocholic acid	0.001	0.005	15 - 750	0.995	7	61

4. Analysis of neutral steroids, steroid acids and sterol sulfates

3.4 *Application on biological samples*

Results of analysis of liver, brain and cell samples are shown in Table 9. The results obtained with this method fit in most cases with previously published values. It should be mentioned that published data on endogenous steroid concentrations have noticeable variations. Concentrations are also dependent on age, gender and diet of the animals. Furthermore the determined concentrations can also vary on the used analytical procedure. With this approach cholesterol precursors, oxysterols, neurosteroids, unconjugated steroid acids and sterol sulfates can be analyzed. However some sterols (e.g. bile acids) are preferably present as taurine- or glycine-conjugates, which cannot be determined by this approach (see 1. Introduction).

4. Analysis of neutral steroids, steroid acids and sterol sulfates

Table 9 Identified and quantified steroids of mouse brain and liver tissue and cell samples. The concentrations measured with targeted analysis are given as **mean ± SD** [ng/mg] (n=3) or < LOQ for brain and liver tissue. The concentrations measured with targeted analysis are given as **mean ± SD** [ng/mg] (n=6) or < LOQ for N2a cells. Steroids only detected with the screening method (scan) are marked with +. Steroids that could not be detected are marked with n.d.; The unknown muricholic acids **52** and **53** are likely β- and ω-muricholic acid. Results are compared with published data [ng/mg], if available. Cholesterol biosynthesis precursors, oxysterols, C₁₉/C₂₁ steroids and sterol sulfates were measured as MO-TMS derivatives (Chapter 2.6.2). Steroid acids were measured as Me-TMS derivatives (Chapter 2.6.3).

No.	Trivial name	Brain						Liver			N2a cells	References	
		animal	3 weeks			10 months			10 months				1
			1	2	3	1	2	3	1	2	3		
Cholesterol biosynthesis precursors													
1	Squalene	n.d.	n.d.	n.d.	n.d.	n.d.	n.d.	+	+	+	n.d.	Cultured cells: 35.05 [60]	
3	Lanosterol	10.42 ± 0.09	10.84 ± 0.84	11.46 ± 3.16	4.83 ± 0.59	5.74 ± 0.67	6.14 ± 1.69	1.04 ± 0.14	0.87 ± 0.08	1.05 ± 0.14	0.92 ± 0.19	Liver: 1.3-4.9 (2-5 months) [96] Cultured cells: 3.17 [60]	
4	Dihydrolanosterol	1.95 ± 0.07	1.66 ± 0.08	1.32 ± 0.15	0.31 ± 0.01	0.34 ± 0.01	0.18 ± 0.05	0.31 ± 0.12	0.11 ± 0.01	0.38 ± 0.06	n.d.	Liver: 0.15-0.5 (2-5 months) [96] Cultured cells: 1.21 [60]	
5	4,4-Dimethylcholesta-8,14-dienol	33.00 ± 1.28	27.43 ± 4.93	22.90 ± 3.62	2.66 ± 0.13	2.71 ± 0.19	1.45 ± 0.38	0.08 ± 0.04	0.03 ± 0.00	0.05 ± 0.01	0.01 ± 0.00		
6	4,4-Dimethylcholest-8-enol	+	+	+	n.d.	n.d.	n.d.	n.d.	n.d.	n.d.	n.d.		
7	Zymostenol	+	+	+	+	+	+	n.d.	n.d.	n.d.	+		
8	Lathosterol	83.91 ± 2.13	87.79 ± 7.13	97.11 ± 17.39	23.70 ± 11.98	27.79 ± 4.48	28.48 ± 6.62	0.43 ± 0.11	0.24 ± 0.00	0.39 ± 0.02	3.26 ± 1.38	Brain: 20-30 (16-18 weeks) [76] Liver: 1.7-2.1 (2-5 months) [96] Cultured cells: 7.50 [60]	
9	7-Dehydrocholesterol	3.36 ± 0.12	3.81 ± 0.30	4.02 ± 1.11	1.13 ± 0.34	1.44 ± 0.15	1.25 ± 0.43	0.47 ± 0.09	0.34 ± 0.00	0.55 ± 0.05	2.26 ± 0.37	Cultured cells: 1.48 [60] Liver: 0.5-1 (2-5 months) [96] Brain: n.d. (15 weeks) [42]	
10	Cholesterol	8810 ± 65	8000 ± 23	8040 ± 80	12020 ± 48	11700 ± 77	13210 ± 105	1990 ± 40	2080 ± 43	1790 ± 0.8	1500 ± 137	Brain: 16000 (15 weeks) [97] Liver: 1800 (2-5 months) [96] Cultured cells: 8608 [60]	
11	Cholestanol	+	n.d.	+	n.d.	+	+	n.d.	n.d.	n.d.	n.d.		

4. Analysis of neutral steroids, steroid acids and sterol sulfates

12	Zymosterol	13.73 ± 0.51	12.18 ± 0.33	11.97 ± 0.29	8.01 ± 0.49	7.94 ± 0.25	8.25 ± 0.17	0.04 ± 0.01	0.04 ± 0.01	0.03 ± 0.00	0.18 ± 0.07	Liver: 0.1-0.7 (19 weeks, high fat diet) [98] Cultured cells: 0.00 [60]
13	Desmosterol	220 ± 11	253 ± 21	284 ± 60	77.56 ± 8	84.04 ± 12	81.73 ± 17.2	0.44 ± 0.10	0.24 ± 0.11	0.43 ± 0.04	5.14 ± 0.65	Brain: 100 (15 weeks) [97] Liver: 1.2-1.8 (2-5 months) [96] Cultured cells: 2.30 [60]
15	4,4-Dimethylcholesta-5,7-dienol	6.13 ± 0.11	4.96 ± 0.03	4.73 ± 0.13	0.61 ± 0.02	0.62 ± 0.04	0.45 ± 0.06	0.02 ± 0.00	0.01 ± 0.00	0.02 ± 0.00	0.04 ± 0.01	
Oxysterols												
18	7-Ketocholesterol	2.69 ± 0.20	3.49 ± 0.67	2.57 ± 0.36	3.68 ± 1.00	2.88 ± 0.52	2.49 ± 0.48	0.65 ± 0.05	1.59 ± 0.10	0.75 ± 0.24	7.58 ± 2.56	
19	7β-Hydroxycholesterol	0.76 ± 0.02	1.14 ± 0.20	1.55 ± 0.19	1.22 ± 0.04	1.27 ± 0.09	1.82 ± 0.40	0.74 ± 0.18	4.73 ± 0.96	1.43 ± 0.36	3.15 ± 12.7	Brain: <0.05 (15 weeks) [97]
20	7α-Hydroxycholesterol	+	+	+	+	+	+	n.d.	n.d.	n.d.	+	Liver: 0.087 [77]
21	Trihydroxycoprostan	n.d.	n.d.	n.d.	+	n.d.	n.d.	n.d.	n.d.	n.d.	n.d.	
22	24S-Hydroxycholesterol	30.45 ± 0.83	33.40 ± 2.25	39.16 ± 9.92	38.30 ± 5.92	40.60 ± 6.87	39.21 ± 9.27	0.08 ± 0.02	0.22 ± 0.04	0.25 ± 0.04	0.26 ± 0.07	Brain: 27.91±0.73 (15 weeks) [97] Liver: 0.009-0.027 (2-5 months) [96], 0.004 (8 weeks) [77]
23	27-Hydroxycholesterol	0.33 ± 0.00	0.31 ± 0.01	0.31 ± 0.00	0.28 ± 0.01	0.27 ± 0.01	0.31 ± 0.01	0.09 ± 0.06	0.13 ± 0.03	0.06 ± 0.01	0.06 ± 0.02	Brain: 3.9-6 (3-18 months) [17] Liver: 0.013-0.019 (2-5 months) [96], 0.083 (8 weeks) [77]
24	25-Hydroxycholesterol	< 0.032	< 0.032	< 0.032	< 0.032	< 0.032	< 0.032	< 0.013	0.030 ± 0.01	0.04 ± 0.02	0.03 ± 0.01	Brain: <0.05 (15 weeks) [97] Liver: 0.015 (8 weeks) [77] Liver: 0.01-0.013 (2-5 months) [96]
C₁₉/C₂₁ steroids												
26	Pregnenolone	0.06 ± 0.01	0.09 ± 0.04	0.05 ± 0.00	0.08 ± 0.01	0.07 ± 0.02	0.07 ± 0.02	0.02 ± 0.00	0.02 ± 0.00	0.03 ± 0.01	0.02 ± 0.02	Brain: 0.00165±0.00023 (8 weeks) [99] 0.00167 (male rat) [100] 0.015 (female rat) [101]
28	17-Hydroxypregnenolone	n.d.	n.d.	n.d.	n.d.	n.d.	n.d.	n.d.	n.d.	n.d.	n.d.	Brain: n.d. (rat) [100]
29	Progesterone	< 0.002	n.d.	n.d.	0.003 ± 0.00	< 0.002	< 0.002	n.d.	n.d.	n.d.	n.d.	Brain: 0.001-0.02 (rat) [43] 0.008 (female rat) [101] 0.0007 (male rat) [100]

4. Analysis of neutral steroids, steroid acids and sterol sulfates

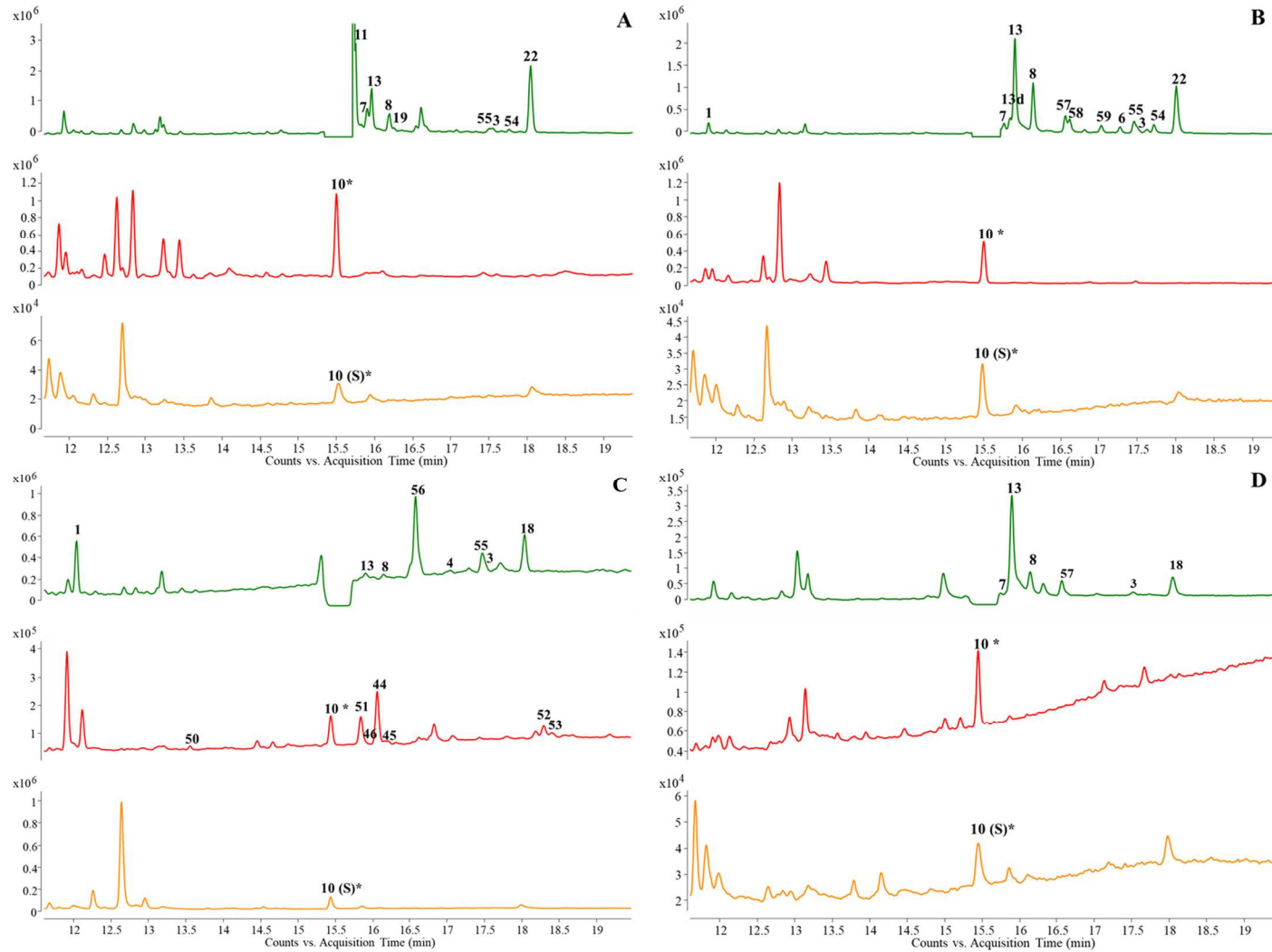
30	17-Hydroxyprogesterone	n.d.	n.d.	n.d.	n.d.	n.d.	n.d.	n.d.	n.d.	n.d.	n.d.	Brain: n.d. (rat) [100]
31	Dehydroepiandrosterone	0.01 ± 0.00	0.03 ± 0.00	0.02 ± 0.00	0.02 ± 0.00	0.02 ± 0.00	0.02 ± 0.002	< 0.002	< 0.002	< 0.002	0.05 ± 0.01	Brain: 0.00004-0.00011 (rat) [43] 0.00027 (male rat) [100] 0.012 (female rat) [101]
34	Epiandrosterone	n.d.	n.d.	n.d.	n.d.	n.d.	n.d.	n.d.	n.d.	n.d.	n.d.	Brain: n.d. (male rat) [100]
37	20-Hydroxyprogesterone	n.d.	n.d.	n.d.	n.d.	n.d.	n.d.	n.d.	n.d.	n.d.	n.d.	Brain: 0.00019 (male rat) [100]
38	Allopregnanolone	n.d.	< 0.002	n.d.	n.d.	n.d.	< 0.002	n.d.	n.d.	n.d.	n.d.	Brain: 0.00402±0.00031 (8 weeks) [99] 0.00042-0.038 (rat) [43]
39	Pregnanolone	n.d.	n.d.	n.d.	n.d.	n.d.	n.d.	n.d.	n.d.	n.d.	n.d.	n.d.-0.00016 (rat) [43]
Steroid acids												
43	Trihydroxycoprostanoic acid	n.d.	n.d.	n.d.	n.d.	n.d.	n.d.	0.52 ± 0.05	0.27 ± 0.01	0.31 ± 0.05	n.d.	
44	Cholic acid	0.47 ± 0.01	0.44 ± 0.00	0.44 ± 0.00	0.38 ± 0.00	0.37 ± 0.01	0.38 ± 0.00	96.79 ± 20.02	0.47 ± 0.05	41.65 ± 13.07	0.23 ± 0.04	Brain: 0.047±0.077 (rat) [102] Liver: 20-40 [79] 8.9-22.7 (rat) [103]
45	Chenodeoxycholic acid	< 0.033	< 0.033	< 0.033	< 0.033	< 0.033	< 0.033	0.36 ± 0.02	0.12 ± 0.01	0.21 ± 0.01	0.28 ± 0.05	Brain: 0.630±0.23 [102] Liver: 0.98-2.6 (rat) [103]
46	Deoxycholic acid	0.04 ± 0.01	0.05 ± 0.01	0.04 ± 0.00	0.04 ± 0.00	0.06 ± 0.00	0.05 ± 0.01	0.38 ± 0.04	0.03 ± 0.01	0.12 ± 0.02	n.d.	Brain: 0.025±0.020 (rat) [102] Liver: 2.7-5.1 (rat) [103]
47	Lithocholic acid	n.d.	n.d.	n.d.	n.d.	n.d.	n.d.	0.12 ± 0.05	0.28 ± 0.21	0.08 ± 0.02	0.50 ± 0.25	Liver 1.5-2.6 (rat) [103]
Sterol sulfates												
26S	Pregnenolone sulfate	< 0.010	0.10 ± 0.07	< 0.010	< 0.010	< 0.010	< 0.010	< 0.004	< 0.004	< 0.004	0.01 ± 0.00	Brain: .n.d.-0.00028 (rat) [39] n.d. (male rat) [100] Liver: n.d. (rat) [39]
31S	Dehydroepiandrosterone sulfate	0.03 ± 0.01	0.08 ± 0.04	0.04 ± 0.00	0.03 ± 0.01	0.13 ± 0.09	0.03 ± 0.01	n.d.	n.d.	< 0.003	0.01 ± 0.00	Brain: n.d. (rat) [39] 0.00104 (male rat) [100] Liver: 0.00041-0.00074 (rat) [39]
33S	Androsterone sulfate	n.d.	n.d.	n.d.	n.d.	n.d.	n.d.	n.d.	n.d.	< 0.004	n.d.	

4. Analysis of neutral steroids, steroid acids and sterol sulfates

34S	Epiandrosterone sulfate	0.05 ± 0.01	0.14 ± 0.07	0.04 ± 0.01	0.06 ± 0.01	0.09 ± 0.04	< 0.031	0.01 ± 0.00	0.02 ± 0.00	0.05 ± 0.05	0.05 ± 0.01	Brain: n.d. (male rat) [100]]
38S	Allopregnanolone sulfate	< 0.002	0.16 ± 0.10	< 0.002	< 0.002	< 0.002	< 0.002	< 0.001	< 0.001	< 0.001	n.d.	
39S	Pregnanolone sulfate	< 0.002	0.14 ± 0.09	n.d.	< 0.002	< 0.002	n.d.	< 0.001	< 0.001	< 0.001	< 0.001	
24S	25-Hydroxycholesterol sulfate	0.01 ± 0.00	0.020 ± 0.01	0.01 ± 0.00	0.01 ± 0.01	0.06 ± 0.04	0.01 ± 0.00	n.d.	n.d.	< 0.002	n.d.	
others												
51	α-Muricholic acid	n.d.	n.d.	n.d.	n.d.	n.d.	n.d.	+	+	+	n.d.	Brain: n.d. (rat) [102]
52	unknown Muricholic acid 1	n.d.	n.d.	n.d.	n.d.	n.d.	n.d.	+	+	+	n.d.	
53	unknown Muricholic acid 2	n.d.	n.d.	n.d.	n.d.	n.d.	n.d.	+	+	+	n.d.	
54	T-MAS	+	+	+	+	+	+	n.d.	n.d.	n.d.	+	Cultured cells: 1.32 [60]
55	Sitosterol	+	+	n.d.	n.d.	n.d.	+	+	+	+	n.d.	Cultured cells: 3.45[60]
56	Campesterol	n.d.	n.d.	n.d.	n.d.	n.d.	n.d.	+	+	+	n.d.	Cultured cells: 8.22 [60]
57	Cholesta-7,24-dienol	+	+	+	n.d.	n.d.	n.d.	n.d.	n.d.	n.d.	+	
58	Lophenol	+	+	+	n.d.	n.d.	n.d.	n.d.	n.d.	n.d.	n.d.	
59	4-Methylcholesta-7,24-dienol	+	+	+	+	+	+	n.d.	n.d.	n.d.	n.d.	

4. Analysis of neutral steroids, steroid acids and sterol sulfates

Figure 4 Total ion chromatograms from GC-IT-MS (full scan m/z 50 – 650). A: Mouse brain; 10 months old; B: Mouse brain; 3 weeks old; C: Mouse liver, 10 months old; D: N2a cells. Neutral steroids: green; steroid acids: red; sterol sulfates: yellow. **10*/10*(S)**: cholesterol detected in steroid acid and sterol sulfates fractions. Numbers in the diagram represent the detected steroids as are given in Table 2.



4. Analysis of neutral steroids, steroid acids and sterol sulfates

Scan chromatograms measured with IT-MS are shown in Figure 4. Here some additional compounds could be identified by comparing with literature data, for example the phytosterols sitosterol (**55**) and campesterol (**56**) and murine bile acids. Small amounts of residual cholesterol were detected in the steroid acids and sterol sulfate groups, where it could not be distinguished from cholesterol sulfate. Cholesterol (**10**, RRT 1.226) and their nearly identical relative retention times a reliable quantification of **11**, **20**, and **21** was not possible.

4. Conclusion

The described GC-MS method allows the analysis of neutral steroids, steroid acids and sterol sulfates from one single sample. This method is suitable for brain and liver tissue and is also applicable on cultured cells. The combination of scan and dMRM measurement allows identification of unknown or unexpected compounds and quantification of targeted compounds in trace amounts. Especially the peak spectra obtained in scan mode can help to identify unexpected compounds by comparing with MS databases or literature data. The method has some limitations due to the large amounts of cholesterol in most biological samples. A complete elution in the group of neutral steroids is not guaranteed and residual cholesterol is then found in the following eluates. This makes an indirect measurement of cholesterol sulfate impossible. For this compound direct analysis in presence of cholesterol like LC-MS analysis is an alternative [64]. In some cases, the high on column concentration of cholesterol also leads to a strong peak tailing which could make the proper analysis of compounds eluting right after cholesterol difficult. This is the case for some intermediates of cholesterol biosynthesis, then injection of a smaller sample volume, as described for GC-IT-MS analysis, can be a solution, as shown for lathosterol (**8**) and desmosterol (**13**) in brain samples. There are few methods covering a higher number of analytes (Table 1), but we present here the up to our knowledge first method covering this large range of different steroid classes including cholesterol precursors, oxysterols, C₁₉ and C₂₁ steroids, steroid acids and sterol sulfates. The list of analyzed steroids can certainly be extended with further compounds of interest. To improve precision of quantification of certain analytes and to minimize matrix effects, the use of the respective isotope-labelled internal standards is recommended for targeted analysis. As our method has the potential for untargeted screening and steroid profiling in different tissues it could be used for further investigation and comprehension of diseases like AD, CAH, CTX, SLOS and more.

Author contributions

Conceptualization, JJ, CM; Methodology, JJ, CM; Validation, JJ; Formal Analysis, JJ, CM; Investigation, JJ; Resources, FK, EW, HS, FB; Data Curation; JJ, Writing - Original Draft, JJ; Writing - Review and Editing, CM, FB; Visualization, JJ; Supervision, HS, FB; Funding Acquisition, FK, HS, FB.

Conflicts of interest

The authors declare no competing financial interest.

Acknowledgments

We thank Dr. Alessio Colombo for help with tissue preparation. This work was supported by the Deutsche Forschungsgemeinschaft (DFG) grant STE 847/6-1 (HS) and the VERUM Stiftung für Verhalten und Umwelt (FK).

References

4. Analysis of neutral steroids, steroid acids and sterol sulfates

- [1] W.J. Griffiths, Y. Wang, Sterolomics in biology, biochemistry, medicine, *Trends Analyt. Chem.*, 120 (2019) 115280. <https://doi.org/10.1016/j.trac.2018.10.016>
- [2] S. Christakoudi, D.A. Cowan, N.F. Taylor, Steroids excreted in urine by neonates with 21-hydroxylase deficiency. 3. Characterization, using GC–MS and GC–MS/MS, of androstanes and androstenes, *Steroids*, 77 (2012) 1487-1501. <https://doi.org/10.1016/j.steroids.2012.08.012>
- [3] S. Christakoudi, D.A. Cowan, N.F. Taylor, Steroids excreted in urine by neonates with 21-hydroxylase deficiency: Characterization, using GC–MS and GC–MS/MS, of the D-ring and side chain structure of pregnanes and pregnenes, *Steroids*, 75 (2010) 34-52. <https://doi.org/10.1016/j.steroids.2009.09.011>
- [4] S. Christakoudi, D.A. Cowan, N.F. Taylor, Steroids excreted in urine by neonates with 21-hydroxylase deficiency. 2. Characterization, using GC–MS and GC–MS/MS, of pregnanes and pregnenes with an oxo- group on the A- or B-ring, *Steroids*, 77 (2012) 382-393. <https://doi.org/10.1016/j.steroids.2011.12.018>
- [5] S. Christakoudi, D.A. Cowan, N.F. Taylor, Steroids excreted in urine by neonates with 21-hydroxylase deficiency. 4. Characterization, using GC–MS and GC–MS/MS, of 11oxo-pregnanes and 11oxo-pregnenes, *Steroids*, 78 (2013) 468-475. <https://doi.org/10.1016/j.steroids.2013.02.008>
- [6] G. Salen, R. Steiner, Epidemiology, diagnosis, and treatment of cerebrotendinous xanthomatosis (CTX), *J. Inher. Metab. Dis.*, 40 (2017). <https://doi.org/10.1007/s10545-017-0093-8>
- [7] G. Testa, E. Staurengi, C. Zerbinati, S. Gargiulo, L. Iuliano, G. Giaccone, F. Fantò, G. Poli, G. Leonarduzzi, P. Gamba, Changes in brain oxysterols at different stages of Alzheimer's disease: Their involvement in neuroinflammation, *Redox Biol.*, 10 (2016) 24-33. <https://doi.org/10.1016/j.redox.2016.09.001>
- [8] M. Vaňková., M. Hill, M. Velíková, J. Včelák., G. Vacínová, K. Dvořáková, P. Lukášová, R. Rusina, I. Holmerová, E. Jarolímová, H. Vaňková, R. Kancheva, B. Bendlová, L. Stárka, Preliminary evidence of altered steroidogenesis in women with Alzheimer's disease: Have the patients "OLDER" adrenal zona reticularis?, *J. Steroid Biochem. Mol. Biol.*, 158 (2016) 157-177. <https://doi.org/10.1016/j.jsbmb.2015.12.011>
- [9] S. Weill-Engerer, J.P. David, V. Sazdovitch, P. Liere, B. Eychenne, A. Pianos, M. Schumacher, A. Delacourte, E.E. Baulieu, Y. Akwa, Neurosteroid quantification in human brain regions: comparison between Alzheimer's and nondemented patients, *J. Clin. Endocrinol. Metab.*, 87 (2002) 5138-5143. <https://doi.org/10.1210/jc.2002-020878>
- [10] M.J.M. Nowaczyk, M.B. Irons, Smith–Lemli–Opitz syndrome: Phenotype, natural history, and epidemiology, *Am. J. Med. Genet. C Semin. Med. Genet.*, 160C (2012) 250-262. <https://doi.org/10.1002/ajmg.c.31343>
- [11] M.H. Choi, B.C. Chung, Bringing GC–MS profiling of steroids into clinical applications, *Mass Spectrom. Rev.*, 34 (2015) 219-236. <https://doi.org/10.1002/mas.21436>
- [12] B.G. Keevil, LC–MS/MS analysis of steroids in the clinical laboratory, *Clin. Biochem.*, 49 (2016) 989-997. <https://doi.org/10.1016/j.clinbiochem.2016.04.009>
- [13] V.M. Olkkonen, R. Hynynen, Interactions of oxysterols with membranes and proteins, *Mol. Asp. Med.*, 30 (2009) 123-133. <https://doi.org/10.1016/j.mam.2009.02.004>
- [14] D. Zhu, B.L. Bungart, X. Yang, Z. Zhumadilov, J.C.M. Lee, S. Askarova, Role of membrane biophysics in Alzheimer's–related cell pathways, *Front. Neurosci.*, 9 (2015) 186. <https://doi.org/10.3389/fnins.2015.00186>
- [15] E. Winkler, F. Kamp, J. Scheuring, A. Ebke, A. Fukumori, H. Steiner, Generation of Alzheimer disease-associated amyloid beta42/43 peptide by gamma-secretase can be inhibited directly by modulation of membrane thickness, *J. Biol. Chem.*, 287 (2012) 21326-21334. <https://doi.org/10.1074/jbc.M112.356659>
- [16] X. Fu, J.G. Menke, Y. Chen, G. Zhou, K.L. MacNaul, S.D. Wright, C.P. Sparrow, E.G. Lund, 27-Hydroxycholesterol is an endogenous ligand for liver X receptor in cholesterol-loaded cells, *J. Biol. Chem.*, 276 (2001) 38378-38387. <https://doi.org/10.1074/jbc.M105805200>
- [17] M. Heverin, N. Bogdanovic, D. Lütjohann, T. Bayer, I. Pikuleva, L. Bretillon, U. Diczfalusy, B. Winblad, I. Björkhem, Changes in the levels of cerebral and extracerebral sterols in the brain of

4. Analysis of neutral steroids, steroid acids and sterol sulfates

patients with Alzheimer's disease, *J. Lipid Res.*, 45 (2004) 186-193.

<https://doi.org/10.1194/jlr.M300320-JLR200>

[18] S. Hannedouche, J. Zhang, T. Yi, W. Shen, D. Nguyen, J.P. Pereira, D. Guerini, B.U. Baumgarten, S. Roggo, B. Wen, R. Knochenmuss, S. Noël, F. Gessier, L.M. Kelly, M. Vanek, S. Laurent, I. Preuss, C. Miault, I. Christen, R. Karuna, W. Li, D.-I. Koo, T. Suply, C. Schmedt, E.C. Peters, R. Falchetto, A. Katopodis, C. Spanka, M.-O. Roy, M. Detheux, Y.A. Chen, P.G. Schultz, C.Y. Cho, K. Seuwen, J.G. Cyster, A.W. Sailer, Oxysterols direct immune cell migration via EB12, *Nature*, 475 (2011) 524-527. <https://doi.org/10.1038/nature10280>

[19] T. Yi, X. Wang, L.M. Kelly, J. An, Y. Xu, A.W. Sailer, J.-A. Gustafsson, D.W. Russell, J.G. Cyster, Oxysterol gradient generation by lymphoid stromal cells guides activated B cell movement during humoral responses, *Immunity*, 37 (2012) 535-548. <https://doi.org/10.1016/j.immuni.2012.06.015>

[20] M.D. Majewska, Neurosteroids: endogenous bimodal modulators of the GABA_A receptor. Mechanism of action and physiological significance, *Prog. Neurobiol.*, 38 (1992) 379-395. [https://doi.org/10.1016/0301-0082\(92\)90025-a](https://doi.org/10.1016/0301-0082(92)90025-a)

[21] N.A. Compagnone, S.H. Mellon, Neurosteroids: biosynthesis and function of these novel neuromodulators, *Front. Neuroendocrinol.*, 21 (2000) 1-56. <https://doi.org/10.1006/frne.1999.0188>

[22] E.E. Baulieu, Neurosteroids: A novel Function of the brain, *Psychoneuroendocrinology*, 23 (1998) 963-987. [https://doi.org/10.1016/S0306-4530\(98\)00071-7](https://doi.org/10.1016/S0306-4530(98)00071-7)

[23] J. Teubel, M.K. Parr, Determination of neurosteroids in human cerebrospinal fluid in the 21st century: A review, *J. Steroid Biochem. Mol. Biol.*, 204 (2020) 105753.

<https://doi.org/10.1016/j.jsbmb.2020.105753>

[24] C.C. Smith, T.T. Gibbs, D.H. Farb, Pregnenolone sulfate as a modulator of synaptic plasticity, *Psychopharmacology (Berl.)*, 231 (2014) 3537-3556. <https://doi.org/10.1007/s00213-014-3643-x>

[25] M. Vallée, W. Mayo, M. Darnaudéry, C. Corpéchet, J. Young, M. Koehl, M. Le Moal, E.-E. Baulieu, P. Robel, H. Simon, Neurosteroids: Deficient cognitive performance in aged rats depends on low pregnenolone sulfate levels in the hippocampus, *Proc. Natl. Acad. Sci. USA*, 94 (1997) 14865-14870. <https://doi.org/10.1073/pnas.94.26.14865>

[26] M. Vaňková, M. Hill, M. Velíková, J. Včelák, G. Vacínová, P. Lukášová, D. Vejražková, K. Dvořáková, R. Rusina, I. Holmerová, E. Jarolímová, H. Vaňková, B. Bendlová, Reduced sulfotransferase SULT2A1 activity in patients with Alzheimer's disease, *Physiol. Res.*, 64 Suppl 2 (2015) S265-273. <https://doi.org/10.33549/physiolres.933160>

[27] J.I. Jung, T.B. Ladd, T. Kukar, A.R. Price, B.D. Moore, E.H. Koo, T.E. Golde, K.M. Felsenstein, Steroids as γ -secretase modulators, *FASEB J.*, 27 (2013) 3775-3785. <https://doi.org/10.1096/fj.12-225649>

[28] S. Luchetti, I. Huitinga, D.F. Swaab, Neurosteroid and GABA-A receptor alterations in Alzheimer's disease, Parkinson's disease and multiple sclerosis, *Neuroscience*, 191 (2011) 6-21. <https://doi.org/10.1016/j.neuroscience.2011.04.010>

[29] B. Lindenthal, A.L. Holleran, T.A. Aldaghlis, B. Ruan, J. George J. Schropfer, W.K. Wilson, J.K. Kelleher, Progestins block cholesterol synthesis to produce meiosis-activating sterols, *FASEB J.*, 15 (2001) 775-784. <https://doi.org/10.1096/fj.00-0214com>

[30] H. Kölsch, R. Heun, F. Jessen, J. Popp, F. Hentschel, W. Maier, D. Lutjohann, Alterations of cholesterol precursor levels in Alzheimer's disease, *Biochim. Biophys. Acta*, 1801 (2010) 945-950. <https://doi.org/10.1016/j.bbali.2010.03.001>

[31] T. Wisniewski, K. Newman, N.B. Javitt, Alzheimer's disease: brain desmosterol levels, *J. Alzheimers Dis.*, 33 (2013) 881-888. <https://doi.org/10.3233/JAD-2012-121453>

[32] M.P. Burns, G.W. Rebeck, Intracellular cholesterol homeostasis and amyloid precursor protein processing, *Biochim. Biophys. Acta*, 1801 (2010) 853-859. <https://doi.org/10.1016/j.bbali.2010.03.004>

[33] M. Sjögren, K. Blennow, The link between cholesterol and Alzheimer's disease, *World J. Biol. Psychiatry*, 6 (2005) 85-97. <https://doi.org/10.1080/15622970510029795>

4. Analysis of neutral steroids, steroid acids and sterol sulfates

- [34] J.C. Cossec, C. Marquer, M. Panchal, A.N. Lazar, C. Duyckaerts, M.C. Potier, Cholesterol changes in Alzheimer's disease: methods of analysis and impact on the formation of enlarged endosomes, *Biochim. Biophys. Acta*, 1801 (2010) 839-845. <https://doi.org/10.1016/j.bbali.2010.03.010>
- [35] J.I. Jung, A.R. Price, T.B. Ladd, Y. Ran, H.-J. Park, C. Ceballos-Diaz, L.A. Smithson, G. Hochhaus, Y. Tang, R. Akula, S. Ba, E.H. Koo, G. Shapiro, K.M. Felsenstein, T.E. Golde, Cholestenoic acid, an endogenous cholesterol metabolite, is a potent γ -secretase modulator, *Mol. Neurodegener.*, 10 (2015) 29. <https://doi.org/10.1186/s13024-015-0021-z>
- [36] M. Ogundare, S. Theofilopoulos, A. Lockhart, L.J. Hall, E. Arenas, J. Sjövall, A.G. Brenton, Y. Wang, W.J. Griffiths, Cerebrospinal fluid steroidomics: are bioactive bile acids present in brain?, *J. Biol. Chem.*, 285 (2010) 4666-4679. <https://doi.org/10.1074/jbc.M109.086678>
- [37] H.D. Ackerman, G.S. Gerhard, Bile acids in neurodegenerative disorders, *Front. Aging Neurosci.*, 8 (2016) 1-13. <https://doi.org/10.3389/fnagi.2016.00263>
- [38] M. Hill, A. Pařízek, R. Kancheva, M. Dušková, M. Velíková, L. Kříž, M. Klímková, A. Pašková, Z. Žižka, P. Matucha, M. Meloun, L. Stárka, Steroid metabolome in plasma from the umbilical artery, umbilical vein, maternal cubital vein and in amniotic fluid in normal and preterm labor, *J. Steroid Biochem. Mol. Biol.*, 121 (2010) 594-610. <http://dx.doi.org/10.1016/j.jsbmb.2009.10.012>
- [39] P. Liere, A. Pianos, B. Eychenne, A. Cambourg, S. Liu, W. Griffiths, M. Schumacher, J. Sjövall, E.-E. Baulieu, Novel lipoidal derivatives of pregnenolone and dehydroepiandrosterone and absence of their sulfated counterparts in rodent brain, *J. Lipid Res.*, 45 (2004) 2287-2302. <https://doi.org/10.1194/jlr.M400244-JLR200>
- [40] M. Hill, V. Hána Jr., M. Velíková, A. Pařízek, L. Kolátorová, J. Vítků, T. Škodová, M. Šimková, P. Šimják, R. Kancheva, M. Koucký, Z. Korkdová, K. Amcová, A. Černý, Z. Hájek, M. Dušková, J. Bulant, L. Stárka, A method for determination of one hundred endogenous steroids in human serum by gas chromatography-tandem mass spectrometry *Physiol. Res.*, (2019) 179-207. <https://doi.org/10.33549/physiolres.934124>
- [41] P. Liere, Y. Akwa, S. Weill-Engerer, B. Eychenne, A. Pianos, P. Robel, J. Sjövall, M. Schumacher, E.E. Baulieu, Validation of an analytical procedure to measure trace amounts of neurosteroids in brain tissue by gas chromatography-mass spectrometry, *J. Chromatogr. B Biomed. Sci. Appl.*, 739 (2000) 301-312. [https://doi.org/10.1016/S0378-4347\(99\)00563-0](https://doi.org/10.1016/S0378-4347(99)00563-0)
- [42] A. Meljon, S. Theofilopoulos, C.H.L. Shackleton, G.L. Watson, N.B. Javitt, H.-J. Knölker, R. Saini, E. Arenas, Y. Wang, W.J. Griffiths, Analysis of bioactive oxysterols in newborn mouse brain by LC/MS, *J. Lipid Res.*, 53 (2012) 2469-2483. <https://doi.org/10.1194/jlr.D028233>
- [43] S. Liu, J. Sjövall, W.J. Griffiths, Neurosteroids in rat brain: Extraction, isolation, and analysis by nanoscale liquid chromatography-electrospray mass spectrometry, *Anal. Chem.*, 75 (2003) 5835-5846. <https://doi.org/10.1021/ac0346297>
- [44] W.J. Griffiths, J. Abdel-Khalik, P.J. Crick, E. Yutuc, Y. Wang, New methods for analysis of oxysterols and related compounds by LC-MS, *J. Steroid Biochem. Mol. Biol.*, 162 (2016) 4-26. <https://doi.org/10.1016/j.jsbmb.2015.11.017>
- [45] A. Honda, K. Yamashita, T. Hara, T. Ikegami, T. Miyazaki, M. Shirai, G. Xu, M. Numazawa, Y. Matsuzaki, Highly sensitive quantification of key regulatory oxysterols in biological samples by LC-ESI-MS/MS, *J. Lipid Res.*, 50 (2009) 350-357. <https://doi.org/10.1194/jlr.D800040-JLR200>
- [46] C. Rustichelli, D. Pinetti, C. Lucchi, F. Ravazzini, G. Puia, Simultaneous determination of pregnenolone sulphate, dehydroepiandrosterone and allopregnanolone in rat brain areas by liquid chromatography-electrospray tandem mass spectrometry, *J. Chromatogr. B*, 930 (2013) 62-69. <https://doi.org/10.1016/j.jchromb.2013.04.035>
- [47] J. Teubel, B. Wüst, C.G. Schipke, O. Peters, M.K. Parr, Methods in endogenous steroid profiling – A comparison of gas chromatography mass spectrometry (GC-MS) with supercritical fluid chromatography tandem mass spectrometry (SFC-MS/MS), *J. Chromatogr. A*, 1554 (2018) 101-116. <https://doi.org/10.1016/j.chroma.2018.04.035>
- [48] C. Corpéchet, P. Robel, M. Axelson, J. Sjövall, E.E. Baulieu, Characterization and measurement of dehydroepiandrosterone sulfate in rat brain, *Proc Natl Acad Sci U S A*, 78 (1981) 4704-4707. <https://doi.org/10.1073/pnas.78.8.4704>

4. Analysis of neutral steroids, steroid acids and sterol sulfates

- [49] C. Corpéchet, M. Synguelakis, S. Talha, M. Axelson, J. Sjövall, R. Vihko, E.-E. Baulieu, P. Robel, Pregnenolone and its sulfate ester in the rat brain, *Brain Res.*, 270 (1983) 119-125. [https://doi.org/10.1016/0006-8993\(83\)90797-7](https://doi.org/10.1016/0006-8993(83)90797-7)
- [50] H.-F. Schött, D. Lütjohann, Validation of an isotope dilution gas chromatography–mass spectrometry method for combined analysis of oxysterols and oxyphytosterols in serum samples, *Steroids*, 99, Part B (2015) 139-150. <http://dx.doi.org/10.1016/j.steroids.2015.02.006>
- [51] K. Karu, M. Hornshaw, G. Woffendin, K. Bodin, M. Hamberg, G. Alvelius, J. Sjövall, J. Turton, Y. Wang, W.J. Griffiths, Liquid chromatography-mass spectrometry utilizing multi-stage fragmentation for the identification of oxysterols, *J. Lipid Res.*, 48 (2007) 976-987. <https://doi.org/10.1194/jlr.M600497-JLR200>
- [52] W.J. Griffiths, P.J. Crick, Y. Wang, M. Ogundare, K. Tuschl, A.A. Morris, B.W. Bigger, P.T. Clayton, Y. Wang, Analytical strategies for characterization of oxysterol lipidomes: Liver X receptor ligands in plasma, *Free Radic. Biol. Med.*, 59 (2013) 69-84. <https://doi.org/10.1016/j.freeradbiomed.2012.07.027>
- [53] A. Saeed, F. Floris, U. Andersson, I. Pikuleva, A. Lövgren-Sandblom, M. Bjerke, M. Paucar, A. Wallin, P. Svenningsson, I. Björkhem, 7 α -Hydroxy-3-oxo-4-cholestenoic acid in cerebrospinal fluid reflects the integrity of the blood-brain barrier, *J. Lipid Res.*, 55 (2014) 313-318. <https://doi.org/10.1194/jlr.P044982>
- [54] P.J. Crick, L. Beckers, M. Baes, P.P. Van Veldhoven, Y. Wang, W.J. Griffiths, The oxysterol and cholestenic acid profile of mouse cerebrospinal fluid, *Steroids*, 99 (2015) 172-177. <https://doi.org/10.1016/j.steroids.2015.02.021>
- [55] I. Björkhem, U. Andersson, E. Ellis, G. Alvelius, L. Ellegård, U. Diczfalusy, J. Sjövall, C. Einarsson, From Brain to Bile: Evidence that conjugation and ω -hydroxylation are important for elimination of 24S-hydroxycholesterol (cerebrosterol) in humans, *J. Biol. Chem.*, 276 (2001) 37004-37010. <https://doi.org/10.1074/jbc.M103828200>
- [56] W.J. Griffiths, I. Gilmore, E. Yutuc, J. Abdel-Khalik, P.J. Crick, T. Hearn, A. Dickson, B.W. Bigger, T.H. Wu, A. Goenka, A. Ghosh, S.A. Jones, Y. Wang, Identification of unusual oxysterols and bile acids with 7-oxo or 3 β ,5 α ,6 β -trihydroxy functions in human plasma by charge-tagging mass spectrometry with multistage fragmentation, *J. Lipid Res.*, 59 (2018) 1058-1070. <https://doi.org/10.1194/jlr.D083246>
- [57] B.S. Kumar, B.C. Chung, Y.-J. Lee, H.J. Yi, B.-H. Lee, B.H. Jung, Gas chromatography–mass spectrometry-based simultaneous quantitative analytical method for urinary oxysterols and bile acids in rats, *Anal. Biochem.*, 408 (2011) 242-252. <https://doi.org/10.1016/j.ab.2010.09.031>
- [58] W.J. Griffiths, M. Hornshaw, G. Woffendin, S.F. Baker, A. Lockhart, S. Heidelberger, M. Gustafsson, J. Sjövall, Y. Wang, Discovering oxysterols in plasma: A window on the metabolome, *J. Proteome Res.*, 7 (2008) 3602-3612. <https://doi.org/10.1021/pr8001639>
- [59] S. Dzeletovic, O. Breuer, E. Lund, U. Diczfalusy, Determination of cholesterol oxidation products in human plasma by isotope dilution-mass spectrometry, *Anal. Biochem.*, 225 (1995) 73-80. <https://doi.org/10.1006/abio.1995.1110>
- [60] J. Acimovic, A. Lövgren-Sandblom, K. Monostory, D. Rozman, M. Golicnik, D. Lutjohann, I. Björkhem, Combined gas chromatographic/mass spectrometric analysis of cholesterol precursors and plant sterols in cultured cells, *J. Chromatogr. B*, 877 (2009) 2081-2086. <https://doi.org/10.1016/j.jchromb.2009.05.050>
- [61] S.-J.J. Tsai, Y.-S. Zhong, J.-F. Weng, H.-H. Huang, P.-Y. Hsieh, Determination of bile acids in pig liver, pig kidney and bovine liver by gas chromatography-chemical ionization tandem mass spectrometry with total ion chromatograms and extraction ion chromatograms, *J. Chromatogr. A*, 1218 (2011) 524-533. <https://doi.org/10.1016/j.chroma.2010.11.062>
- [62] S. Matysik, G. Schmitz, Determination of steroid hormones in human plasma by GC–triple quadrupole MS, *Steroids*, 99 (2015) 151-154. <http://dx.doi.org/10.1016/j.steroids.2015.01.016>
- [63] C. Müller, J. Junker, F. Bracher, M. Giera, A gas chromatography-mass spectrometry-based whole-cell screening assay for target identification in distal cholesterol biosynthesis, *Nat. Protoc.*, 14 (2019) 2546-2570. <https://doi.org/10.1038/s41596-019-0193-z>

4. Analysis of neutral steroids, steroid acids and sterol sulfates

- [64] A. Sánchez-Guijo, V. Oji, M.F. Hartmann, H. Traupe, S.A. Wudy, Simultaneous quantification of cholesterol sulfate, androgen sulfates, and progestagen sulfates in human serum by LC-MS/MS, *J. Lipid Res.*, 56 (2015) 1843-1851. <https://doi.org/10.1194/jlr.D061499>
- [65] P.J. Crick, T. William Bentley, J. Abdel-Khalik, I. Matthews, P.T. Clayton, A.A. Morris, B.W. Bigger, C. Zerbinati, L. Tritapepe, L. Iuliano, Y. Wang, W.J. Griffiths, Quantitative charge-tags for sterol and oxysterol analysis, *Clin. Chem.*, 61 (2015) 400-411. <https://doi.org/10.1373/clinchem.2014.231332>
- [66] S. Matysik, G. Liebisch, Quantification of steroid hormones in human serum by liquid chromatography-high resolution tandem mass spectrometry, *J. Chromatogr. A*, 1526 (2017) 112-118. <https://doi.org/10.1016/j.chroma.2017.10.042>
- [67] T. Yang, T. Shu, G. Liu, H. Mei, X. Zhu, X. Huang, L. Zhang, Z. Jiang, Quantitative profiling of 19 bile acids in rat plasma, liver, bile and different intestinal section contents to investigate bile acid homeostasis and the application of temporal variation of endogenous bile acids, *J. Steroid Biochem. Mol. Biol.*, 172 (2017) 69-78. <https://doi.org/10.1016/j.jsbmb.2017.05.015>
- [68] A. Gomez-Gomez, J. Miranda, G. Feixas, A. Arranz Betegon, F. Crispi, E. Gratacós, O.J. Pozo, Determination of the steroid profile in alternative matrices by liquid chromatography tandem mass spectrometry, *J. Steroid Biochem. Mol. Biol.*, 197 (2020) 105520. <https://doi.org/10.1016/j.jsbmb.2019.105520>
- [69] C. Shackleton, O.J. Pozo, J. Marcos, GC/MS in recent years has defined the normal and clinically disordered steroidome: Will it soon be surpassed by LC/tandem MS in this role?, *J. Endocr. Soc.*, 2 (2018) 974-996. <https://doi.org/10.1210/js.2018-00135>
- [70] P.J. Taylor, Matrix effects: the Achilles heel of quantitative high-performance liquid chromatography–electrospray–tandem mass spectrometry, *Clin. Biochem.*, 38 (2005) 328-334. <https://doi.org/10.1016/j.clinbiochem.2004.11.007>
- [71] W.J. Griffiths, J. Sjövall, Bile Acids: analysis in biological fluids and tissues, *Journal of lipid research*, (2009). 10.1194/jlr.R001941
- [72] J. Sjövall, K.D.R. Setchell, Techniques for Extraction and Group Separation of Bile Acids, in: K.D.R. Setchell, D. Kritchevsky, P.P. Nair (Eds.) *The Bile Acids: Chemistry, Physiology, and Metabolism: Volume 4: Methods and Applications*, Springer US, Boston, MA, 1988, pp. 1-42.
- [73] K.D.R. Setchell, A.M. Lawson, N. Tanida, J. Sjövall, General methods for the analysis of metabolic profiles of bile acids and related compounds in feces, *Journal of lipid research*, 24 (1983) 1085-1100. 10.1016/S0022-2275(20)37923-2
- [74] J.M. Gilbert, K.D.R. Setchell, A.M. Lawson, J.P. Royston, J. Worthington, A. Kark, Detailed faecal bile acid profile: a diagnostic test for colorectal cancer?, *European journal of surgical oncology : the journal of the European Society of Surgical Oncology and the British Association of Surgical Oncology*, 12 (1986) 359-365.
- [75] Y. Yang, W.J. Griffiths, H. Nazer, J. Sjövall, Analysis of Bile Acids and Bile Alcohols in Urine by Capillary Column Liquid Chromatography–Mass Spectrometry using Fast Atom Bombardment or Electrospray Ionization and Collision-induced Dissociation, 11 (1997) 240-255. [https://doi.org/10.1002/\(SICI\)1099-0801\(199707\)11:4<240::AID-BMC686>3.0.CO;2-6](https://doi.org/10.1002/(SICI)1099-0801(199707)11:4<240::AID-BMC686>3.0.CO;2-6)
- [76] A. Båvner, M. Shafaati, M. Hansson, M. Olin, S. Shpitzen, V. Meiner, E. Leitersdorf, I. Björkhem, On the mechanism of accumulation of cholestanol in the brain of mice with a disruption of sterol 27-hydroxylase, *J. Lipid Res.*, 51 (2010) 2722-2730. <https://doi.org/10.1194/jlr.M008326>
- [77] T. Raselli, T. Hearn, A. Wyss, K. Atrott, A. Peter, I. Frey-Wagner, M.R. Spalinger, E.M. Maggio, A.W. Sailer, J. Schmitt, P. Schreiner, A. Moncsek, J. Mertens, M. Scharl, W.J. Griffiths, M. Bueter, A. Geier, G. Rogler, Y. Wang, B. Misselwitz, Elevated oxysterol levels in human and mouse livers reflect non-alcoholic steatohepatitis, *J. Lipid Res.*, (2019). <https://doi.org/10.1194/jlr.M093229>
- [78] D.-P. Kloos, E. Gay, H. Lingeman, F. Bracher, C. Müller, O.A. Mayboroda, A.M. Deelder, W.M.A. Niessen, M. Giera, Comprehensive gas chromatography–electron ionisation mass spectrometric analysis of fatty acids and sterols using sequential one-pot silylation: quantification and isotopologue analysis, *Rapid Commun. Mass Spectrom.*, 28 (2014) 1507-1514. <https://doi.org/10.1002/rcm.6923>

4. Analysis of neutral steroids, steroid acids and sterol sulfates

- [79] S. Nishida, J. Ozeki, M. Makishima, Modulation of bile acid metabolism by 1 α -hydroxyvitamin D₃ administration in mice, *Drug Metab. Dispos.*, 37 (2009) 2037-2044.
<https://doi.org/10.1124/dmd.109.027334>
- [80] A.M. Lawson, K.D.R. Setchell, Mass Spectrometry of Bile Acids, in: K.D.R. Setchell, D. Kritchevsky, P.P. Nair (Eds.) *The Bile Acids: Chemistry, Physiology, and Metabolism: Volume 4: Methods and Applications*, Springer US, Boston, MA, 1988, pp. 167-267.
- [81] Data from NIST Standard Reference Database 69: NIST Chemistry WebBook, Sitosterol TMS, NIST Mass Spectrometry Data Center,
<https://webbook.nist.gov/cgi/inchi?ID=C2625469&Mask=200#Mass-Spec> (accessed 25 September 2020).
- [82] Data from NIST Standard Reference Database 69: NIST Chemistry WebBook, Campesterol TMS, NIST Mass Spectrometry Data Center,
<https://webbook.nist.gov/cgi/inchi?ID=C55429624&Mask=200#Mass-Spec> (accessed 25 September 2020).
- [83] J. Junker, I. Chong, F. Kamp, H. Steiner, M. Giera, C. Müller, F. Bracher, Comparison of strategies for the determination of sterol sulfates via GC-MS leading to a novel deconjugation-derivatization protocol, *Molecules*, 24 (2019) 2353. <https://doi.org/10.3390/molecules24132353>
- [84] European Commission, 2019. Analytical quality control and method validation procedures for pesticide residues analysis in food and feed (SANTE/12682/2019).
- [85] DIN 32645:2008-11. <https://dx.doi.org/10.31030/1465413>
- [86] J. Folch, M. Lees, G.H. Sloane Stanley, A simple method for the isolation and purification of total lipides from animal tissues, *J. Biol. Chem.*, 226 (1957) 497-509.
- [87] E.G. Bligh, W.J. Dyer, A rapid method of total lipid extraction and purification, *Can. J. Biochem. Physiol.*, 37 (1959) 911-917. <https://doi.org/10.1139/o59-099>
- [88] J.-H. Lin, L.-Y. Liu, M.-H. Yang, M.-H. Lee, Ethyl acetate/ethyl alcohol mixtures as an alternative to folch reagent for extracting animal lipids, *J. Agric. Food Chem.*, 52 (2004) 4984-4986.
<https://doi.org/10.1021/jf049360m>
- [89] C. Breil, M. Abert Vian, T. Zemb, W. Kunz, F. Chemat, "Bligh and Dyer" and Folch methods for solid-liquid-liquid Extraction of lipids from microorganisms. comprehension of solvation mechanisms and towards substitution with alternative solvents, *Int. J. Mol. Sci.*, 18 (2017).
<https://doi.org/10.3390/ijms18040708>
- [90] M. Giera, C. Müller, F. Bracher, Analysis and experimental inhibition of distal cholesterol biosynthesis, *Chromatographia*, 78 (2015) 343-358. <https://doi.org/10.1007/s10337-014-2796-4>
- [91] W.J. Griffiths, P.J. Crick, Y. Wang, Methods for oxysterol analysis: Past, present and future, *Biochem. Pharmacol.*, 86 (2013) 3-14. <https://doi.org/10.1016/j.bcp.2013.01.027>
- [92] A. Ruokonen, T. Laatikainen, E.A. Laitinen, R. Vihko, Free and sulfate-conjugated neutral steroids in human testis tissue, *Biochemistry*, 11 (1972) 1411-1416. <https://doi.org/10.1021/bi00758a013>.
- [93] W.J. Griffiths, J. Sjövall, Analytical strategies for characterization of bile acid and oxysterol metabolomes, *Biochemical and Biophysical Research Communications*, 396 (2010) 80-84.
<https://doi.org/10.1016/j.bbrc.2010.02.149>
- [94] Richtlinien und Empfehlungen der GTFCh, Richtlinie zur Qualitätssicherung bei forensisch-toxikologischen Untersuchungen, Anhang B - Anforderungen an die Validierung von Analysenmethoden, *Toxichem. Krimtech.* (2009) 76 (3): 185 - 208.
- [95] M.M. Rahman, A.M. Abd El-Aty, J.-H. Shim, Matrix enhancement effect: A blessing or a curse for gas chromatography?—A review, *Anal. Chim. Acta*, 801 (2013) 14-21.
<https://doi.org/10.1016/j.aca.2013.09.005>
- [96] M. Heverin, Z. Ali, M. Olin, V. Tillander, M.M. Joibari, E. Makoveichuk, E. Leitersdorf, M. Warner, G. Olivercrona, J.-Å. Gustafsson, I. Björkhem, On the regulatory importance of 27-hydroxycholesterol in mouse liver, *J. Steroid Biochem. Mol. Biol.*, 169 (2017) 10-21.
<https://doi.org/10.1016/j.jsbmb.2016.02.001>

4. Analysis of neutral steroids, steroid acids and sterol sulfates

- [97] A. Meljon, Y. Wang, W.J. Griffiths, Oxysterols in the brain of the cholesterol 24-hydroxylase knockout mouse, *Biochem. Biophys. Res. Commun.*, 446 (2014) 768-774. <https://doi.org/10.1016/j.bbrc.2014.01.153>
- [98] G. Lorbek, M. Perse, S. Horvat, I. Björkhem, D. Rozman, Sex differences in the hepatic cholesterol sensing mechanisms in mice, *Molecules (Basel, Switzerland)*, 18 (2013) 11067-11085. <https://doi.org/10.3390/molecules180911067>
- [99] C.E. Marx, P. Yuan, J.D. Kiltz, R.D. Madison, L.J. Shampine, H.K. Manji, Neuroactive steroids, mood stabilizers, and neuroplasticity: alterations following lithium and changes in Bcl-2 knockout mice, *Int. J. Neuropsychopharmacol.*, 11 (2008) 547-552. <https://doi.org/10.1017/S1461145708008444>
- [100] M.J. Ebner, D.I. Corol, H. Havlíková, J.W. Honour, J.P. Fry, Identification of neuroactive steroids and their precursors and metabolites in adult male rat brain, *Endocrinology*, 147 (2006) 179-190. <https://doi.org/10.1210/en.2005-1065>
- [101] D. Caruso, M. Pesaresi, F. Abbiati, D. Calabrese, S. Giatti, L.M. Garcia-Segura, R.C. Melcangi, Comparison of plasma and cerebrospinal fluid levels of neuroactive steroids with their brain, spinal cord and peripheral nerve levels in male and female rats, *Psychoneuroendocrinology*, 38 (2013) 2278-2290. <https://doi.org/10.1016/j.psyneuen.2013.04.016>
- [102] N. Mano, T. Goto, M. Uchida, K. Nishimura, M. Ando, N. Kobayashi, J. Goto, Presence of protein-bound unconjugated bile acids in the cytoplasmic fraction of rat brain, *J. Lipid. Res.*, 45 (2004) 295-300. <https://doi.org/10.1194/jlr.M300369-JLR200>
- [103] K.D.R. Setchell, C.M. Rodrigues, C. Clerici, A. Solinas, A. Morelli, C. Gartung, J. Boyer, Bile acid concentrations in human and rat liver tissue and in hepatocyte nuclei, *Gastroenterology*, 112 (1997) 226-235. [https://doi.org/10.1016/S0016-5085\(97\)70239-7](https://doi.org/10.1016/S0016-5085(97)70239-7)

5. Characterization of inhibitors of cholesterol biosynthesis

C. Müller, J. Junker, F. Bracher, M. Giera, A gas chromatography-mass spectrometry-based whole-cell screening assay for target identification in distal cholesterol biosynthesis, Nature Protocols, 14 (2019) 2546-2570

5.1. Summary

Cholesterol biosynthesis is the target of cholesterol lowering drugs, which are frequently used in therapy of cardiovascular diseases to decrease morbidity and mortality [66, 79]. The most commonly used cholesterol lowering drugs are statins, which interfere at an early stage in pre-squalene pathway of cholesterol biosynthesis. Other drugs, such as triparanolol (MER-29) [80] and AY-9944 [81], which interfere in a later stage of cholesterol biosynthesis have not been successfully applied due to severe side effects [82]. Some of these side effects could be explained by intrinsic effects of accumulating cholesterol precursors [82]. This accumulation of cholesterol precursors was also observed in some congenital diseases, like SLOS [12, 16]. In other cases, an accumulation of steroid precursors seems to be beneficial, for example desmosterol which exhibits antiphlogistic effects *via* LXR activation [83, 84], or C8-C9 unsaturated sterols which could enhance remyelination [85]. It is further known that other drugs, *e.g.* neuroleptics, show off target effects and interfere with cholesterol biosynthesis [86-88], which is particularly critical in the treatment of pregnant women [86]. It therefore appears important to have a method that allows the identification and characterization of potential cholesterol biosynthesis inhibitors. However, identification and characterization of inhibitors of cholesterol biosynthesis is challenging. The enzymes involved in cholesterol biosynthesis are membrane bound enzymes and as such hardly available as isolated enzymes that could be used for *in vitro* binding studies or similar assays [13, 14]. This problem could be circumvented by an analytical procedur based on whole cells. This procedure was first developed by Dr. Martin Giera in the course of his dissertation [89] and was part of earlier publications [66, 90]. With this whole cell assay, possible inhibitors of the post-squalene pathway of cholesterol biosynthesis could be identified and IC₅₀ values could be determined [66, 89]. In the article presented here a further improved and refined whole cell assay, covering all enzymes of the post-squalene pathway of cholesterol biosynthesis, is described in detail. The assay utilized HL-60 cells, which were incubated with potential inhibitors for 24 h. Then the cells were hydrolyzed with aqueous NaOH and the sterols were extracted with methyl-*tert*-butyl ether (MtBE) using a liquid-liquid extraction. The sterols were then derivatized to the respective sterol TMS ethers, which were then analyzed with GC-MS. The sterol TMS ethers were

5. Characterization of inhibitors of cholesterol biosynthesis

identified using their relative retention times (RRT) based on cholestane and their obtained mass spectra. Therefore, a mass spectral library was created which contained 22 cholesterol precursors. An observed accumulation of certain sterols indicates the inhibition of the corresponding enzymes. For IC_{50} value determination, the cells were incubated with different inhibitor concentrations and ^{13}C labeled acetate. The incorporation of ^{13}C in cholesterol in relation to inhibitor concentration can then be analyzed. This protocol is designed to be adapted in other laboratories. The necessary digital library for sterol identification is provided alongside this protocol and well-known inhibitors as AY-9944 and clotrimazole are described and should be used for verification. On basis of this protocol, the integration of the cholesterol biosynthesis precursors into the new method for simultaneous determination of neutral steroids, steroid acids and sterol sulfates was possible (Chapter 4).

5.2. Personal contribution

The basic development of this assay was done by Dr. Martin Giera [66, 89, 90] and further implementation was carried on by Dr. Christoph Müller [71, 91]. These previous works were the prerequisite for this publication of the whole protocol. They contributed in writing of the manuscript as well as design and performance of the experiments.

My contributions to this article were the performance of the experiments concerning the mass spectral library and method validation, as well as editing and proof reading of the manuscript. I further prepared Figure 2 and Table S8, containing the mass spectral library. Therefore, the raw data were deconvoluted and formatted for the printed data sheets, as well as for the digital library (NIST) by me. The spectra included in the Supplementary Figures S1, S2 and S3 were processed by me in the same manner. I further determined and compiled the analytical data for Table S1, as well as the validation data in Table S2, the performance of the necessary experiments and formal analysis were also done by me.

Prof. Dr. Franz Bracher was involved in the initial method development and design of the protocol [66, 90]. He also contributed in editing and reviewing of the manuscript.

5.3. Article

The following article is printed in the original wording. The formatting may vary slightly compared to the original article.

A gas chromatography–mass spectrometry-based whole-cell screening assay for target identification in distal cholesterol biosynthesis

Christoph Müller¹, Julia Junker¹, Franz Bracher¹ and Martin Giera^{1,2*}

Distal cholesterol biosynthesis (CB) has recently taken center stage as a promising drug target in several diseases previously not linked to this biochemical pathway, including cardiovascular disease, cancer, multiple sclerosis and Alzheimer's disease. Most enzymes involved in this pathway are hard to isolate, warranting dedicated analytical tools for biochemical screening. We describe the use of gas chromatography–electron ionization mass spectrometry (GC–MS) in a whole-cell screening assay aimed at monitoring interactions with all enzymes of distal CB in a single experiment. Following cell culture and lipid extraction, the trimethylsilyl ethers of sterols are analyzed by GC–MS. Analytical data for 23 relevant sterols (intermediates) are provided, allowing their unambiguous identification. Sterol pattern analysis reveals the target enzyme on the basis of characteristic marker sterols, whereas quantification of 2-¹³C-acetate incorporation correlates with the inhibitory activity of drug candidates. The protocol can be used by both experienced scientists and newcomers to the field, allowing detection and quantification of small molecule–enzyme interactions in distal CB. The entire protocol can be carried out within two working days.

Introduction

Distal CB (Fig. 1; all substance numbers and enzyme letters used hereafter correspond to those in Fig. 1, Table 1 and Supplementary Table 1) can be defined as the biosynthetic part of CB, starting with the triterpene squalene (**1**)¹. Downstream of the first sterol, lanosterol (**3**), the biosynthesis process is divided into the Bloch and Kandutsch–Russell pathways. The Bloch pathway contains the Δ^{24} -unsaturated intermediates and is interconnected with the Kandutsch–Russell branch by the actions of the enzyme Δ^{24} -dehydrocholesterol reductase (sterol C24-reductase, DHCR24, **C**) on the respective Δ^{24} intermediates¹. Cholesterol (**11**) has long been recognized as an important storage lipid and a critical component of biomembranes, and it plays an essential role during embryonic development. Mutations in CB genes have been associated with several inborn disorders that lead to severe malformations (Table 2). Most of these defects are linked to decreased cholesterol and increased precursor levels (e.g., 7-dehydrocholesterol (**10**), desmosterol (**18**)) or the formation of abnormal sterols such as 8-dehydrocholesterol (**23**). However, the physiological and biological functions of cholesterol precursors have only recently been

¹ Department of Pharmacy, Center for Drug Research, Ludwig-Maximilians University Munich, Munich, Germany. ² Center for Proteomics and Metabolomics, Leiden University Medical Center (LUMC), Leiden, The Netherlands. *e-mail: m.a.giera@lumc.nl

5. Characterization of inhibitors of cholesterol biosynthesis

investigated and described, probably because of the low amounts present under physiological conditions as compared to cholesterol. Byskov et al.² were the first to discover critical biological functions of the precursors 4,4-dimethylcholesta-8,14,24-trien-3 β -ol (FF-MAS) (**12**) and 4,4-dimethylcholesta-8,24-dien-3 β -ol (T-MAS) (**13**) as meiosis-activating sterols. In the middle of the 20th century, several companies pursued distal CB as a possible drug target for lowering blood cholesterol. A series of promising inhibitors were developed, e.g., BIBX 79, NB-598 and MER-29 (triparanol). However, the discovery of the statins and the detrimental effects seen following AY-9944 administration in animal models³; as well as the market retraction of MER29 due to severe side effects⁴ slowed progress and diminished interest in distal CB. Therefore, it is not surprising that critical functions and roles of several cholesterol precursors have only recently been investigated and described. Important examples include cholesta-5,24-dien-3 β -ol (desmosterol) (**18**) and its hydroxylated metabolites as key regulators of liver X receptor (LXR) and sterol response element-binding protein (SREBP)⁵. Another recent example is $\Delta^{8(9)}$ -unsaturated sterols, which have been found to play a critical role in the remyelination of oligodendrocytes⁶, an important process fundamental to numerous neurological diseases (e.g., multiple sclerosis). Moreover, it has recently been discovered that several drug substances, for example, neuroleptic drugs (e.g., haloperidol)⁷⁻⁹, the anti-arrhythmic drug amiodarone¹⁰, the selective estrogen receptor modulator tamoxifen¹¹ and certain antifungals such as fluconazole¹², interfere with distal CB, possibly explaining certain activities and side effects of these drugs. Given the abovementioned birth defects, related to genetic mutations and possibly increased cholesterol precursor levels due to inhibition of certain enzymes, monitoring of distal CB might be warranted, particularly in pregnant women under treatment with drugs suspected to interfere with the biosynthetic pathway¹³. Taken together, these examples underline the critical roles and activities of several cholesterol precursors, sparking increased interest in distal CB as a bioactive pathway and possible drug target¹⁴⁻¹⁷.

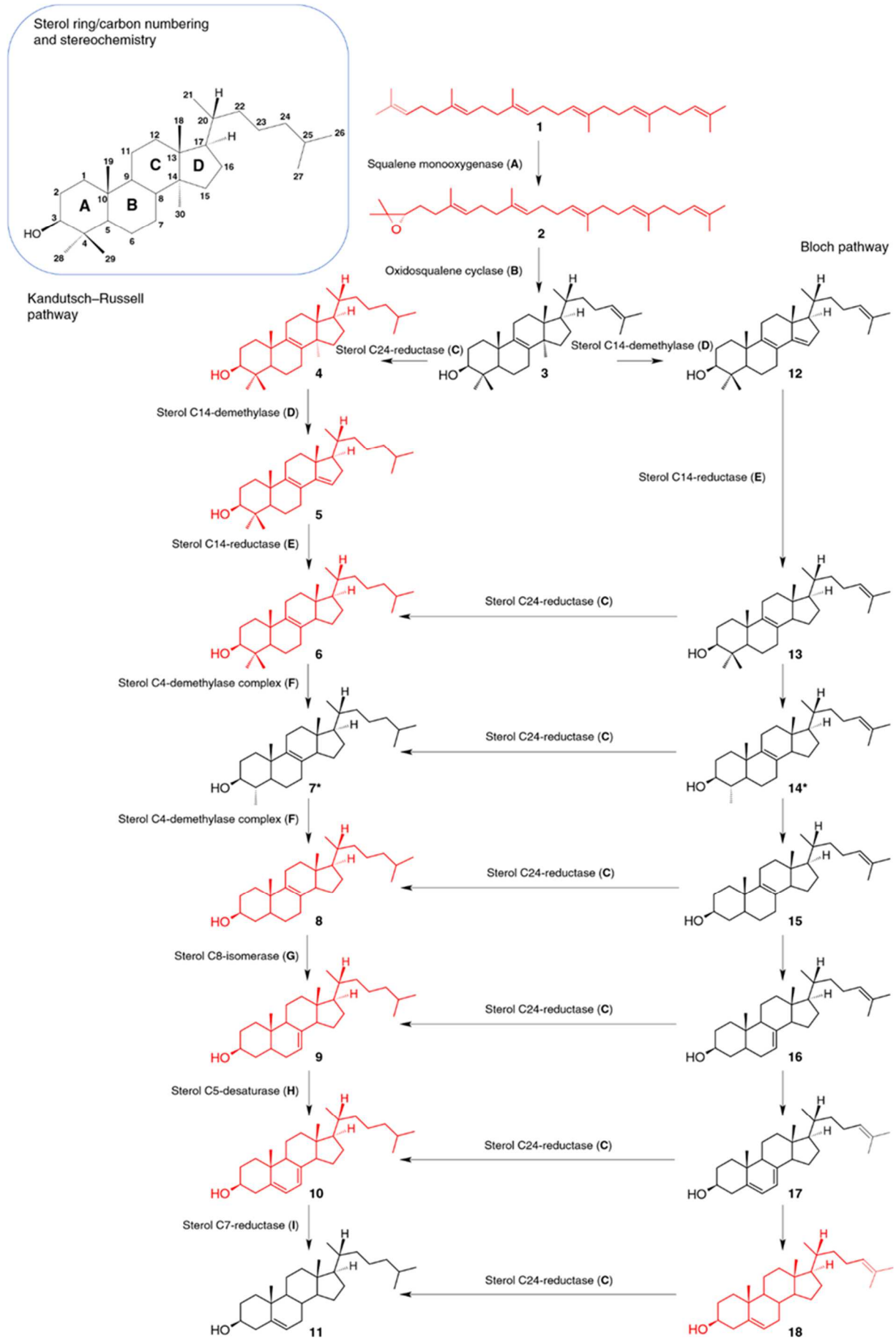
Technological solutions that allow qualitative and quantitative determination of the interaction of (drug) substances with distal CB are of great interest. However, screening for inhibitors of distal CB is not a straightforward task. Most of the enzymes involved in the transformation of squalene (**1**) to cholesterol (**11**) (Fig. 1) are membrane associated and hard to isolate and rapidly lose activity after isolation¹. Together this renders classic biochemical approaches relying on the availability of the isolated enzymes very cumbersome, demanding a dedicated assay for each enzyme of the cascade. A solution to these pitfalls is the targeted analysis of mammalian sterol patterns after incubation with test substances. Monitoring metabolic activity and molecular composition provides insights into target enzymes and allows the construction of IC₅₀ curves for test substances^{18,19}. For the targeted identification of sterol intermediates, high chromatographic separation efficiency, in combination with a characteristic information-rich detection technique, is mandatory due to the high structural similarity of the sterols of interest. GC-MS is a technique that fulfills these demands. GC-MS allows for a very high separation efficiency in combination with isomer-specific retention behavior. As an example, Fig. 2 shows the separation of the isomeric $\Delta^{7(8)}$ - and $\Delta^{8(9)}$ -sterols, lathosterol (**9**) and zymostenol (**8**), giving rise to almost identical mass spectra. Electron ionization (EI) mass spectra of the sterol trimethylsilyl (TMS) ethers present characteristic fragments that are very meaningful for structural elucidation^{20,21}. For identifying the quantitative effects of test substances on CB, we found it useful to determine 2-¹³C-acetate incorporation into the ultimate product of the biosynthetic cascade, cholesterol^{18,22}. In this way, multiple enzyme interactions can be described in one nominal value, allowing for a more facile comparison, whereas selectivity can be investigated using qualitative sterol pattern analysis. Moreover, this approach allows the quantification of the overall influence of a substance on CB, even if inhibition takes place outside distal CB. We identified HL-60 cells, a human leukemia suspension cell line characterized by high growth rates (doubling time 40 h) and active CB, as a suitable mammalian source for the study of metabolic activity of distal CB under treatment with test substances. We also carried out the procedure with a series of other cell lines, for example HEK²³ and TR146²⁴ cells, as well as induced pluripotent stem cell (iPSC)-derived neurons²⁵. However, the high growth rates in suspension, which make EDTA-trypsin treatment unnecessary, plus the robustness of the HL-60 cell line, led us to primarily use this cell line. We describe here how GC-MS-based sterol pattern analysis of the unsaponifiable matter

5. Characterization of inhibitors of cholesterol biosynthesis

obtained from the incubation of test substances with HL-60 cells can be used to identify enzyme inhibition in distal CB. In addition, we use 2-¹³C-acetate and its incorporation into cholesterol for the construction of IC₅₀ curves. We present the chromatographic data for 23 sterol TMS ethers and other relevant intermediates, as well as their characteristic EI mass spectra, used for unambiguous substance identification and sterol pattern analysis for target identification in distal CB. The protocol can be used to identify and quantify interactions in distal CB in various cell types. The protocol is useful in drug-screening campaigns aimed at distal CB, as well as for the identification of possible off-target effects.

Fig. 1 | Main cholesterol biosynthesis pathways. The predominantly observed intermediates are shown. Enzymes: **A** squalene monooxygenase, marker substance for inhibition: squalene (**1**); **B** 2,3-oxidosqualene cyclase, marker substance for inhibition: squalene epoxide (**2**); **C** sterol C24-reductase, marker sterol for inhibition: desmosterol (**18**); **D** sterol C14-demethylase, marker sterol for inhibition: dihydrolanosterol (**4**); **E** sterol C14-reductase, marker sterol for inhibition: 4,4-dimethylcholesta-8,14-dien-3 β -ol (**5**); **F** sterol C4-demethylase complex (sterol C4-methyl oxidase/ sterol C3-dehydrogenase/sterol C3-keto reductase), marker sterol for inhibition: 4,4-dimethylcholest-8-en-3 β -ol (**6**); **G** sterol C8-isomerase, marker sterol for inhibition: zymostenol (**8**); **H** sterol C5-desaturase, marker sterol for inhibition: lathosterol (**9**); **I** sterol C7-reductase (**10**). Marker sterols are shown in red. * *Mass spectrum of the sterol TMS ether is not listed in the cholesterol database (Supplementary File S1) or in Supplementary Table 1. For detailed information about the enzymes and sterols, see Table 1 and Supplementary Table 1.

5. Characterization of inhibitors of cholesterol biosynthesis



5. Characterization of inhibitors of cholesterol biosynthesis

Table 1 | Classification of enzymes, along with Enzyme Commission (EC) number, established selective inhibitors and marker sterols

Letter	Enzyme	EC no.	Established inhibitor	Marker sterol for inhibition
A	Squalene monooxygenase (SqMO)	1.14.13.132	NB-598 ^{18,82} TU-2078 ⁸³	Squalene (1)
B	Oxidosqualene cyclase (OSC)	5.4.99.7	BIBX 79 ^{18,84} Ro 48-8071 ⁸⁵	Squalene epoxide (2)
C	Sterol C24-reductase (DHCR24)	1.3.1.72	DMHCA ⁸⁶ SH-42 ²⁶	Desmosterol (18)
D	Sterol C14-demethylase (CYP51)	1.14.13.70	Clotrimazole ^{18,87}	Dihydrolanosterol (4)
E	Sterol C14-reductase (DHCR14)	1.3.1.70	Clotrimazole ^{18,87}	4,4-Dimethylcholesta-8,14-dien-3 β -ol (5)
F	Sterol C4-methyl oxidase	1.14.13.72	Aminotriazole ^{18,88}	4,4-Dimethylcholest-8-en-3 β -ol (6)
	Sterol C3-dehydrogenase	1.1.1.170	Aminotriazole ^{18,88}	
	Sterol C3-keto reductase	1.1.1.270	Aminotriazole ^{18,88}	
G	Sterol C8-isomerase (EBP)	5.3.3.5	Aminoindenols ²⁹	Zymostenol (8)
H	Sterol C5-desaturase (SC5D)	1.14.21.6	MGI-39 ¹⁹	Lathosterol (9)
I	Sterol C7-reductase (DHCR7)	1.3.1.21	Phenethyltetrahydroisoquinolines ²² BM 15766 ^{22,89}	7-Dehydrocholesterol (10)

Compound numbers refer to Supplementary Table 1.

Table 2 | Malformation syndromes caused by disorders of cholesterol biosynthesis

Associated disorder			Biochemistry			References
Name	OMIM no.	Inheritance pattern	Defective gene	Affected enzyme	Increased serum or plasma levels of marker sterols	
Desmosterolosis	602398	AR	DHCR24	Sterol C24-reductase (C)	7-Dehydrocholesterol (10), desmosterol (18)	66,90–92
Antley-Bixler-syndrome (ABS) and cytochrome P450 oxidoreductase (POR) deficiency ^a	207410 (ABS) 124015 (POR)	AR	CYP51A1 and other cytochrome P450 oxidoreductase genes	Sterol C14-demethylase (D)	Lanosterol (3), dihydrolanosterol (4), pregnenolone ^a , 17-hydroxyprogesterone ^b	58,90,91,93
Greenberg dysplasia ^a also called HEM dysplasia ^a (hydrops-ectopic calcificationmoth-eaten skeletal)	215140	AR	DHCR14 and LBR	Sterol C14-reductase (E) and lamin B receptor (LBR)	Cholesta-8,14-dien-3 β -ol (19), cholesta-8,14,24-trien-3 β -ol (20)	60,67,90,91
CHILD syndrome (congenital hemidysplasia with ichthyosiform erythroderma and limb defects syndrome) also called SC4MOL syndrome (sterol-C4 methyl oxidase-like)	308050	XL	SC4MOL, NSHDL, HSD17B7	Sterol C4-demethylase complex (F), sterol C4-methyl oxidase (SC4MOL), sterol C3-dehydrogenase (NSHDL), sterol C3-keto reductase (HSD17B7)	4,4-Dimethylcholest-8-en-3 β -ol (6), 4-methylzymostenol (7), T-MAS (13), lophenol (21)	61,68,69,90,91
CDPX2 syndrome (X-linked dominant chondrodysplasia punctata) also called Conradi–Hünemann–Happle syndrome	302960	XL	EBP	Sterol C8-isomerase (G)	Zymostenol (8), 8-dehydrocholesterol (23)	62,90,91
Lathosterolosis	607330	AR	SC5D	Sterol C5-desaturase (H)	Lathosterol (9), zymostenol (8), 7-dehydrocholesterol (10)	61,69,90,91,94
Smith-Lemli-Opitz syndrome (SLOS)	270400	AR	DHCR7	Sterol C7-reductase (I)	7-Dehydrocholesterol (10), 8-dehydrocholesterol (23)	9,58,63,64,90,91,95

AR, autosomal recessive; OMIM, Online Mendelian Inheritance in Man; XL, X-linked dominant. ^aNot dependent only on affected enzyme. ^bNot characterized here; see Hill et al.⁵⁵ for GC–MS data.

Development of the protocol

When we started our work in the field of distal CB, we wanted an assay that would allow us to interrogate all enzymes of the pathway to help us to rationally design our synthetic efforts^{26–31} and determine the target enzyme, selectivity and inhibitory efficiency. Owing to the aforementioned pitfalls concerning isolation and stability of the enzymes involved in

5. Characterization of inhibitors of cholesterol biosynthesis

the pathway, we quickly realized that isolation and testing of single enzymes or mixtures would not be practical, and we rationalized

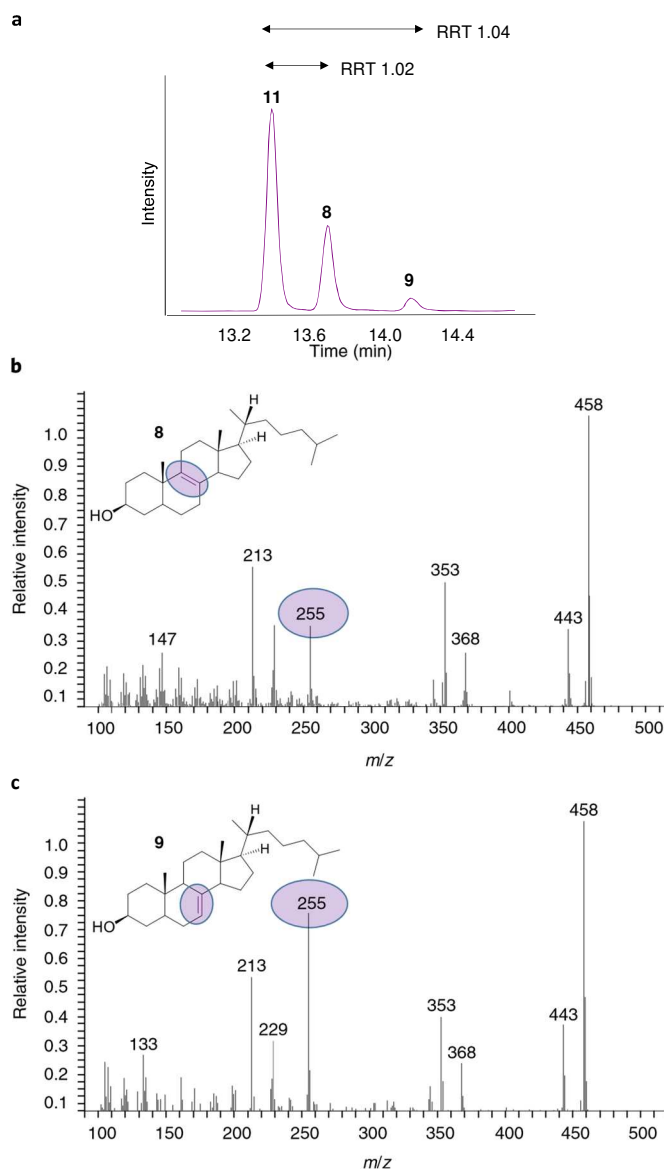


Fig. 2 | Separation of Δ^7 - and Δ^8 -sterol isomers. a–c, Although the isomeric pair zymostenol (8)/lathosterol (9) present very similar EI mass spectra (b and c, respectively), with a base peak of m/z 458 and a characteristic fragment at m/z 255, GC-based separation (a) allows for their facile separation and hence unambiguous identification.

that monitoring enzyme inhibition at the metabolic level in a whole-cell assay would be a much more straightforward and meaningful approach. We therefore sought to adapt our concept of whole-cell incubation and metabolic sterol pattern analysis—which we had developed for the screening of antifungal drugs^{21,32}—to a mammalian cell system. Initially we adapted parts of the HPLC scintillation-based method described by Fernández et al.³³. In their assay, the authors incorporate ¹⁴C-acetate into cholesterol and its precursors, followed by reverse-phase chromatographic separation and scintillation counting. Although this is a highly sensitive and useful assay, we wished for faster run times, higher throughput and the possibility of identifying unknown sterols accumulating due to (multiple) enzyme inhibition. In addition, the use of radioactively labeled materials, which is possible only in specialized laboratories and with permission, would limit flexibility. In turn, we adapted the cell culture conditions described by Fernández et al.³³ and combined

5. Characterization of inhibitors of cholesterol biosynthesis

these with GC–MS analysis and the incorporation of non-radioactive 2-¹³C-acetate for isotope labeling¹⁸. Many intermediates of distal CB are, chemically speaking, highly similar, being positional double-bond isomers or they

Table 3 | Sources of established cholesterol biosynthesis inhibitors

Inhibitor	CAS no.	Source	Item no.
Aminoindenols	ExI	Ref. ²⁹	ExI
Aminotriazole	61-82-5	Sigma-Aldrich	A8053
AY-9944	366-93-8	Cayman Chemicals	14611
BIBX 79	ExI	Ref. ⁸⁴	ExI
BM 15766	86621-94-5	Sigma-Aldrich	B8685
Clotrimazole	23593-75-1	Sigma-Aldrich	C6019
DMHCA	79066-03-8	Sigma-Aldrich	700125P
Haloperidol	52-86-8	Sigma-Aldrich	H1512
MGI-39	ExI	Ref. ¹⁹	ExI
NB-598	131060-14-5	AdooQ Bioscience	A14131
Phenethyltetrahydroisoquinolines	ExI	Ref. ²²	ExI
Ro 48-8071	161582-11-2	Cayman Chemicals	10006415
SH-42	ExI	Ref. ²⁶	ExI
Tamoxifen	10540-29-1	Sigma-Aldrich	T5648
TU-2078	ExI	Ref. ⁸³	ExI

ExI, experimental inhibitor.

present differential degrees of unsaturation and/or methylation (at C4 and C14). From an analytical perspective, this favored the use of GC–MS in combination with EI, tailor-made for the intermediates of distal CB. In comparison with HPLC, GC usually allows for higher separation efficiencies, as Eddy diffusion in the gas phase is limited, and EI-MS facilitates the ionization of neutral molecules and the generation of highly informative mass spectra (after derivatization) for substance identification^{34,35}. Initially, we developed a six-well screening assay based on liquid/liquid extraction (LLE) of neutral lipids after saponification using iso-hexane. We adapted this assay to create a 24-well assay that makes use of methyl tert-butyl ether (MtBE), as this solvent has superior solubilizing properties for sterols. The recovery for the surrogate analytes (squalene (**1**), dihydrolanosterol (**4**), lathosterol (**9**)) was tested with this solvent and found to be >80%^{18,36}. We also determined the linear regression, limit of quantification (LOQ) and limit of detection (LOD) for 15 relevant sterols (Supplementary Table 2). The detector response, expressed as the slope of the regression line of each sterol, was quite similar, with a somewhat lower value found for the Δ^{24} -unsaturated sterol, desmosterol (**18**) and a higher value found for cholesta-8,14-dien-3 β -ol (**19**) (Supplementary Table 2; ref. ³⁵). The LOD in scan mode ranged between 0.01 and 0.10 $\mu\text{g/ml}$ and the LOQ ranged between 0.02 and 0.40 $\mu\text{g/ml}$. Compared to a specific liquid chromatography–tandem mass spectrometry (LC–MS/MS) approach, the LODs for GC–MS-based analysis are ~20-fold higher (20 pg versus 1 pg on column)³⁷. We circumvented the classic lipid extraction protocols of Folch³⁸ and Bligh and Dyer³⁹, which make use of chlorinated solvents, thus causing the organic extract to be the lower phase during LLE, rendering recovery of the organic extract rather tedious. Instead, we used a facile LLE with MtBE, which has a lower density compared to water, thus being the upper organic phase for collection. Moreover, as we focused our efforts toward distal CB, we carried out a saponification step, allowing investigation of the total sterol pool. When we started to work on our protocol, numerous intermediates of distal CB were not commercially available; therefore, we carried out organic synthesis for several cholesterol precursors of the Kandutsch–Russell pathway and identified members of the Bloch pathway using inhibitor combinations and characteristic retention time shifts caused by the Δ^{24} -unsaturation in combination with the evaluation of EI mass spectra^{18–20}. For details about

5. Characterization of inhibitors of cholesterol biosynthesis

all identified sterols, see Supplementary Table 1. To validate our system, we utilized well-described inhibitors of several enzymes of distal CB (Table 3) and recorded the observed changes in sterol patterns upon incubation with the respective inhibitors, thereby allowing the identification of marker sterols characteristic of specific enzyme inhibition. Later on, we developed numerous novel experimental inhibitors to cover the remaining gaps in the pathway (see below). However, care must be taken, as several marketed inhibitors of distal CB are claimed to be selective, but when used in a whole-cell assay and depending on the applied concentrations, multiple enzyme inhibitions were observed. Striking examples are AY-9944 and MER-29 (triparanol)⁴⁰ (see Supplementary Table 3 for non-selective inhibitors).

Applications of the protocol

We have listed several example applications of the protocol below.

Drug screening approaches aimed at elucidating target enzymes in distal CB

Test substances can be evaluated for their activity in distal CB using GC-MS analysis followed by sterol pattern analysis. In addition, the described quantitative workflow allows for the generation of IC₅₀ values. Together these permit medicinal chemistry efforts to be steered in terms of selectivity and inhibitory activity. Using our approach, we have successfully characterized novel inhibitors of hitherto underexplored enzymes in distal CB, including the development of inhibitors of lathosterol oxidase (sterol C5-desaturase, **H**)^{6,19}, selective inhibitors of sterol C8-isomerase (**G**)²⁹, and selective, in vivo active inhibitors of DHCR24 (**C**)²⁶.

Evaluation of interactions of drugs with distal CB

We and others have used the described protocol for evaluating the effects of well-known, registered drugs, such as neuroleptics, on CB. Considering the recent interest in distal CB, this is an upcoming field of research with several topical contributions^{41,42}. However, the concept is not limited to neuroleptics, but can also be expanded to other substance classes and diseases^{43,44}. Identification of such previously unknown effects enables drug repurposing as an attractive new option for the fast generation of therapeutics for novel drug targets.

Diagnosis of inherited disorders in CB

The presented analytical data and approach could also be useful for the diagnosis of malformation syndromes such as the Smith-Lemli-Opitz syndrome (SLOS) and CHILD syndrome (congenital hemidysplasia with ichthyosiform erythroderma and limb defects syndrome) (Table 2), as such diseases are characterized by a substantial accumulation of cholesterol precursors in patient-derived blood^{20,26}, feces⁴⁵, tissues⁴⁵ or other matrices. The presented MS data (Supplementary Table 1) allow for the identification of 16 biosynthetic precursors of cholesterol; several non-physiological marker sterols (**19–21**, **23**), indicative of some malformation syndromes, can also be detected.

Experimental design

A detailed depiction of the Procedure can be found in Fig. 3. Experimentally, some steps could be modified or carried out in an alternative manner; however, in our experience, the described Procedure is the most practical and facile approach. Below we will use Fig. 3 as a guideline for the step-by-step description of the entire protocol.

Cell lysis and extraction of the unsaponifiable matter

As we focused our attention on distal CB, we opted for alkaline hydrolysis using sodium hydroxide, followed by the extraction of the unsaponifiable matter (neutral lipids). This procedure has the advantages that (i) no measures have to be taken in order to break the cell membrane, and (ii) no dedicated lipid extraction protocol such as those published by Bligh and Dyer³⁹ or Folch³⁸ must be applied. A point of attention is the facile autoxidation of $\Delta^{5,7}$ -sterols, in particular; hence, samples should be flooded with nitrogen or argon gas before being heated. The detection of oxysterols, e.g., 7-ketocholesterol, can be indicative of sample autoxidation⁴⁶. If autoxidation is observed, the addition of antioxidants such as

5. Characterization of inhibitors of cholesterol biosynthesis

butylated hydroxytoluene and triphenylphosphine should be considered. For more information about peroxidation of sterols, see Lamberson et al.⁴⁷. In addition, alkaline hydrolysis should be performed in glass vessels, as heating of aqueous suspensions of neutral lipids (sterols) in plastic vessels may result in the loss of these analytes, probably due to diffusion into the plastic. Moreover, extraction of leachables and extractables from polymers can occur, causing pollution of the analytical system. For extraction, we advise use of MtBE, as it is an excellent solvent for neutral lipids, and sterols in particular, and its low boiling point allows facile removal. Moreover, compared to chlorinated organic solvents, waste management is less problematic. To correct for fluctuations of sample preparation, cholestane (**26**), a non-physiological steroid, is added as an internal standard (IS) after saponification and before extraction with MtBE. The organic extracts are dried over anhydrous sodium sulfate, as any residual sodium hydroxide solution from the hydrolysis step might severely damage the GC column and diminish derivatization efficiency. Furthermore, our method uses a dispersive solid-phase extraction (dSPE) step, using a mixture of the 'primary secondary amine' (PSA) reagent and anhydrous sodium sulfate⁴⁸. This step is not critical to the approach and is hence optional; it does, however, remove residual fatty acids, which results in much cleaner extracts and improved chromatograms. During longer sequences (>100 samples), we found the dSPE protocol quite useful in limiting pollution of the GC inlet.

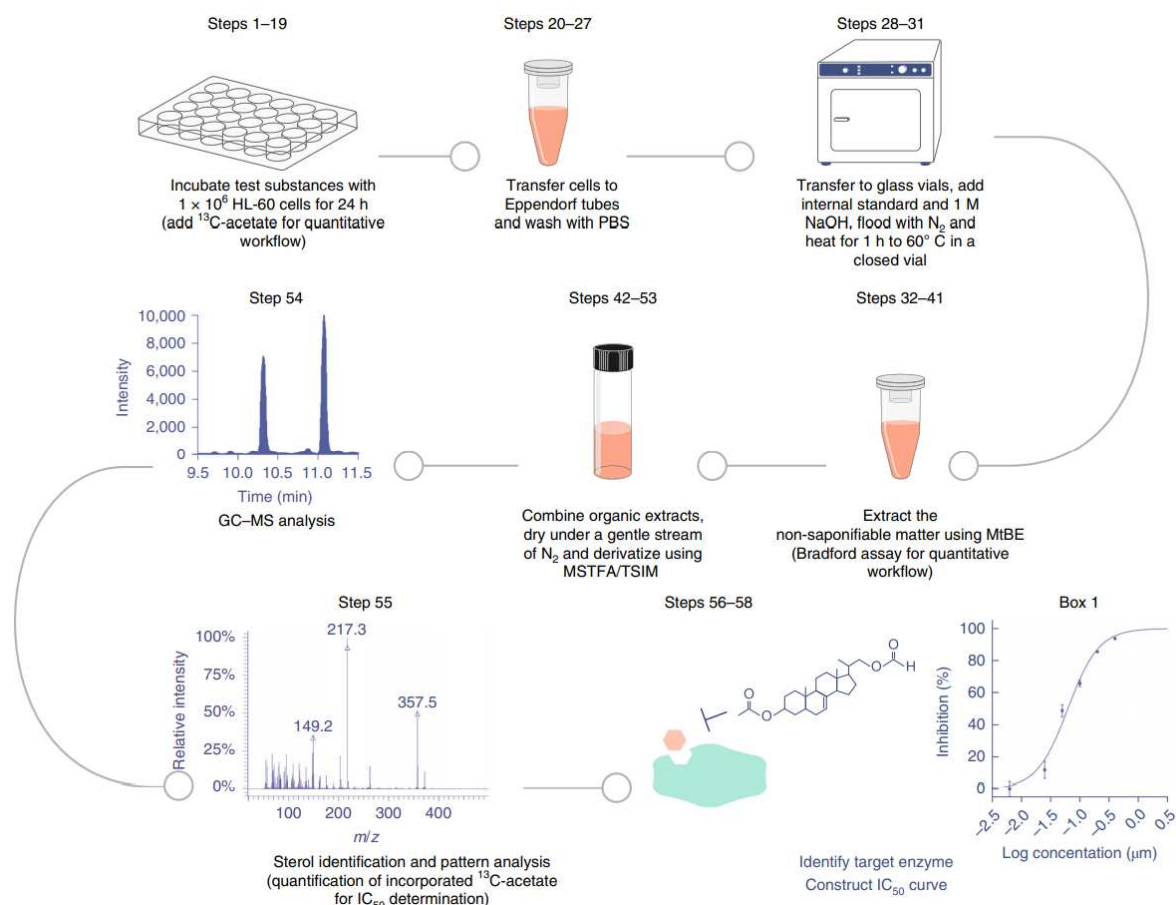


Fig. 3 | Workflow for target identification (and IC_{50} determination) in distal cholesterol biosynthesis.

Derivatization and GC-MS analysis

Although underivatized sterols can, in principle, be analyzed using GC-MS, we found that derivatization leads to increased sensitivity as well as sharper and more symmetric peak shapes. Sterol TMS ethers show characteristic fragmentations in MS, which allows distinct identification of closely related analytes. Sterols, being secondary alcohols, can present some difficulties during derivatization because of incomplete conversion. Although many

5. Characterization of inhibitors of cholesterol biosynthesis

procedures for sterol derivatization have been described^{34,49,50}, in our experience, the most straightforward one remains trimethylsilylation. We tested several reagents and combinations and found a combination of N-methyl-N-trimethylsilyl-trifluoroacetamide (MSTFA) and 10% (vol/vol) N-trimethylsilyl-imidazole (TSIM) most effective, even at room temperature (22 °C). Generally, MSTFA can be used alone; however, in this case, small amounts of pyridine should be used in order to prevent incomplete derivatization. Care must be taken here to ensure that dry and high-purity pyridine is applied. For the determination of squalene epoxide (which is analyzed in its underivatized form), a mixture of MSTFA/TSIM (1:1) is recommended; when using other silylation reagents, analyte breakdown can occur (data not shown).

Many different stationary phases have been applied in the GC-based separation of sterols. However, we make use of a highly inert 5% (vol/vol) phenylmethyl polysiloxane column. This stationary phase is broadly applicable and allows high flexibility. Particularly in combination with pre-column derivatization and mass spectrometric detection, the use of polyethylene glycol-based columns is not advisable. For a detailed discussion of the advantages and disadvantages of certain column types, we refer to the work of Gerst et al.⁵¹ and Giera et al.³⁴.

In principle, GC-MS analysis of sterols can be carried out in combination with quadrupole or ion trap (IT)-type mass analyzers. However, IT-type instruments tend to result in better quality of the obtained spectra, particularly in the full-scan mode. We observed that quadrupoles can lead to an increased intensity of low-mass fragments ($m/z < 200$), which in the case of polyunsaturated sterols can lead to a loss of the molecular ion, especially when analytes are present in minute amounts. Nevertheless, the use of an IT-type mass analyzer is not a requirement, and we have run our assay on both types of instruments, including triple-quadrupoles.

The choice for GC-MS analysis

LC-MS has become the most prominent technique for the analysis of certain classes of steroids, such as bile acids^{52,53}, conjugated sterols⁵⁴, hormones^{55,56} and oxysterols^{57,58}. However, GC-MS analysis is still the most common technique for the analysis of neutral sterols^{21,51,53,59}, such as cholesterol⁶⁰⁻⁶⁴ and its precursors^{51,60-69}. Nevertheless, some LC-based approaches are described with^{17,65} or even without derivatization^{70,71} of neutral sterols. With respect to the different detection possibilities, MS-based detection is the most used technique in sterolomics^{53,72,73}. Both LC and GC have some advantages and disadvantages (which we summarize in Supplementary Table 4). As can be seen, the two techniques are highly complementary³⁵. Krone et al.⁷⁴ have presented a comparison of the performance of GC-MS and LC-MS/MS for steroid analysis. The approach we present here aims to use GC-MS analysis to produce a screening assay based on determination of patterns of neutral sterols⁵⁰. A decade ago, when we started our research in the field of distal CB, we argued that most available knowledge described the GC-MS-based analysis of sterols, including retention time data and detailed descriptions of the EI-MS fragmentation patterns⁷⁵. Taken together, these facts let us choose GC-MS rather than LC-MS analysis as the method of choice for establishing the protocol presented here.

Biochemical evaluation and target identification

On the basis of sterol pattern analysis of the accumulation of cholesterol precursors, the target enzyme in distal CB of different low-molecular-weight inhibitors can be deduced. The accumulating precursors, in most cases, represent the target enzymes' substrates (Fig. 1 and Table 1). However, inhibiting an enzyme in distal CB does not simply stop the cascade; rather, the accumulating sterols might become substrates of downstream enzymes, resulting in the formation of non-physiological, yet very characteristic, marker sterols. One such example is cholesta-8,14-dien-3 β -ol (**19**), a nonphysiological sterol resulting from the inhibition of sterol C14-reductase (**E**) and sterol C8-isomerase (**G**), typically found when high (10 μ M) concentrations of AY-9944 are used³³. A list of all enzymes involved in distal CB, corresponding marker sterols and selective inhibitors can be found in Table 1. Cerqueira et al.⁷⁶ and Nes¹ have presented excellent overviews of the enzymes involved in CB.

5. Characterization of inhibitors of cholesterol biosynthesis

Validation of the test system with established enzyme inhibitors

To calibrate target identification in a certain cell line or type, we recommend evaluating the described procedure in-house with well-established and selective enzyme inhibitors as outlined in Tables 1 and 3.

Quantitative assay

To allow a quantitative assessment of a test substance's effects on distal CB, we opted for the use of sodium 2-¹³C-acetate. Of course, one could argue that the accumulating precursor could be quantified and used for the construction of IC₅₀ curves as described for DHCR24 (ref. 77). However, when evaluating the entire distal CB, we rationalized that multiple enzyme inhibition might occur, rendering the assessment of the quantitative effect on a specific enzyme rather complicated. Upstream blockage of the biosynthetic pathway normally limits downstream substrate accessibility in a concentration-dependent manner, thereby causing multiple enzyme inhibitions to be intertwined, influencing each other. In turn, we argued that for our purposes of comparing the efficiency of novel inhibitors of distal CB, we would prefer a single nominal value. Therefore, we evaluated the quantitation of 2-¹³C-acetate incorporation into the target molecule cholesterol. To prevent deuterium effects, carbon labeling was applied. Considering that cholesterol (**11**) is biosynthesized entirely from the acetate source acetyl-coenzyme A, a total of fifteen 2-¹³C-acetate units could be incorporated into the molecule¹ (Fig. 4). To keep this quantification as simple as possible, we decided to quantify all the ¹³C-labeled cholesterol.

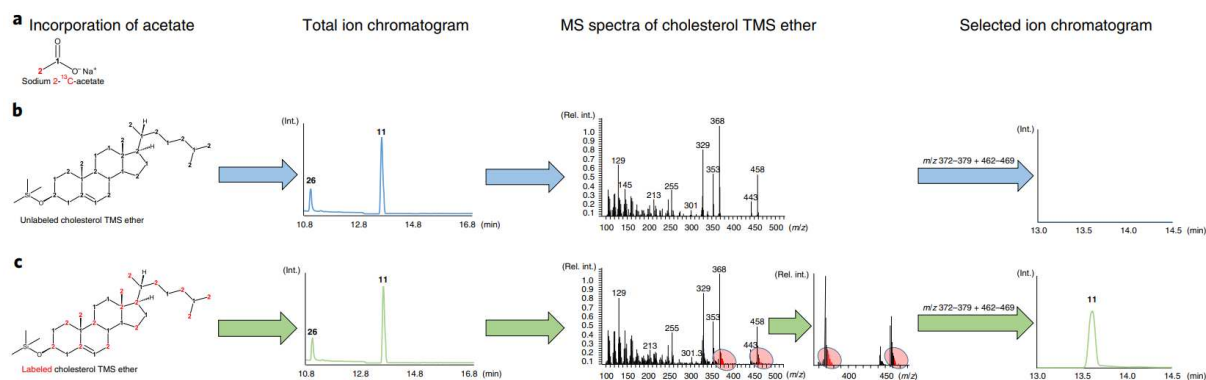


Fig. 4 | Quantitation of 2-¹³C-acetate incorporation. a–c, Structure of sodium 2-¹³C-acetate (a), black number 1 = ¹²C, red number 2 = ¹³C; incorporation of unlabeled acetate into cholesterol and its characteristic MS spectrum (b); incorporation of labeled acetate under control conditions into cholesterol and its corresponding MS spectrum (c). Internal standard cholestane (**26**), cholesterol (**11**) TMS ether. Int., intensity; Rel. int., relative intensity.

To achieve this, we validated our system and applied mass ranges of m/z 372–379 and 462–469, referring to the most abundant isotope fraction of incorporated 2-¹³C-acetate units that has a sufficient mass distance from naturally occurring isotopes. Preventing overlap with the isotopes of unlabeled cholesterol is important; otherwise, these might interfere with the analysis. Although isotopolog or flux analysis might give a more accurate view, we argued that for the purposes of substance comparison within a group of inhibitors, an easy-to-apply, facile and robust approach would be preferred and still fulfill our requirements. We tested this by evaluating the intra- and interday repeatability of the method as applied to two test substances over several days and obtained highly repeatable results¹⁸. Importantly, for this assessment, we needed to adopt a correction for the overall biomass in each experiment. As manual cell counting of dozens of samples can be very tedious, we decided to apply determination of total protein content for correction. For this purpose, we adopted the Bradford⁷⁸ method, which can be directly applied to the hydrolyzed samples just before sterol extraction. As only a very small aliquot is required for this determination, this does not result in a noteworthy influence on the outcome of the sterol assay. Importantly, the applied quantification of 2-¹³C-acetate incorporation does ultimately quantify a substances' effect on the entire CB pathway but does not allow the determination of individual IC₅₀ values for specific enzymes. We chose this approach because it allows the comparison of IC₅₀ values based on a common denominator, total CB. Such an approach allows a more

5. Characterization of inhibitors of cholesterol biosynthesis

facile adaptation of the described protocol, as it omits tedious validation procedures for each accumulating sterol. Moreover, when multiple enzyme inhibition occurs, accumulation of precursors might influence upstream and/or downstream enzymatic reactions, thereby making the comparison of multiple enzyme inhibition very challenging. Nevertheless, use of our described protocol's alternative strategies for selectively investigating specific enzymatic conversions might include the following examples. First, quantification of the accumulating precursor(s) or area ratio analysis compared to those of total cholesterol could be of value. Second, quantification of 2-¹³C-acetate incorporation into accumulating precursors might be an alternative as well. As can be seen from Supplementary Tables 5–7 (experimental data for three inhibitors of distal CB) and the corresponding MS data (some exemplary data are presented in Supplementary Figs. 1–3), as well as the recorded IC₅₀ curves (Supplementary Figs. 4–6), such analysis is in principle possible, and indications about specific enzyme inhibitions can be obtained. Another possible approach for investigating specific enzymatic activities lies in the use of labeled substrates as, for example, recently shown by Prabhu et al.⁷⁷, who studied the activity of DHCR24. Taken together, several possibilities for deciphering multi-enzyme inhibition and obtaining enzyme-specific IC₅₀ values exist. However, when applying our protocol for more than a decade, we had positive experiences quantifying total CB and here focus on our proven approach, quantifying 2-¹³C-acetate incorporation into cholesterol.

Testing of alternative materials

The presented protocol can also be applied to the characterization of physiological cholesterol precursors in blood samples^{20,26}, feces⁴⁵, tissues⁴⁵ and other matrices. The quantitative aspect of 2-¹³C-acetate incorporation is not limited to inhibitors of distal CB, but also allows a rapid assessment of if, and to what extent, a test substance affects overall CB, even for compounds inhibiting enzymes in the proximal (pre-squalene) part of CB.

Limitations of the protocol

We list some imitations below:

- Metabolomics approaches are usually designed to study hundreds of metabolites in a single analytical run. However, these approaches are usually not designed to differentiate between analytes showing only minute structural differences⁷⁹. We describe here an approach selectively aimed at the analysis of intermediates of distal CB. In turn, our approach can identify only drug targets within this pathway. As we wanted to keep the assay as simple and focused as possible, we omitted additional derivatization steps for other classes of steroids (lacking relevance in CB), for example, oxime or imine functionalization of oxosteroids (e.g., using methoxyamine in pyridine)⁴⁹.
- If full blockage of an early enzyme in the pathway occurs, inhibitory effects of the same inhibitor on downstream enzymes might be occluded. We account for this by recommending that the screening always be undertaken using both a high and a low inhibitor concentration (e.g., 1 and 50 μM). See, for example, Horling et al.²².
- This protocol has been set up as a screening tool for medicinal chemistry purposes. In turn, we focused our attention on the main metabolites in CB and marker sterols. Hence, the approach might not give full coverage of all (minute) intermediates possible. For an in-depth analysis, several sterol analysis approaches should be applied. Excellent sources of such protocols are, for example, book chapters by Goad and Akihisa⁵⁰ and Nes⁸⁰. For a recent example, impressively showing an in-depth analysis of a sterol metabolome, see ref. ⁸¹.
- Most of the sterols described here have been identified using synthetic reference materials³⁴. However, some intermediates, mainly of the Bloch pathway, were identified only on the basis of characteristic retention time differences as compared to those of their Δ²⁴-saturated counterparts from the Bloch pathway and characteristic fragmentations patterns matching those previously published (Supplementary Table 1). For these components, some care should be taken when assigning identity.

Our quantitative approach using 2-¹³C-acetate incorporation does not allow enzymes to be assigned to specific IC₅₀ values and might be jeopardized by substances inhibiting enzymes in distal as well as proximal CB

5. Characterization of inhibitors of cholesterol biosynthesis

Materials

Biological materials

- HL-60 cells (DSMZ, cat. no. ACC 3) **!CAUTION** Handle cell lines according to your institutional regulations and inform yourself about necessary bacterial and viral testing. **!CAUTION** The cell lines used in your research should be regularly checked to ensure they are authentic and are not infected with mycoplasma.

Reagents

!CAUTION Use gloves and a lab coat and ensure that work using organic solvents is carried out in a fume hood.

Cell culture

- Dimethyl sulfoxide (DMSO; >99.9% (vol/vol); Sigma-Aldrich, cat. no. D8418)
- Ethanol, absolute (for analysis; Sigma-Aldrich, cat. no. 1009831011)
- FBS (Sigma-Aldrich, cat. no. F7524)
- Lipoprotein-deficient serum (LPDS; Sigma Aldrich, cat. no. S5394)
- Medium for HL-60 cells without cholesterol (PAN Biotech, cat. no. P04-00800); alternatively, RPMI₁₆₄₀ can be used (see below)
- PBS (Sigma-Aldrich, cat. no. P4417)
- RPMI₁₆₄₀ (with phenol red; Sigma Aldrich, cat. no. R6504)
- Sterile purified water (Sigma-Aldrich, cat. no. W3500)
- Clotrimazole (as reference inhibitor; Sigma-Aldrich, cat. no. C6019)
- AY-9944 (as reference inhibitor; Cayman Chemicals, cat. no. 14611)
- Butylated hydroxytoluene (Sigma Aldrich, cat. no. W218405)
- Triphenylphosphine (Sigma Aldrich, cat. no. T84409)

(Optional) For the quantitative assay, 2-¹³C-acetate incorporation

- Sodium 2-¹³C-acetate (Sigma-Aldrich, cat. no. 279315)
- Sterile purified water (Sigma-Aldrich, cat. no. W3500)

Workup

- 5 α -Cholestane (\geq 97% (HPLC); Sigma-Aldrich, cat. no. C8003)
- Helium (99.999%; Air Liquide, cat. no. P0251S10R2A001) **!CAUTION** Helium is an asphyxiant. Use in a well-ventilated area.
- Methyl tert-butyl ether, HPLC Plus, for GC (MtBE; Sigma-Aldrich, cat. no. 650560) **!CAUTION** Use MtBE in a chemical hood and wear protective gloves, safety glasses and suitable protective clothing. MtBE is flammable, is acutely toxic and causes skin and eye irritation.
- Nitrogen (99.999%; Air Liquide, cat. no. P0271L50R2A001) **!CAUTION** Nitrogen is an asphyxiant. Use in a well-ventilated area.
- N-Methyl-N-trimethylsilyl-trifluoroacetamide (MSTFA; Macherey-Nagel, cat. no. 701270.201) **!CAUTION** Wear protective gloves, safety glasses and suitable protective clothing. MSTFA is flammable and is acutely toxic.
- N-Trimethylsilyl-imidazole (TSIM; Macherey-Nagel, cat. no. 701310.201) **!CAUTION** Wear protective gloves, safety glasses and suitable protective clothing. TSIM is flammable, corrosive and acutely toxic.
- Sodium hydroxide solution (NaOH; 1 M, reagent grade, European Pharmacopoeia; Sigma Aldrich, cat. no. 1091371000) **!CAUTION** Wear protective gloves, safety glasses and suitable protective clothing.
- Sodium hydroxide is corrosive and causes serious eye damage.

(Optional) For dSPE

- Agilent SPE bulk sorbent, primary secondary amine (PSA; Agilent, cat. no. 5982-8382)

5. Characterization of inhibitors of cholesterol biosynthesis

- Sodium sulfate, anhydrous ($\geq 99.0\%$; Sigma-Aldrich, cat. no. 239313) ▲**CRITICAL** Make sure that this reagent is dry by heating it in a laboratory cabinet to $>125\text{ }^{\circ}\text{C}$ for at least 1 h.

(Optional) For the quantitative assay, 2- ^{13}C -acetate incubation

- BSA (Albumin Fraction V, $\geq 98\%$, powdered; Carl Roth, cat. no. 8076.2)
- 96-well plate (polystyrene; Greiner Bio-One; VWR, cat. no. 391-3605)
- Hydrochloric acid (1 M; bioreagent; Sigma-Aldrich, cat. no. H9892) **!CAUTION** Wear protective gloves, safety glasses and suitable protective clothing. Hydrochloric acid is corrosive and causes serious eye damage.
- Roti-Quant Bradford reagent (Carl Roth, cat. no. K015.2)

Equipment

Cell culture

- Flow cabinet (Thermo, cat. no. 51029701)
- Centrifuge tubes (50 ml, polypropylene, sterile; VWR, cat. no. 521-1890)
- Centrifuge, benchtop (Heraeus Megafuge 8; VWR, cat. no. 525-0156)
- CO_2 incubator (37°C , 5% CO_2 ; Binder C series; VWR, cat. no. 390-0925)
- Plastic microcentrifuge Safe-Lock tube (2 ml; Eppendorf; VWR, cat. no. 20901-540)
- Fuchs–Rosenthal counting chamber (chamber depth: 0.2 mm; VWR, cat. no. 631-1171)
- Culture flask (250 ml, 75 cm^2 , polystyrene, sterile; Greiner Bio-One; VWR, cat. no. 391-3106)
- Plate (24-well; polystyrene, sterile; Greiner Bio-One; VWR, cat. no. 82050-892)
- Microscope (Zeiss Axio Observer 3; Zeiss, cat. no. 491915-0001-000)
- Serological pipette (10 ml, polystyrene, sterile; VWR, cat. no. 612-3700)

Workup

- Plastic microcentrifuge Safe-Lock tube (2 ml; Eppendorf; VWR, cat. no. 20901-540) ▲**CRITICAL** Only the highest-quality plastic material should be used.
- Benchtop microcentrifuge (Eppendorf, model no. 5415 with rotor F-45-24-11; Sigma-Aldrich, cat. no. Z604062)
- GC glass vial with screw neck (N9, amber, flat bottom, scale, wide opening (Macherey-Nagel, cat. no. 702284)
- Glass vial (4 ml, VWR screw-thread vial; VWR, cat. no. 66010-562)
- Hamilton gas-tight syringe (no. 1750 LT, 500 μl ; VWR, cat. no. 549-1184)
- Laboratory drying cabinet (Binder ED23; VWR, cat. no. 466-3251)
- Polypropylene top, screw-cap, polypropylene, white silicone septa for 4-ml glass vials (VWR, cat. no. 46610-706)
- Screw cap, N9 polypropylene (blue, center hole, silicone white/polytetrafluoroethylene red, hardness:
 - 45° shore A, thickness: 1.0 mm; Macherey-Nagel, cat. no. 702287.1)
- Ultrasonic bath (Bandelin Sonorex, model no. RK100; Bandelin, cat. no. 301)

GC–MS analysis

- GC–MS instrument (Varian, model nos. GC 3800 and MS 2200 IT)
- GC injector (Varian, model no. 1177 with split/splitless option)
- GC inlet liner (2 mm i.d., split/splitless, gooseneck; Agilent, part. no. 8004-0119)
- GC column (Agilent, model no. VF-5MS; 30-m length plus 10-m EZ-Guard, 0.25-mm i.d., 0.25- μm film thickness; Agilent, part. no. CP9013) ▲**CRITICAL** The retention times of sterol TMS ethers can strongly depend on the manufacturer of the column. The use of a column from the same type and manufacturer is recommended. If a column from a different manufacturer is used, (relative) retention times might differ from the values described here.
- GC autosampler (CTC Analytics, Combi PAL model)

5. Characterization of inhibitors of cholesterol biosynthesis

Quantitative assay, 2-¹³C-acetate incubation

- Greiner Bio-One 96-well plate (polystyrene; VWR, cat. no. 391-3605)
- Plate reader (ELISA reader; Dynex Technologies, model no. MRX II) or similar

Software

- NIST MS search v.2.0 (or higher) if use of the presented database is intended (Supplementary Data) (<https://chemdata.nist.gov/mass-spc/ms-search/>)
- Prism v.7 (GraphPad: <https://www.graphpad.com/scientific-software/prism/>)

Reagent setup

RPMI₁₆₄₀ medium containing 10% FBS (cultivation medium)

In a flow cabinet under sterile conditions, add 50 ml of FBS to 500 ml of RPMI₁₆₄₀, mix it well and store at 5 °C. The solution can be stored for 2 weeks. ▲**CRITICAL** Sterile conditions are mandatory.

Check the sterility of the medium before use.

Medium for HL-60 cells or RPMI₁₆₄₀ (test medium) containing 1% LPDS

In a flow cabinet under sterile conditions, add 5 ml of LPDS to 500 ml of medium for HL-60 cells or RPMI₁₆₄₀, mix well and store at 5 °C. The solution can be stored for 2 weeks.

▲**CRITICAL** Sterile conditions are mandatory. Check the sterility of the medium before use.

Preparation of test compound solution

The test compound must be dissolved in either RPMI₁₆₄₀, sterile purified water, ethanol or DMSO. The final concentrations of the test compound should be 1 μM and 50 μM. Prepare a 50 μM test compound solution and dilute 1:50 to obtain the 1 μM test compound solution.

▲**CRITICAL** For ethanol and DMSO, a maximum final concentration of 1.0% (vol/vol) in the test well is allowed. Prepare the test compound solution on the day of experiment.

Cholestane IS solution (10 μg/ml) for workup

Prepare a 10 μg/ml solution of 5α-cholestane in MtBE, mix it well and store it in a glass volumetric flask at 5 °C. The solution can be stored up to 6 months. **!CAUTION** MtBE is flammable and toxic. See notes above.

PBS (pH 7.4, 0.01 M phosphate buffer, 0.0027 M potassium chloride, 0.137 M sodium chloride)

In a flow cabinet under sterile conditions, dissolve one tablet in 200 ml of sterile water.

(Optional) Dispersive solid-phase adsorbent (40 mg per tube)

Mix anhydrous sodium sulfate (if necessary, dried at >125 °C for 1 h) and Agilent SPE bulk sorbent in a ratio of 7:1. The weight per tube can vary between 35 and 45 mg. This mixture should be freshly prepared on a weekly basis, ensuring dryness of the sodium sulfate used. Bulk preparations can be stored in a closed Falcon tube for up to 1 week.

Silylation reagent mixture

Add 100 μl of TSIM with a Hamilton syringe to one vial of MSTFA (1,000 μl). Shake it carefully. Keep at 5 °C. The mixture can be stored for up to 1 week. **!CAUTION** TSIM and MSTFA are flammable and toxic. See notes above. ▲**CRITICAL** The mixture is sensitive to water. It can be stored refrigerated for 1 week.

BSA calibration standards for quantitative assay, 2-¹³C-acetate incubation

Prepare the calibration standards at a concentration range of 0–140 μg/ml (0, 40, 60, 80, 100, 120, 140 μg/ml) BSA. Prepare a stock solution of 140 μg/ml in sterile water and serially dilute to reach the other concentrations. The solutions can be stored for up to 3 months at –20 °C.

5. Characterization of inhibitors of cholesterol biosynthesis

Roti-Quant solution (Bradford reagent)

Mix 5 ml of Roti-Quant with 13.75 ml of water and shake the solution well in a 50-ml centrifuge tube. This volume allows pipetting into 84 wells. ▲**CRITICAL** Prepare the solution immediately before use and mix it well.

Sodium acetate-2-¹³C solution (6.25 mg/ml)

In a flow cabinet, prepare a 6.25 mg/ml solution of sodium 2-¹³C-acetate in sterile water and mix it well. The solution can be stored for up to 3 months at -20 °C. ▲**CRITICAL** Prepare the solution under sterile conditions.

Equipment setup

Injection parameters for GC-MS analysis of squalene, squalene epoxide and sterol TMS ethers

Inject 1 µl of the sample (splitless). After 1 min, set the injector to a split ratio of 1:25. Hold the inlet at 250 °C.

Chromatographic parameters for GC-MS analysis of squalene, squalene epoxide and sterol TMS ethers

In our labs, the column we most often use for this analysis is an inert 5% phenylmethyl polysiloxane column (e.g., the VF-5MS from Agilent). Use the carrier gas helium at a constant flow rate of 1.4 ml/min. After injection, hold the column oven at 50 °C for 1 min, then ramp up at a rate of 50 °C/min to 260 °C, followed by a ramp rate of 4 °C/min to the final temperature of 310 °C, and then hold for 0.3 min. The total run time is 18.0 min.

Mass spectrometer settings for (qualitative) analysis

Set the solvent delay at 9 min. Operate the mass spectrometer in scan mode from m/z 50 to 450 for between 9 and 12 min, and implement a second segment from 12 to 18 min with a scan range from m/z 100 to 600. Sterol TMS ethers start eluting at ~13 min. Hold the MS transfer line at 270 °C. Set the manifold temperature to 50 °C and the trap temperature to 200 °C. ▲**CRITICAL** The first scan segment is required only for detecting squalene and squalene epoxide. The chromatogram might be polluted with low-molecular-weight substances, especially in the first segment. If there is no interest in detecting squalene and/or squalene epoxide, set the solvent delay to 11 min and the scan range to m/z 100–600 during the whole run. It is advisable to obtain full spectral data for each sterol TMS ether in scan mode. For identifying the sterol TMS ethers, the use of the single-ion monitoring (SIM) mode in combination with relative retention time (RRT) is not sufficient, as this would, in particular, not allow detection of possible co-elutions of critical peak pairs.

Mass spectrometer settings for IC₅₀ analysis (quantitative assay)

Quantify ¹³C-labeled cholesterol by analyzing the ions' m/z 372–379 and 462–469 values corresponding to carbon-labeled cholesterol TMS ether (11). Plot the percentage inhibition (see equation for the calculation in Box 1, step 16) relative to untreated control samples (0% inhibition) against the logarithmic inhibitor. Normalize all samples to their protein content, determined using the Bradford protein assay, as a surrogate for the respective cell count.

5. Characterization of inhibitors of cholesterol biosynthesis

Box 1 | Optional additional assays

Quantitative assay: 2-¹³C-acetate incubation • Timing 1–2 h hands-on time for 21 samples

- 1 Carry out Steps 1–11 as described in the main Procedure.
- 2 Calculate the required volume of medium. Use the following equation:

$$1,000 \mu\text{l} - (\text{volume } 1 \times 10^6 \text{ cell} + 10 \mu\text{l test compound solution} + 10 \mu\text{l } ^{13}\text{C} - \text{acetate solution}) = \text{necessary volume of medium.}$$

- 3 Add the calculated volume of medium for HL-60 cells to 21 wells of a 24-well plate.
▲ CRITICAL STEP Do not reverse the mixing steps. If the test compound solution is placed first in each 24-well plate, the solvent of the solution can evaporate. In addition, the cell suspension should not be mixed with the test compound solution to avoid temporarily increased concentrations of test compound, ethanol or DMSO.
- 4 Add 10 μl of the test compound solution in six appropriate concentrations with each concentration in triplicate.
- 5 Add 10 μl of the test compound solvent in triplicate; use the test compound solvent in triplicate as control samples.
- 6 Add the calculated volume of cell suspension.
- 7 Carry out Steps 17–32 as described in the main procedure.

Quantitative assay: Bradford protein assay • Timing 1–2 h hands-on time for 21 samples

- 8 Pipette 50 μl of the calibration standards at 0, 40, 60, 80, 100, 120, 140 $\mu\text{g/ml}$ (in triplicates) into a 96-well plate.
- 9 Pipette 25 μl (in triplicates) of each sample into a 96-well plate.
- 10 Add 25 μl of 1 M hydrochloric acid.
!CAUTION Wear protective gloves, goggles and suitable protective clothing. Hydrochloric acid is corrosive and causes serious eye damage.
▲ CRITICAL STEP Hydrochloric acid is added only to the sample wells, not the calibration standard wells. This is to neutralize the sodium hydroxide stemming from the hydrolysis step.
- 11 Add 200 μl of Roti-Quant solution (Bradford reagent) to each well.
- 12 Incubate the plate for 5 min at room temperature.
▲ CRITICAL STEP Timing is essential for this step. Make sure that you measure your samples within 5–15 min after you added the reagent.
- 13 Measure the plate with the plate reader (ELISA reader) at OD₅₉₅. Determine the concentration of each sample by plotting the OD₅₉₅ values of the calibration curve and construct the calibration function. Use the calibration function in order to calculate the protein content of your samples. **!CAUTION** The concentration of the samples must be multiplied by two.

Quantification of 2-¹³C-acetate incorporation and construction of IC₅₀ curves • Timing 0.5–1 h per sample

- 14 Carry out Steps 33–54 as described in the main Procedure.
- 15 Integrate the peak areas of cholestane (**26**) and labeled cholesterol (**11**) TMS ether. For cholestane, use m/z 217 and 357; for cholesterol, use m/z 372–379 + 462–469.
- 16 Calculate the amount of newly synthesized cholesterol by using the following equation, where As is the area of labeled cholesterol TMS ether in the samples, aISc the average of the area of the IS in the control sample (no inhibitor added), aPCc the average of the protein content of the control sample, aAc the average area of labeled cholesterol TMS ether in the control sample, ISs the area of the IS in the sample and PCs the protein content of the sample.

$$\% \text{Inhibition} = \left[1 - \left(\frac{As \times aISc \times aPCc}{aAc \times ISs \times PCs} \right) \right]$$

- 17 Plot the results in a sigmoidal curve-fitting model and calculate the IC₅₀ value. We usually carry out this step using the GraphPad Prism software. Also calculate R² values to obtain an estimate of the goodness of fit. Usually R² values >0.90–0.95 are obtained. The calculation of the 95% confidence intervals can be useful for comparing compound activities.

Procedure

▲ CRITICAL When working with lipids, laboratory glassware should be used wherever possible. In cases in which, for example, high centrifugal forces are applied, plastic cannot be circumvented. In such cases, we explicitly specify the plastic material to use.

5. Characterization of inhibitors of cholesterol biosynthesis

Incubation of test organisms with test substances • Timing 26 h; 1–2 h hands-on time for 24 samples

- 1 Cultivate HL-60 cells in 25 ml of RPMI₁₆₄₀ medium containing 10% FBS without antibiotics (Reagent setup) at 37 °C in a humidified atmosphere containing 5% CO₂.
▲ CRITICAL STEP All cell-handling steps must be carried out under sterile conditions in a flow cabinet.
- 2 Maintain the cells at 0.5–1.0 × 10⁶ cells/ml and split the cells every 2–3 d. The residual cells can be used for incubation with test substances. Normally, split cells 1:2 –1:5. 3 Transfer the residual cell culture to a 50-ml centrifuge tube. **▲ CRITICAL STEP** Transfer all the cells.
- 4 Centrifuge the tube at 1,500g for 5 min at room temperature.
- 5 Discard the supernatant, and resuspend the pellet in 10 ml of medium for HL-60 cells (or RPMI₁₆₄₀) with 1% LPDS.
- 6 Transfer 100 µl of the resuspended cell pellet to a 2-ml microcentrifuge Safe-Lock tube.
- 7 Add 900 µl of cold PBS, close the tube and manually swirl gently.
- 8 Transfer 20 µl to a Fuchs–Rosenthal counting chamber.
- 9 Count the cells.
▲ CRITICAL STEP We recommend counting two big squares of a hemocytometer, each equaling 0.2 µl (verify the size of your own counting chamber).
- 10 Calculate the number of cells in 10 ml. One big square of the recommended counting chamber equals 0.2 µl (0.2 mm³); hence, the average of the two counted big squares must be multiplied by a factor of 500,000.
- 11 Calculate the volume containing an absolute number of 1.0 × 10⁶ cells.
- 12 Calculate the volume of medium necessary to make up each well to 1,000 µl. Use the following equation:

$$1,000 \mu\text{l} - \text{volume } 1 \times 10^6 \text{ cell} + 10 \mu\text{l test compound solution}$$

$$= \text{necessary volume of medium}$$

- 13 Add the calculated volume of medium to each well of a 24-well plate.
 - 14 Add 10 µl of the test compound solution to reach final concentrations of 1 µM and 50 µM, both for each test compound. Perform each experiment in duplicate for screening purposes and triplicate in the case of IC₅₀ determination.
 - 15 Add the calculated volume of medium containing 1.0 × 10⁶ cells from Step 11.
▲ CRITICAL STEP Do not invert when mixing in Steps 13–15. If the test compound solution is placed first in each 24-well plate, the solvent of the solution can evaporate. In addition, the cell suspension should not be mixed with the test compound solution, as this might temporarily increase the concentration of the test compound, ethanol or DMSO.
- ? TROUBLESHOOTING**
- 16 Always use two control wells; to these, add the same amount of solvent as used for dissolving the test compound(s). These wells represent the untreated controls.
▲ CRITICAL STEP In addition, we also advise using a well-established inhibitor as a positive control (e.g., clotrimazole, AY-9944 or NB-598; see Table 1 and Supplementary Table 3 for additional inhibitors).
 - 17 Manually swirl the plate carefully.
▲ CRITICAL STEP The test compound solution should be mixed with the test culture without splashing into other wells or onto the cover.
 - 18 Incubate the 24-well plate for 24 ± 2 h at 37 °C in a humidified atmosphere containing 5% CO₂.
 - 19 After incubation, check all wells under a suitable light microscope. Check for bacterial or fungal contamination (i.e., the presence of smaller, frequently rapidly moving, cells) and note the morphology of the HL-60 cells. Healthy HL-60 cells should be seen in the control wells and should have a round shape.

? TROUBLESHOOTING

5. Characterization of inhibitors of cholesterol biosynthesis

Transfer of cells and preparation for cell lysis and extraction • **Timing** 0.5–1 h total time for 24 samples

- 20 Pipette the cells from all incubations into individual 2-ml plastic microcentrifuge Safe-Lock tubes. One tube per well.
- 21 Wash each well of the 24-well plate with 1 ml of cold PBS and combine with the cell suspension from Step 20.
- 22 Centrifuge the tubes at 540g for 5 min at room temperature.
- 23 Discard the supernatants, and resuspend the pellets in 1 ml of cold PBS.
- 24 Centrifuge the tubes at 540g for 5 min at room temperature.
- 25 Discard the supernatants and resuspend the pellets in 1 ml of 1 M NaOH.
!CAUTION Wear protective gloves, goggles and suitable protective clothing. Sodium hydroxide is corrosive and causes serious eye damage.
- 26 Close the tubes.
!CAUTION Close the tube tightly. Otherwise, there is a danger of loss of material and a health risk in case of spilling.
- 27 Vortex the tubes for 10 s.
!CAUTION Wear protective goggles.
▲CRITICAL STEP The pellets must be fully resuspended in sodium hydroxide solution.
- 28 Transfer the solutions to 4-ml glass vials.
▲CRITICAL STEP Only glass vials are suitable for cell lysis and saponification. Using glass avoids the extraction of leachables and extractables from the plastic tubes and overcomes loss of analytes due to adsorption to the plastic material.
- 29 Flood the glass vials with nitrogen (alternatively argon) and close the vials tightly with a PTFE screw cap.
▲CRITICAL STEP Nitrogen (or argon) prevents the oxidation of sterols. However, if oxysterols are detected, autoxidation should be considered. If autoxidation is observed, the addition of antioxidants such as butylated hydroxytoluene and triphenylphosphine should be considered.
? TROUBLESHOOTING
■ PAUSE POINT At this point, the samples can be stored at 5 °C for up to 24 h.

Cell lysis, lipid extraction and detection of squalene, squalene epoxide and sterol TMS ethers • Timing 2–3 h total time for 24 samples

- 30 Place the glass vial at 60 °C in a laboratory drying cabinet or water bath for 1 h. Vortex the vial for 10 s occasionally during the incubation (at least twice).
- 31 Allow the suspension to cool to room temperature. **!CAUTION** Wear protective goggles.
▲CRITICAL STEP Do not add MtBE to the hot mixture, as the MtBE might evaporate because its boiling point is 55 °C.
? TROUBLESHOOTING
- 32 Transfer the lysed cell suspension to a 2-ml plastic microcentrifuge Safe-Lock tube.
▲CRITICAL STEP Plastic must be used because high centrifugal forces will be required. In the presence of MtBE, notable diffusion of lipids into the plastic walls is not observed. Use only high-quality plastic, ideally the tubes from Eppendorf in the Equipment list.
▲CRITICAL STEP For quantification of de novo synthesized cholesterol, also carry out protein quantification according to Bradford as described in Box 1.
- 33 Add 650 µl of MtBE.
? TROUBLESHOOTING
- 34 Add 100 µl of IS solution (10 µg/ml).
? TROUBLESHOOTING
- 35 Close the tube.

5. Characterization of inhibitors of cholesterol biosynthesis

!CAUTION The tube must be tightly closed. Otherwise, part of the suspension will be lost during shaking or centrifugation. 36 For the first extraction step, shake the tube vigorously for 1 min by hand.

!CAUTION Wear protective goggles.

37 Centrifuge the tube at 10,000g for 5 min at room temperature.

38 Use a glass pipette to transfer ~550 μ l of the organic upper layer to a glass GC vial.

!CAUTION Avoid transferring any of the aqueous layer. Sodium hydroxide damages the GC column.

▲CRITICAL STEP If dSPE is to be applied, transfer the 550 μ l of the organic upper layer to a 2-ml plastic microcentrifuge Safe-Lock tube containing the dispersive solid-phase adsorbent. **? TROUBLESHOOTING**

39 Add 750 μ l of MtBE to the 2-ml plastic microcentrifuge Safe-Lock tube containing the lysed cell suspension.

? TROUBLESHOOTING

40 Close the tube.

!CAUTION The tube must be tightly closed. Otherwise, part of the suspension will be lost during shaking or centrifugation.

41 For the second extraction step, shake the tube vigorously for 1 min by hand.

42 Centrifuge the tube at 10,000g for 5 min at room temperature.

43 Use a glass pipette to combine the organic extracts by transferring ~650 μ l of the organic upper layer to the GC glass vial.

!CAUTION Avoid transfer of any of the aqueous layer. Sodium hydroxide damages the stationary phase of the GC column.

■ PAUSE POINT At this point, the sample can be stored at -20 °C for up to 24 h in the dark.

(Optional) Dispersive solid-phase extraction • Timing 15 min for 24 samples

▲CRITICAL Steps 44–47 are optional and are required only if performing dSPE. Otherwise, proceed directly to Step 48.

44 Combine the organic extracts by transferring 650 μ l of the organic upper layer to the 2-ml plastic microcentrifuge Safe-Lock tube, which already contains 550 μ l of extract plus dSPE sorbent from Step 38.

45 Shake the tube vigorously for 1 min by hand.

!CAUTION The tube must be tightly closed. Otherwise, a part of the suspension will be lost during shaking or centrifugation.

46 Centrifuge the tube at 10,000g for 5 min at room temperature.

47 Transfer 1,000 μ l of the (cleaned) extract to a GC glass vial (as in Step 43).

!CAUTION Pipette carefully, making sure to aspirate only the organic phase; avoid pipetting solid particles. Particles can plug the GC syringe or the GC column.

■ PAUSE POINT At this point, the sample can be stored at -20 °C for up to 24 h in the dark.

Sterol derivatization • Timing 1–2 h for 24 samples

48 Evaporate the extract to dryness under a gentle stream of nitrogen at room temperature.

!CAUTION Evaporate in a fume hood. MtBE is flammable and acutely toxic.

▲CRITICAL STEP Avoid splashing the organic phase out of the vial. If the sample cannot be evaporated to dryness, it is probable that some aqueous phase was transferred during the extraction step. Such a sample is not suitable for GC-MS analysis and should be discarded.

? TROUBLESHOOTING

■ PAUSE POINT At this point, the sample can be stored at -20 °C for up to 24 h.

49 Dissolve the dried lipid fraction in 950 μ l of MtBE.

? TROUBLESHOOTING

50 Use a Hamilton glass syringe to add 50 μ l of the silylation reagent mixture.

!CAUTION The silylation reagent mixture is flammable and toxic. See notes above.

5. Characterization of inhibitors of cholesterol biosynthesis

▲ CRITICAL STEP The mixture is sensitive to water (humidity).

- 51 Close the GC glass vial with a screw cap.
- 52 Mix the vial with a vortex mixer for 10 s.

! CAUTION Wear protective glasses and work in a fume hood. The silylation mixture is corrosive and causes severe eye damage.

- 53 Maintain the vial at room temperature for at least 30 min for complete silylation.

GC–MS analysis and identification of CB intermediates • Timing ~23 min per sample

- 54 Transfer the silylated sample to the GC–MS autosampler for analysis (Equipment setup). Analyze using the described settings.

Data analysis: identification and semi-quantitative assessment of CB intermediates

• Timing ~5 min per sample

- 55 For each peak in the GC–MS trace, calculate the RRT, i.e., the retention time relative to that of the IS. Compare the obtained RRT and mass spectra with the data in Supplementary Table 1 and the supplied mass spectral library (Supplementary Data or Supplementary Table 8, PDF of database entries).

▲ CRITICAL STEP The sterol database gives MS spectra of sterol TMS ethers and can be run using the NIST MS search program. A free downloadable version of the NIST MS search program with which our library can be browsed is available at <http://chemdata.nist.gov/mass-spc/ms-search/>. Install the program and extract the Supplementary Data S1_substance library.7z into the NISTDEMO/MSSEARCH folder. The library should now be visible. To use it for search queries, use the ‘options’ > ‘library search options’ tab. All spectra should be visible under the ‘Names’ tab. The NIST MS search program usually allows searching for mass spectra directly out of raw data files. For further information, refer to <http://www.chemdata.nist.gov/mass-spc/ms-search/>. The MS search program also allows other search terms, such as name, molecular weight and several other options, which can be found under the ‘search’ menu. Alternatively, use our spectra catalog (Supplementary Table 8).

▲ CRITICAL STEP Both the mass spectrum and the RRT must match in order to achieve an unambiguous identification. Empirically, no more than a 0.5% RRT shift is tolerated. Some mass spectra of sterol TMS ether isomers, especially pairs of Δ^7 - and Δ^8 -isomers, are very similar (Fig. 2, Supplementary Data, or Supplementary Table 8).

? TROUBLESHOOTING

Identification of the target enzyme in CB • Timing ~10 min per sample

- 56 Compare the obtained peak patterns for the identified squalene, squalene epoxide or sterol TMS ethers between sample and control.
- 57 Evaluate the differences between the two chromatograms, looking, for example, for any intermediates that accumulate only in the treated sample. Usually only cholesterol (11) can be found at significant levels in the control samples.

? TROUBLESHOOTING

- 58 Plot your accumulated sterols in the biosynthesis scheme (Fig. 1). The inhibited enzyme can now be evaluated. In addition, you can use Table 1 (marker sterols).

? TROUBLESHOOTING

5. Characterization of inhibitors of cholesterol biosynthesis

Troubleshooting

Troubleshooting advice can be found in Table 4.

Table 4 Troubleshooting table			
Step	Problem	Possible reason	Solution
15	Test substance insoluble	Insolubility	Try a different solvent: DMSO, ethanol, medium or water. In our experience, up to 1.0% (vol/vol) ethanol or DMSO does not affect the experiment
19	No cell growth	Wrong dilution of cells	Check the calculation and repeat the experiment
	Growth in negative control sample	Bacterial or fungal growth (cross-contamination)	Repeat the experiment under sterile conditions and sterilize all your consumables before use. The main reason is often a contamination of the medium used
29	Detection of significant amounts of oxysterols	Autoxidation	Addition of antioxidants such as butylated hydroxytoluene and triphenylphosphine should be considered
31, 33, 34, 38, 39, 43–49	Dripping pipette while working with MtBE	Insufficient saturation of the headspace when using air-displacement pipettes	Pipette MtBE up and down three or four times before the actual pipetting; use Hamilton glass syringes
48	Sample does not fully dry	Parts of the aqueous phase entered the extract	Discard the sample or re-dissolve the sample and start again from Step 39
55	No GC-MS signal	Clogged injection needle	Replace the syringe or try to flush out solid particles from the back by taking out the plunger, filling the syringe with hexane, and subsequently replacing the plunger and ejecting the hexane
	Only cholestane (IS) is detected and no other sterol TMS ether can be detected	Derivatization reaction did not work Insufficient cell density, insufficient cell lysis or insufficient saponification of the sterol esters; bacterial contamination	Use fresh derivatization reagents Control the cell number, reduce the inhibitor concentration. Shake the samples vigorously during cell lysis. Repeat the experiments under sterile conditions

Table continued

5. Characterization of inhibitors of cholesterol biosynthesis

Table 4 (continued)			
Step	Problem	Possible reason	Solution
	Sterol TMS ether peaks and underivatized sterol peaks are detected	Incomplete derivatization	Use fresh derivatization reagents; homogenize your sample by vortexing after addition of the silylation reagent mixture
	Poor chromatographic separation	Column degradation	Clean the column by heating to 320 °C, cut 5–10 cm off the column on the injector side or replace the column and change the liner
	Peak tailing	Too much sample was injected Column degradation, poor column installation, or, in rare cases, activation of ion trap electrodes	Dilute the sample or change to a higher split ratio in the GC settings. Replace the column, check column installation in injector, or use new deactivated IT electrodes
	Detection of peaks with similar time intervals and similar mass spacing (m/z 72) (detection of siloxane)	Column bleeding	Cut the GC column and change the liner. A possible reason is that parts of the NaOH solution were injected. Pipette the MtBE phase carefully from the NaOH solution and clean the extract well by dSPE
	The spectra are not or only partially visible in the MS Search program	Damaged file; in the 'names' tab 'a-z' is switched on	Download and extract the file again or turn off the 'a-z' function
	No or fluctuant cholestane (IS) or sterol TMS ether peak areas are detected	Poor extraction owing to poor reagents or insufficient saponification; insufficient hardware settings	Use fresh NaOH solution and shake the tubes well. The relative standard deviation of the cholestane (IS) peak area should be <20%. Check for the correct positioning of septum, liner, inlet seal and the installation depth of the column
	Unexpected mass spectra of commercial standard or more peaks	Commercial standards are not always pure or can even have incorrect labeling	Interpret the peak spectrum and compare it with Supplementary File S1, or Supplementary Table 8, PDF of database entries
57, 58	No difference in the sterol pattern of the treated sample as compared to the control sample	The peak areas of the accumulating sterols are too small or the accumulating sterols co-elute with other sterols Substance does not inhibit CB under experimental conditions	Use appropriate m/z fragments (base peaks, see Supplementary Table 1) and then compare extracted ion chromatograms. Quantify the newly synthesized cholesterol by using 2- ¹³ C-acetate (Fig. 4).
	Changes in the sterol pattern were detected, but they do not fit to one enzyme inhibition	Multi-enzyme inhibition	Use either higher or lower concentrations of the inhibitor; sometimes the effect is dose dependent
	Unknown sterols or sterols that are not in the database were detected. Detection of oxysterols	The presented database contains a broad spectrum of sterols, but not all possible sterols are mentioned	Carry out literature search and interpret the spectral data using, for example, refs. ^{34,50,51,80,96} If autoxidation is observed, the addition of antioxidants such as butylated hydroxytoluene and triphenylphosphine should be considered

Timing

Steps 1–19, incubation of HL-60 cells with test compounds: 26 h; 1–2 h hands-on time for 24 samples
 Steps 20–29, transfer and preparation for cell lysis and extraction: 0.5–1 h for 24 samples
 Steps 30–47, cell lysis, lipid extraction, preparation: 2–3 h for 24 samples
 Steps 48–53, sterol derivatization procedure: 1–2 h for 24 samples
 Step 54, GC–MS separation and detection of intermediates: 23 min per sample
 Step 55, data analysis: identification and semi-quantitative assessment of CB intermediates: ~5 min per sample for experienced users
 Steps 56–58, identification of the target enzyme in CB: ~10 min per sample for experienced users
 Box 1, steps 1–7, optional quantitative assay: 1–2 h for 21 test samples
 Box 1, steps 8–13, Bradford protein assay: 1–2 h hands-on time for 21 samples
 Box 1, steps 14–17, quantification of 2-¹³C-acetate incorporation and construction of IC₅₀ curves: 0.5–1 h per sample

5. Characterization of inhibitors of cholesterol biosynthesis

Anticipated results

Figure 5 shows typical test results for target identification, as well as IC_{50} determination. As can be seen from the upper left plot (blue), treatment of HL-60 cells using an inhibitor of proximal CB

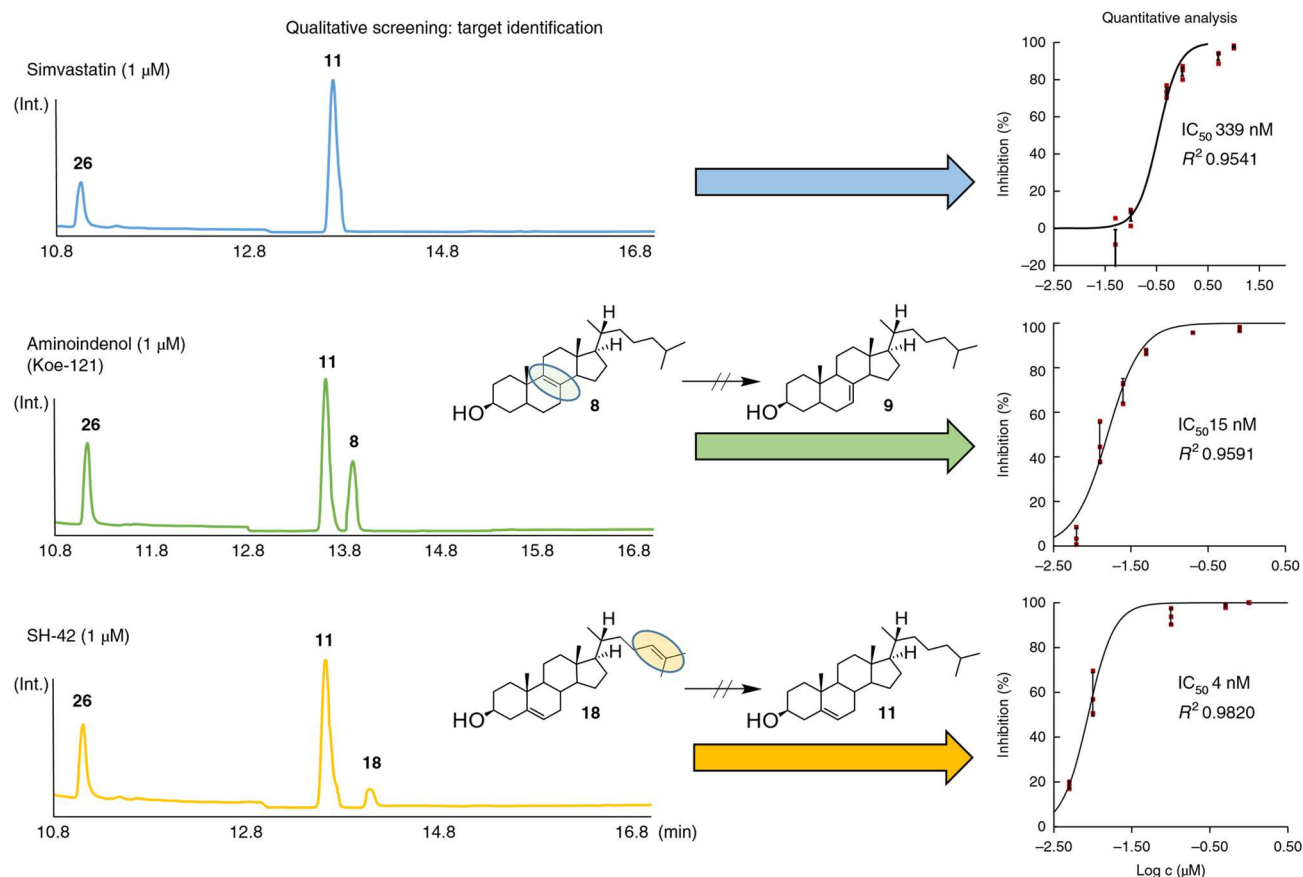


Fig. 5 | Anticipated results. The left panels show the total ion current (TIC) chromatograms obtained after incubation with the three listed inhibitors. From the chromatographic traces, the interaction with distal CB can be elucidated. No interaction with distal CB is observed for the HMG CoA-reductase inhibitor simvastatin, as no substrate of an enzyme of distal CB is detected. Inhibition of sterol C8-isomerase (G), characterized by an accumulation of zymostenol (8), is detected for Koe-121²⁹, and inhibition of DHCR24 (C), characterized by the accumulation of desmosterol (18), is observed for SH-42²⁶. On the right side, the corresponding IC_{50} curves as obtained with the described $2\text{-}^{13}\text{C}$ -acetate incorporation assay are shown ($n = 3$ for each data point; error bars show ± 1 s.d.).

(simvastatin) does not lead to a detectable accumulation of CB precursors. Nevertheless, the approach presented here can still be used to assess the overall effect of simvastatin on the incorporation of $2\text{-}^{13}\text{C}$ -acetate into the target molecule cholesterol (11). The middle (green) and lower (yellow) panels show the selective inhibition of distal CB by Koe-121 and SH-42, respectively. Koe-121 leads to an accumulation of zymostenol (8), which is characteristic for an inhibition of sterol C8-isomerase (G). SH-42 causes a selective accumulation of desmosterol (18), indicating inhibition of DHCR24 (C). Following these observations, $2\text{-}^{13}\text{C}$ -acetate incorporation analysis allows the assessment of the inhibitory potential of these components. These were found to be 15 and 4 nM, respectively. Identification of the accumulating sterols should be done on matching RRTs relative to the IS (26) and the full-scan MS spectrum (see Table 1 and Supplementary Table 8). Further examples in which the in vivo activity of SH-42 has subsequently also been established can be found in ref. ²⁶.

5. Characterization of inhibitors of cholesterol biosynthesis

Reporting Summary

Further information on research design is available in the Nature Research Reporting Summary linked to this article.

Data availability

The datasets generated and analyzed during the current study are available from the corresponding author on reasonable request.

5. Characterization of inhibitors of cholesterol biosynthesis

References

1. Nes, W. D. Biosynthesis of cholesterol and other sterols. *Chem. Rev.* 111, 6423–6451 (2011).
2. Byskov, A. G. et al. Chemical structure of sterols that activate oocyte meiosis. *Nature* 374, 559–562 (1995).
3. Roux, C., Horvath, C. & Dupuis, R. Teratogenic action and embryo lethality of AY 9944R: prevention by a hypercholesterolemia-provoking diet. *Teratology* 19, 35–38 (1979).
4. Kirby, T. J. Cataracts produced by triparanol (MER-29). *Trans. Am. Ophthalmol. Soc.* 65, 494–543 (1967).
5. Zerenturk, E. J., Sharpe, L. J., Ikonen, E. & Brown, A. J. Desmosterol and DHCR24: unexpected new directions for a terminal step in cholesterol synthesis. *Prog. Lipid Res.* 52, 666–680 (2013).
6. Hubler, Z. et al. Accumulation of 8,9-unsaturated sterols drives oligodendrocyte formation and remyelination. *Nature* 560, 372–376 (2018).
7. Canfrán-Duque, A. et al. Atypical antipsychotics alter cholesterol and fatty acid metabolism in vitro. *J. Lipid Res.* 54, 310–324 (2013).
8. Sánchez-Wandelmer, J. et al. Haloperidol disrupts lipid rafts and impairs insulin signaling in SH-SY5Y cells. *Neuroscience* 167, 143–153 (2010).
9. Boland, M. R. & Tatonetti, N. P. Investigation of 7-dehydrocholesterol reductase pathway to elucidate off-target prenatal effects of pharmaceuticals: a systematic review. *Pharmacogenomics J.* 16, 411–429 (2016).
10. Simonen, P. et al. Desmosterol accumulation in users of amiodarone. *J. Intern. Med.* 283, 93–101 (2017).
11. Kedjouar, B. et al. Molecular characterization of the microsomal tamoxifen binding site. *J. Biol. Chem.* 279, 34048–34061 (2004).
12. Giavini, E. & Menegola, E. Are azole fungicides a teratogenic risk for human conceptus? *Toxicol. Lett.* 198, 106–111 (2010).
13. Pilmis, B. et al. Antifungal drugs during pregnancy: an updated review. *J. Antimicrob. Chemother.* 70, 14–22 (2014).
14. Brown, A. J., Ikonen, E. & Olkkonen, V. M. Cholesterol precursors: more than mere markers of biosynthesis. *Curr. Opin. Lipidol.* 25, 133–139 (2014).
15. Sharpe, L. J. & Brown, A. J. Controlling cholesterol synthesis beyond 3-hydroxy-3-methylglutaryl-CoA reductase (HMGCR). *J. Biol. Chem.* 288, 18707–18715 (2013).
16. Rozman, D. & Monostory, K. Perspectives of the non-statin hypolipidemic agents. *Pharmacol. Ther.* 127, 19–40 (2010).
17. Kim, H.-Y. H. et al. Inhibitors of 7-dehydrocholesterol reductase: screening of a collection of pharmacologically active compounds in Neuro2a cells. *Chem. Res. Toxicol.* 29, 892–900 (2016).
18. Giera, M., Plössl, F. & Bracher, F. Fast and easy in vitro screening assay for cholesterol biosynthesis inhibitors in the post-squalene pathway. *Steroids* 72, 633–642 (2007).
19. Giera, M., Renard, D., Plössl, F. & Bracher, F. Lathosterol side chain amides—a new class of human lathosterol oxidase inhibitors. *Steroids* 73, 299–308 (2008).
20. Kloos, D.-P. et al. Comprehensive gas chromatography–electron ionisation mass spectrometric analysis of fatty acids and sterols using sequential one-pot silylation: quantification and isotopologue analysis. *Rapid Commun. Mass Spectrom.* 28, 1507–1514 (2014).
21. Müller, C., Binder, U., Bracher, F. & Giera, M. Antifungal drug testing by combining minimal inhibitory concentration testing with target identification by gas chromatography–mass spectrometry. *Nat. Protoc.* 12, 947–963 (2017).
22. Horling, A., Müller, C., Barthel, R., Bracher, F. & Imming, P. A new class of selective and potent 7-dehydrocholesterol reductase inhibitors. *J. Med. Chem.* 55, 7614–7622 (2012).
23. Müller, C. et al. Fungal sterol C22-desaturase is not an antimycotic target as shown by selective inhibitors and testing on clinical isolates. *Steroids* 101, 1–6 (2015).
24. Mailänder-Sánchez, D. et al. Antifungal defense of probiotic *Lactobacillus rhamnosus* GG is mediated by blocking adhesion and nutrient depletion. *PLoS ONE* 12, e0184438 (2017).
25. van der Kant, R. et al. Cholesterol metabolism is a druggable axis that independently regulates tau and amyloid-beta in iPSC-derived Alzheimer’s disease neurons. *Cell Stem Cell* 24, 363–375.e369 (2019).
26. Müller, C. et al. New chemotype of selective and potent inhibitors of human delta 24-dehydrocholesterol reductase. *Eur. J. Med. Chem.* 140, 305–320 (2017).
27. Krojer, M., Müller, C. & Bracher, F. Steroidomimetic aminomethyl spiroacetals as novel inhibitors of the enzyme $\Delta 8,7$ -sterol isomerase in cholesterol biosynthesis. *Arch. Pharm. (Weinheim)* 347, 108–122 (2014).
28. Keller, M. et al. Arylpiperidines as a new class of oxidosqualene cyclase inhibitors. *Eur. J. Med. Chem.* 109, 13–22 (2016).
29. König, M., Müller, C. & Bracher, F. Stereoselective synthesis of a new class of potent and selective inhibitors of human $\Delta 8,7$ -sterol isomerase. *Bioorg. Med. Chem.* 21, 1925–1943 (2013).
30. Fanter, L., Müller, C., Schepmann, D., Bracher, F. & Wünsch, B. Chiral-pool synthesis of 1,2,4-trisubstituted 1,4-diazepanes as novel $\sigma 1$ receptor ligands. *Bioorg. Med. Chem.* 25, 4778–4799 (2017).
31. Knappmann, I. et al. Lipase-catalyzed kinetic resolution as key step in the synthesis of enantiomerically pure ligands with 2-benzopyran structure. *Bioorg. Med. Chem.* 25, 3384–3395 (2017).
32. Renard, D., Perruchon, J., Giera, M., Müller, J. & Bracher, F. Side chain azasteroids and thia steroids as sterol methyltransferase inhibitors in ergosterol biosynthesis. *Bioorg. Med. Chem.* 17, 8123–8137 (2009).

5. Characterization of inhibitors of cholesterol biosynthesis

33. Fernández, C., Martín, M., Gómez-Coronado, D. & Lasunción, M. A. Effects of distal cholesterol biosynthesis inhibitors on cell proliferation and cell cycle progression. *J. Lipid Res.* 46, 920–929 (2005).
34. Giera, M., Müller, C. & Bracher, F. Analysis and experimental inhibition of distal cholesterol biosynthesis. *Chromatographia* 78, 343–358 (2015).
35. Shackleton, C., Pozo, O. J. & Marcos, J. GC/MS in recent years has defined the normal and clinically disordered steroidome: will it soon be surpassed by LC/tandem MS in this role? *J. Endocr. Soc.* 2, 974–996 (2018).
36. Müller, C., Staudacher, V., Krauss, J., Giera, M. & Bracher, F. A convenient cellular assay for the identification of the molecular target of ergosterol biosynthesis inhibitors and quantification of their effects on total ergosterol biosynthesis. *Steroids* 78, 483–493 (2013).
37. Honda, A. et al. Highly sensitive analysis of sterol profiles in human serum by LC-ESI-MS/MS. *J. Lipid Res.* 49, 2063–2073 (2008).
38. Folch, J., Lees, M. & Stanley, G. H. S. A simple method for the isolation and purification of total lipides from animal tissues. *J. Biol. Chem.* 226, 497–509 (1957).
39. Bligh, E. G. & Dyer, W. J. A rapid method of total lipid extraction and purification. *Can. J. Biochem. Physiol.* 37, 911–917 (1959).
40. Sánchez-Wandelmer, J. et al. Inhibition of cholesterol biosynthesis disrupts lipid raft/caveolae and affects insulin receptor activation in 3T3-L1 preadipocytes. *Biochim. Biophys. Acta* 1788, 1731–1739 (2009).
41. Korade, Ž. et al. Effect of psychotropic drug treatment on sterol metabolism. *Schizophr. Res.* 187, 74–81 (2017).
42. Korade, Z. et al. Vulnerability of DHCR7+/- mutation carriers to aripiprazole and trazodone exposure. *J. Lipid Res.* 58, 2139–2146 (2017).
43. Chua, N. K., Coates, H. W. & Brown, A. J. Cholesterol, cancer, and rebooting a treatment for athlete's foot. *Sci. Transl. Med.* 10, eaat3741 (2018).
44. Brown, A. J. & Gelissen, I. C. Cholesterol and desmosterol dancing to the beat of a different drug. *J. Intern. Med.* 283, 102–105 (2018).
45. Grimm, C. et al. High susceptibility to fatty liver disease in two-pore channel 2-deficient mice. *Nat. Commun.* 5, 4699 (2014).
46. Mutemberezi, V., Guillemot-Legris, O. & Muccioli, G. G. Oxysterols: from cholesterol metabolites to key mediators. *Prog. Lipid Res.* 64, 152–169 (2016).
47. Lamberson, C. R. et al. Propagation rate constants for the peroxidation of sterols on the biosynthetic pathway to cholesterol. *Chem. Phys. Lipids* 207, 51–58 (2017).
48. Plössl, F., Giera, M. & Bracher, F. Multiresidue analytical method using dispersive solid-phase extraction and gas chromatography/ion trap mass spectrometry to determine pharmaceuticals in whole blood. *J. Chromatogr. A* 1135, 19–26 (2006).
49. Kloos, D. et al. Analysis of biologically-active, endogenous carboxylic acids based on chromatography-mass spectrometry. *Trends Anal. Chem.* 61, 17–28 (2014).
50. Goad, L. J. & Akihisa, T. *Analysis of Sterols* 115–143 (Springer, Netherlands, 1997).
51. Gerst, N., Ruan, B., Pang, J., Wilson, W. K. & Schroepfer, G. J. An updated look at the analysis of unsaturated C27 sterols by gas chromatography and mass spectrometry. *J. Lipid Res.* 38, 1685–1701 (1997).
52. Griffiths, W. J. & Sjövall, J. Bile acids: analysis in biological fluids and tissues. *J. Lipid Res.* 51, 23–41 (2010).
53. Griffiths, W. J. et al. Cholesterolomics: an update. *Anal. Biochem.* 524, 56–67 (2017).
54. Bowers, L. D. & Sanaullah Direct measurement of steroid sulfate and glucuronide conjugates with high-performance liquid chromatography-mass spectrometry. *J. Chromatogr. B Biomed. Appl.* 687, 61–68 (1996).
55. Hill, M. et al. Steroid metabolome in plasma from the umbilical artery, umbilical vein, maternal cubital vein and in amniotic fluid in normal and preterm labor. *J. Steroid Biochem. Mol. Biol.* 121, 594–610 (2010).
56. Häkkinen, M. R. et al. Analysis by LC-MS/MS of endogenous steroids from human serum, plasma, endometrium and endometriotic tissue. *J. Pharm. Biomed. Anal.* 152, 165–172 (2018).
57. Griffiths, W. J. & Wang, Y. Analysis of oxysterol metabolomes. *Biochim. Biophys. Acta* 1811, 784–799 (2011).
58. Herron, J. et al. Identification of environmental quaternary ammonium compounds as direct inhibitors of cholesterol biosynthesis. *Toxicol. Sci.* 151, 261–270 (2016).
59. Saraiva, D., Semedo, R., Castilho, Md. C., Silva, J. M. & Ramos, F. Selection of the derivatization reagent—the case of human blood cholesterol, its precursors and phytosterols GC-MS analyses. *J. Chromatogr. B Analyt. Technol. Biomed. Life Sci.* B 879, 3806–3811 (2011).
60. Wassif, C. A. et al. HEM dysplasia and ichthyosis are likely laminopathies and not due to 3 β -hydroxysterol Δ 14-reductase deficiency. *Hum. Mol. Genet.* 16, 1176–1187 (2007).
61. Brunetti-Pierri, N. et al. Lathosterolosis, a novel multiple-malformation/mental retardation syndrome due to deficiency of 3 β -hydroxysteroid- Δ 5-desaturase. *Am. J. Hum. Genet.* 71, 952–958 (2002).
62. Has, C. et al. Gas chromatography-mass spectrometry and molecular genetic studies in families with the Conradi-Hünemann-Happle syndrome. *J. Invest. Dermatol.* 118, 851–858 (2002).
63. Kelley, R. I. Diagnosis of Smith-Lemli-Opitz syndrome by gas chromatography/mass spectrometry of 7-dehydrocholesterol in plasma, amniotic fluid and cultured skin fibroblasts. *Clin. Chim. Acta* 236, 45–58 (1995).
64. Blassberg, R., Macrae, J. I., Briscoe, J. & Jacob, J. Reduced cholesterol levels impair Smoothed activation in Smith-Lemli-Opitz syndrome. *Hum. Mol. Genet.* 25, 693–705 (2016).

5. Characterization of inhibitors of cholesterol biosynthesis

65. Korade, Z. et al. The effect of small molecules on sterol homeostasis: measuring 7-dehydrocholesterol in Dhcr7-deficient Neuro2a cells and human fibroblasts. *J. Med. Chem.* 59, 1102–1115 (2016).
66. Dias, C. et al. Desmosterolosis: an illustration of diagnostic ambiguity of cholesterol synthesis disorders. *Orphanet J. Rare Dis.* 9, 94 (2014).
67. Thompson, E. et al. Lamin B receptor-related disorder is associated with a spectrum of skeletal dysplasiaphenotypes. *Bone* 120, 354–363 (2019).
68. He, M., Smith, L. D., Chang, R., Li, X. & Vockley, J. The role of sterol-C4-methyl oxidase in epidermalbiology. *Biochim. Biophys. Acta* 1841, 331–335 (2014).
69. Acimovic, J. et al. Combined gas chromatographic/mass spectrometric analysis of cholesterol precursors and plant sterols in cultured cells. *J. Chromatogr. B Analyt. Technol. Biomed. Life Sci.* 877, 2081–2086 (2009).
70. McDonald, J. G., Smith, D. D., Stiles, A. R. & Russell, D. W. A comprehensive method for extraction and quantitative analysis of sterols and secosteroids from human plasma. *J. Lipid Res.* 53, 1399–1409 (2012).
71. Herron, J., Hines, K. M. & Xu, L. Assessment of altered cholesterol homeostasis by xenobiotics using ultrahigh performance liquid chromatography–tandem mass spectrometry. *Curr. Protoc. Toxicol.* 78, e65 (2018).
72. Griffiths, W. J. & Wang, Y. Sterolomics: state of the art, developments, limitations and challenges. *Biochim. Biophys. Acta Mol. Cell Biol. Lipids* 1862, 771–773 (2017).
73. Liere, P. & Schumacher, M. Mass spectrometric analysis of steroids: all that glitters is not gold. *Expert Rev. Endocrinol. Metab.* 10, 463–465 (2015).
74. Krone, N. et al. Gas chromatography/mass spectrometry (GC/MS) remains a pre-eminent discovery tool in clinical steroid investigations even in the era of fast liquid chromatography tandem mass spectrometry (LC/MS/MS). *J. Steroid Biochem. Mol. Biol.* 121, 496–504 (2010).
75. Nicholson, J. D. Derivative formation in the quantitative gas-chromatographic analysis of pharmaceuticals. Part II. A review. *Analyst* 103, 193–222 (1978).
76. Cerqueira, N. M. F. S. A. et al. Cholesterol biosynthesis: a mechanistic overview. *Biochemistry* 55, 5483–5506 (2016).
77. Prabhu, A. V., Luu, W. & Brown, A. J. in *Cholesterol Homeostasis: Methods and Protocols* (eds Gelissen, I. C. & Brown, A. J.) 211–219 (Springer, New York, 2017).
78. Bradford, M. M. A rapid and sensitive method for the quantitation of microgram quantities of protein utilizing the principle of protein-dye binding. *Anal. Biochem.* 72, 248–254 (1976).
79. Kohler, I., Verhoeven, A., Derks, R. J. & Giera, M. Analytical pitfalls and challenges in clinical metabolomics. *Bioanalysis* 8, 1509–1532 (2016).
80. Nes, W. R. in *Methods in Enzymology*, Vol. 111 (eds Law, J. H. & Rilling, H. C.) 3–37 (Academic Press, 1985).
81. Zhou, W. et al. Functional importance for developmental regulation of sterol biosynthesis in *Acanthamoeba castellanii*. *Biochim. Biophys. Acta Mol. Cell Biol. Lipids* 1863, 1164–1178 (2018).
82. Chugh, A., Ray, A. & Gupta, J. B. Squalene epoxidase as hypocholesterolemic drug target revisited. *Prog. Lipid Res.* 42, 37–50 (2003).
83. Matzno, S. et al. Inhibition of cholesterol biosynthesis by squalene epoxidase inhibitor avoids apoptotic cell death in L6 myoblasts. *J. Lipid Res.* 38, 1639–1648 (1997).
84. Mark, M., Muller, P., Maier, R. & Eisele, B. Effects of a novel 2,3-oxidosqualene cyclase inhibitor on the regulation of cholesterol biosynthesis in HepG2 cells. *J. Lipid Res.* 37, 148–158 (1996).
85. Chuang, J.-C. et al. Sustained and selective suppression of intestinal cholesterol synthesis by Ro 48-8071, an inhibitor of 2,3-oxidosqualene:lanosterol cyclase, in the BALB/c mouse. *Biochem. Pharmacol.* 88, 351–363 (2014).
86. Pfeifer, T. et al. Synthetic LXR agonist suppresses endogenous cholesterol biosynthesis and efficiently lowers plasma cholesterol. *Curr. Pharm. Biotechnol.* 12, 285–292 (2011).
87. Lepesheva, G. I. & Waterman, M. R. Sterol 14 α -demethylase cytochrome P450 (CYP51), a P450 in all biological kingdoms. *Biochim. Biophys. Acta* 1770, 467–477 (2007).
88. Beynen, A. C., Buechler, K. F. & J. Van Der Molen, A. Inhibition of lipogenesis in isolated hepatocytes by 3-amino-1,2,4-triazole. *Toxicology* 22, 171–178 (1981).
89. Shefer, S. et al. Regulation of rat hepatic 3 β -hydroxysterol Δ 7-reductase: substrate specificity, competitive and non-competitive inhibition, and phosphorylation/dephosphorylation. *J. Lipid Res.* 39, 2471–2476 (1998).
90. Porter, F. D. & Herman, G. E. Malformation syndromes caused by disorders of cholesterol synthesis. *J. Lipid Res.* 52, 6–34 (2011).
91. Kanungo, S., Soares, N., He, M. & Steiner, R. D. Sterol metabolism disorders and neurodevelopment—an update. *Dev. Disabil. Res. Rev.* 17, 197–210 (2013).
92. Rohanizadegan, M. & Sacharow, S. Desmosterolosis presenting with multiple congenital anomalies. *Eur. J. Med. Genet.* 61, 152–156 (2018).
93. Tomková, M., Marohnic, C., Baxová, A. & Martasek, P. Antley-Bixler syndrome or POR deficiency? *Cas Lek Cesk* 147, 261–265 (2008).
94. Ho, A. C. C. et al. Lathosterolosis: a disorder of cholesterol biosynthesis resembling smith-lemli-opitz syndrome. *JIMD Rep.* 12, 129–134 (2013).
95. DeBarber, A. E., Eroglu, Y., Merkens, L. S., Pappu, A. S. & Steiner, R. D. Smith–Lemli–Opitz syndrome. *Expert Rev. Mol. Med.* 13, e24 (2011).

5. Characterization of inhibitors of cholesterol biosynthesis

96. Brooks, C. J. W., Horning, E. C. & Young, J. S. Characterization of sterols by gas chromatography–mass spectrometry of the trimethylsilyl ethers. *Lipids* 3, 391–402 (1968).

Acknowledgements

We thank Niki Zervoudi for the artwork of Fig. 3.

Author contributions

C.M., J.J. and M.G. carried out the experiments. C.M., F.B. and M.G. designed the protocol. All authors contributed to writing the protocol.

Competing interests

The authors declare no competing interests.

Additional information

Supplementary information is available for this paper at <https://doi.org/10.1038/s41596-019-0193-z>.

Reprints and permissions information is available at www.nature.com/reprints.

Correspondence and requests for materials should be addressed to M.G.

Publisher's note: Springer Nature remains neutral with regard to jurisdictional claims in published maps and institutional affiliations.

Received: 9 October 2018; Accepted: 16 May 2019;

Published online: 24 July 2019

Related links

Key references using this protocol

Van der Kant, R. et al. *Cell Stem Cell* 24, 363–375.e9 (2019): [https://www.cell.com/cell-stem-cell/fulltext/S1934-5909\(18\)30603-9](https://www.cell.com/cell-stem-cell/fulltext/S1934-5909(18)30603-9)

Müller, C. et al. *Eur. J. Med. Chem.* 140, 305–320 (2017): <https://www.sciencedirect.com/science/article/pii/S0223523417306141>

Keller, M. et al. *Eur. J. Med. Chem.* 109, 13–22 (2016): <https://www.sciencedirect.com/science/article/pii/S0223523415304086>

Horling, A., Müller, C., Barthel, R., Bracher, F. & Imming, P. *J. Med. Chem.* 55, 7614–7622 (2012): <https://pubs.acs.org/doi/10.1021/jm3006096>

Sánchez-Wandelmer, J. et al. *Neuroscience* 167, 143–153 (2010): <https://www.sciencedirect.com/science/article/abs/pii/S0306452210001430>

Giera, M., Renard, D., Plössl, F. & Bracher, F. *Steroids* 73, 299–308 (2008): <https://www.sciencedirect.com/science/article/pii/S0039128X07002139>

Key data used in this protocol

Kloos, D.-P. et al. *Rapid Commun. Mass Spectrom.* 28, 1507–1514 (2014): <https://onlinelibrary.wiley.com/doi/abs/10.1002/rcm.6923>

Giera, M., Plössl, F. & Bracher, F. *Steroids* 72, 633–642 (2007): <https://www.sciencedirect.com/science/article/pii/S0039128X07000736>

5.4. Supplementary material

nature
protocols

SUPPLEMENTARY INFORMATION

<https://doi.org/10.1038/s41596-019-0193-z>

In the format provided by the authors and unedited.

A gas chromatography–mass spectrometrybased whole-cell screening assay for target identification in distal cholesterol biosynthesis

Christoph Müller¹, Julia Junker¹, Franz Bracher¹ and Martin Giera^{1,2*}

¹Department of Pharmacy, Center for Drug Research, Ludwig-Maximilians University Munich, Munich, Germany. ²Center for Proteomics and Metabolomics, Leiden University Medical Center (LUMC), Leiden, The Netherlands. *e-mail: m.a.giera@lumc.nl

5. Characterization of inhibitors of cholesterol biosynthesis

Compound			Substance information						Chromatographic characteristics RRT TMS ether		MS characteristics TMS ether		Reference
No.	IUPAC Name	Trivial Name	Chemical Formula	M [g/mol]	CAS Number	Origin	Distributor	Order Number	Cholestane	Cholesterol	M [g/mol]	Base peak [m/z]	
1	(6E,10E,14E,18E)-2,6,10,15,19,23Hexamethyltetracosahexaene	Squalene	C ₃₀ H ₅₀	410.4	111-02-4	C	Sigma-Aldrich	S3626	0.95	0.76		69	1
2	2,2-Dimethyl-(S)-((3E,7E,11E,15E)3,7,12,16,20pentamethylhenicosahenicosapentaenyl)oxirane	Squalene epoxide	C ₃₀ H ₅₀ O	426.4	7200-26-2	OS ²	Sigma-Aldrich	41043	1.05	0.83		81	3
3	4,4,14-Trimethylcholesta-8,24dien-3β-ol	Lanosterol	C ₃₀ H ₅₀ O	426.4	79-63-0	C	Sigma-Aldrich	L5768	1.44	1.16	498.4	393	4,5
4	4,4,14-Trimethylcholest-8-en-3β-ol	Dihydrolanosterol	C ₃₀ H ₅₂ O	428.4	79-62-9	OS ⁶	Toronto Research Chemicals	D449855	1.40	1.12	500.4	395	1,4
5	4,4-Dimethylcholesta-8,14-dien-3β-ol		C ₂₉ H ₄₈ O	412.4	19456-83-8	OS ⁷			1.42	1.13	484.5	379	8
6	4,4-Dimethylcholest-8en-3β-ol		C ₂₉ H ₅₀ O	414.4	5241-24-7	OS ⁷	Toronto Research Chemicals	D230905	1.43	1.14	486.4	486	
7	4-Methylcholest-8-en-3β-ol	4-Methylzymostenol	C ₂₈ H ₄₈ O	400.4	5241-22-5						472.4		
8	Cholest-8-en-3β-ol	Zymostenol	C ₂₇ H ₄₆ O	386.4	566-97-2	OS ⁶	Sigma-Aldrich	700118P	1.27	1.02	458.4	458	9,10
9	Cholest-7-en-3β-ol	Lathosterol	C ₂₇ H ₄₆ O	386.4	80-99-9	OS ⁶	Sigma-Aldrich	C3652	1.31	1.04	458.4	458	4,10

5. Characterization of inhibitors of cholesterol biosynthesis

10	Cholesta-5,7-dien-3 β -ol	7-Dehydrocholesterol	C ₂₇ H ₄₄ O	384.3	434-16-2	C	Sigma-Aldrich	30800	1.29	1.03	456.4	351	4,10
11	Cholest-5-en-3 β -ol	Cholesterol	C ₂₇ H ₄₆ O	386.4	57-88-5	C	Sigma-Aldrich	C8667	1.26	1.00	458.4	368	4,10
12	4,4-Dimethylcholesta-8,14,24-trien-3 β -ol	FF-MAS	C ₂₉ H ₄₄ O	410.4	64284-64-6	MS (I)	Sigma-Aldrich	700077P	1.47	1.17	482.4	482	1
13	4,4-Dimethylcholesta-8,24-dien-3 β -ol	T-MAS	C ₂₉ H ₄₈ O	412.4	7448-02-4	MS (II)	Sigma-Aldrich	700073P	1.48	1.18	484.4	379	1
14	4-Methylcholesta-8,24dien-3 β -ol	4-Methylzymosterol	C ₂₈ H ₄₆ O	398.4	7448-03-5		Toronto Research Chemicals	M338615			470.4		
15	Cholesta-8,24-dien-3 β -ol	Zymosterol	C ₂₇ H ₄₄ O	384.3	128-33-6	Isol.	Sigma-Aldrich	700068P	1.32	1.06	456.4	351	4,10
16	Cholesta-7,24-dien-3 β ol		C ₂₇ H ₄₄ O	384.3	651-54-7	MS (III)	Sigma-Aldrich	700114P	1.34	1.09	456.4	343	5,10
17	Cholesta-5,7,24-trien-3 β -ol	7-Dehydrodesmosterol	C ₂₇ H ₄₂ O	382.3	1715-86-2	MS (IV)	Sigma-Aldrich	700138P	1.33	1.06	454.4	349	5,11
18	Cholesta-5,24-dien-3 β -ol	Desmosterol	C ₂₇ H ₄₄ O	384.3	313-04-2	C	Sigma-Aldrich	D6513	1.29	1.03	456.4	253	1,4
19	Cholesta-8,14-dien-3 β -ol		C ₂₇ H ₄₄ O	384.3	17608-73-0	OS ¹²			1.27	1.02	456.4	351	10
20	Cholesta-8,14,24-trien3 β -ol		C ₂₇ H ₄₂ O	382.3	64284-65-7	MS (V)			1.31	1.05	454.4	454	11
21	4-Methylcholest-7-en3 β -ol	Lophenol	C ₂₈ H ₄₈ O	400.4	481-25-4	MS (VI)	Toronto Research Chemicals	M260640	1.37	1.09	472.4	472	4
22	4-Methylcholesta-7,24dien-3 β -ol		C ₂₈ H ₄₆ O	398.4	24778-51-6	MS (VII)			1.40	1.12	470.4	365	
23	Cholesta-5,8-dien-3 β -ol	8-Dehydrocholesterol	C ₂₇ H ₄₄ O	384.3	70741-38-7	OS ¹²	Toronto Research Chemicals	D230295	1.26	1.01	456.4	351	9,10
24	Cholesta-5,8,24-trien3 β -ol		C ₂₇ H ₄₂ O	382.3	70441-40-6	MS (VIII)			1.30	1.04	454.4	349	

5. Characterization of inhibitors of cholesterol biosynthesis

25	4,4-Dimethylcholesta-5,7-dien-3 β -ol		C ₂₉ H ₄₈ O	412.4	53296-71-2	OS ¹²			1.43	1.14	484.4	379	
26	Cholestane		C ₂₇ H ₄₈	372.4	481-21-0	C	Sigma Aldrich	C8003	1.00	0.80		217	10

Supplementary Table S1, Analytical details of cholesterol biosynthesis intermediates. RRT relative retention time, C, commercial source, MS mass spectral analysis, OS organic synthesis, (I) incubation of *Aspergillus fumigatus*¹³, (II) incubation of *Aspergillus fumigatus*¹³, (III) incubation of HL-60 cells with experimental inhibitor (ethyl side chain) see reference¹⁴, (IV) incubation of HL-60 cells with DR 258⁶, (V) incubation of HL-60 cells with AY-9944, and experimental inhibitor¹⁴, (VI) incubation of HL-60 cells with aminotriazole⁶, (VII) incubation of HL-60 cells with aminotriazole, AY9944, MGI-21¹⁵ (VIII) incubation of HL-60 cells with experimental inhibitor¹⁵, **Isol.** Isolated from yeast fat.

- 1 Acimovic, J. *et al.* Combined gas chromatographic/mass spectrometric analysis of cholesterol precursors and plant sterols in cultured cells. *Journal of Chromatography B* **877**, 2081-2086, doi:<https://doi.org/10.1016/j.jchromb.2009.05.050> (2009).
- 2 Ceruti, M. *et al.* Stereospecific synthesis of squalenoid epoxide vinyl ethers as inhibitors of 2,3-oxidosqualene cyclase. *Journal of the Chemical Society, Perkin Transactions 1*, 461-469, doi:10.1039/P19880000461 (1988).
- 3 Santivañez-Veliz, M. *et al.* Development, validation and application of a GC–MS method for the simultaneous detection and quantification of neutral lipid species in *Trypanosoma cruzi*. *Journal of Chromatography B* **1061-1062**, 225-232, doi:<https://doi.org/10.1016/j.jchromb.2017.07.031> (2017).
- 4 Brooks, C. J. W., Horning, E. C. & Young, J. S. Characterization of sterols by gas chromatography-mass spectrometry of the trimethylsilyl ethers. *Lipids* **3**, 391-402, doi:doi:10.1007/BF02531277 (1968).
- 5 Nakanishi, S., Nishtno, T., Nagai, J. & Katsuki, H. Characterization of Nystatin-Resistant Mutants of *Saccharomyces cerevisiae* and Preparation of Sterol Intermediates Using the Mutants. *The Journal of Biochemistry* **101**, 535-544 (1987).
- 6 Giera, M., Plössl, F. & Bracher, F. Fast and easy in vitro screening assay for cholesterol biosynthesis inhibitors in the post-squalene pathway. *Steroids* **72**, 633-642, doi:<https://doi.org/10.1016/j.steroids.2007.04.005> (2007).
- 7 Kloos, D.-P. *et al.* Comprehensive gas chromatography–electron ionisation mass spectrometric analysis of fatty acids and sterols using sequential onepot silylation: quantification and isotopologue analysis. *Rapid Communications in Mass Spectrometry* **28**, 1507-1514, doi:doi:10.1002/rcm.6923 (2014).
- 8 NKININ, S. W. *et al.* Pneumocystis carinii Sterol 14 α -Demethylase Activity in *Saccharomyces cerevisiae* erg11 Knockout Mutant: Sterol Biochemistry. *Journal of Eukaryotic Microbiology* **58**, 383-392, doi:doi:10.1111/j.1550-7408.2011.00556.x (2011).
- 9 Wolthers, B. G. *et al.* Use of determinations of 7-lathosterol (5 α -cholest-7-en-3 β -ol) and other cholesterol precursors in serum in the study and treatment of disturbances of sterol metabolism, particularly cerebrotendinous xanthomatosis. *Journal of Lipid Research* **32**, 603-612 (1991).
- 10 Gerst, N., Ruan, B., Pang, J., Wilson, W. K. & Schroepfer, G. J. An updated look at the analysis of unsaturated C27 sterols by gas chromatography and mass spectrometry. *Journal of Lipid Research* **38**, 1685-1701 (1997).
- 11 Ogihara, N. & Morisaki, M. FACILE SYNTHESIS OF ZYMOSTEROL AND RELATED COMPOUNDS. *CHEMICAL & PHARMACEUTICAL BULLETIN* **36**, 2724-2725, doi:10.1248/cpb.36.2724 (1988).

5. Characterization of inhibitors of cholesterol biosynthesis

- 12 Boer, D. R. *et al.* Calculated heats of formation of sterol diene isomers compared with synthetic yields of isomerisation reactions of $\Delta^{5,7}$ sterols. *Journal of the Chemical Society, Perkin Transactions 2*, 1701-1704, doi:10.1039/B002212H (2000).
- 13 Müller, C., Binder, U., Bracher, F. & Giera, M. Antifungal drug testing by combining minimal inhibitory concentration testing with target identification by gas chromatography–mass spectrometry. *Nature Protocols* **12**, 947, doi:10.1038/nprot.2017.005 <https://www.nature.com/articles/nprot.2017.005#supplementary-information> (2017).
- 14 Giera, M., Renard, D., Plössl, F. & Bracher, F. Lathosterol side chain amides—A new class of human lathosterol oxidase inhibitors. *Steroids* **73**, 299-308, doi:<https://doi.org/10.1016/j.steroids.2007.10.015> (2008).
- 15 Giera, M., Müller, C. & Bracher, F. Analysis and Experimental Inhibition of Distal Cholesterol Biosynthesis. *Chromatographia* **78**, 343-358, doi:10.1007/s10337-014-2796-4 (2015).

5. Characterization of inhibitors of cholesterol biosynthesis

Supplementary table S2 Linear regression, LOD, and LOQ of prominent sterols The limit of detection (LOD) was determined at a signal/noise ratio of 3 in the total ion chromatogram. The limit of quantification (LOQ) was set where the RSD (n=6) was < 20% using the base peak chromatograms. All compounds were linear in a range between LOQ and 1.40 µg/mL.

No.	IUPAC Name	Trivial Name	Base peak [m/z]	Slope	Y - intercept	R ²	LOD [µg/mL]	LOQ [µg/mL]	LOQ on column [pg]
1	(6E,10E,14E,18E)-2,6,10,15,19,23-Hexamethyltetracosane	Squalene	69	0.4329	-0.0019	0.960	0.05	0.05	50
2	2,2-Dimethyl-(S)-3-((3E,7E,11E,15E)3,7,12,16,20-pentamethylhenicosa-3,7,11,15,19pentaenyl)-oxirane	Squalene epoxide	81	0.1088	-0.0133	0.953	0.20	0.40	400
3	4,4,14-Trimethylcholesta-8,24-dien-3β-ol	Lanosterol	393	0.6388	-0.0500	0.979	0.01	0.02	20
4	4,4,14-Trimethylcholest-8-en-3β-ol	Dihydrolanosterol	395	1.342	-0.0127	0.996	0.02	0.02	20 All
5	4,4-Dimethylcholesta-8,14-dien-3β-ol		379	0.5721	-0.0606	0.991	0.05	0.10	100
6	4,4-Dimethylcholest-8-en-3β-ol		486	0.1762	-0.0007	0.996	0.02	0.02	20
8	Cholest-8-en-3β-ol	Zymostenol	458	0.1762	-0.0007	0.996	0.02	0.02	20
9	Cholest-7-en-3β-ol	Lathosterol	458	0.5883	-0.0474	0.988	0.02	0.20	200
10	Cholesta-5,7-dien-3β-ol	7-Dehydrocholesterol	351	0.6525	-0.0574	0.979	0.02	0.20	200
11	Cholest-5-en-3β-ol	Cholesterol	368	0.3788	0.0077	0.998	0.02	0.02	20
15	Cholesta-8,24-dien3β-ol	Zymosterol	351	0.2560	-0.0015	0.989	0.05	0.05	50
18	Cholesta-5,24-dien3β-ol	Desmosterol	253	0.3159	-0.0433	0.990	0.10	0.20	200
19	Cholesta-8,14-dien3β-ol		351	1.756	-0.0359	0.991	0.02	0.02	20
23	Cholesta-5,8-dien-3β-ol	8-Dehydrocholesterol	351	0.8237	-0.0227	0.998	0.05	0.05	50
25	4,4-Dimethylcholesta-5,7-dien-3β-ol		379	0.8891	-0.0389	0.989	0.05	0.05	50

5. Characterization of inhibitors of cholesterol biosynthesis

Inhibitor				Inhibited enzymes
Inhibitor	CAS-Number	Distributor	Item Number	
AY-9944	366-93-8	Cayman Chemicals	Cay14611-1	C _{3,4} , E _{5,6} , G ₃ , I _{1,2,4,7}
BM 15766 sulfate ^{1,2}	86621-94-5	Sigma-Aldrich	B8685	
Haloperidol	52-86-8	Sigma-Aldrich	H1512	E ⁸ , G ⁸ , I ⁸ ,
SR 31747	132173-06-9	MuseChem	I013540	C ₉ , G _{3,6,9}
Tamoxifene	10540-29-1	Sigma-Aldrich	T5648	C _{6,10,11} , G _{6,10,11}
Trifluoperazine dihydrochloride	440-17-5	Sigma-Aldrich	T8516	C _{4,12} , H ₁₂
Triparanol	78-41-1	Sigma-Aldrich	T5200	C _{1,6,12} , G ₁₂ , H ₁₂
U18666A	3039-71-2	Sigma-Aldrich	U3633	B _{1,13} , C _{1,6,13} , G ₁₃

Supplementary Table S3

5. Characterization of inhibitors of cholesterol biosynthesis

- 1 Rozman, D. & Monostory, K. Perspectives of the non-statin hypolipidemic agents. *Pharmacology & Therapeutics* **127**, 19-40, doi:<https://doi.org/10.1016/j.pharmthera.2010.03.007> (2010).
- 2 Shefer, S. *et al.* Regulation of rat hepatic 3 β -hydroxysterol Δ 7-reductase: substrate specificity, competitive and non-competitive inhibition, and phosphorylation/dephosphorylation. *Journal of Lipid Research* **39**, 2471-2476 (1998).
- 3 Fernández, C., Martín, M., Gómez-Coronado, D. & Lasunción, M. A. Effects of distal cholesterol biosynthesis inhibitors on cell proliferation and cell cycle progression. *Journal of Lipid Research* **46**, 920-929, doi:10.1194/jlr.M400407-JLR200 (2005).
- 4 BAE, S.-H. & PAIK, Y.-K. Cholesterol biosynthesis from lanosterol: development of a novel assay method and characterization of rat liver microsomal lanosterol Δ ²⁴-reductase. *Biochemical Journal* **326**, 609-616, doi:10.1042/bj3260609 (1997).
- 5 Gatticchi, L. *et al.* Selected cholesterol biosynthesis inhibitors produce accumulation of the intermediate FF-MAS that targets nucleus and activates LXR α in HepG2 cells. *Biochimica et Biophysica Acta (BBA) - Molecular and Cell Biology of Lipids* **1862**, 842-852, doi:<https://doi.org/10.1016/j.bbalip.2017.05.004> (2017).
- 6 Lasunción, M. A., Martín-Sánchez, C., Canfrán-Duque, A. & Busto, R. Post-lanosterol biosynthesis of cholesterol and cancer. *Current Opinion in Pharmacology* **12**, 717-723, doi:<https://doi.org/10.1016/j.coph.2012.07.001> (2012).
- 7 Kraml, M., Bagli, J. F. & Dvornik, D. Inhibition of the conversion of 7-dehydrocholesterol to cholesterol by AY-9944. *Biochemical and Biophysical Research Communications* **15**, 455-457, doi:[https://doi.org/10.1016/0006-291X\(64\)90485-1](https://doi.org/10.1016/0006-291X(64)90485-1) (1964).
- 8 Canfrán-Duque, A. *et al.* Atypical antipsychotics alter cholesterol and fatty acid metabolism in vitro. *Journal of Lipid Research* **54**, 310-324, doi:10.1194/jlr.M026948 (2013).
- 9 Labit-Le Bouteiller, C. *et al.* Antiproliferative effects of SR31747A in animal cell lines are mediated by inhibition of cholesterol biosynthesis at the sterol isomerase step. *European Journal of Biochemistry* **256**, 342-349, doi:doi:10.1046/j.1432-1327.1998.2560342.x (1998).
- 10 König, M., Müller, C. & Bracher, F. Stereoselective synthesis of a new class of potent and selective inhibitors of human Δ 8,7-sterol isomerase. *Bioorganic & Medicinal Chemistry* **21**, 1925-1943, doi:<https://doi.org/10.1016/j.bmc.2013.01.041> (2013).
- 11 Suarez, Y. *et al.* Synergistic upregulation of low-density lipoprotein receptor activity by tamoxifen and lovastatin. *Cardiovasc Res* **64**, 346355, doi:10.1016/j.cardiores.2004.06.024 (2004).
- 12 Müller, C. *et al.* New chemotype of selective and potent inhibitors of human delta 24-dehydrocholesterol reductase. *European Journal of Medicinal Chemistry* **140**, 305-320, doi:<https://doi.org/10.1016/j.ejmech.2017.08.011> (2017).
- 13 Cenedella, R. J. Cholesterol Synthesis Inhibitor U18666A and the Role of Sterol Metabolism and Trafficking in Numerous Pathophysiological Processes. *Lipids* **44**, 477-487, doi:doi:10.1007/s11745-009-3305-7 (2009).

5. Characterization of inhibitors of cholesterol biosynthesis

	LC-MS/MS	GC-EI-MS (scan mode)
Advantages	<ul style="list-style-type: none"> <input type="checkbox"/> Short analysis times^{1,2}, favored for high throughput analysis³ but long run time for cholesterol precursors after derivatization (40 min)⁴ <input type="checkbox"/> Analysis of non-hydrolysable and derivatization-resistant metabolites^{1,3,5} <input type="checkbox"/> Sensitive and specific technique for clinical steroid analysis⁶ (e.g. cortisol precursors, hormonal 3α-Δ^4 steroids^{1,2}) and cholesterol precursors (LOD < 1pg on-column after derivatization)⁴ <input type="checkbox"/> Suited to commercial routine analysis⁶ and targeted steroidomics^{1,4} 	<ul style="list-style-type: none"> <input type="checkbox"/> Unprecedented separation capacity¹ <input type="checkbox"/> Minimal matrix effects¹ <input type="checkbox"/> Derivatized sterols can be subjected to untargeted and/or targeted analysis^{1,2} <input type="checkbox"/> Comparable MS spectra (libraries) are available⁷ (see Supporting information) <input type="checkbox"/> Fragmentation of derivatized sterols allows characterization of unexpected or novel compounds^{1,3,5} <input type="checkbox"/>
Disadvantages	<ul style="list-style-type: none"> <input type="checkbox"/> Authentic reference material should be available¹ <input type="checkbox"/> Analysis of steroids without 3α-Δ^4 unconjugated ring system, by ESI sources is challenging^{1,4} <input type="checkbox"/> Derivatization step is necessary for the high sensitivity analysis cholesterol precursors⁴ <input type="checkbox"/> Lower sensitivities are achieved when analysing underivatized sterols⁸ 	<ul style="list-style-type: none"> <input type="checkbox"/> Extensive sample workup¹, conjugated sterols (sulfates and glucuronides) require a hydrolysis step^{1,3,5-7} <input type="checkbox"/> Sterols with $\Delta^{5,7}$-diene structure may be labile under basic conditions (saponification step)⁵ <input type="checkbox"/> Derivatization step is necessary to improve steroid volatility and stability¹ <input type="checkbox"/> Scan mode lacks sensitivity for identifying and quantifying minor sterols¹

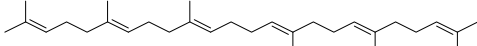
Supplementary Table S4

- 1 Shackleton, C., Pozo, O. J. & Marcos, J. GC/MS in Recent Years Has Defined the Normal and Clinically Disordered Steroidome: Will It Soon Be Surpassed by LC/Tandem MS in This Role? *Journal of the Endocrine Society* **2**, 974-996, doi:10.1210/js.2018-00135 (2018).
- 2 Krone, N. *et al.* Gas chromatography/mass spectrometry (GC/MS) remains a pre-eminent discovery tool in clinical steroid investigations even in the era of fast liquid chromatography tandem mass spectrometry (LC/MS/MS). *The Journal of Steroid Biochemistry and Molecular Biology* **121**, 496-504, doi:<https://doi.org/10.1016/j.jsbmb.2010.04.010> (2010).
- 3 Griffiths, W. J. & Wang, Y. Analysis of oxysterol metabolomes. *Biochimica et Biophysica Acta (BBA) - Molecular and Cell Biology of Lipids* **1811**, 784-799, doi:<https://doi.org/10.1016/j.bbalip.2011.05.012> (2011).
- 4 Honda, A. *et al.* Highly sensitive analysis of sterol profiles in human serum by LC-ESI-MS/MS. *Journal of Lipid Research* **49**, 2063-2073, doi:10.1194/jlr.D800017-JLR200 (2008).

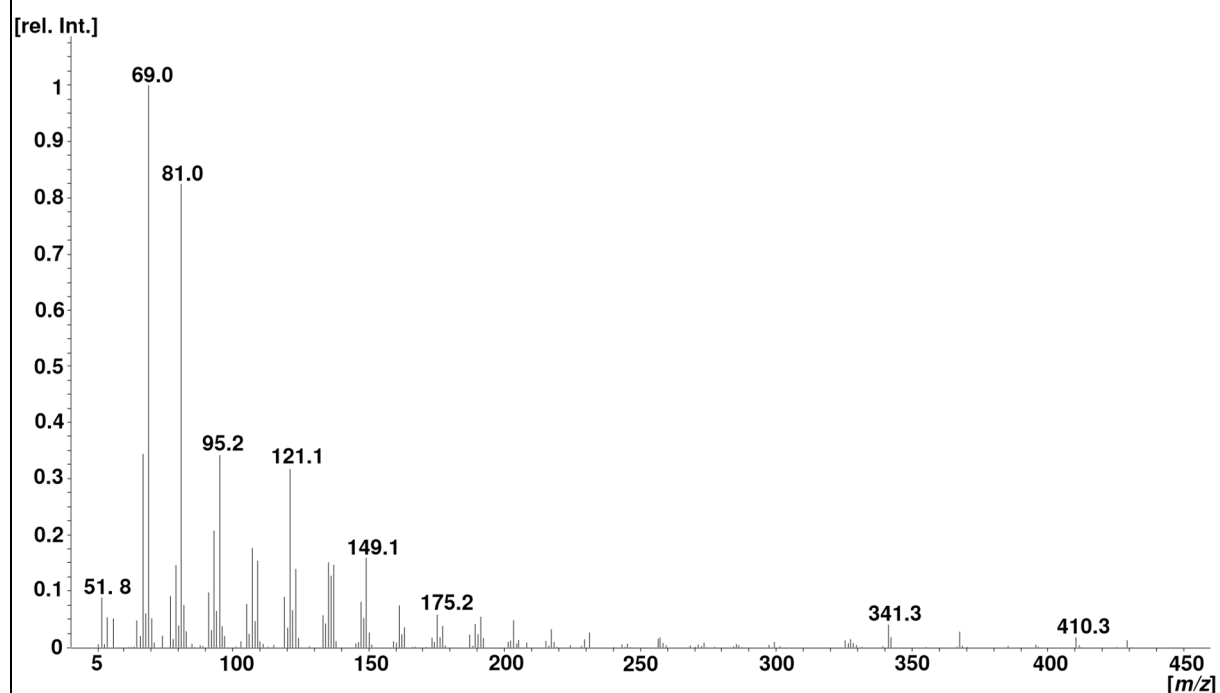
5. Characterization of inhibitors of cholesterol biosynthesis

- 5 Griffiths, W. J. & Wang, Y. Sterolomics: State of the art, developments, limitations and challenges. *Biochimica et Biophysica Acta (BBA) - Molecular and Cell Biology of Lipids* **1862**, 771-773, doi:<https://doi.org/10.1016/j.bbalip.2017.03.001> (2017).
- 6 Shackleton, C. Clinical steroid mass spectrometry: A 45-year history culminating in HPLC–MS/MS becoming an essential tool for patient diagnosis. *The Journal of Steroid Biochemistry and Molecular Biology* **121**, 481-490, doi:<https://doi.org/10.1016/j.jsbmb.2010.02.017> (2010).
- 7 Jeanneret, F. *et al.* Evaluation of steroidomics by liquid chromatography hyphenated to mass spectrometry as a powerful analytical strategy for measuring human steroid perturbations. *Journal of Chromatography A* **1430**, 97-112, doi:<https://doi.org/10.1016/j.chroma.2015.07.008> (2016).
- 8 Herron, J., Hines, K. M. & Xu, L. Assessment of Altered Cholesterol Homeostasis by Xenobiotics Using Ultra-High Performance Liquid Chromatography–Tandem Mass Spectrometry. *Current Protocols in Toxicology* **78**, e65, doi:doi:10.1002/cptx.65 (2018).

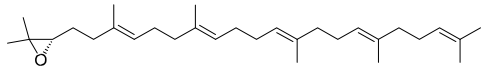
Supplementary Table S8 - Spectral database

Compound No.	1		
IUPAC Name	(6E,10E,14E,18E)-2,6,10,15,19,23-Hexamethyltetracosane-2,6,10,14,18,22-hexaene		
Trivial Name	Squalene		
CAS Number	111-02-4	M [g/mol]	410.4
Chemical Formula	C ₃₀ H ₅₀	M TMS ether [g/mol]	
Structure		RRT TMS ether (Cholestane)	0.95
		RRT TMS ether (Cholesterol)	0.76

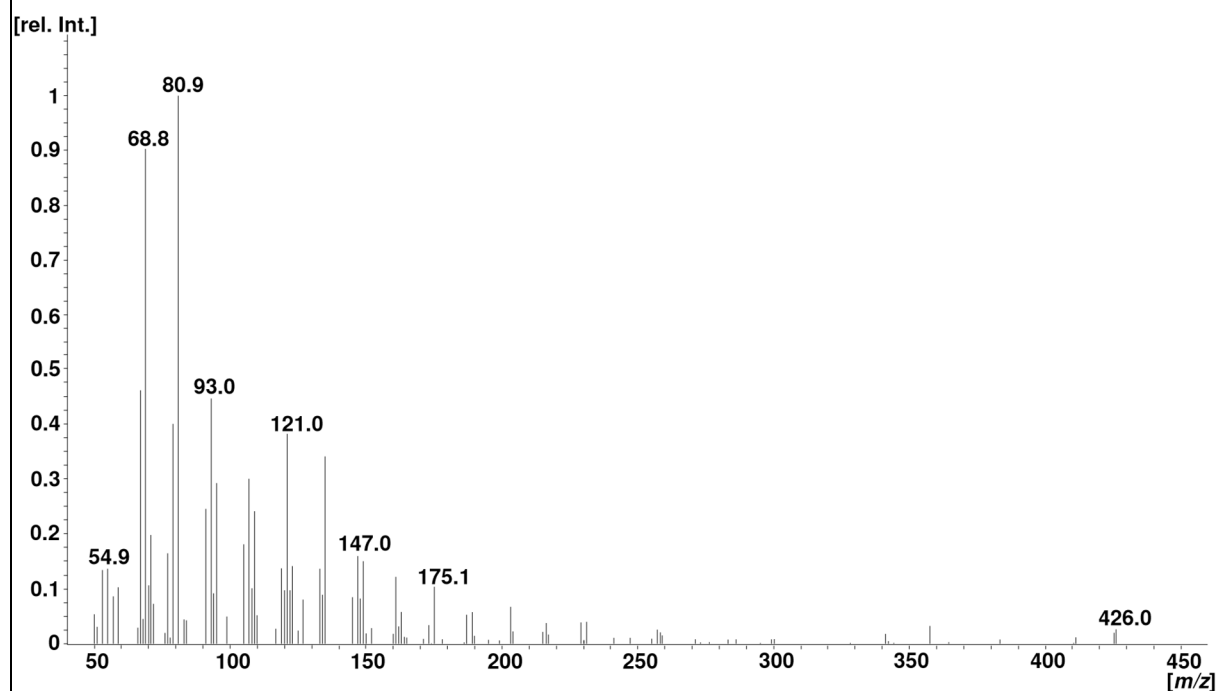
MS spectrum



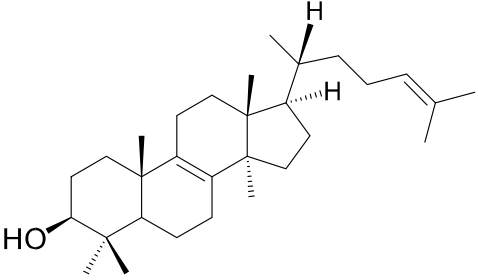
5. Characterization of inhibitors of cholesterol biosynthesis

Compound No.	2		
IUPAC Name	(3S)-2,2-Dimethyl-3-((3E,7E,11E,15E)-3,7,12,16,20pentamethylhenicosa-3,7,11,15,19-pentaenyl)-oxirane		
Trivial Name	Squalene epoxide		
CAS Number	7200-26-2	M [g/mol]	426.4
Chemical Formula	C ₃₀ H ₅₀ O	M TMS ether [g/mol]	
Structure		RRT TMS ether (Cholestane)	1.05
		RRT TMS ether (Cholesterol)	0.83

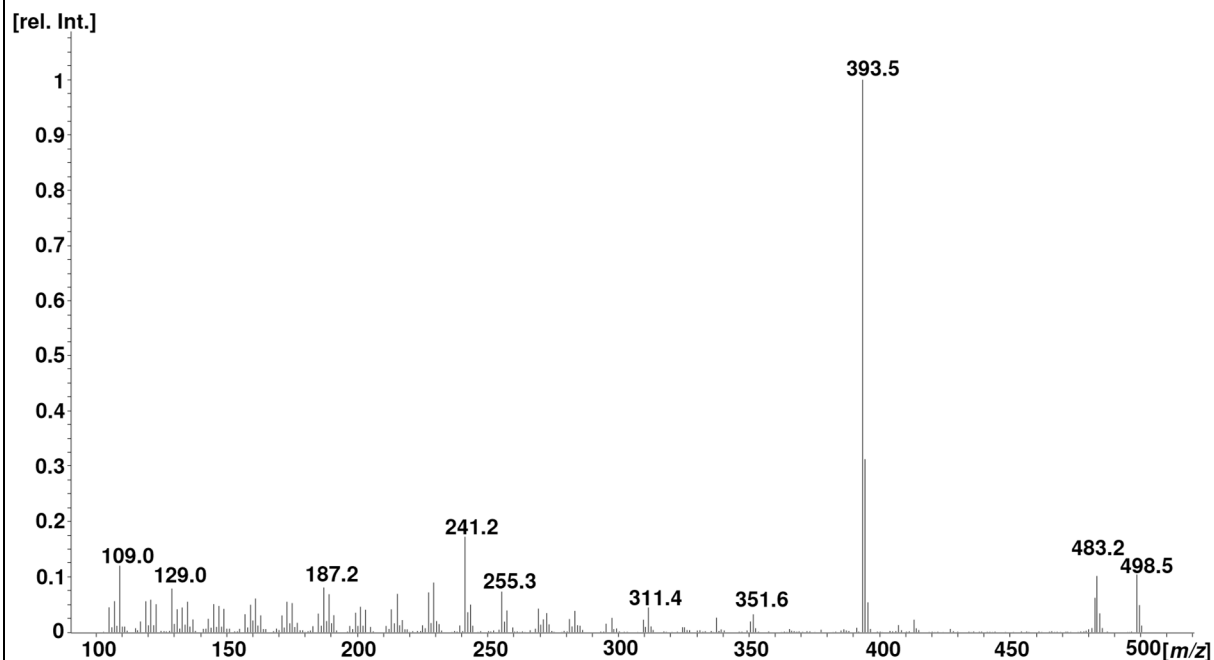
MS spectrum



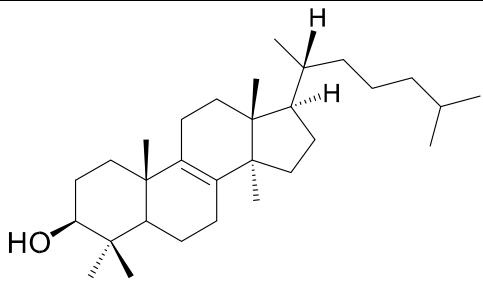
5. Characterization of inhibitors of cholesterol biosynthesis

Compound No.	3		
IUPAC Name	4,4,14-Trimethylcholesta-8,24-dien-3 β -ol		
Trivial Name	Lanosterol		
CAS Number	79-63-0	M [g/mol]	426.4
Chemical Formula	C ₃₀ H ₅₀ O	M TMS ether [g/mol]	498.4
Structure		RRT TMS ether (Cholestane)	1.44
		RRT TMS ether (Cholesterol)	1.16

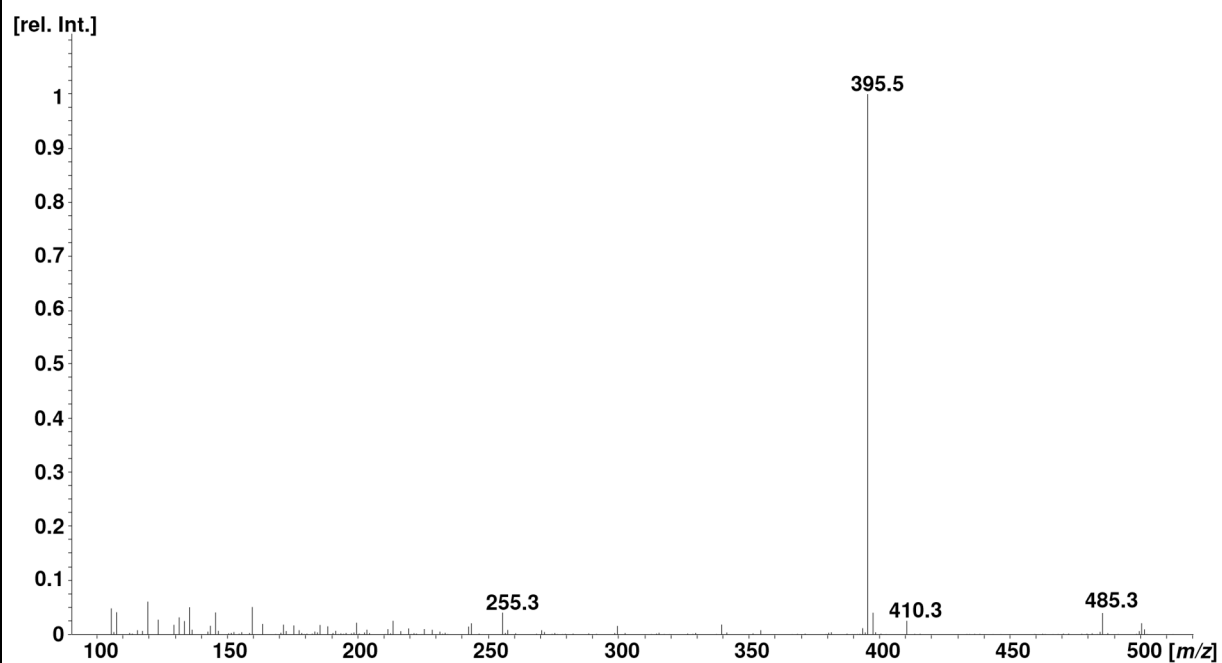
MS spectrum TMS ether



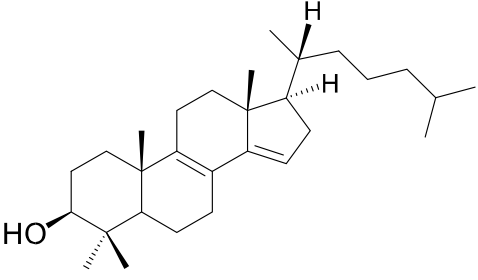
5. Characterization of inhibitors of cholesterol biosynthesis

Compound No.	4		
IUPAC Name	4,4,14-Trimethylcholest-8-en-3 β -ol		
Trivial Name	Dihydrolanosterol		
CAS Number	79-62-9	M [g/mol]	428.4
Chemical Formula	C ₃₀ H ₅₂ O	M TMS ether [g/mol]	500.4
Structure		RRT TMS ether (Cholestane)	1.40
		RRT TMS ether (Cholesterol)	1.12

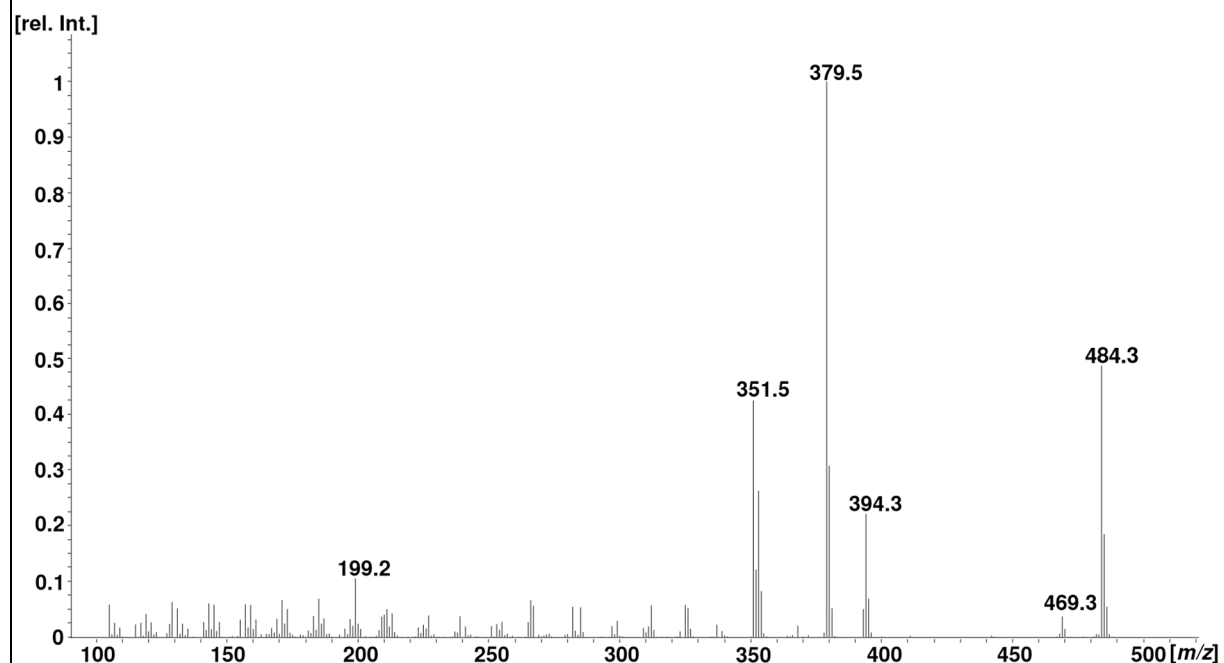
MS spectrum TMS ether



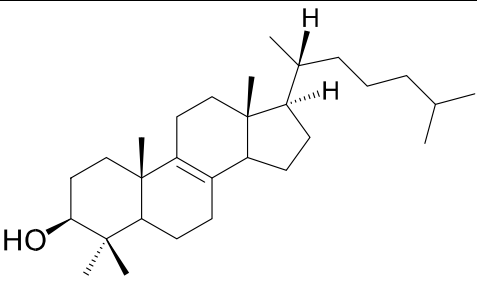
5. Characterization of inhibitors of cholesterol biosynthesis

Compound No.	5		
IUPAC Name	4,4-Dimethylcholesta-8,14-dien-3 β -ol		
Trivial Name			
CAS Number	19456-83-8	M [g/mol]	412.4
Chemical Formula	C ₂₉ H ₄₈ O	M TMS ether [g/mol]	484.5
Structure		RRT TMS ether (Cholestane)	1.42
		RRT TMS ether (Cholesterol)	1.13

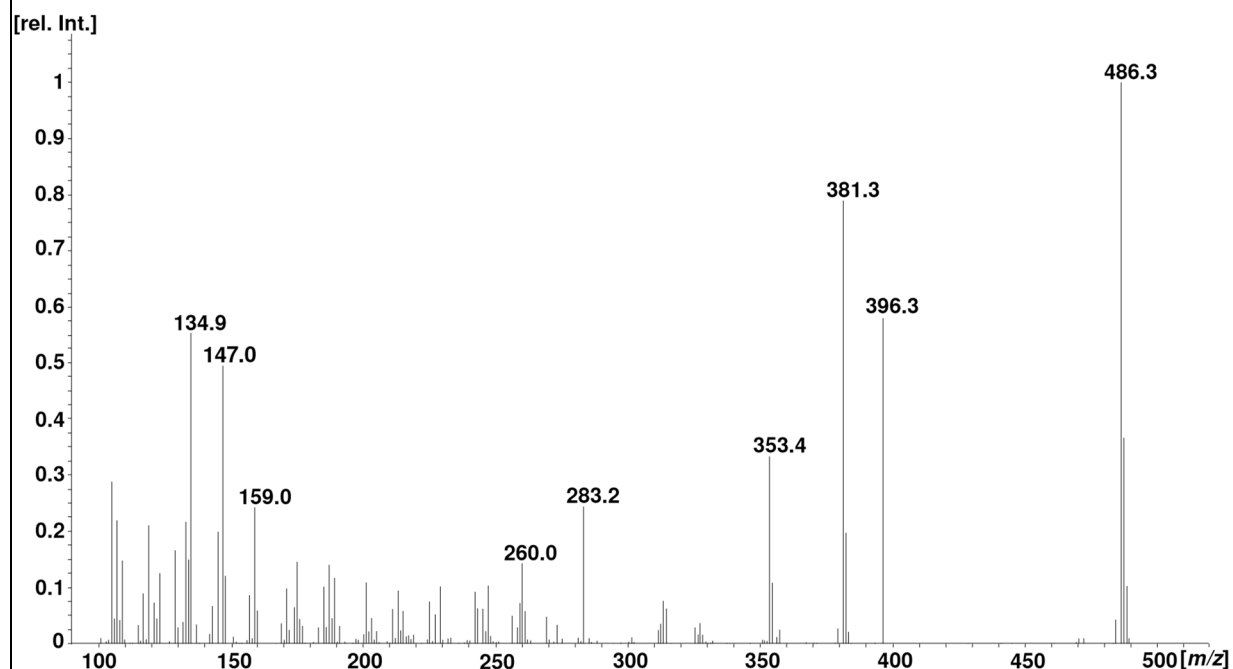
MS spectrum TMS ether



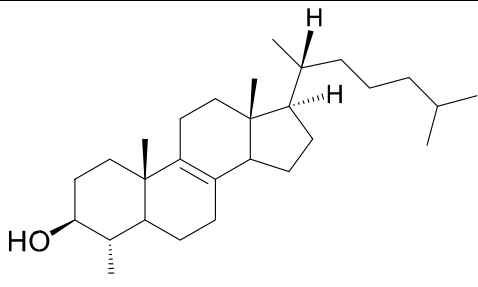
5. Characterization of inhibitors of cholesterol biosynthesis

Compound No.	6		
IUPAC Name	4,4-Dimethylcholest-8-en-3 β -ol		
Trivial Name			
CAS Number	5241-24-7	M [g/mol]	414.4
Chemical Formula	C ₂₉ H ₅₀ O	M TMS ether [g/mol]	486.4
Structure		RRT TMS ether (Cholestane)	1.43
		RRT TMS ether (Cholesterol)	1.14

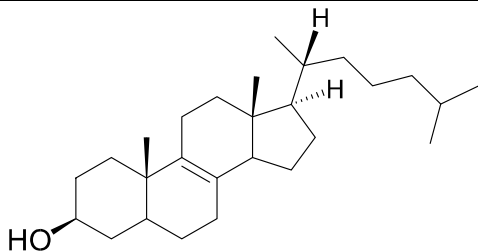
MS spectrum TMS ether



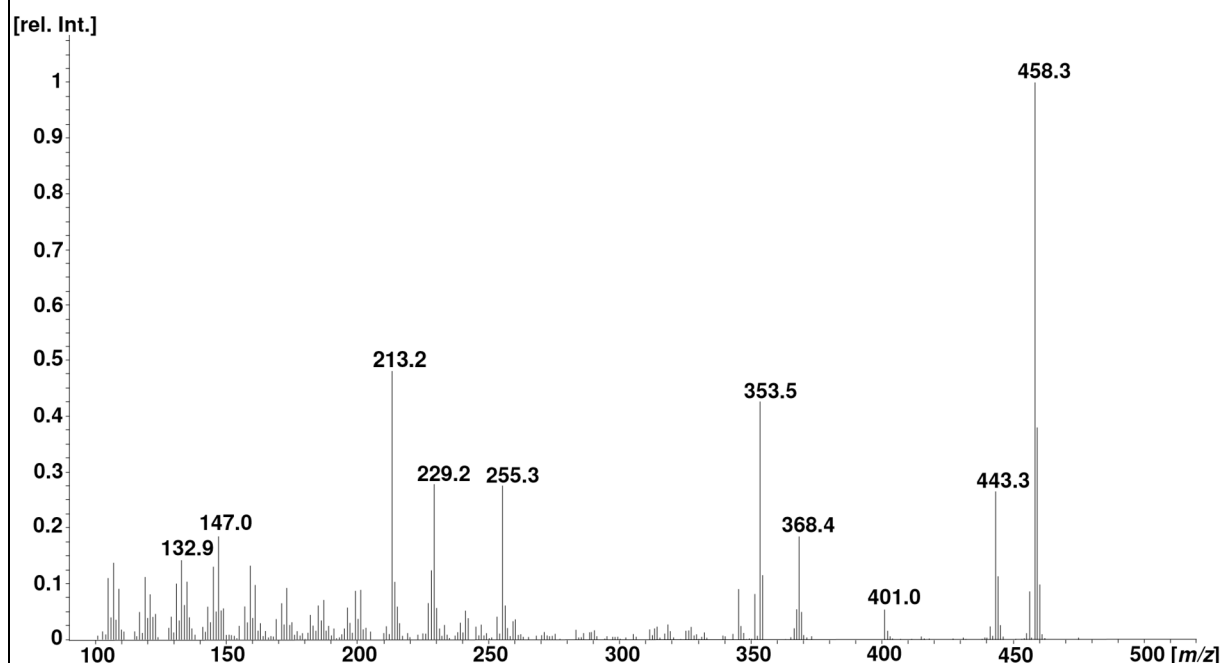
5. Characterization of inhibitors of cholesterol biosynthesis

Compound No.	7		
IUPAC Name	4 α -Methylcholest-8-en-3 β -ol		
Trivial Name	4-Methylzymostenol		
CAS Number	5241-22-5	M [g/mol]	400.4
Chemical Formula	C ₂₈ H ₄₈ O	M TMS ether [g/mol]	472.4
Structure		RRT TMS ether (Cholestane)	
		RRT TMS ether (Cholesterol)	
MS spectrum TMS ether not available			

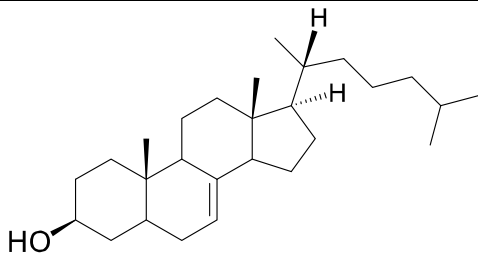
5. Characterization of inhibitors of cholesterol biosynthesis

Compound No.	8		
IUPAC Name	Cholest-8-en-3 β -ol		
Trivial Name	Zymostenol		
CAS Number	566-97-2	M [g/mol]	386.4
Chemical Formula	C ₂₇ H ₄₆ O	M TMS ether [g/mol]	458.4
Structure		RRT TMS ether (Cholestane)	1.27
		RRT TMS ether (Cholesterol)	1.02

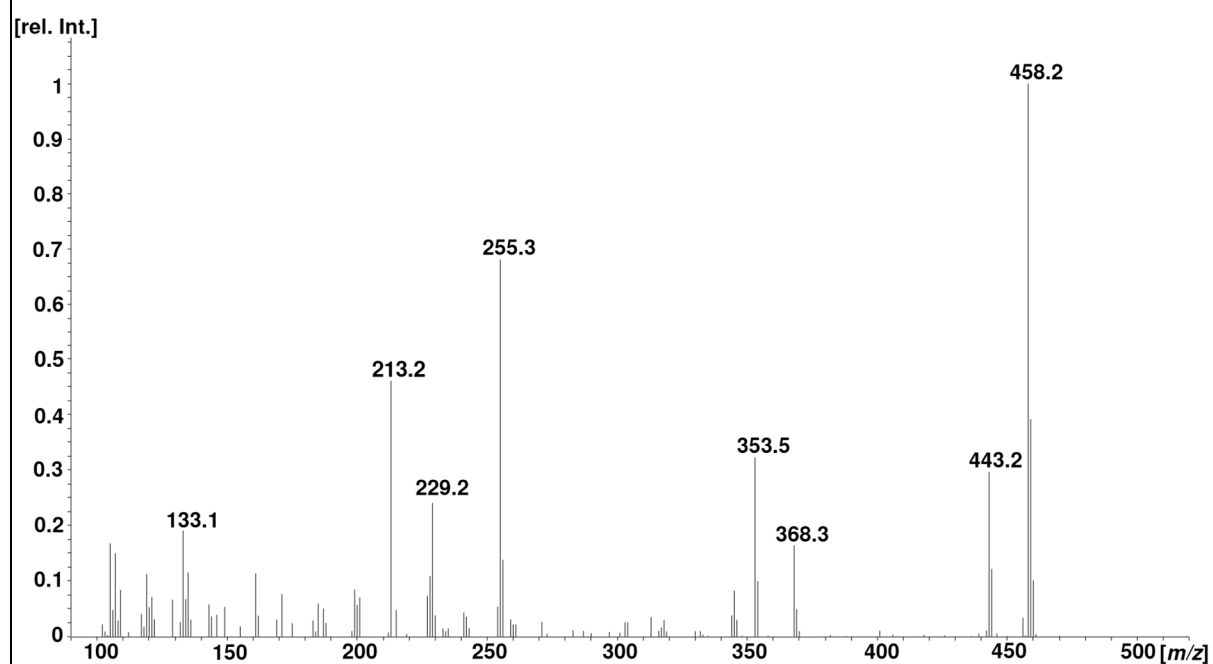
MS spectrum TMS ether



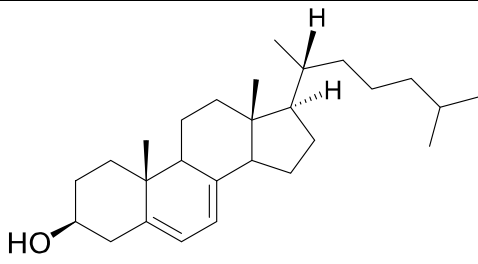
5. Characterization of inhibitors of cholesterol biosynthesis

Compound No.	9		
IUPAC Name	Cholest-7-en-3 β -ol		
Trivial Name	Lathosterol		
CAS Number	80-99-9	M [g/mol]	386.4
Chemical Formula	C ₂₇ H ₄₆ O	M TMS ether [g/mol]	458.4
Structure		RRT TMS ether (Cholestane)	1.31
		RRT TMS ether (Cholesterol)	1.04

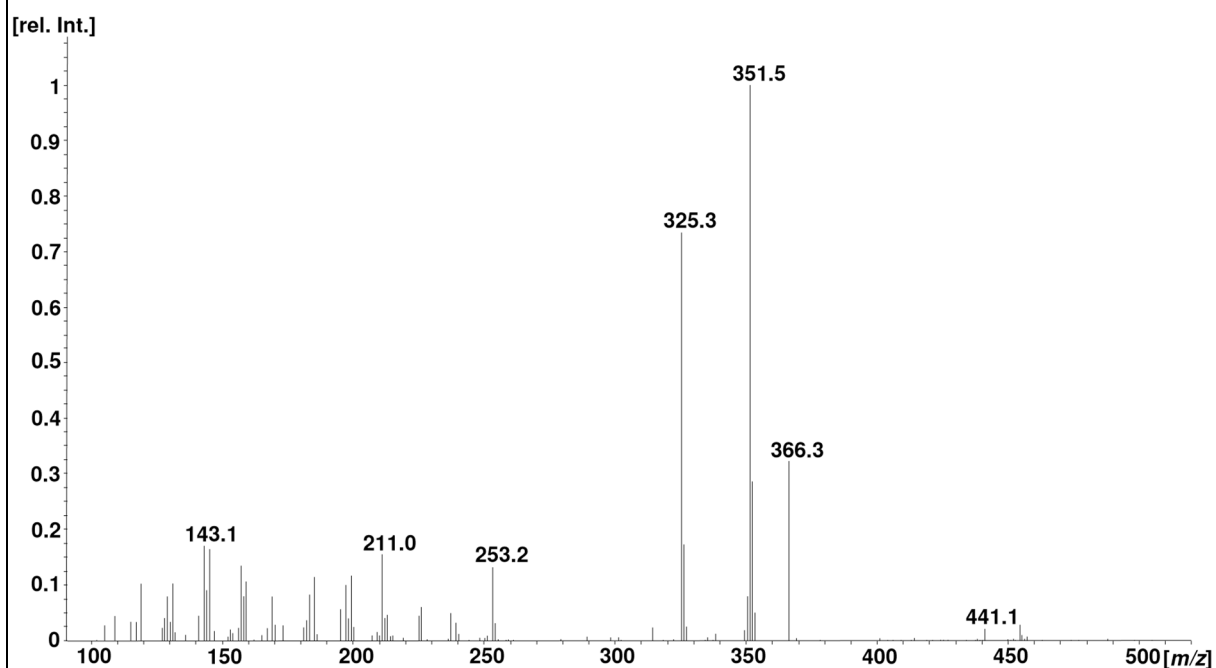
MS spectrum TMS ether



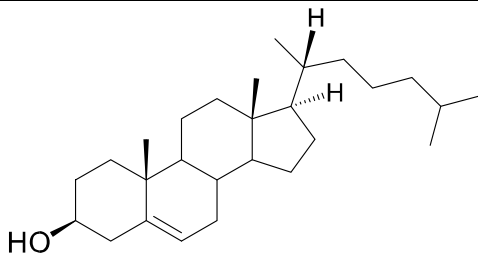
5. Characterization of inhibitors of cholesterol biosynthesis

Compound No.	10		
IUPAC Name	Cholesta-5,7-dien-3 β -ol		
Trivial Name	7-Dehydrocholesterol		
CAS Number	434-16-2	M [g/mol]	384.3
Chemical Formula	C ₂₇ H ₄₄ O	M TMS ether [g/mol]	456.4
Structure		RRT TMS ether (Cholestane)	1.29
		RRT TMS ether (Cholesterol)	1.03

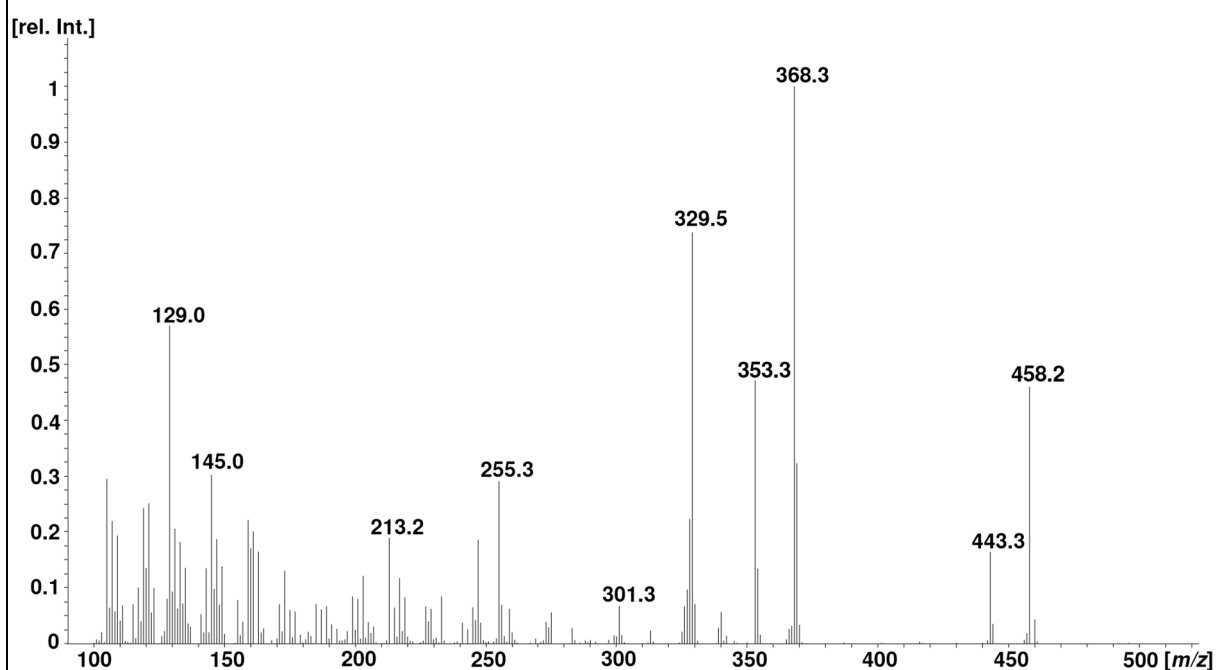
MS spectrum TMS ether



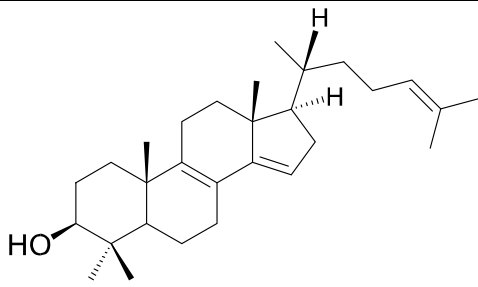
5. Characterization of inhibitors of cholesterol biosynthesis

Compound No.	11		
IUPAC Name	Cholest-5-en-3 β -ol		
Trivial Name	Cholesterol		
CAS Number	57-88-5	M [g/mol]	386.4
Chemical Formula	C ₂₇ H ₄₆ O	M TMS ether [g/mol]	458.4
Structure		RRT TMS ether (Cholestane)	1.26
		RRT TMS ether (Cholesterol)	1.00

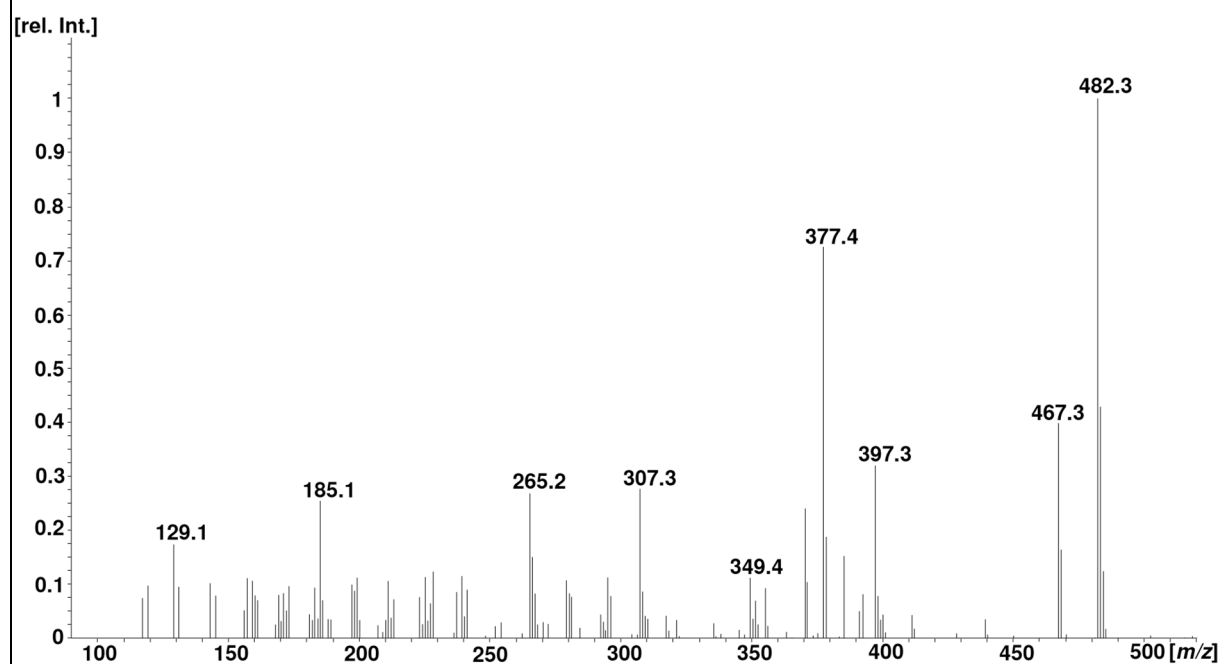
MS spectrum TMS ether



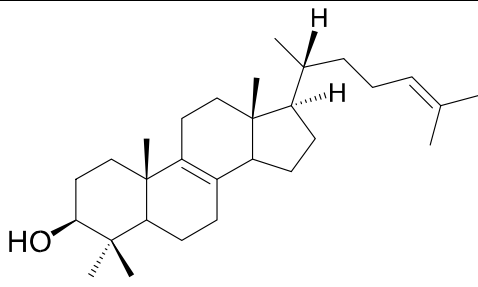
5. Characterization of inhibitors of cholesterol biosynthesis

Compound No.	12		
IUPAC Name	4,4-Dimethylcholesta-8,14,24-trien-3 β -ol		
Trivial Name	FF-MAS		
CAS Number	64284-64-6	M [g/mol]	410.4
Chemical Formula	C ₂₉ H ₄₄ O	M TMS ether [g/mol]	482.4
Structure		RRT TMS ether (Cholestane)	1.47
		RRT TMS ether (Cholesterol)	1.17

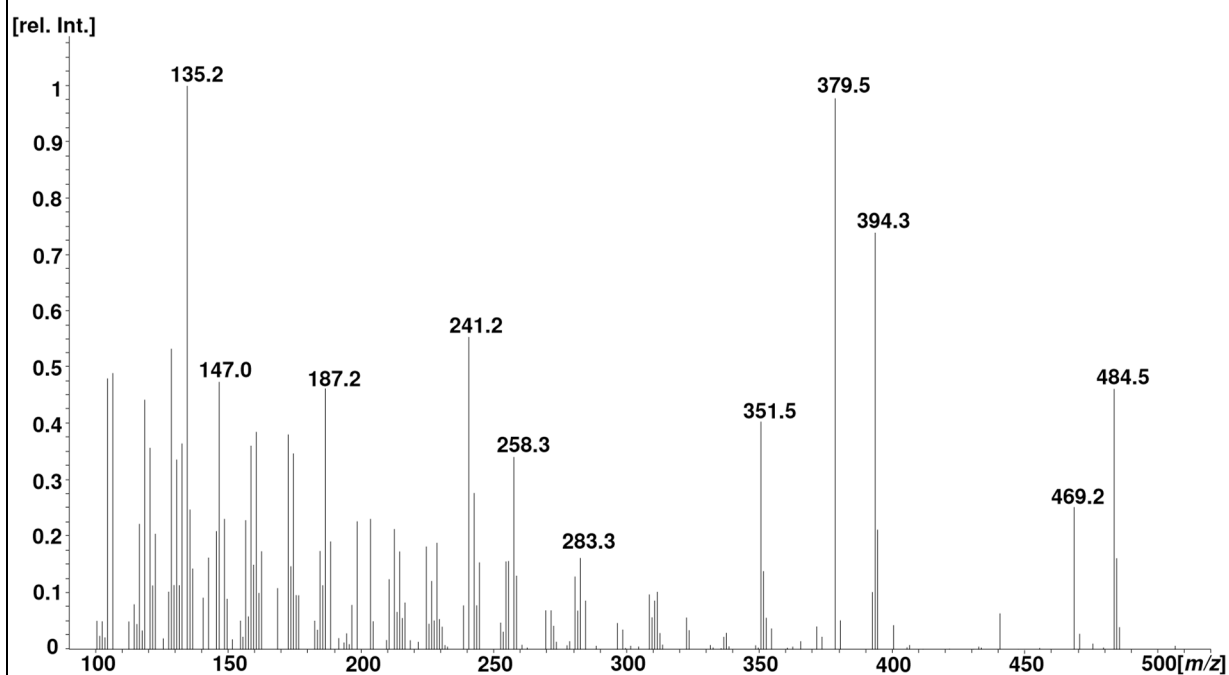
MS spectrum TMS ether



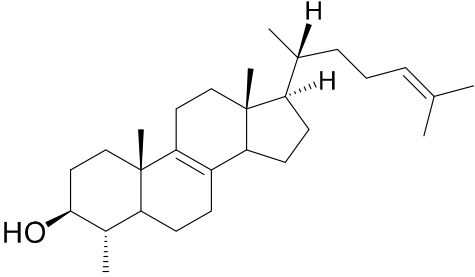
5. Characterization of inhibitors of cholesterol biosynthesis

Compound No.	13		
IUPAC Name	4,4-Dimethylcholesta-8,24-dien-3 β -ol		
Trivial Name	T-MAS		
CAS Number	7448-02-4	M [g/mol]	412.4
Chemical Formula	C ₂₉ H ₄₈ O	M TMS ether [g/mol]	484.4
Structure		RRT TMS ether (Cholestane)	1.48
		RRT TMS ether (Cholesterol)	1.18

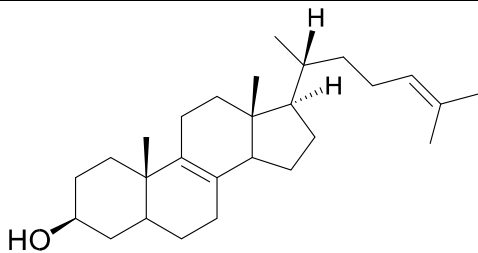
MS spectrum TMS ether



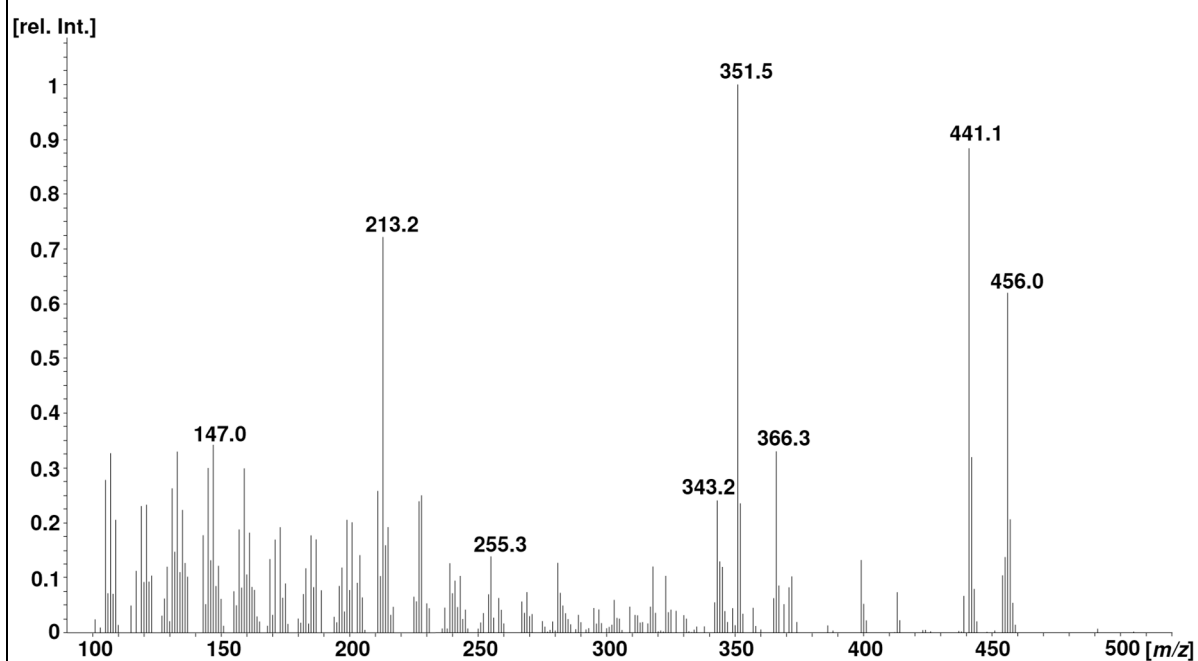
5. Characterization of inhibitors of cholesterol biosynthesis

Compound No.	14		
IUPAC Name	4 α -Methylcholesta-8,24-dien-3 β -ol		
Trivial Name	4-Methylzymosterol		
CAS Number	7448-03-5	M [g/mol]	398.4
Chemical Formula	C ₂₈ H ₄₆ O	M TMS ether [g/mol]	470.4
Structure		RRT TMS ether (Cholestane)	
		RRT TMS ether (Cholesterol)	
MS spectrum TMS ether not available			

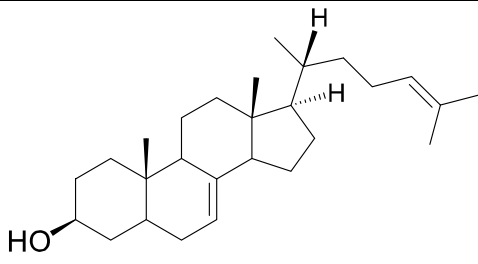
5. Characterization of inhibitors of cholesterol biosynthesis

Compound No.	15		
IUPAC Name	Cholesta-8,24-dien-3 β -ol		
Trivial Name	Zymosterol		
CAS Number	128-33-6	M [g/mol]	384.3
Chemical Formula	C ₂₇ H ₄₄ O	M TMS ether [g/mol]	456.4
Structure		RRT TMS ether (Cholestane)	1.32
		RRT TMS ether (Cholesterol)	1.06

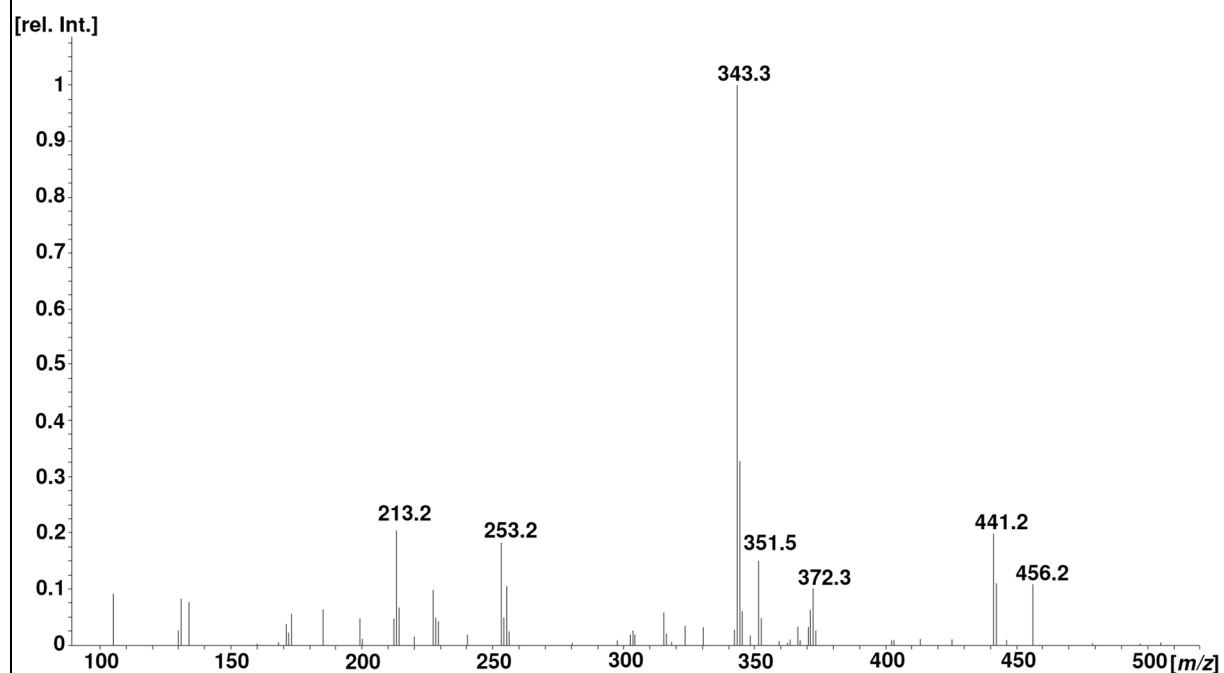
MS spectrum TMS ether



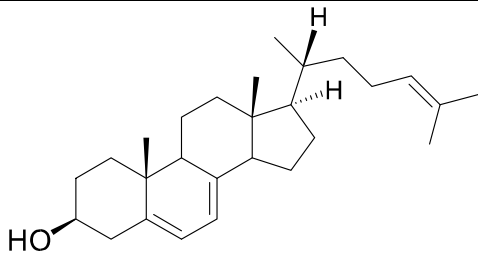
5. Characterization of inhibitors of cholesterol biosynthesis

Compound No.	16		
IUPAC Name	Cholesta-7,24-dien-3 β -ol		
Trivial Name			
CAS Number	651-54-7	M [g/mol]	384.3
Chemical Formula	C ₂₇ H ₄₄ O	M TMS ether [g/mol]	456.4
Structure		RRT TMS ether (Cholestane)	1.34
		RRT TMS ether (Cholesterol)	1.09

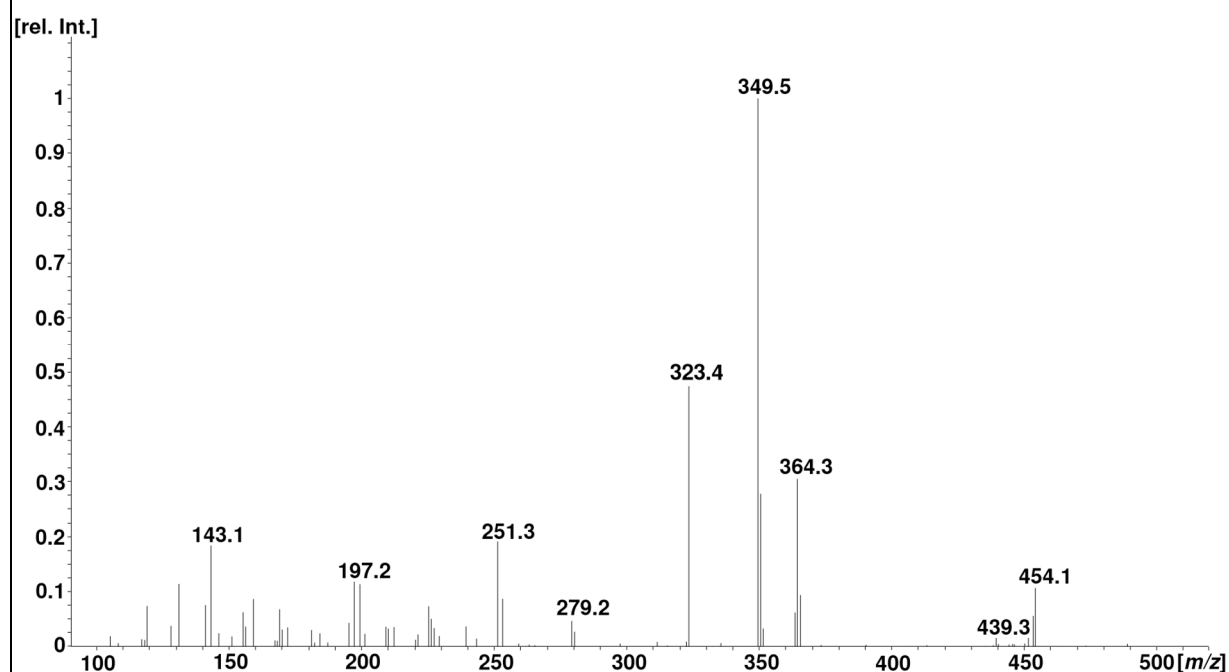
MS spectrum TMS ether



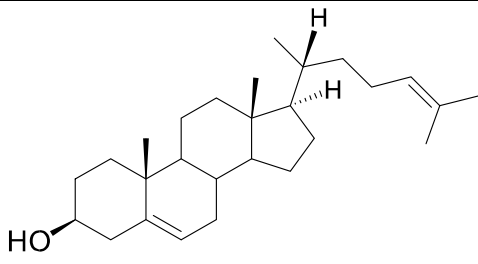
5. Characterization of inhibitors of cholesterol biosynthesis

Compound No.	17		
IUPAC Name	Cholesta-5,7,24-trien-3 β -ol		
Trivial Name	7-Dehydrodesmosterol		
CAS Number	1715-86-2	M [g/mol]	382.3
Chemical Formula	C ₂₇ H ₄₂ O	M TMS ether [g/mol]	454.4
Structure		RRT TMS ether (Cholestane)	1.33
		RRT TMS ether (Cholesterol)	1.06

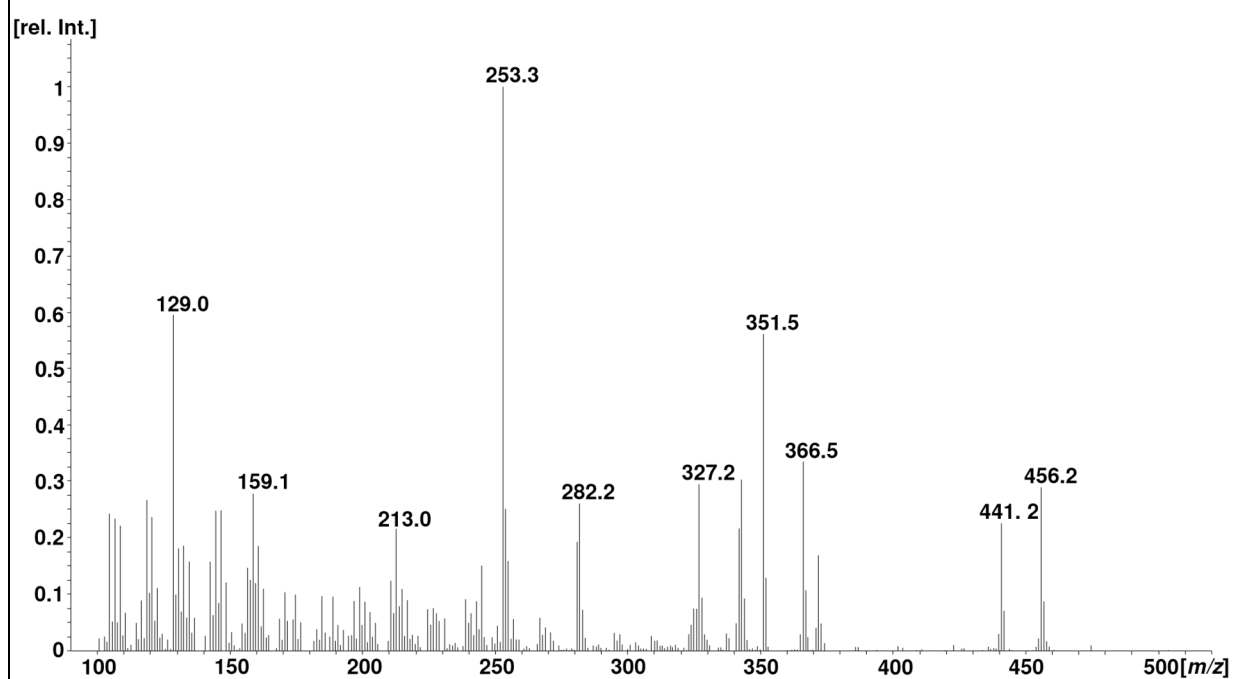
MS spectrum TMS ether



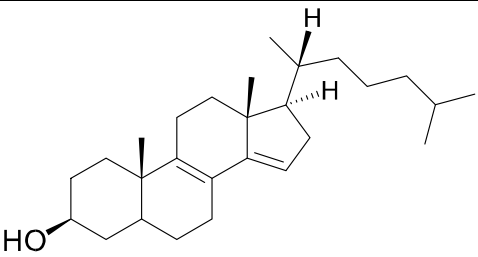
5. Characterization of inhibitors of cholesterol biosynthesis

Compound No.	18		
IUPAC Name	Cholesta-5,24-dien-3 β -ol		
Trivial Name	Desmosterol		
CAS Number	313-04-2	M [g/mol]	384.3
Chemical Formula	C ₂₇ H ₄₄ O	M TMS ether [g/mol]	456.4
Structure		RRT TMS ether (Cholestane)	1.29
		RRT TMS ether (Cholesterol)	1.03

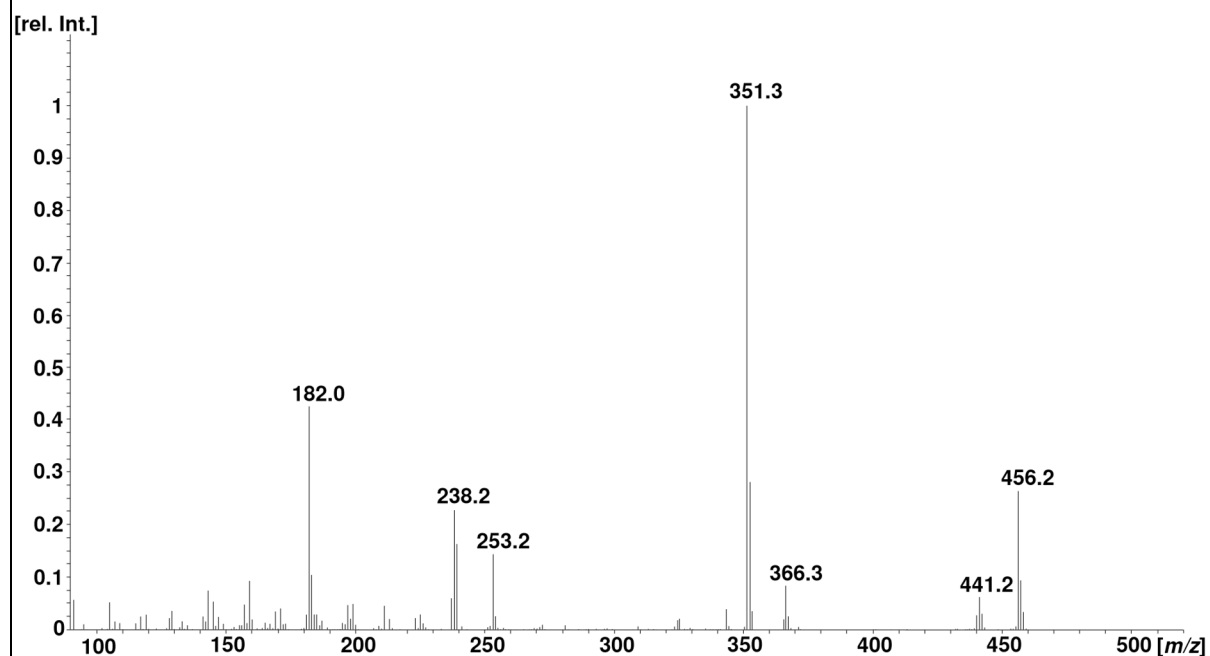
MS spectrum TMS ether



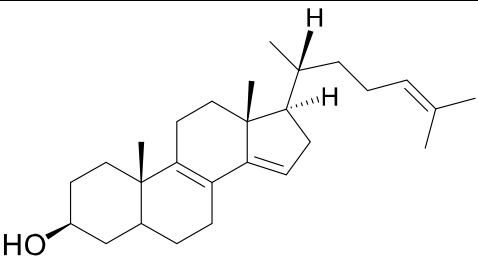
5. Characterization of inhibitors of cholesterol biosynthesis

Compound No.	19		
IUPAC Name	Cholesta-8,14-dien-3 β -ol		
Trivial Name			
CAS Number	17608-73-0	M [g/mol]	384.3
Chemical Formula	C ₂₇ H ₄₄ O	M TMS ether [g/mol]	456.4
Structure		RRT TMS ether (Cholestane)	1.27
		RRT TMS ether (Cholesterol)	1.02

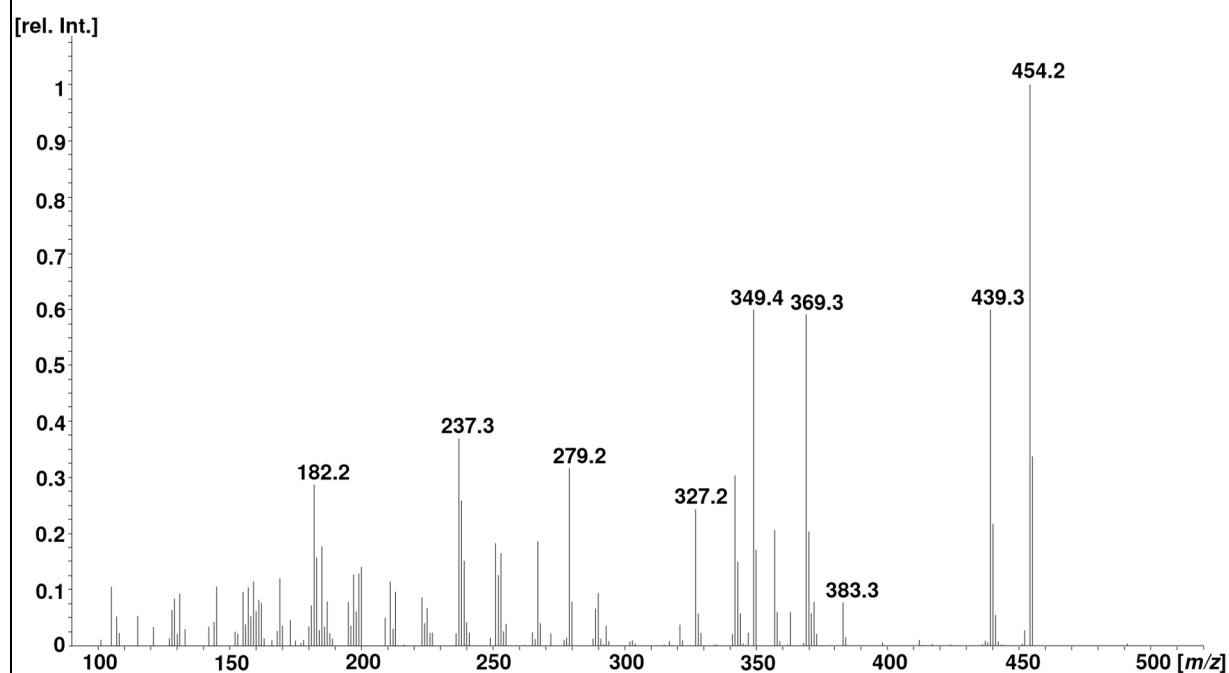
MS spectrum TMS ether



5. Characterization of inhibitors of cholesterol biosynthesis

Compound No.	20		
IUPAC Name	Cholesta-8,14,24-trien-3 β -ol		
Trivial Name			
CAS Number	64284-65-7	M [g/mol]	382.3
Chemical Formula	C ₂₇ H ₄₂ O	M TMS ether [g/mol]	454.4
Structure		RRT TMS ether (Cholestane)	1.31
		RRT TMS ether (Cholesterol)	1.05

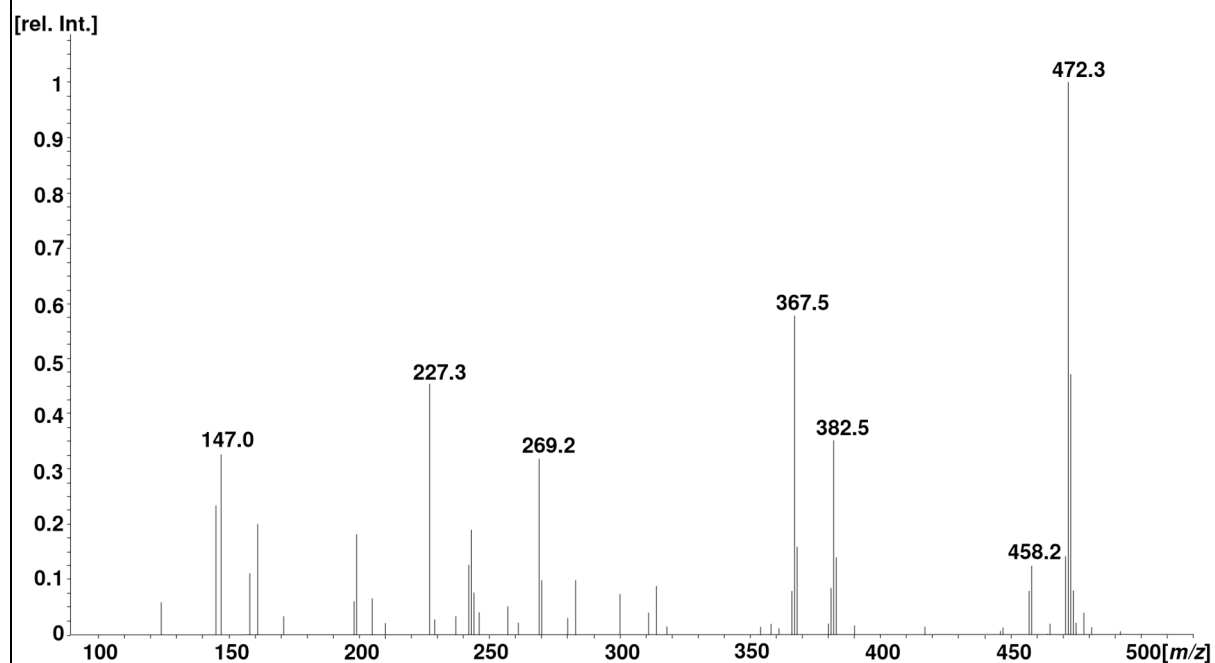
MS spectrum TMS ether



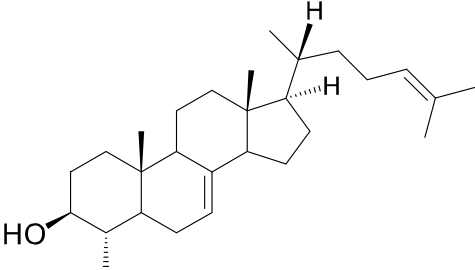
5. Characterization of inhibitors of cholesterol biosynthesis

Compound No.	21		
IUPAC Name	4 α -Methylcholest-7-en-3 β -ol		
Trivial Name	Lophenol		
CAS Number	481-25-4	M [g/mol]	400.4
Chemical Formula	C ₂₈ H ₄₈ O	M TMS ether [g/mol]	472.4
Structure		RRT TMS ether (Cholestane)	1.37
		RRT TMS ether (Cholesterol)	1.09

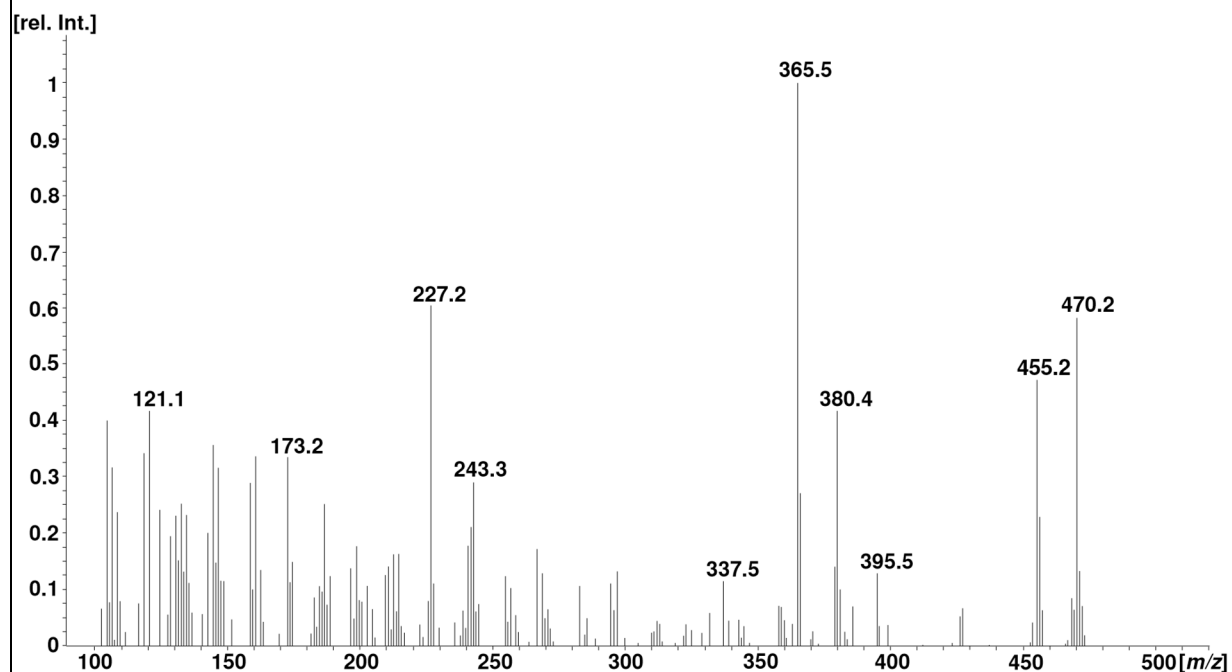
MS spectrum TMS ether



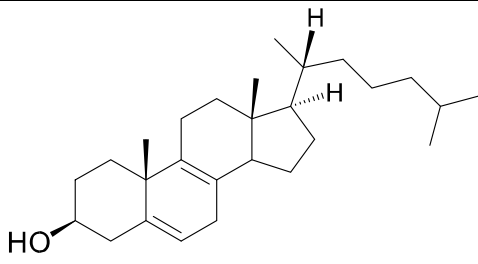
5. Characterization of inhibitors of cholesterol biosynthesis

Compound No.	22		
IUPAC Name	4 α -Methylcholesta-7,24-dien-3 β -ol		
Trivial Name			
CAS Number	24778-51-6	M [g/mol]	398.4
Chemical Formula	C ₂₈ H ₄₆ O	M TMS ether [g/mol]	470.4
Structure		RRT TMS ether (Cholestane)	1.40
		RRT TMS ether (Cholesterol)	1.12

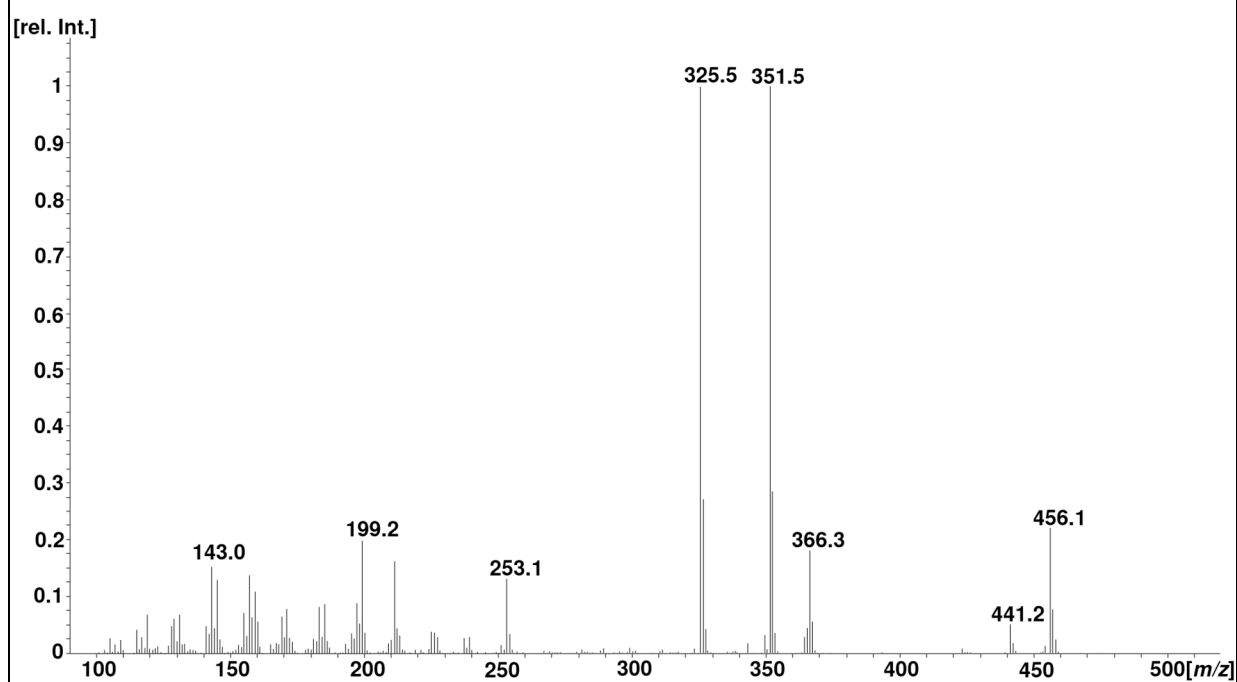
MS spectrum TMS ether



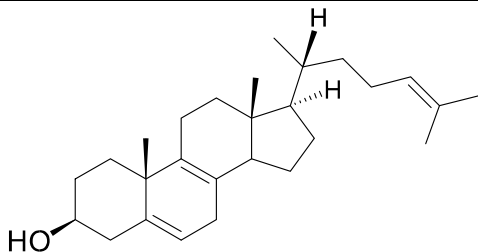
5. Characterization of inhibitors of cholesterol biosynthesis

Compound No.	23		
IUPAC Name	Cholesta-5,8-dien-3 β -ol		
Trivial Name	8-Dehydrocholesterol		
CAS Number	70741-38-7	M [g/mol]	384.3
Chemical Formula	C ₂₇ H ₄₄ O	M TMS ether [g/mol]	456.4
Structure		RRT TMS ether (Cholestane)	1.26
		RRT TMS ether (Cholesterol)	1.01

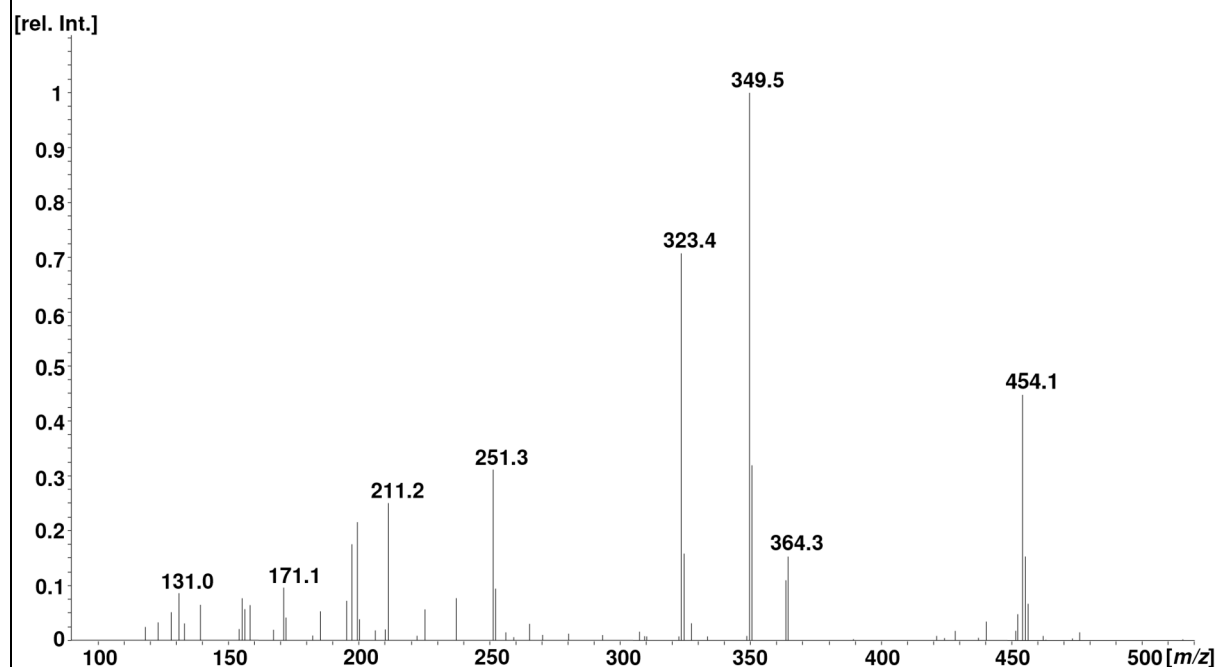
MS spectrum TMS ether



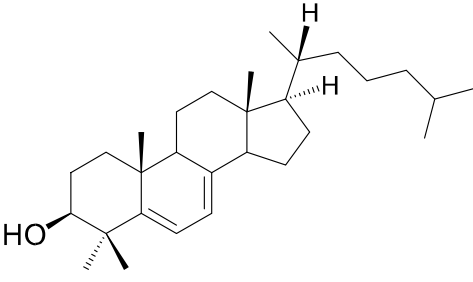
5. Characterization of inhibitors of cholesterol biosynthesis

Compound No.	24		
IUPAC Name	Cholesta-5,8,24-trien-3 β -ol		
Trivial Name			
CAS Number	70441-40-6	M [g/mol]	382.3
Chemical Formula	C ₂₇ H ₄₂ O	M TMS ether [g/mol]	454.4
Structure		RRT TMS ether (Cholestane)	1.30
		RRT TMS ether (Cholesterol)	1.04

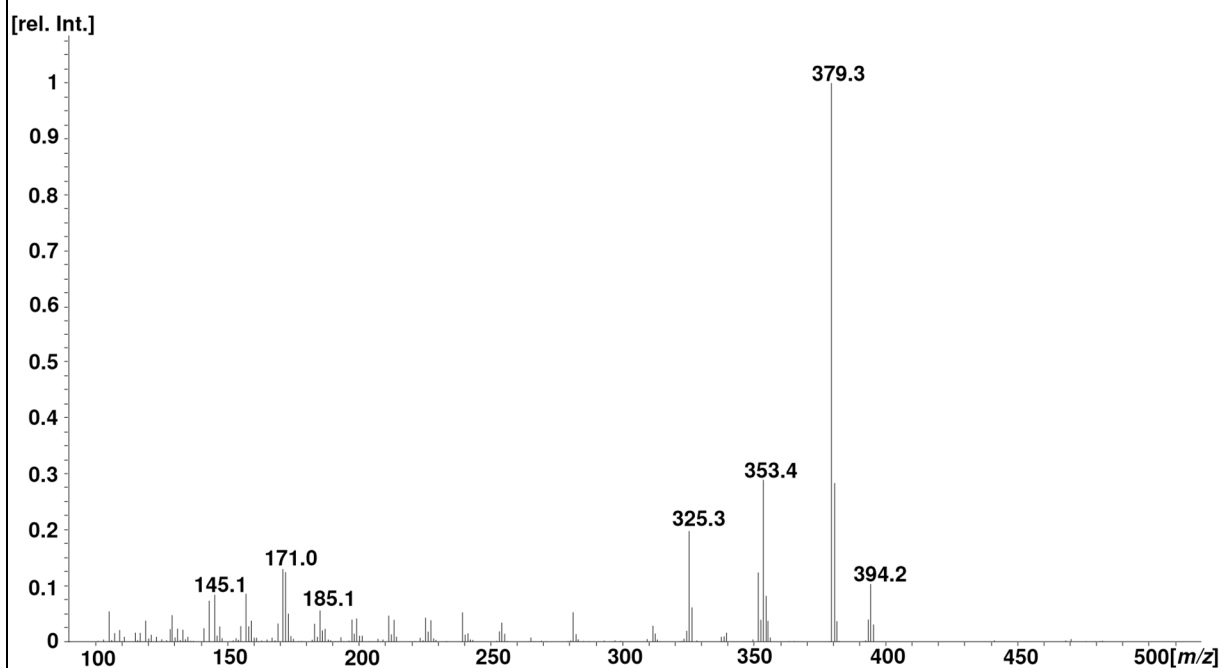
MS spectrum TMS ether



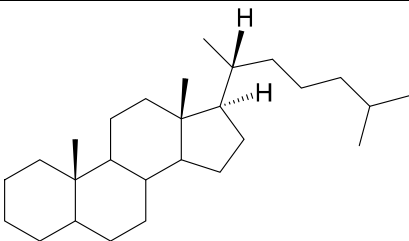
5. Characterization of inhibitors of cholesterol biosynthesis

Compound	25		
IUPAC Name	4,4-Dimethylcholesta-5,7-dien-3 β -ol		
Trivial Name			
CAS Number	53296-71-2	M_R [g/mol]	412.4
Chemical Formula	C ₂₉ H ₄₈ O	M_R TMS ether [g/mol]	484.4
Structure		RRT TMS ether (Cholestane)	1.43
		RRT TMS ether (Cholesterol)	1.14

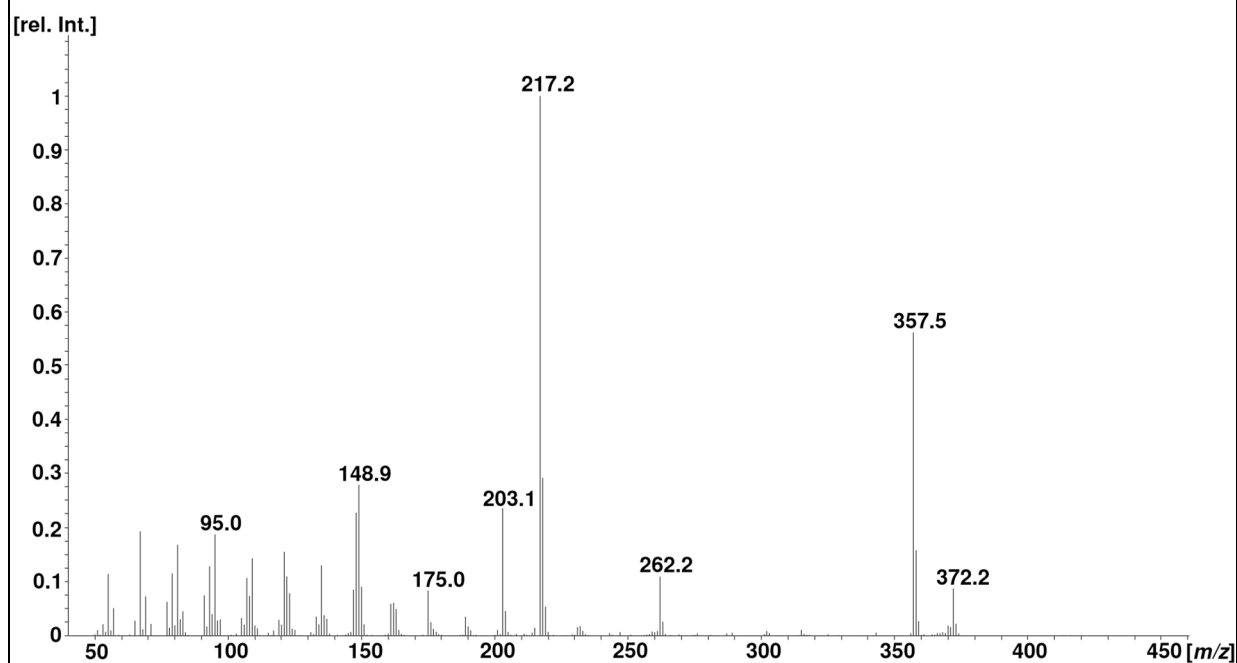
MS spectrum TMS ether



5. Characterization of inhibitors of cholesterol biosynthesis

Compound No.	26		
IUPAC Name	Cholestane		
Trivial Name			
CAS Number	481-21-0	M [g/mol]	372.4
Chemical Formula	C ₂₇ H ₄₈	M TMS ether [g/mol]	
Structure		RRT TMS ether (Cholestane)	1.00
		RRT TMS ether (Cholesterol)	0.80

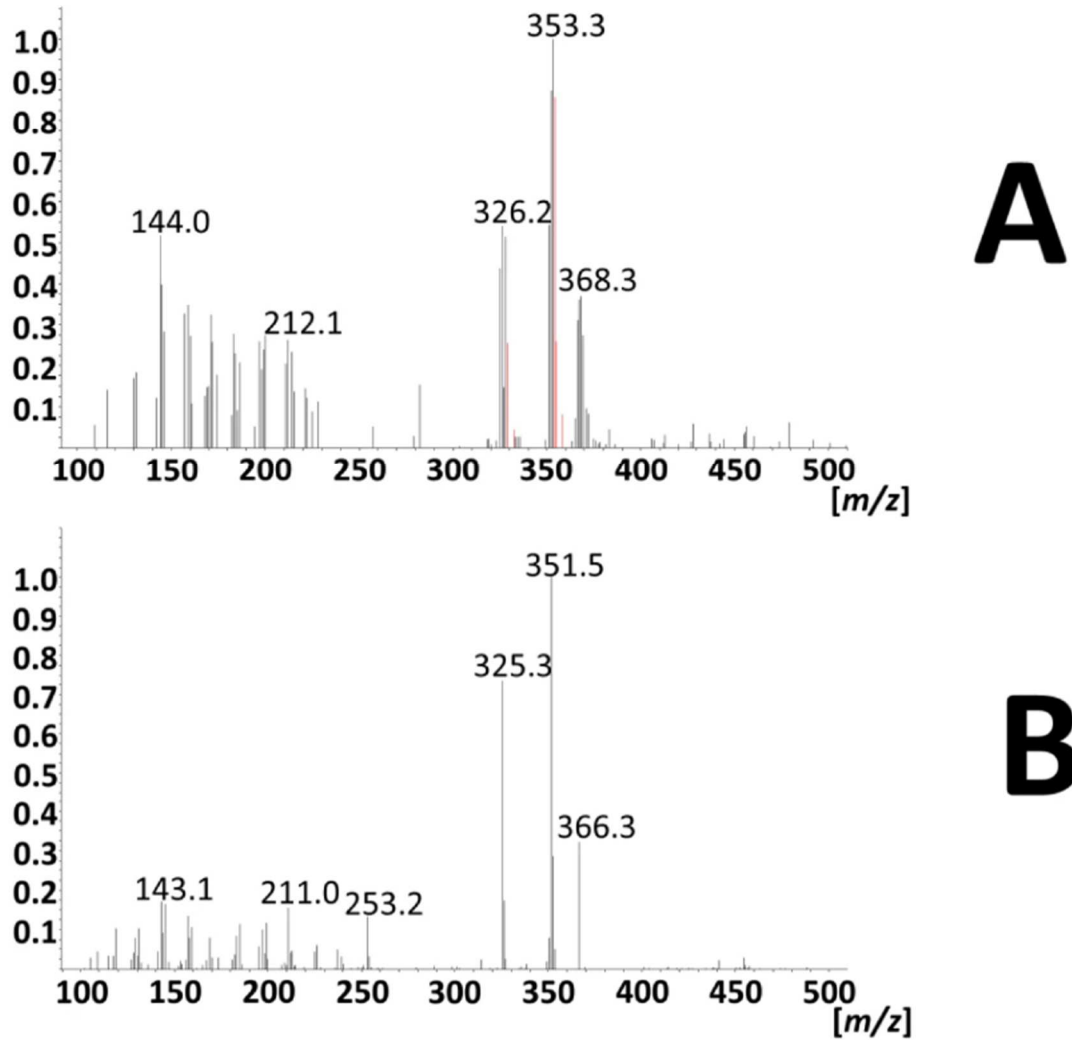
MS spectrum



5. Characterization of inhibitors of cholesterol biosynthesis

Supplementary Fig. 1: Comparison of labeled and unlabeled 7-Dehydrocholesterol.

From: A gas chromatography–mass spectrometry-based whole-cell screening assay for target identification in distal cholesterol biosynthesis

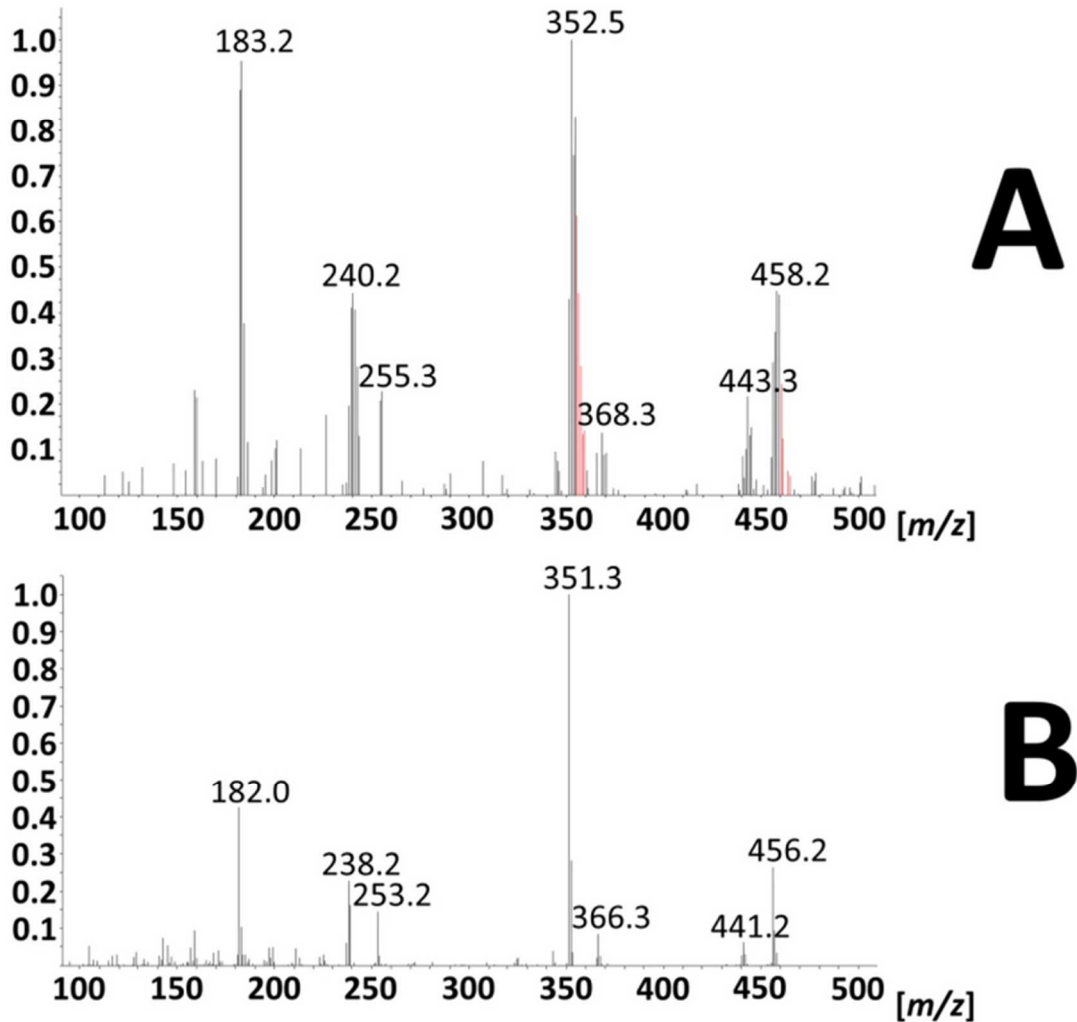


A) Labeled 7-Dehydrocholesterol after incubation of HL60 cells with AY9944 and 2- ^{13}C -acetate. The red lines denote the isotopes +4 to +11 of the two most prominent peaks in the spectrum, used for quantification. B) unlabeled control.

5. Characterization of inhibitors of cholesterol biosynthesis

Supplementary Fig. 2: Comparison of labeled and unlabeled cholesta-8,14-dien-3 β -ol.

From: A gas chromatography–mass spectrometry-based whole-cell screening assay for target identification in distal cholesterol biosynthesis



A) labeled Cholesta-8,14-dien-3 β -ol after incubation of HL60 cells with AY9944 and 2-¹³C-acetate. The red lines denote the isotopes +4 to +11 of the two most prominent peaks in the spectrum, used for quantification. B) unlabeled control.

5. Characterization of inhibitors of cholesterol biosynthesis

Supplementary Fig. 3: Comparison of labeled and unlabeled zymostenol.

From: A gas chromatography–mass spectrometry-based whole-cell screening assay for target identification in distal cholesterol biosynthesis

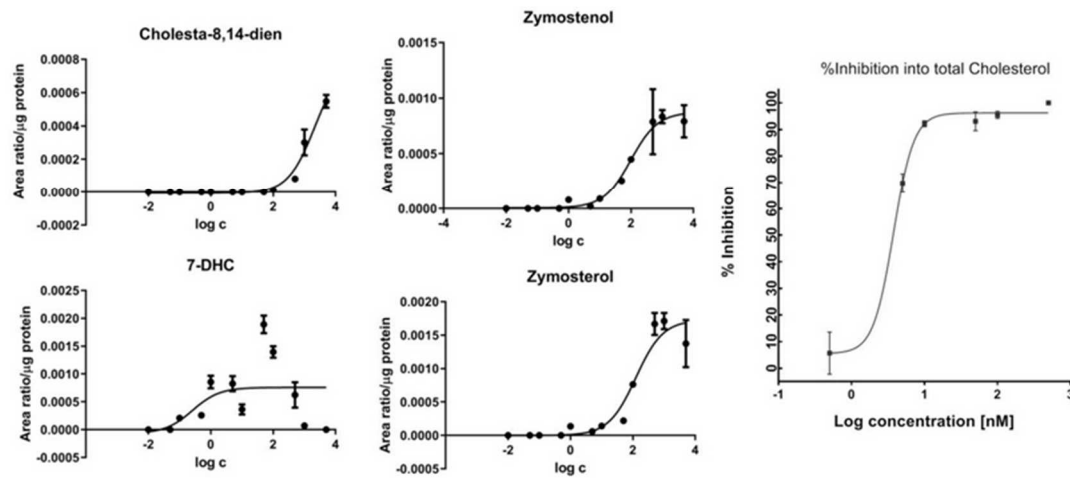


A) Labeled Zymostenol after incubation of HL60 cells with AY9944 and 2-¹³C-acetate. The red lines denote the isotopes +4 to +11 of the two most prominent peaks in the spectrum, used for quantification. B) unlabeled control.

5. Characterization of inhibitors of cholesterol biosynthesis

Supplementary Fig. 4: IC50 comparison for AY 9944.

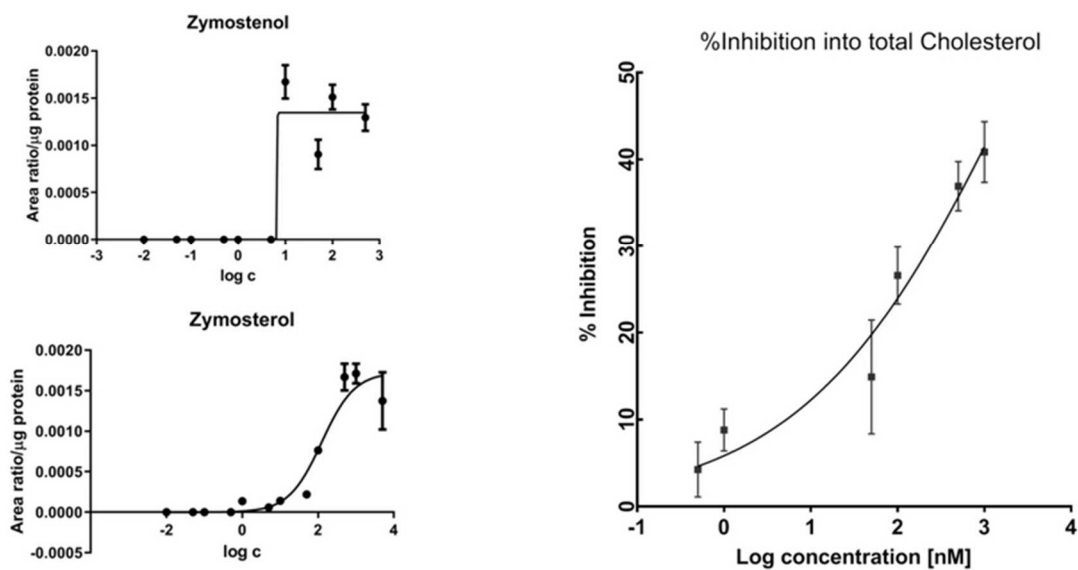
From: A gas chromatography–mass spectrometry–based whole-cell screening assay for target identification in distal cholesterol biosynthesis



IC50 curves constructed using precursor sterols versus 2-13C acetate accumulation in total cholesterol (right side).

Supplementary Fig. 5: IC50 comparison for tamoxifen.

From: A gas chromatography–mass spectrometry–based whole-cell screening assay for target identification in distal cholesterol biosynthesis

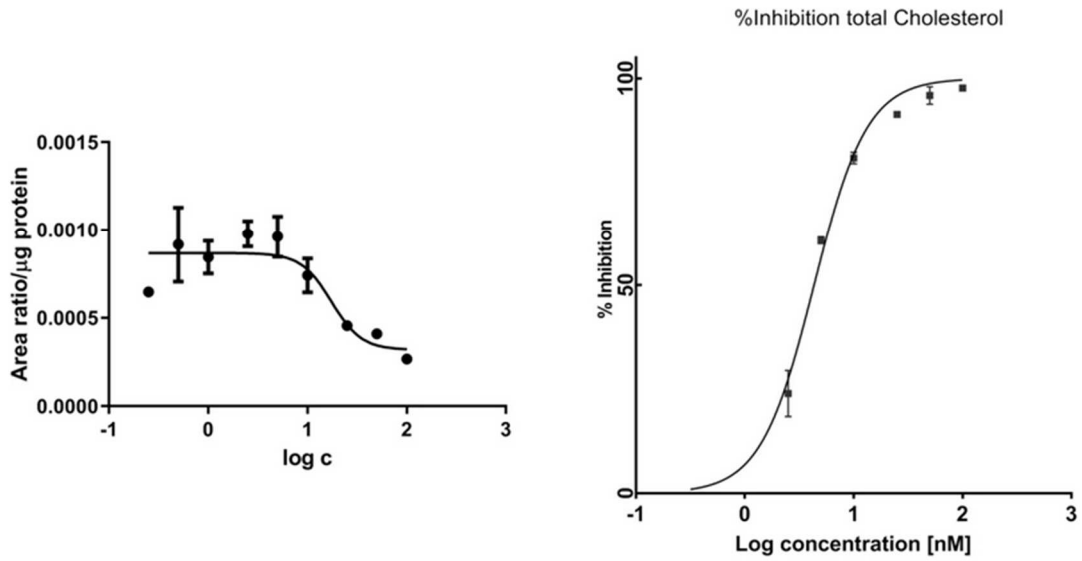


IC50 curves constructed using precursor sterols versus 2-13C acetate accumulation in total cholesterol (right side).

5. Characterization of inhibitors of cholesterol biosynthesis

Supplementary Fig. 6: IC₅₀ comparison for SH42.

From: A gas chromatography–mass spectrometry–based whole-cell screening assay for target identification in distal cholesterol biosynthesis



IC₅₀ curves constructed using precursor sterols versus 2-¹³C acetate accumulation in total cholesterol (right side).

6. Traceless isoprenylation

D. Heerdegen, J. Junker, S. Dittrich, P. Mayer, F. Bracher, Traceless Isoprenylation of Aldehydes via N-Boc-N-(1,1-dimethylallyl)hydrazones, European Journal of Organic Chemistry, 24 (2020) 3680-3687.

6.1. Summary

Isoprenylation is a typical biological process which takes place in posttranslational modifications of proteins [92] and in the biosynthesis of terpenes like sterols by addition of isopentenyl diphosphate building blocks as shown in Figure 2 (Chapter 1.2.1) [13]. In this article, a new approach for the introduction of an isoprenyl group into organic molecules is presented. Using the traceless bond construction developed by Thomson et al. [93] *N*-Boc-*N*-allylhydrazines were used, which after condensation with appropriate aldehydes undergo [3,3]-sigmatropic rearrangement leading to the desired isoprenylated compounds. The rearrangement here is named traceless bond construction, since only gaseous by-products (N_2 , *iso*-butylene (C_4H_8) and CO_2) were formed during the C-C bond formation and the product does not contain any retron, which could reveal the used synthetic pathway [93]. The required *N*-Boc-*N*-allylhydrazone was synthesized from a novel *N*-Boc-*N*-allyl-hydrazine building block by condensation with the appropriate aldehyde. The resulting hydrazone underwent the [3,3] sigmatropic in the presence of catalytic amounts of the superacid triflimide.



Figure 11 Graphical abstract of the article showing the condensation of the *N*-Boc-*N*-allylhydrazine with an aldehyde leading to a *N*-Boc-*N*-allylhydrazone. After [3,3]-sigmatropic rearrangement the desired isoprenylated product is formed

This article describes the synthesis of the required *N*-Boc-*N*-allyl-hydrazine building block, the condensation reactions with various aldehydes and the subsequent rearrangement. It was crucial, to first optimize the [3,3]-sigmatropic rearrangement by changing the solvent, acid, temperature and reaction times by using a model compound. All in all, 33 optimization reactions were performed for one model product. This high number of experiments could be achieved using GC-MS monitoring, which was the ideal method to analyze the very volatile model product ((4-methylpent-3-en-1-yl)cyclohexane). As the cumbersome preparative

6. Traceless isoprenylation

cleanup and weighting of the product could be avoided, the optimization reactions could be performed much faster and in smaller synthesis approaches.

6.2. Personal contribution

Conceptualization of the project, as well as planning and implementation of the synthesis was done by Dr. Desiree Heerdegen. In addition, she wrote the original draft and also the preliminary investigations and experiments were part of her contribution to the article.

My contribution to this article were the development of the GC-MS method for the analysis of the prenylated products. The conceptualization of the analytical procedure for the optimization experiments, the performance of the respective GC-MS measurements and the analysis of the measurement data (see Chapter 6.4) was also part of my contribution to this article. This GC-MS based method was crucial for the screening of multiple different reaction conditions without time consuming workup.

The crystallization experiments were done by Dr. Peter Mayer.

The project based on previously developed traceless bond constructions, that were published by Dr. Sebastian Dittrich and Prof. Dr. Franz Bracher [94, 95]. Both supported the conceptualization of this project and further contributed in editing and reviewing of the original draft. Dr. Sebastian Dittrich was further involved in parts of the synthesis. Prof. Dr. Franz Bracher further contributed by providing the necessary resources.

6.3. Article

The following article is printed in the original wording. The formatting may vary slightly compared to the original article.

Traceless Isoprenylation

Traceless Isoprenylation of Aldehydes via *N*-Boc-*N*-(1,1-dimethylallyl)hydrazones

Desirée Heerdegen,^[a] Julia Junker,^[a] Sebastian Dittrich,^[a] Peter Mayer,^[b] and Franz Bracher*^[a]

Abstract: A short isoprenylation protocol starting from nonconjugated *N*-Boc-*N*-(1,1-dimethylallyl)hydrazones was developed utilising Thomson's traceless bond construction. This type of [3,3]-sigmatropic rearrangement is catalysed by the Brønsted acid triflimide and liberates only gaseous by-products. The required *N*-Boc-*N*-allylhydrazine precursor is available in three steps starting from a known diazene using

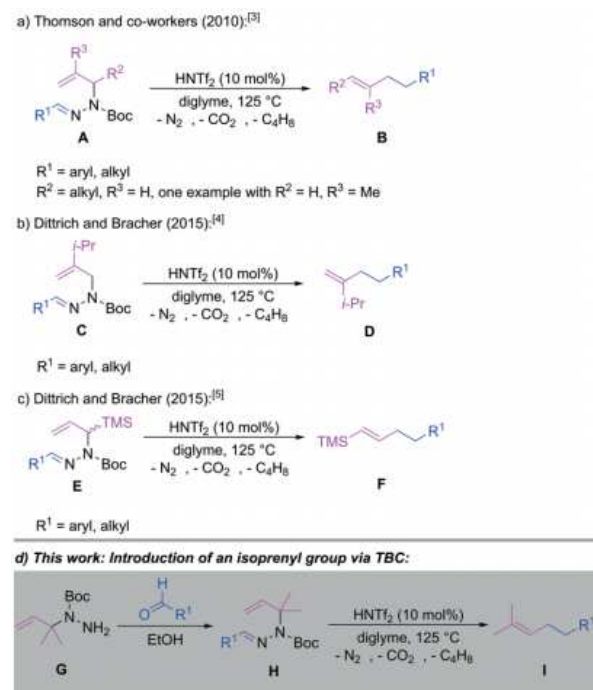
which permits use, distribution and reproduction in any medium, provided the original work is properly cited.

biocatalytic aldol addition and Tebbe olefination as key steps. Allylhydrazones are prepared via condensation with appropriate aldehydes. Scope and limitations of the [3,3]-sigmatropic rearrangements are analysed.

Introduction

The [3,3]-sigmatropic rearrangement is a common but impressive tool for the formation of new C–C-bonds in synthetic chemistry.^[1] In 1973 Stevens showed that *N*-allylhydrazones undergo such a rearrangement under release of N₂ as well, but due to very harsh reaction conditions (300 °C) and low yields, this reaction was limited in its applicability.^[2] For several decades, synthetic chemists did not see any real benefit of this unique rearrangement, until 2010, when Thomson and co-workers published the traceless bond construction (TBC), an improved variant of Stevens' [3,3]-sigmatropic rearrangement, working with *N*-Boc-*N*-allylhydrazones (**A**, Scheme 1a) and catalytic amounts of the Brønsted superacid triflimide (HNTf₂).^[3] It was now possible to lower the temperature of the rearrangement to 125 °C and the yields of the products could be increased. This pioneering work of Thomson allowed the synthesis of various 1,2-disubstituted olefins (**B**) and one 1,1-disubstituted olefin (Scheme 1a). Mono-substituted olefins could not be obtained by this way. Later our group extended the scope to the synthesis of 1,1-disubstituted olefins (**D**, Scheme 1b), bearing an isopropyl group in 1-position, which resulted in a methylene branched end, a motif which is found in the side chains of steroidal natural products, e.g. episterol.^[4] In the same year we reported the synthesis of

terminal vinylsilanes (**F**, Scheme 1c) using TBC, which opened a new route to diversely substituted olefins.^[5]



Scheme 1. a) Original TBC by Thomson and co-workers.^[3] b) Extension of the TBC to the synthesis of 1,1-disubstituted olefins bearing an isopropyl group.^[4] c) TBC yielding terminal vinylsilanes.^[5] d) Introduction of an isoprenyl group via TBC developed in this work.

In this work we present a protocol for the introduction of an isopentenyl (isoprenyl) residue to aldehydes (Scheme 1d). The isoprenyl function is a common structural element in terpenoid biomolecules and natural secondary

[a] D. Heerdegen, J. Junker, Dr. S. Dittrich, Prof. Dr. F. Bracher
Department of Pharmacy - Center for Drug Research, Ludwig-Maximilians University,
Butenandtstr. 5-13, 81377 Munich, Germany
<https://bracher.cup.uni-muenchen.de/>

[b] Dr. P. Mayer
Department of Chemistry, Ludwig-Maximilians University,
Butenandtstr. 5-13, 81377 Munich, Germany
Supporting information and ORCID(s) from the author(s) for this article are available
on the WWW under <https://doi.org/10.1002/ejoc.202000382>.

© 2020 The Authors. Published by Wiley-VCH Verlag GmbH & Co. KGaA. - This is an
open access article under the terms of the Creative Commons Attribution License,

6. Traceless isoprenylation

metabolites.^[6] The natural isoprene building block in terpenoid biosynthesis is dimethylallyl pyrophosphate (DMAPP).^[7,8] Steroids like cholesterol as a membrane component,^[9] pigments like β -carotene,^[10] or cortisone or progesterone to name a few hormones,^[11] are naturally occurring terpenoid derivatives, derived from DMAPP.

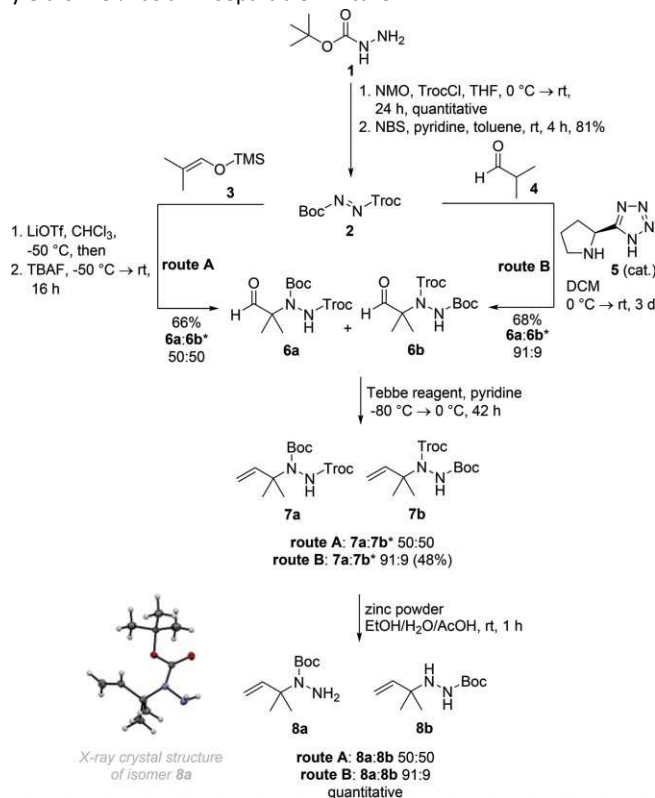
At the biological level, protein prenyltransferases attach terpenoid residues like farnesyl (C₁₅) or geranylgeranyl (C₂₀) groups to cysteinyl residues of proteins in posttranslational modifications. Due to the introduction of this hydrophobic group, the proteins can anchor in biomembranes resulting in altered biological activities.^[12] In synthetic chemistry, organometallic building blocks like 3-methyl-2-butenylmagnesium chloride are commonly used for the introduction of an isoprenyl group.^[13] Utilising inverse reactivities, 3,3-dimethylallyl bromide can be applied as an electrophilic isoprenyl building block,^[14] as exemplified by the total syntheses of natural products, e.g. (\pm)-eldanolid^[15] and (\pm)-fumagillin.^[16] Besides direct isoprenylation, eliminations can lead to the isoprenyl function by forming the thermodynamically most stable double bond, e.g. from tertiary alcohols by dehydration.^[17] An intramolecular isoprenylation, in which the group is constructed during a rearrangement, is to the best of our knowledge, not described in literature yet.

A further centrepiece of this work is the synthesis of the required, hitherto unknown, *N*-Boc-*N*-(1,1-dimethylallyl)hydrazine building block (**G**, Scheme 1d), bearing two geminal methyl groups in α -position to the hydrazine moiety to receive the desired isoprenylated products (**I**, Scheme 1d) via *N*-Boc-*N*-allylhydrazones (**H**, Scheme 1d). In our previous investigations leading to 1,1-disubstituted olefins,^[4] undesired subsequent acidcatalysed isomerisations of the formed olefinic double bond were observed,^[18] which led occasionally to isomeric mixtures of product alkenes. In the present case this is not expected to happen, since the resulting trisubstituted olefin should be the thermodynamically most stable isomer. An additional benefit of the two geminal methyl groups in precursor **G** is on the one hand that product **I** cannot be formed as mixture of *E/Z* isomers and on the other hand it is expected to facilitate the rearrangement due to the Thorpe-Ingold effect (gem-dimethyl effect).^[19] As a result, less drastic reaction temperatures and shortened reaction times may be employable.^[20]

Results and Discussion

The synthesis of the required *N*-Boc-*N*-(1,1-dimethylallyl)hydrazine building block **8a** (Scheme 2; **G** in Scheme 1d) started with the two-step synthesis of known *N*-Troc-*N*-Boc-protected diazene **2**.^[21] Conversion into aldehyde **6a** was performed on two different routes. Route A used commercially available silyl enol ether **3**, which was activated by LiOTf and TBAF. The idea was to achieve a controlled O-Si-bond cleavage in **3** by slow addition of the

fluoride source. Simultaneously, the presence of significant amounts of lithium ions should lead to an immediate formation of the lithium enolate. However, the addition of **3** to **2** did not proceed in a regioselective manner, and a 50:50 mixture of the isomeric aldehydes **6a** and its regioisomer **6b** was obtained. It is noteworthy, that the regioselectivity of this reaction could not be measured in this step, hence, it was determined retrospectively after conversion into **8a/8b** after the last step. Both isomers showed identical chromatographic behaviour and no distinct signals enabling quantification of the ratio of regioisomers could be observed by NMR spectroscopy until reaching **8a/8b**. Because of the lack of regioselectivity, an alternative approach to intermediate **6a** utilising organocatalysis^[22,23] was worked out (route B). For this Aldol-type reaction with isobutyraldehyde (**4**), three catalysts were explored: L-proline,^[24] L-phenylalanine,^[25] and Ley's (*S*)-5-(pyrrolidin-2-yl)1*H*-tetrazole (**5**).^[21,26] Tetrazole catalyst **5** gave the best result with 68 % yield and the isomeric ratio could be improved to 91:9 (determined retrospectively by ¹H NMR spectroscopy) of the desired aldehyde **6a** and its regioisomer **6b**. Methylenation of the aldehyde function of **6a/6b** gave the olefins **7a** and **7b**. Different methods like Wittig,^[27] Nysted-Takai^[28] and Tebbe^[29] olefination were tested, whereby the first two methods did not result in any product. Under Tebbe conditions the desired terminal olefin **7a** and its regioisomer **7b** were obtained in an acceptable yield of 48 % as an inseparable mixture.



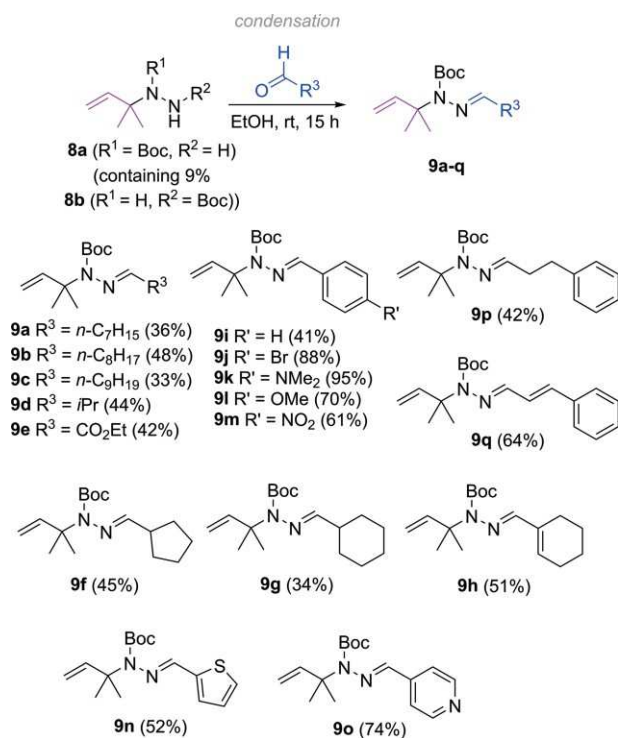
Scheme 2. Route A leading to an equimolar mixture of **8a/8b** starting from silyl enol ether **3**. Route B provides **8a**, contaminated with 9 % of isomer **6b** starting from aldehyde **4**. *The ratios of the isomers were determined retrospectively by NMR spectroscopy of the product **8a/8b**.

6. Traceless isoprenylation

The X-ray crystal structure of the desired isomer **8a** is shown on the left. Diazene **2** was synthesised according to literature.^[21]

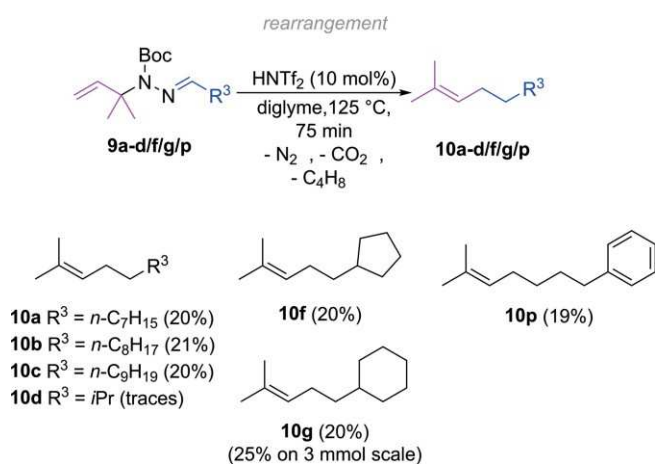
Chemoselective reductive Troc cleavage with zinc powder gave a still inseparable mixture of the desired olefin **8a** and its constitutional isomer **8b** in excellent yield. However, at this stage NMR spectroscopy enabled determination of the ratio of isomers (route A 50:50, route B 91:9). The structure of the desired *N*-Boc-*N*-allylhydrazone **8a** was unambiguously confirmed by X-ray crystal structure analysis (see Supporting Information). The enriched isomeric mixture of building block **8a** and **8b** could be used for the next step without further purification, since exclusively **8a** undergoes condensation with the employed aldehydes to give the *N*-Boc-*N*-allylhydrazones **9**, whereas the isomer **8b** remains unreacted. Scheme 3 shows the prepared allylhydrazones **9a–q**. Aliphatic (**9a–d**, **9f**, **9g**, **9p**), allylic (**9h**, **9q**) and aromatic (**9i–9o**) and ester-bearing (**9e**) allylhydrazones were synthesised by reacting the appropriate aldehydes with building block mixture **8a/b** in ethanol (yields 33 – 95 %). Especially non-conjugated allylhydrazones slowly decomposed during the purification process, which is reflected in the yields. Before we studied the capability of our *N*-Boc-*N*-allylhydrazone building block **8a**, we identified the optimum reaction conditions for the rearrangement utilising cyclohexanecarboxaldehyde-derived hydrazone **9g** as a model compound. Overall, 33 test reactions were performed with variations of temperature (23 to 125 °C), time (15 to 75 min) and solvents (THF and diglyme) (see Supporting Information). Significant rearrangement was only accomplished at temperatures of 75 °C and above. Besides HNTf₂ (pK_a –12.0, measured in DCE),^[30] triflic acid (TfOH, pK_a –11.3, measured in DCE)^[30] and trifluoroacetic acid (TFA, pK_a 0.23)^[31] were tested. All in all, the hitherto used conditions of Thomson^[3] (HNTf₂, diglyme, 125 °C) gave the best results for this conversion, closely followed by the rearrangement with triflic acid in diglyme at 125 °C, which would be a rewarding alternative to HNTf₂, which decomposes immediately in air and requires extremely dry reaction conditions. As the main side product, and even right at the beginning of the reaction, the corresponding Boc-protected allylhydrazone was observed, a compound which does not undergo the rearrangement. This is in accordance with the observations of Thomson and could not be prevented.^[3] This prompted us to further investigate an alternative carbamate residue, which might be less prone to premature acidic cleavage. We prepared the ethyl carbamate analogue S5a of **8a** starting from ethyl carbamate on a route analogous to route B shown in Scheme 2 (for details, see Supporting Information). Two *N*-Boc-*N*-allylhydrazones S6g and S6i derived thereof were subjected to the previously determined best reaction conditions for rearrangement (HNTf₂, diglyme, 125 °C), but though the starting materials were fully consumed, none of the expected rearrangement products could be identified by GC/MS analysis. Consequently, the Boc group cannot be

replaced in this protocol by the smaller ethoxycarbonyl group.



Scheme 3. *N*-Boc-*N*-allylhydrazones **9a–q** prepared via condensation reaction between *N*-Boc-*N*-allylhydrazone **8a** and appropriate aldehydes. The yields refer to the content of *N*-Boc-*N*-allylhydrazone **8a** in the applied **8a/8b** mixture.

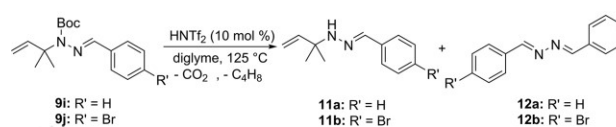
Scheme 4 shows the following rearrangement of substrates **9**. The allylhydrazones **9a–c** derived from *n*-alkanal underwent sigmatropic rearrangement providing the appropriate olefins **10a–c** in 20–21 % isolated yields. The poor yields are in part due to the high volatility of the olefinic products, as demonstrated by an increased yield (25 %) of **10g** on a larger scale (3 mmol). The rearrangement product **10d** of isobutyraldehyde-derived *N*-allylhydrazone **9d** could be detected by GC/MS, but could not be isolated due to its very high volatility (b.p. 135– 136 °C^[32]). Ester **9e** did not undergo rearrangement to the corresponding olefin and only the Boc-protected allylhydrazone was found.



6. Traceless isoprenylation

Scheme 4. Successful rearrangements of *N*-Boc-*N*-allylhydrazones using the standard conditions of the TBC. The reactions were performed at least in a 0.5 mmol scale. Isolated yields are given.

N-Allylhydrazones derived from cycloalkane carboxaldehydes (**9f**, **9g**) underwent rearrangement to olefins **10f** and **10g** with a yield of 20 % for both compounds (Scheme 4). In contrast, allylhydrazone **9h** derived from an α,β -unsaturated aldehyde did not undergo rearrangement and again only Boc-deprotected allylhydrazone was isolated. The attempted rearrangements of variously substituted arylidene hydrazones failed as well (**9i–m**). During the purification process of the attempted rearrangements of **9i** and **9j** crystalline solids were obtained, which were identified as the symmetric bis-hydrazones **12a/b** (Scheme 5).



Scheme 5. Attempted rearrangements of allylhydrazones **9i** and **9j** leading to deprotected allylhydrazones **11a/b** and bis-hydrazones **12a/b**.

Obviously, acid-mediated removal of both the Boc and the dimethylallyl residue took place in these experiments. Next to those, once again Boc-deprotected allylhydrazones **11a/b** were formed. Introduction of both electron-donating (methoxy compound **9l**) and electron-withdrawing groups (nitro compound **9m**) did not lead to successful rearrangements, and the same holds for hydrazones derived from heteroaromatic aldehydes (thiophene **9n** and pyridine **9o**). After these experiments it became evident which type of allylhydrazones would undergo the attempted acid-catalysed rearrangement. Non-conjugated allylhydrazones, like aliphatic systems **9a–d**, **9f**, and **9g** form the corresponding olefins, in contrast to allylhydrazones conjugated with aryl or ester groups, which do not show any rearrangement. The following experiments supported this assumption: Non-conjugated *N*-allylhydrazone **9p** derived from phenylpropanal showed a successful rearrangement with 19 % yield, whereas its cinnamaldehyde-derived congener **9q** did not give the desired alkene **10q** and only Boc-deprotected allylhydrazone was obtained. Thomson also reported on problems during the development of methods for hydrazone rearrangements, but with aliphatic systems,^[3,33] which resulted in unidentified decomposition products. However, the rearrangement of aryl-substituted allylhydrazones worked well in his setup. Boc-deprotected allylhydrazones were observed in every reaction as by-products by GC/MS analysis, but no rearrangement takes place with these deprotected forms under our conditions. The deprotection reaction outcompetes the rearrangement and is a possible reason for the observed yields. This finding validates computational studies towards the mechanism of the triflimidecatalysed [3,3]-sigmatropic rearrangement by

Gutierrez et al. indicating that conversion of deprotected allylhydrazones does not proceed well or not at all.^[34]

Conclusion

In summary, we present a unique method for traceless isoprenylation of aliphatic aldehydes via triflimide-catalysed [3,3]-sigmatropic rearrangement of *N*-Boc-*N*-allylhydrazones. The central *N*-Boc-*N*-allylhydrazine building block **8a** is available in four steps utilising organocatalysis and Tebbe methylenation. This method opens a new route to isoprenyl compounds. This novel protocol is compromised by poor yields in the final step and its limitation to non-conjugated systems. Nevertheless, it broadens the scope of Stevens-type traceless bond constructions and represents the first example of a TBC for the introduction of an isoprenyl group into readily available aliphatic aldehydes. Therefore, this work extends the repertoire of methods for the total synthesis of isoprenoid natural products.

Experimental Section

General Information: All reactions were carried out in oven-dried Schlenk flasks equipped with a septum and a magnetic stirring bar which were evacuated and back filled with dry nitrogen. Solvents were dried according to standard methods by distillation over drying agents. Thin layer chromatography (TLC) was performed using polyester sheets polygram SIL G/UV254 covered with SiO₂ (layer thickness 0.2 mm, 40 × 80 mm) from Macherey-Nagel. Spots were visualized with a CAM (ceric ammonium molybdate) solution followed by heating. Flash column chromatography was performed using SiO₂ 60 (0.040–0.063 mm, 230–400 mesh ASTM) from Merck. For chromatography distilled solvents were used. NMR spectra were recorded on JNM-Eclipse 400 (400 MHz), JNM-Eclipse 500 (500 MHz), Avance III HD 400 MHz Bruker Biospin (400 MHz) and Avance III HD 500 MHz Bruker Biospin (500 MHz) with CryoProbe™ Prodigy. Chemical shifts δ are reported as δ values in ppm relative to the deuterated solvent peak. The chemical shifts are reported in parts per million [ppm] and refer to the δ scale. Coupling constants *J* are indicated in Hertz [Hz]. For the characterization of the observed signal multiplicities the following abbreviations were applied: s (singlet), d (doublet), dd (doublet of doublet), dt (doublet of triplet), t (triplet), q (quartet), quint (quintet), m (multiplet), br (broad). Infrared spectra were recorded from 4000–650 cm⁻¹ on a PERKIN ELMER Spectrum BX-59343 FT-IR instrument. For detection a Smiths Detection DuraSamp IR II Diamond ATR sensor was used. The absorption bands are reported in wave numbers (cm⁻¹). High resolution mass spectra (HRMS) were recorded on a Jeol Mstation 700 (Fa. Jeol, Peabody, USA) or JMS GCmate II Jeol instrument for electron impact ionisation (EI) equipped with a quadrupole doublet based lens system. Thermo Finnigan LTQ FT (Fa. Thermo Electron Corporation, Bremen, Germany) was used for electrospray ionization (ESI) equipped with an ion trap. Melting points were measured with a Büchi apparatus B-540 (Büchi, Flawill, Switzerland) and are reported in °C and are

6. Traceless isoprenylation

not corrected. Gas chromatography (GC) was performed on a Varian 3800 gas chromatograph coupled to a Saturn 2200 ion trap from Varian (Darmstadt, Germany). The autosampler was from CTC Analytics (Zwingen, Switzerland) and the split/splitless injector was a Varian 1177 (Darmstadt, Germany). Instrument control and data analysis were carried out with Varian Workstation 6.9 SP1 software (Darmstadt, Germany). A Varian VF-5ms capillary column of 30 m length, 0.25 mm i.d. and 0.25 μm film thickness (Darmstadt, Germany) was used at a constant flow rate of 1.4 mL/min. Carrier gas was helium 99.999 % from Air Liquide (Düsseldorf, Germany). The inlet temperature was kept at 300 °C and injection volume was 1 μL with splitless time 1.0 min. The initial column temperature was 50 °C and was held for 1.0 min. Then the temperature was ramped up to 250 °C with 50 °C/min. Then the products were eluted at a rate of 5 °C/min until 310 °C (hold time 3 min). Total run time was 20 min. Transfer line temperature was 300 °C and the ion trap temperature was 150 °C. The ion trap was operated with electron ionization (EI) at 70 eV in scan mode (m/z 50–650) with a solvent delay of 6.3 min.

Crystallography: All X-ray intensity data were measured on a Bruker D8 Venture TXS system equipped with a multilayer mirror optics monochromator and a Mo K_{α} rotating-anode X-ray tube ($\lambda = 0.71073 \text{ \AA}$). The data collections were performed at 103 K. The frames were integrated with the Bruker SAINT Software package.^[35] Data were corrected for absorption effects using the Multi-Scan method (SADABS).^[36] The structures were solved and refined using the Bruker SHELXTL Software Package.^[37] All C-bound hydrogen atoms were calculated in positions having ideal geometry riding on their parent atoms.

Deposition Number(s) 1907495 (for **8a**) contain(s) the supplementary crystallographic data for this paper. These data are provided free of charge by the joint Cambridge Crystallographic Data Centre and Fachinformationszentrum Karlsruhe Access Structures service www.ccdc.cam.ac.uk/structures.

Synthesis of Compounds

Diazene **2** was synthesised according to a literature protocol^[21] in two steps and a total yield of 81 %.

1-(tert-Butyl) 2-(2,2,2-Trichloroethyl) 1-(2-Methyl-1-oxopropan-2-yl)hydrazine-1,2-dicarboxylate (6a) and 2-(tert-Butyl) 1-(2,2,2-Trichloroethyl) 1-(2-Methyl-1-oxopropan-2-yl)hydrazine-1,2-dicarboxylate (6b): *Route A:* A suspension of LiOTf (875 mg, 5.61 mmol, 1.52 equiv.) in dry CHCl_3 (20 mL) was cooled to -50 °C. A solution of diazene **2** (1.70 g, 5.56 mmol, 1.5 equiv.) in CHCl_3 (10 mL), 2-methyl-1-(trimethylsilyloxy)-1-propene (**3**) (533 mg, 3.70 mmol, 1.0 equiv.) in CHCl_3 (10 mL) was added, followed by TBAF (1 M in THF, 3.7 mL, 3.7 mmol, 1.0 equiv.). The resulting reaction mixture was warmed to room temperature and stirred for 16 h. The reaction was stopped with aq. sat. NH_4Cl solution (10 mL) and the layers were separated. The organic layer was washed with aq. sat.

NaHCO_3 solution (10 mL), dried with MgSO_4 , filtered and the solvent was removed in vacuo. The title compound was purified by flash column chromatography (hexanes/ EtOAc , 8:1). An inseparable mixture of aldehydes **6a/6b** (911 mg, 2.43 mmol, 66 %) were obtained as a colourless solid in an isomeric mixture of 50:50 (determined retrospectively via ^1H NMR). *Route B:* Diazene **2** (690 mg, 2.26 mmol, 1.0 equiv.) and (*S*)-5-(pyrrolidin-2-yl)-1*H*-tetrazole (**5**) (31.4 mg, 0.226 mmol, 10 mol-%) were dissolved in dry dichloromethane (15 mL) and the solution was cooled to 0 °C. Isobutyraldehyde (**4**) (0.25 mL, 2.71 mmol, 1.2 equiv.) was added slowly and the reaction mixture was warmed to room temperature. After completion of the reaction, the solvent was removed in vacuo and the product was purified by flash column chromatography (hexanes/ EtOAc , 8:1). An inseparable mixture of aldehydes **6a/6b** (580 mg, 1.53 mmol, 68 %) were obtained as a colourless solid in an isomeric mixture of 91:9 (determined retrospectively via ^1H NMR): $R_f = 0.17$ (hexanes/ EtOAc , 8:1); m.p. 128–129 °C; ^1H NMR (500 MHz, $[\text{D}]\text{chloroform}$) $\delta/\text{ppm} = 9.49$ (s, 1H), 6.70 (s, 1H), 4.93–4.51 (m, 2H), 1.44 (s, 9H), 1.36 (s, 3H), 1.29 (s, 3H); ^{13}C NMR (101 MHz, $[\text{D}]\text{chloroform}$) $\delta/\text{ppm} = 198.1, 155.4, 154.3, 94.9, 84.3, 75.2, 67.4, 28.2, 20.5$; IR (ATR) $\tilde{\nu} = / \text{cm}^{-1} = 3255, 3013, 2980, 2936, 1771, 1723, 1694, 1528, 1457, 1391, 1380, 1365, 1358, 1287, 1254, 1220, 1161, 1108, 1054, 992, 945, 916, 882, 858, 834, 817, 799, 763, 750, 724, 709, 658$; HRMS (ESI): m/z calcd. For $\text{C}_{12}\text{H}_{18}\text{Cl}_3\text{N}_2\text{O}_5$ $[\text{M} - \text{H}]^-$ 375.0287, found 375.0287.

1-(tert-Butyl) 2-(2,2,2-Trichloroethyl) 1-(2-Methylbut-3-en-2-yl)hydrazine-1,2-dicarboxylate (7a) and 2-(tert-Butyl) 1-(2,2,2-Trichloroethyl) 1-(2-Methylbut-3-en-2-yl)hydrazine-1,2-dicarboxylate (7b):

The isomeric mixture of aldehydes **6a/6b** (569 mg, 1.51 mmol, 1.0 equiv.) and pyridine (0.22 mL, 2.7 mmol, 1.8 equiv.) were added to a flame dried flask and the mixture was blended to a gel via ultrasound bath. The suspension was cooled to -80 °C and Tebbe reagent (0.5 M in toluene, 3.92 mL, 1.96 mmol, 1.3 equiv.) was added carefully by adding it along the flask. The reaction mixture was warmed to 0 °C and stirred 48 h. The reaction was quenched with a saturated aqueous NaHCO_3 solution (6 mL) at -80 °C and extracted with dichloromethane ($3 \times 10 \text{ mL}$). The combined organic layers were dried with MgSO_4 , filtered and the solvent was removed in vacuo. Purification by flash column chromatography (hexanes/ EtOAc , 9:1) gave an inseparable mixture of olefins **7a/7b** (270 mg, 0.719 mmol, 48 %) as a colourless solid in an isomeric mixture of 91:9 (determined retrospectively via ^1H NMR): $R_f = 0.29$ (hexanes/ EtOAc , 9:1); m.p. 103–104 °C; ^1H NMR (500 MHz, $[\text{D}]\text{chloroform}$) $\delta/\text{ppm} = 6.68$ (s, 1H), 6.10 (dd, $^3J_{\text{H,H}} = 17.4, 11.0 \text{ Hz}$, 1H), 5.08 (d, $^3J_{\text{H,H}} = 17.1 \text{ Hz}$, 1H), 5.00 (d, $^3J_{\text{H,H}} = 10.9 \text{ Hz}$, 1H), 4.87 (d, $^2J_{\text{H,H}} = 11.5 \text{ Hz}$, 1H), 4.68 (d, $^2J_{\text{H,H}} = 11.8 \text{ Hz}$, 1H), 1.50 (s, 3H), 1.44 (s, 9H), 1.42 (s, 3H); ^{13}C NMR (126 MHz, $[\text{D}]\text{chloroform}$) $\delta/\text{ppm} = 155.4, 154.5, 144.6, 111.2, 95.2, 82.1, 75.1, 62.9, 28.4, 26.6, 26.4$; IR (ATR) $\tilde{\nu} = / \text{cm}^{-1} = 3323, 2924, 2854, 1733, 1706, 1644, 1522, 1456, 1414, 1386, 1359, 1274, 1253, 1233, 1156, 1101, 1078, 1044, 1011, 990, 967, 922, 907, 851, 815, 759$,

6. Traceless isoprenylation

741, 724, 688; HRMS (ESI): m/z calcd. for $C_{13}H_{20}O_4N_2Cl_3 [M - H]^-$ 373.0494, found 373.0499.

tert-Butyl 1-(2-Methylbut-3-en-2-yl)hydrazine-1-carboxylate (8a) and tert-Butyl 2-(2-Methylbut-3-en-2-yl)hydrazine-1-carboxylate (8b): The mixture of olefins **7a/7b** (95.6 mg, 0.254 mmol, 1.0 equiv.) was dissolved in a mixture of ethanol (0.3 mL), water (0.3 mL) and acetic acid (0.3 mL). Zinc powder (582 mg, 8.91 mmol, 35.0 equiv.) was added and the reaction mixture was stirred for 10 minutes at room temperature. After filtration of the reaction mixture, the filtrate was extracted with dichloromethane (3 × 3 mL) and the residue was extracted. The combined organic layers were washed with saturated aqueous $NaHCO_3$ solution (5 mL) and the organic layer was dried with $MgSO_4$, filtered and the solvent was removed in vacuo. The product was used without purification. **8a/8b** (57 mg, 0.28 mmol, quantitative) was obtained as a colourless oil in an isomeric mixture of 91:9; $R_f = 0.15$ (hexanes/EtOAc, 8:2); 1H NMR (**8a**) (400 MHz, $[D_6]DMSO$) $\delta/ppm = 6.00$ (dd, $^3J_{H,H} = 17.5, 10.7$ Hz, 1H), 4.87 (dd, $^3J_{H,H} = 17.5, 10.8$, 2H), 4.24 (s, 2H), 1.38 (s, 9H), 1.33 (s, 6H); ^{13}C NMR (**8a**) (126 MHz, $[D_6]DMSO$) $\delta/ppm = 156.4, 146.2, 108.8, 79.3, 60.6, 28.1, 26.5$; 1H NMR (**8b**) (500 MHz, $[D_6]DMSO$) $\delta/ppm = 7.95$ (s, 1H), 5.81 (dd, $^3J_{H,H} = 17.6, 10.8$ Hz, 1H), 5.08–4.92 (m, 2H), 4.07 (s, 1H), 1.38 (s, 9H), 1.03 (s, 6H); ^{13}C NMR (**8b**) (126 MHz, $[D_6]DMSO$) $\delta/ppm = 155.6, 145.0, 112.2, 78.1, 57.8, 28.2, 24.8$; IR (ATR) $\tilde{\nu} = /cm^{-1} = 3334, 2977, 2932, 1679, 1477, 1455, 1412, 1365, 1249, 1163, 1101, 1005, 994, 948, 907, 868, 766, 724, 687$; HRMS (ESI): m/z calcd. for $C_{10}H_{21}N_2O_2 [M + H]^+$ 201.1597, found 201.1597.

General Procedure 1 (GP1) for the Synthesis of *N*-Boc-*N*-(1,1-Dimethylallyl)hydrazones **9a–q:** The mixture of *N*-(1,1-dimethylallyl)hydrazines **8a/8b** (1.0 equiv.) was dissolved in absolute EtOH and the appropriate aldehyde (1.0 equiv.) was added. The reaction mixture was stirred at room temperature for 15 h, then the solvent was removed in vacuo and the crude product was purified by flash column chromatography. Isolated yields are correlated to the amount of **8a** in the isomeric mixture **8a/8b**.

tert-Butyl 1-(2-methylbut-3-en-2-yl)-2-octylidenehydrazine-1-carboxylate (9a): Mixture of allylhydrazines **8a/8b** (250 mg, 1.75 mmol 1.59 mmol of isomer **8a**) and octanal (0.298 mL, 1.75 mmol) gave *N*-Boc-*N*-allylhydrazone **9a** (178 mg, 0.576 mmol, 36 % referred to isomer **8a**) as colourless oil via GP1: $R_f = 0.58$ (hexanes/EtOAc, 9:1); 1H NMR (400 MHz, $[D]chloroform$) $\delta/ppm = 7.71$ (t, $^3J_{H,H} = 5.6$ Hz, 1H), 6.11 (dd, $^3J_{H,H} = 17.5, 10.8$ Hz, 1H), 5.07–4.86 (m, 2H), 2.35 (td, $^3J_{H,H} = 5.6$ Hz, 2H), 1.59–1.50 (m, 2H), 1.42 (s, 9H), 1.39 (s, 6H), 1.34–1.24 (m, 8H), 0.87 (m, 3H); ^{13}C NMR (101 MHz, $[D]chloroform$) $\delta/ppm = 169.5, 154.3, 146.3, 109.4, 80.9, 61.7, 33.0, 31.9, 29.5, 29.2, 28.6, 26.7, 26.2, 22.8, 14.3$; IR (ATR) $\tilde{\nu} = /cm^{-1} = 3084, 3004, 2972, 2958, 2927, 2857, 1698, 1641, 1455, 1412, 1391, 1366, 1302, 1244, 1157, 1101, 1003,$

991, 901, 855, 757, 724, 686; HRMS (ESI): m/z calcd. for $C_{18}H_{35}N_2O_2 [M + H]^+$ 311.2693, found 311.2694.

tert-Butyl 1-(2-Methylbut-3-en-2-yl)-2-nonylidenehydrazine-1-carboxylate (9b): Mixture of allylhydrazines **8a/8b** (404 mg, 2.02 mmol 1.83 mmol of isomer **8a**) and nonanal (0.346 mL, 2.02 mmol) gave *N*-Boc-*N*-allylhydrazone **9b** (284 mg, 0.877 mmol, 48 % referred to isomer **8a**) as colourless oil via GP1: $R_f = 0.58$ (hexanes/EtOAc, 9:1); 1H NMR (500 MHz, $[D]chloroform$) $\delta/ppm = 7.71$ (t, $^3J_{H,H} = 5.6$ Hz, 1H), 6.11 (dd, $^3J_{H,H} = 17.5, 10.8$ Hz, 1H), 5.05–4.89 (m, 2H), 2.34 (td, $^3J_{H,H} = 5.6$ Hz, 2H), 1.55 (m, 2H), 1.42 (s, 9H), 1.39 (s, 6H), 1.36–1.21 (m, 10H), 0.89–0.85 (m, 3H); ^{13}C NMR (101 MHz, $[D]chloroform$) $\delta/ppm = 169.4, 154.3, 146.3, 109.4, 80.9, 61.7, 33.0, 31.9, 29.5, 29.4, 29.3, 28.5, 26.7, 26.2, 22.8, 14.2$; IR (ATR) $\tilde{\nu} = /cm^{-1} = 3086, 2972, 2956, 2926, 2856, 1698, 1640, 1455, 1412, 1390, 1366, 1302, 1244, 1157, 1100, 1003, 992, 900, 874, 857, 783, 756, 723, 687, 599$; HRMS (ESI): m/z calcd. for $C_{19}H_{37}N_2O_2 [M + H]^+$ 325.2849, found 325.2849.

tert-Butyl 2-Decylidene-1-(2-methylbut-3-en-2-yl)hydrazine-1-carboxylate (9c): Mixture of allylhydrazines **8a/8b** (115 mg, 0.574 mmol 0.522 mmol of isomer **8a**) and decanal (0.108 mL, 0.574 mmol) gave *N*-Boc-*N*-allylhydrazone **9c** (56 mg, 0.17 mmol, 33 % referred to isomer **8a**) as colourless oil via GP1: $R_f = 0.56$ (hexanes/EtOAc, 9:1). 1H NMR (500 MHz, $[D]chloroform$) $\delta/ppm = 7.71$ (t, $^3J_{H,H} = 5.6$ Hz, 1H), 6.11 (dd, $^3J_{H,H} = 17.5, 10.8$ Hz, 1H), 5.01 (dd, $^3J_{H,H} = 17.5, ^2J_{H,H} = 0.7$ Hz, 1H), 4.92 (dd, $J ^3J_{H,H} = 10.8, ^2J_{H,H} = 0.7$ Hz, 1H), 2.35 (td, $^3J_{H,H} = 5.6$ Hz, 2H), 1.57–1.54 (m, 2H), 1.42 (s, 9H), 1.39 (s, 6H), 1.26 (m, 12H), 0.89–0.86 (m, 3H). ^{13}C NMR (126 MHz, $[D]chloroform$) $\delta/ppm = 169.5, 154.3, 146.3, 109.4, 80.9, 61.7, 33.0, 32.0, 29.6, 29.5, 29.5, 29.4, 28.6, 26.7, 26.2, 22.8, 14.3$. IR (ATR) $\tilde{\nu} = /cm^{-1} = 2924, 2853, 1696, 1458, 1407, 1368, 1310, 1245, 1158, 1101, 990, 903, 852, 754, 719, 665$. HRMS (ESI): m/z calcd. for $C_{20}H_{39}N_2O_2 [M + H]^+$ 339.3006, found 339.3011.

tert-Butyl 1-(2-Methylbut-3-en-2-yl)-2-(2-methylpropylidene)hydrazine-1-carboxylate (9d): Mixture of olefins **8a/8b** (519 mg, 2.59 mmol 2.36 mmol of isomer **8a**) and isobutyraldehyde (**4**) (0.237 mL, 2.59 mmol) gave *N*-Boc-*N*-allylhydrazone **9d** (262 mg, 1.03 mmol, 44 % referred to isomer **8a**) as colourless oil via GP1: $R_f = 0.55$ (hexanes/EtOAc, 9:1); 1H NMR (400 MHz, $[D]chloroform$) $\delta/ppm = 7.61$ (d, $^3J_{H,H} = 5.9$ Hz, 1H), 6.11 (dd, $^3J_{H,H} = 17.6, 10.8$ Hz, 1H), 5.03–4.90 (m, 2H), 2.66–2.56 (m, 1H), 1.42 (s, 9H), 1.39 (s, 6H), 1.13 (s, 3H), 1.12 (s, 3H). ^{13}C NMR (101 MHz, $[D]chloroform$) $\delta/ppm = 173.2, 154.1, 146.3, 109.4, 80.9, 61.9, 32.2, 28.6, 26.6, 19.6$. IR (ATR) $\tilde{\nu} = /cm^{-1} = 3086, 3008, 2973, 2930, 2872, 1698, 1641, 1456, 1412, 1390, 1366, 1304, 1289, 1244, 1156, 1092, 1058, 992, 970, 902, 879, 856, 756, 686, 599, 588$. HRMS (ESI): m/z calcd. for $C_{14}H_{27}N_2O_2 [M + H]^+$ 255.2067, found 255.2066.

6. Traceless isoprenylation

tert-Butyl 2-(2-Ethoxy-2-oxoethylidene)-1-(2-methylbut-3-en-2-yl)hydrazine-1-carboxylate (9e):

Mixture of olefins **8a/8b** (200 mg, 0.990 mmol, 0.901 mmol of isomer **8a**) and ethyl glyoxalate solution (ca. 50 % in toluene, 0.198 mL, 0.990 mmol) gave *N*-Boc-*N*-allylhydrazone **9e** (108 mg, 0.380 mmol, 42 % referred to isomer **8a**) as colourless oil via GP1: $R_f = 0.44$ (hexanes/EtOAc, 9:1); $^1\text{H NMR}$ (400 MHz, [D]chloroform) $\delta/\text{ppm} = 8.41$ (s, 1H), 6.05 (dd, $^3J_{\text{H,H}} = 17.5, 10.8$ Hz, 1H), 5.07–4.93 (m, 2H), 4.26 (q, $^3J_{\text{H,H}} = 7.1$ Hz, 2H), 1.52 (s, 6H), 1.48 (s, 9H), 1.31 (t, $^3J_{\text{H,H}} = 7.1$ Hz, 3H); $^{13}\text{C NMR}$ (101 MHz, [D]chloroform) $\delta/\text{ppm} = 164.9, 151.9, 145.5, 135.7, 110.6, 83.6, 65.9, 60.9, 28.3, 27.7, 14.4$; IR (ATR) $\tilde{\nu} = / \text{cm}^{-1} = 1742, 1708, 1585, 1477, 1456, 1369, 1339, 1288, 1242, 1206, 1181, 1148, 1113, 1093, 1044, 911, 848, 798, 759, 744, 576$; HRMS (EI): m/z calcd. for $\text{C}_9\text{H}_{16}\text{N}_2\text{O}_2$ [M – Boc] $^+$ 184.1206, found 184.1205.

tert-Butyl 2-(Cyclopentylmethylene)-1-(2-methylbut-3-en-2-yl)hydrazine-1-carboxylate (9f):

Mixture of olefins **8a/8b** (430 mg, 2.15 mmol, 1.96 mmol of isomer **8a**) and cyclopentane carboxaldehyde (0.229 mL, 2.15 mmol) gave *N*-Boc-*N*-allylhydrazone **9f** (245 mg, 0.874 mmol, 45 % referred to isomer **8a**) as colourless oil via GP1: $R_f = 0.57$ (hexanes/EtOAc, 9:1); $^1\text{H NMR}$ (400 MHz, [D]chloroform) $\delta/\text{ppm} = 7.62$ (d, $^3J_{\text{H,H}} = 6.8$ Hz, 1H), 6.11 (dd, $^3J_{\text{H,H}} = 17.5, 10.8$ Hz, 1H), 5.08–4.82 (m, 2H), 2.87–2.71 (m, 1H), 1.95–1.79 (m, 2H), 1.73–1.54 (m, 6H), 1.42 (s, 9H), 1.38 (s, 6H); $^{13}\text{C NMR}$ (101 MHz, [D]chloroform) $\delta/\text{ppm} = 172.6, 154.2, 146.2, 109.4, 80.8, 61.8, 42.9, 30.3, 28.6, 28.5, 26.6, 25.7$; IR (ATR) $\tilde{\nu} = / \text{cm}^{-1} = 3084, 2968, 2956, 2869, 1697, 1639, 1476, 1454, 1412, 1390, 1366, 1304, 1244, 1156, 1101, 1061, 1003, 992, 900, 877, 856, 783, 757, 687$; HRMS (ESI): m/z calcd. for $\text{C}_{16}\text{H}_{29}\text{N}_2\text{O}_2$ [M + H] $^+$ 281.2224, found 281.2225.

tert-Butyl 2-(Cyclohexylmethylene)-1-(2-methylbut-3-en-2-yl)hydrazine-1-carboxylate (9g):

Mixture of olefins **8a/8b** (91.6 mg, 0.686 mmol, 0.624 mmol of isomer **8a**) and cyclohexanecarboxaldehyde (55.4 μL , 0.686 mmol) gave *N*-Boc-*N*-allylhydrazone **9g** (63.3 mg, 0.215 mmol, 34 % referred to isomer **8a**) as colourless oil via GP1: $R_f = 0.64$ (hexanes/EtOAc, 9:1); $^1\text{H NMR}$ (500 MHz, [D]chloroform) $\delta/\text{ppm} = 7.58$ (d, $^3J_{\text{H,H}} = 6.0$ Hz, 1H), 6.11 (dd, $^3J_{\text{H,H}} = 17.5, 10.8$ Hz, 1H), 5.01 (dd, $^3J_{\text{H,H}} = 17.5, ^2J_{\text{H,H}} = 0.9$ Hz, 1H), 4.92 (dd, $^3J_{\text{H,H}} = 10.8, ^2J_{\text{H,H}} = 0.9$ Hz, 1H), 2.42–2.25 (m, 1H), 1.89–1.80 (m, 2H), 1.80–1.73 (m, 2H), 1.70–1.64 (m, 1H), 1.41 (s, 9H), 1.39 (s, 6H), 1.35–1.28 (m, 4H), 1.27–1.18 (m, 1H). $^{13}\text{C NMR}$ (101 MHz, [D]chloroform) $\delta/\text{ppm} = 172.6, 154.3, 146.3, 109.4, 80.8, 61.8, 41.5, 29.9, 28.6, 26.7, 26.1, 25.5$; IR (ATR) $\tilde{\nu} = / \text{cm}^{-1} = 2929, 2854, 1709, 1366, 1308, 1244, 1160$; HRMS (ESI): m/z calcd. for $\text{C}_{17}\text{H}_{31}\text{N}_2\text{O}_2$: 295.2380 [M + H] $^+$, found 295.2385.

tert-Butyl 2-(Cyclohex-1-en-1-ylmethylene)-1-(2-methylbut-3-en-2-yl)hydrazine-1-carboxylate (9h):

Mixture of olefins **8a/8b** (200 mg, 0.999 mmol, 0.909 mmol

of isomer **8a**) and 1-cyclohexene-1-carboxaldehyde (0.114 mL, 0.990 mmol) gave *N*-Boc-*N*-allylhydrazone **9h** (135 mg, 0.460 mmol, 51 % referred to isomer **8a**) as colourless oil via GP1: $R_f = 0.52$ (hexanes/EtOAc, 9:1); $^1\text{H NMR}$ (400 MHz, [D]chloroform) $\delta/\text{ppm} = 7.99$ (s, 1H), 6.18–6.05 (m, 2H), 5.05–4.85 (m, 2H), 2.37–2.12 (m, 4H), 1.70–1.61 (m, 4H), 1.43 (s, 9H), 1.41 (s, 6H); $^{13}\text{C NMR}$ (101 MHz, [D]chloroform) $\delta/\text{ppm} = 163.9, 153.9, 146.6, 138.2, 136.3, 109.1, 81.2, 62.7, 28.6, 26.9, 26.3, 23.4, 22.5, 22.1$; IR (ATR) $\tilde{\nu} = / \text{cm}^{-1} = 2976, 2931, 2859, 1697, 1639, 1596, 1366, 1291, 1243, 1152, 1107, 902, 881, 754, 699$; HRMS (ESI): m/z calcd. for $\text{C}_{17}\text{H}_{29}\text{N}_2\text{O}_2$ [M + H] $^+$ 293.2224, found 293.2223.

tert-Butyl 2-Benzylidene-1-(2-methylbut-3-en-2-yl)hydrazine-1-carboxylate (9i):

Mixture of olefins **8a/8b** (580 mg, 2.90 mmol, 2.64 mmol of isomer **8a**) and benzaldehyde (0.294 mL, 2.90 mmol) gave *N*-Boc-*N*-allylhydrazone **9i** (312 mg, 1.08 mmol, 41 % referred to isomer **8a**) as colourless oil via GP1: $R_f = 0.64$ (hexanes/EtOAc, 9:1); $^1\text{H NMR}$ (400 MHz, [D]chloroform) $\delta/\text{ppm} = 8.65$ (s, 1H), 7.74–7.68 (m, 2H), 7.43–7.34 (m, 3H), 6.17 (dd, $^3J_{\text{H,H}} = 17.5, 10.8$ Hz, 1H), 5.11–4.90 (m, 2H), 1.52 (s, 6H), 1.47 (s, 9H); $^{13}\text{C NMR}$ (101 MHz, [D]chloroform) $\delta/\text{ppm} = 157.1, 153.6, 146.4, 135.4, 130.2, 128.7, 127.7, 109.4, 81.8, 63.6, 28.5, 27.2$; IR (ATR) $\tilde{\nu} = / \text{cm}^{-1} = 3083, 3062, 2976, 2932, 1697, 1642, 1574, 1476, 1449, 1412, 1391, 1366, 1289, 1243, 1149, 1109, 1071, 992, 947, 898, 856, 784, 753, 692, 659, 563$; HRMS (ESI): m/z calcd. for $\text{C}_{17}\text{H}_{25}\text{N}_2\text{O}_2$ [M + H] $^+$ 289.1910, found 289.1909.

tert-Butyl 2-(4-Bromobenzylidene)-1-(2-methylbut-3-en-2-yl)hydrazine-1-carboxylate (9j):

Mixture of olefins **8a/8b** (243 mg, 1.21 mmol, 1.10 mmol of isomer **8a**) and 4-bromobenzaldehyde (224 mg, 1.21 mmol) gave *N*-Boc-*N*-allylhydrazone **9j** (356 mg, 0.971 mmol, 88 % referred to isomer **8a**) as colourless oil via GP1: $R_f = 0.64$ (hexanes/EtOAc, 9:1); $^1\text{H NMR}$ (500 MHz, [D]chloroform) $\delta/\text{ppm} = 8.68$ (s, 1H), 7.56 (d, $^3J_{\text{H,H}} = 8.4$ Hz, 2H), 7.50 (d, $^3J_{\text{H,H}} = 8.3$ Hz, 2H), 6.14 (dd, $^3J_{\text{H,H}} = 17.5, 10.8$ Hz, 1H), 5.07–4.92 (m, 2H), 1.51 (s, 6H), 1.47 (s, 9H); $^{13}\text{C NMR}$ (126 MHz, [D]chloroform) $\delta/\text{ppm} = 153.9, 153.5, 146.3, 134.7, 131.9, 128.9, 124.1, 109.6, 82.1, 63.9, 28.5, 27.3$; IR (ATR) $\tilde{\nu} = / \text{cm}^{-1} = 3086, 2979, 2932, 1696, 1643, 1591, 1564, 1487, 1455, 1412, 1392, 1367, 1289, 1244, 1148, 1115, 1098, 1069, 1044, 1009, 992, 953, 929, 901, 856, 819, 786, 752, 708, 691, 667$; HRMS (ESI): m/z calcd. For $\text{C}_{17}\text{H}_{24}\text{BrN}_2\text{O}_2$ [M + H] $^+$ 367.1015, found 367.1026.

tert-Butyl 2-(4-(Dimethylamino)benzylidene)-1-(2-methylbut-3-en-2-yl)hydrazine-1-carboxylate (9k):

Mixture of olefins **8a/8b** (100 mg, 0.499 mmol, 0.454 mmol of isomer **8a**) and 4-dimethylaminobenzaldehyde (74.5 mg, 0.499 mmol) gave *N*-Boc-*N*-allylhydrazone **9k** (143 mg, 0.431 mmol, 95 % referred to isomer **8a**) as white crystalline solid via GP1: $R_f = 0.35$ (hexanes/EtOAc, 9:1); m.p. 73–75 °C; $^1\text{H NMR}$ (400 MHz, [D]chloroform) $\delta/\text{ppm} = 8.30$ (s, 1H), 7.61 (d, $^3J_{\text{H,H}} = 8.9$ Hz, 2H), 6.69 (d, $^3J_{\text{H,H}} = 8.9$ Hz, 2H), 6.19 (dd, $^3J_{\text{H,H}} = 17.5, 10.8$ Hz, 1H), 5.08–4.90 (m, 2H), 3.01 (s, 6H), 1.47 (s,

6. Traceless isoprenylation

6H), 1.44 (s, 9H); ^{13}C NMR (101 MHz, [D]chloroform) δ /ppm = 162.4, 154.2, 152.2, 146.6, 129.4, 122.4, 111.8, 109.2, 80.9, 62.6, 40.4, 28.6, 26.9; IR (ATR) $\tilde{\nu}$ = / cm^{-1} = 2976, 2930, 1693, 1616, 1601, 1528, 1477, 1455, 1363, 1300, 1237, 1155, 1100, 1060, 894, 859, 816, 755, 731; HRMS (ESI): m/z calcd. for $\text{C}_{19}\text{H}_{30}\text{N}_3\text{O}_2$ [M + H] $^+$ 332.2333, found 332.2333.

tert-Butyl 2-(4-Methoxybenzylidene)-1-(2-methylbut-3-en-2-yl)hydrazine-1-carboxylate (9I): Mixture of olefins **8a/8b** (150 mg, 0.749 mmol 0.682 mmol of isomer **8a**) and 4-anisaldehyde (102 mg, 91.1 μL , 0.749 mmol) gave *N*-Boc-*N*-allylhydrazone **9I** (151 mg, 0.475 mmol, 70 % referred to isomer **8a**) as colourless oil via GP1: R_f = 0.42 (hexanes/EtOAc, 9:1); ^1H NMR (400 MHz, [D]chloroform) δ /ppm = 8.48 (s, 1H), 7.66 (d, $^3J_{\text{H,H}}$ = 8.8 Hz, 2H), 6.91 (d, $^3J_{\text{H,H}}$ = 8.9 Hz, 2H), 6.17 (dd, $^3J_{\text{H,H}}$ = 17.5, 10.8 Hz, 1H), 5.08–4.92 (m, 2H), 3.84 (s, 3H), 1.49 (s, 6H), 1.45 (s, 9H); ^{13}C NMR (101 MHz, [D]chloroform) δ /ppm = 161.5, 159.0, 153.9, 146.5, 129.3, 127.8, 114.1, 109.3, 81.4, 63.1, 55.5, 28.6, 27.0; IR (ATR) $\tilde{\nu}$ = / cm^{-1} = 2975, 2932, 1693, 1606, 1512, 1456, 1366, 1293, 1245, 1150, 1104, 1031, 900, 859, 831, 75; HRMS (ESI): m/z calcd. for $\text{C}_{18}\text{H}_{27}\text{N}_2\text{O}_3$ [M + H] $^+$ 319.2016, found 319.2015.

tert-Butyl 1-(2-Methylbut-3-en-2-yl)-2-(4-nitrobenzylidene)hydrazine-1-carboxylate (9m): Mixture of olefins **8a/8b** (250 mg, 1.25 mmol 1.14 mmol of isomer **8a**) and 4-nitrobenzaldehyde (0.126 mL, 1.25 mmol) gave *N*-Boc-*N*-allylhydrazone **9m** (233 mg, 0.698 mmol, 61 % referred to isomer **8a**) as yellow solid via GP1: R_f = 0.51 (hexanes/EtOAc, 9:1); m.p. 67–69 °C; ^1H NMR (400 MHz, [D]chloroform) δ /ppm = 9.02 (s, 1H), 8.24–8.19 (m, 2H), 7.82–7.75 (m, 2H), 6.12 (dd, J = 17.5, 10.8 Hz, 1H), 5.10–4.93 (m, 2H), 1.56 (s, 6H), 1.50 (s, 9H); ^{13}C NMR (101 MHz, [D]chloroform) δ /ppm = 152.9, 148.1, 147.7, 145.9, 142.7, 127.6, 124.0, 110.1, 82.9, 65.0, 28.5, 27.6; IR (ATR) $\tilde{\nu}$ = / cm^{-1} = 1699, 1598, 1572, 1518, 1368, 1343, 1286, 1246, 1146, 1107, 907, 849, 832, 729, 692, 647; HRMS (EI): m/z calcd. for $\text{C}_{17}\text{H}_{23}\text{N}_3\text{O}_4$ [M] $^+$ 333.1683, found 333.1710.

tert-Butyl 1-(2-Methylbut-3-en-2-yl)-2-(thiophen-2-ylmethylene)hydrazine-1-carboxylate (9n): Mixture of olefins **8a/8b** (150 mg, 0.749 mmol 0.681 mmol of isomer **8a**) and 2-thiophenecarboxaldehyde (70 μL , 0.749 mmol) gave *N*-Boc-*N*-allylhydrazone **9n** (104 mg, 0.352 mmol, 52 % referred to isomer **8a**) as light yellow oil via GP1: R_f = 0.60 (hexanes/EtOAc, 9:1); ^1H NMR (400 MHz, [D]chloroform) δ /ppm = 8.85–8.83 (m, 1H), 7.32 (dt, $^3J_{\text{H,H}}$ = 5.0, 1.0 Hz, 1H), 7.24 (dd, $^3J_{\text{H,H}}$ = 3.6, 1.2 Hz, 1H), 7.04 (dd, $^3J_{\text{H,H}}$ = 5.1, 3.6 Hz, 1H), 6.14 (dd, $^3J_{\text{H,H}}$ = 17.5, 10.8 Hz, 1H), 5.08–4.91 (m, 2H), 1.49 (s, 6H), 1.47 (s, 9H); ^{13}C NMR (101 MHz, [D]chloroform) δ /ppm = 153.6, 150.2, 146.3, 140.9, 129.7, 127.9, 127.4, 109.5, 81.9, 63.7, 28.5, 27.2; IR (ATR) $\tilde{\nu}$ = / cm^{-1} = 2985, 2938, 1742, 1708, 1585, 1369, 128, 1242, 1181, 1148, 1113, 1093, 1044, 911, 848, 759, 744, 576; HRMS (EI): m/z calcd. for $\text{C}_{15}\text{H}_{22}\text{N}_2\text{O}_2\text{S}$ [M] $^+$ 294.1396, found 294.1392.

tert-Butyl 1-(2-Methylbut-3-en-2-yl)-2-(pyridin-4-ylmethylene)hydrazine-1-carboxylate (9o): Mixture of olefins **8a/8b** (350 mg, 1.75 mmol 1.59 mmol of isomer **8a**) and 4-pyridinecarboxaldehyde (0.165 mL, 1.75 mmol) gave *N*-Boc-*N*-allylhydrazone **9o** (342 mg, 1.18 mmol, 74 % referred to isomer **8a**) as light yellow oil via GP1: R_f = 0.12 (hexanes/EtOAc, 9:1); ^1H NMR (400 MHz, [D]chloroform) δ /ppm = 8.90 (s, 1H), 8.65–8.55 (m, 2H), 7.50 (dd, $^3J_{\text{H,H}}$ = 6.1, 0.4 Hz, 2H), 6.11 (dd, $^3J_{\text{H,H}}$ = 17.5, 10.8 Hz, 1H), 5.11–4.90 (m, 2H), 1.54 (s, 6H), 1.49 (s, 9H); ^{13}C NMR (101 MHz, [D]chloroform) δ /ppm = 152.9, 150.3, 147.7, 146.0, 143.8, 121.1, 109.9, 82.8, 64.9, 28.5, 27.6; IR (ATR) $\tilde{\nu}$ = / cm^{-1} = 2977, 2933, 1698, 1590, 1367, 1287, 1246, 1147, 989, 903, 859, 814, 755, 732, 656; HRMS (ESI): m/z calcd. for $\text{C}_{16}\text{H}_{24}\text{N}_3\text{O}_2$ [M + H] $^+$ 290.1863, found 290.1862.

tert-Butyl 1-(2-Methylbut-3-en-2-yl)-2-(3-phenylpropylidene)hydrazine-1-carboxylate (9p): Mixture of olefins **8a/8b** (237 mg, 1.18 mmol 1.07 mmol of isomer **8a**) and 3-phenylpropionaldehyde (0.157 mL, 1.18 mmol) gave *N*-Boc-*N*-allylhydrazone **9p** (141 mg, 0.446 mmol, 42 % referred to isomer **8a**) as colourless oil via GP1: R_f = 0.46 (hexanes/EtOAc, 9:1); ^1H NMR (400 MHz, [D₆]DMSO) δ /ppm = 7.75 (t, $^3J_{\text{H,H}}$ = 5.3 Hz, 1H), 7.31–7.22 (m, 4H), 7.18 (m, 1H), 5.99 (dd, $^3J_{\text{H,H}}$ = 17.5, 10.8 Hz, 1H), 4.94 (dd, $^3J_{\text{H,H}}$ = 17.5, $^2J_{\text{H,H}}$ = 1.1 Hz, 1H), 4.86 (dd, $^3J_{\text{H,H}}$ = 10.8, $^2J_{\text{H,H}}$ = 1.1 Hz, 1H), 2.83 (t, $^3J_{\text{H,H}}$ = 7.3 Hz, 2H), 2.59 (ddd, $^3J_{\text{H,H}}$ = 7.3, 5.3 Hz, 2H), 1.36 (s, 9H), 1.25 (s, 6H); ^{13}C NMR (101 MHz, [D₆]DMSO) δ /ppm = 166.7, 153.2, 145.7, 140.9, 128.3, 128.3, 125.9, 109.4, 80.1, 61.1, 33.9, 31.3, 27.9, 26.4; IR (ATR) $\tilde{\nu}$ = / cm^{-1} = 2979, 2929, 1693, 1639, 1455, 1264, 1303, 1241, 1155, 1101, 903, 870, 856, 748; HRMS (ESI): m/z calcd. for $\text{C}_{19}\text{H}_{29}\text{N}_2\text{O}_2$ [M + H] $^+$ 317.2224, found 317.2229.

tert-Butyl 1-(2-Methylbut-3-en-2-yl)-2-((E)-3-phenylallylidene)hydrazine-1-carboxylate (9q): Mixture of olefins **8a/8b** (250 mg, 1.25 mmol 1.13 mmol of isomer **8a**) and cinnamaldehyde (0.157 mL, 1.25 mmol) gave *N*-Boc-*N*-allylhydrazone **9q** (228 mg, 0.725 mmol, 64 % referred to isomer **8a**) as yellow oil via GP1: R_f = 0.56 (hexanes/EtOAc, 9:1); ^1H NMR (500 MHz, [D]chloroform) δ /ppm = 8.33 (dd, $^3J_{\text{H,H}}$ = 7.2, 1.5 Hz, 1H), 7.49–7.47 (m, 2H), 7.38–7.33 (m, 2H), 7.32–7.28 (m, 1H), 6.96–6.93 (m, 2H), 6.14 (dd, $^3J_{\text{H,H}}$ = 17.5, 10.8 Hz, 1H), 5.07–4.92 (m, 2H), 1.47 (s, 6H), 1.46 (s, 9H); ^{13}C NMR (101 MHz, [D]chloroform) δ /ppm = 161.7, 153.7, 146.2, 140.5, 136.2, 128.9, 128.9, 127.2, 126.0, 109.5, 81.6, 62.9, 28.5, 26.9; IR (ATR) $\tilde{\nu}$ = / cm^{-1} = 1694, 1449, 1366, 1289, 1243, 1148, 1109, 1051, 973, 906, 879, 850, 749, 689; HRMS (ESI): m/z calcd. for $\text{C}_{19}\text{H}_{27}\text{N}_2\text{O}_2$ [M + H] $^+$ 315.2067, found 315.2066.

General Procedure for the Synthesis of Olefins via [3,3]-Sigmatropic Rearrangement (GP2): In an oven dried two-necked Schlenk flask HNTf₂ (10 mol-%) was dissolved in dry diglyme (1 mL). A solution of the appropriate *N*-Boc-*N*-allylhydrazone **9** (1.0 equiv.) in dry diglyme (2 mL + 1 mL rinse) was added at room temperature. The reaction

6. Traceless isoprenylation

mixture was fitted with a N₂ flashed reflux condenser and immediately heated to 125 °C in a pre-heated oil bath. After completion of the rearrangement detected by TLC (75 min), the reaction was immediately cooled to room temperature via water bath and then quenched with a sat. aq. NaHCO₃ solution (4 mL). Pentane (10 mL) was added and the organic layer was washed with at least 100 mL water. The solvent was removed in vacuo (30 °C, max. 700 mbar) and the crude product was purified by flash column chromatography.

2-Methylododec-2-ene (10a): Allylhydrazone **9a** (155 mg, 0.500 mmol) and HNTf₂ (14 mg, 0.050 mmol) gave olefin **10a** (18 mg, 0.099 mmol, 20 %) as colourless oil via GP2: *R*_f = 0.94 (pentane); ¹H NMR (400 MHz, [D]chloroform) δ /ppm = 5.15–5.08 (m, 1H), 1.96 (q, ³*J*_{H,H} = 7.1 Hz, 2H), 1.69 (d, ³*J*_{H,H} = 1.4 Hz, 3H), 1.60 (d, ³*J*_{H,H} = 1.3 Hz, 3H), 1.26 (s, 14H), 0.88 (t, ³*J*_{H,H} = 2.9 Hz, 3H). ¹³C NMR (101 MHz, [D]chloroform) δ /ppm = 131.3, 125.1, 32.1, 30.1, 29.8, 29.8, 29.5, 29.5, 28.2, 25.9, 22.9, 17.8, 14.3. IR (ATR) $\tilde{\nu}$ = /cm⁻¹ = 2956, 2922, 2853, 1462, 1376, 1094, 985, 886, 833, 722; HRMS (EI): *m/z* calcd. for C₁₃H₂₆ [M]⁺ 182.2029, found 182.2027.

2-Methyltridec-2-ene(10b): Allylhydrazone **9b** (162 mg, 0.500 mmol) and HNTf₂ (14 mg, 0.050 mmol) gave olefin **10b** (19 mg, 0.10 mmol, 21 %) as colourless oil via GP2: *R*_f = 0.88 (pentane/Et₂O, 9:1); ¹H NMR (400 MHz, [D]chloroform) δ /ppm = 5.12 (tdt, ³*J*_{H,H} = 7.2, 1.5 Hz, 1H), 1.96 (q, ³*J*_{H,H} = 6.8 Hz, 2H), 1.69 (d, ³*J*_{H,H} = 1.4 Hz, 3H), 1.60 (d, ³*J*_{H,H} = 1.3 Hz, 3H), 1.26 (s, 16H), 0.93–0.83 (m, 3H); ¹³C NMR (101 MHz, [D]chloroform) δ /ppm = 131.3, 125.1, 32.1, 30.1, 29.8, 29.8, 29.8, 29.5, 29.5, 28.2, 25.9, 22.9, 17.8, 14.3; IR (ATR) $\tilde{\nu}$ = /cm⁻¹ = 2955, 2922, 2853, 1456, 1376, 1094, 984, 886, 832, 721, 593, 556; HRMS (EI): *m/z* calcd. for C₁₄H₂₈ [M]⁺ 196.2185, found 196.2183.

2-Methyltetradec-2-ene (10c): Allylhydrazone **9c** (169 mg, 0.500 mmol) and HNTf₂ (14 mg, 0.050 mmol) gave olefin **10c** (21 mg, 0.099 mmol, 20 %) as colourless oil via GP2: *R*_f = 0.98 (pentane); ¹H NMR (400 MHz, [D]chloroform) δ /ppm = 5.12 (ddt, ³*J*_{H,H} = 7.1 Hz, 1H), 1.96 (q, ³*J*_{H,H} = 6.9 Hz, 2H), 1.69 (s, 3H), 1.60 (s, 3H), 1.26 (br, 18H), 0.88 (t, ³*J*_{H,H} = 6.8 Hz, 3H); ¹³C NMR (101 MHz, [D]chloroform) δ /ppm = 131.3, 125.1, 34.3, 32.1, 30.1, 29.9, 29.8, 29.8, 29.5, 28.2, 25.9, 22.9, 22.5, 17.8, 14.3; IR (ATR) $\tilde{\nu}$ = /cm⁻¹ = 2958, 2921, 2850, 1461, 1372, 1260, 1090, 1022, 881, 806, 723; HRMS (EI): *m/z* calcd. for C₁₅H₃₀ [M]⁺ 210.2342, found 210.2347.

(4-Methylpent-3-en-1-yl)cyclopentane (10f): Allylhydrazone **9f** (140 mg, 0.500 mmol) and HNTf₂ (14 mg, 0.050 mmol) gave olefin **10f** (15 mg, 0.099 mmol, 20 %) as colourless oil via GP2: *R*_f = 0.95 (pentane); ¹H NMR (500 MHz, [D]chloroform) δ /ppm = 5.15–5.10 (m, 1H), 2.01–1.95 (m, 2H), 1.77–1.73 (m, 2H), 1.69 (d, ³*J*_{H,H} = 1.4 Hz, 3H), 1.60 (d, ³*J*_{H,H} = 1.2 Hz, 3H), 1.52–1.46 (m, 2H), 1.34–1.30 (m, 2H), 1.11–1.05 (m, 2H), 0.91–0.86 (m, 3H); ¹³C NMR (126 MHz, [D]chloroform) δ /ppm = 131.1, 125.2, 39.9, 36.6, 32.8, 27.4, 25.9, 25.4, 17.8; IR (ATR) $\tilde{\nu}$ = /cm⁻¹ = 2983, 2950, 2922, 2857, 1452, 1376, 1105, 985, 907, 830, 735, 650, 574, 560; HRMS (EI): *m/z* calcd. for C₁₁H₂₀ [M]⁺ 152.1559, found 152.1558.

(4-Methylpent-3-en-1-yl)cyclohexane (10g): Allylhydrazone **9g** (147 mg, 0.500 mmol) and HNTf₂ (14 mg, 0.050 mmol) gave olefin **10g** (17 mg, 0.10 mmol, 20 %) as colourless oil via GP2. **(4-Methylpent-3-en-1-yl)cyclohexane (10g, 30 mol-% HNTf₂):** Allylhydrazone **9g** (127 mg, 0.433 mmol) and HNTf₂ (37 mg, 0.13 mmol) gave olefin **10g** (18 mg, 0.11 mmol, 22 %) as colourless oil via GP2. **(4-Methylpent-3-en-1-yl)cyclohexane (10g, 3.00 mmol scale):** Allylhydrazone **9g** (822 mg, 3.00 mmol) and HNTf₂ (84 mg, 0.30 mmol) gave olefin **10g** (129 mg, 0.759 mmol, 25 %) as colourless oil via GP2: *R*_f = 0.91 (pentane); ¹H NMR (500 MHz, [D]chloroform) δ /ppm = 5.15–5.00 (m, 1H), 2.03–1.91 (m, 2H), 1.75–1.57 (m, 11H), 1.25–1.15 (m, 6H), 0.92–0.83 (m, 2H); ¹³C NMR (126 MHz, [D]chloroform) δ /ppm = 131.1, 125.3, 37.8, 37.5, 33.5, 26.9, 26.6, 25.9, 25.5, 17.8; IR (ATR) $\tilde{\nu}$ = /cm⁻¹ = 2923, 2852, 1694, 1448, 1376; HRMS (EI): *m/z* calcd. for C₁₂H₂₂ [M]⁺ 166.1722, found 166.1720.

(6-Methylhept-5-en-1-yl)benzene (10p): Allylhydrazone **9p** (217 mg, 0.686 mmol) and HNTf₂ (14 mg, 0.068 mmol) gave olefin **10p** (25 mg, 0.13 mmol, 19 %) as colourless oil via GP2: *R*_f = 0.48 (pentane); ¹H NMR (400 MHz, dichloromethane-*d*₂) δ /ppm = 7.29–7.23 (m, 2H), 7.20–7.13 (m, 3H), 5.12 (tdt, ³*J*_{H,H} = 7.2, 1.5 Hz, 1H), 2.60 (t, ³*J*_{H,H} = 7.7 Hz, 2H), 2.01 (q, ³*J*_{H,H} = 7.3 Hz, 2H), 1.68 (d, ³*J*_{H,H} = 1.4 Hz, 3H), 1.64–1.58 (m, 5H), 1.41–1.33 (m, 2H); ¹³C NMR (101 MHz, dichloromethane-*d*₂) δ /ppm = 143.6, 131.8, 128.9, 128.7, 126.1, 125.2, 36.4, 31.8, 30.1, 28.4, 25.9, 17.9; IR (ATR) $\tilde{\nu}$ = /cm⁻¹ = 3026, 2922, 2853, 1602, 1494, 1451, 1378, 1108, 1079, 1029, 741, 698, 571; HRMS (EI): *m/z* calcd. for C₁₄H₂₀ [M]⁺ 188.1565, found 188.1565.

Keywords: Hydrazones · Isoprenylation · Sigmatropic rearrangement · Traceless bond construction · Triflimide

- [1] a) E. A. Ildardi, C. E. Stivala, A. Zakarian, *Chem. Soc. Rev.* **2009**, *38*, 3133–3148; b) J. Nowicki, *Molecules* **2000**, *5*, 1033; c) C. M. Rojas (Ed.), *Molecular Rearrangements in Organic Synthesis*, John Wiley & Sons, Inc., Hoboken, New Jersey, **2015**.
- [2] R. V. Stevens, E. E. McEntire, W. E. Barnett, E. Wenkert, *J. Chem. Soc., Chem. Commun.* **1973**, 662–663.
- [3] D. A. Mundal, C. T. Avetta, R. J. Thomson, *Nat. Chem.* **2010**, *2*, 294–297.
- [4] S. Dittrich, F. Bracher, *Tetrahedron* **2015**, *71*, 2530–2539.
- [5] S. Dittrich, F. Bracher, *Eur. J. Org. Chem.* **2015**, *2015*, 8024–8033.
- [6] a) E. Kremers, *J. Am. Chem. Soc.* **1902**, *24*, 1218–1219; b) F. Lynen, *Angew. Chem.* **1965**, *77*, 929–944; c) E. González Burgos, M. Gómez-Serranillos, *Curr. Med. Chem.* **2012**, *19*, 5319–5341.
- [7] E. Oldfield, F.-Y. Lin, *Angew. Chem. Int. Ed.* **2012**, *51*, 1124–1137; *Angew. Chem.* **2012**, *124*, 1150.
- [8] H. Eggerer, *Chem. Ber.* **1961**, *94*, 174–185.
- [9] W. D. Nes, *Chem. Rev.* **2011**, *111*, 6423–6451.
- [10] S. A. R. Paiva, R. M. Russell, *J. Am. Coll. Nutr.* **1999**, *18*, 426–433.
- [11] D. V. Henley, J. Lindzey, K. S. Korach, in *Endocrinology: Basic and Clinical Principles* (Eds.: S. Melmed, P. M. Conn), Humana Press, Totowa, NJ, **2005**, pp. 49–65.
- [12] S. Maurer-Stroh, S. Washietl, F. Eisenhaber, *Genome Biol.* **2003**, *4*, 212.

6. Traceless isoprenylation

- [13] B. H. Lipshutz, S. Saumitra, *Org. React.* **1992**, *41*, 135.
- [14] H. Kaku, M. Ito, M. Horikawa, T. Tsunoda, *Tetrahedron* **2018**, *74*, 124–129.
- [15] C. W. Jefford, A. W. Sledeski, J. Boukouvalas, *Tetrahedron Lett.* **1987**, *28*, 949–950.
- [16] E. J. Corey, B. B. Snider, *J. Am. Chem. Soc.* **1972**, *94*, 2549–2550.
- [17] G. Buchbauer, G. Püspök, A. Angermayer, E. Silbernagel, M. Manz, *Monatsh. Chem.* **1987**, *118*, 387–398.
- [18] A. J. Hubert, H. Reimlinger, *Synthesis* **1970**, *1970*, 405–430.
- [19] a) R. M. Beesley, C. K. Ingold, J. F. Thorpe, *J. Chem. Soc. Trans.* **1915**, *107*, 1080–1106; b) M. E. Jung, G. Piizzi, *Chem. Rev.* **2005**, *105*, 1735–1766.
- [20] M. E. Jung, J. Gervay, *Tetrahedron Lett.* **1988**, *29*, 2429–2432.
- [21] A. J. Oelke, D. J. France, T. Hofmann, G. Wuitschik, S. V. Ley, *Angew. Chem. Int. Ed.* **2010**, *49*, 6139–6142; *Angew. Chem.* **2010**, *122*, 6275.
- [22] B. List, *Tetrahedron* **2002**, *58*, 5573–5590.
- [23] See ref.^[21].
- [24] A. Theodorou, G. N. Papadopoulos, C. G. Kokotos, *Tetrahedron* **2013**, *69*, 5438–5443.
- [25] H. Vogt, S. Vanderheiden, S. Bräse, *Chem. Commun.* **2003**, 2448–2449.
- [26] V. Aureggi, V. Franckevicius, M. O. Kitching, S. V. Ley, D. A. Longbottom, A. J. Oelke, G. Sedelmeier, *Org. Synth.* **2008**, *85*, 72.
- [27] W. Georg, S. Ulrich, *Chem. Ber.* **1954**, *87*, 1318–1330.
- [28] a) K. Takai, Y. Hotta, K. Oshima, H. Nozaki, *Tetrahedron Lett.* **1978**, *19*, 2417–2420; b) L. N. Nysted, *US Pat. 3,865,848* (**1975**); c) L. A. Paquette, R. E. Hartung, J. E. Hofferberth, I. Vilotijevic, J. Yang, *J. Org. Chem.* **2004**, *69*, 2454–2460.
- [29] F. N. Tebbe, G. W. Parshall, G. S. Reddy, *J. Am. Chem. Soc.* **1978**, *100*, 3611–3613.
- [30] E. Paenurk, K. Kaupmees, D. Himmel, A. Kütt, I. Kaljurand, I. A. Koppel, I. Krossing, I. Leito, *Chem. Sci.* **2017**, *8*, 6964–6973.
- [31] J. B. Milne, T. J. Parker, *J. Solution Chem.* **1981**, *10*, 479–487.
- [32] M. E. Lewellyn, D. S. Tarbell, *J. Org. Chem.* **1974**, *39*, 1407–1410.
- [33] D. A. Mundal, J. J. Lee, R. J. Thomson, *J. Am. Chem. Soc.* **2008**, *130*, 1148–1149.
- [34] O. Gutierrez, B. F. Strick, R. J. Thomson, D. J. Tantillo, *Chem. Sci.* **2013**, *4*, 3997–4003.
- [35] Bruker, *SAINT*, Bruker AXS Inc., Madison, Wisconsin, USA, **2012**.
- [36] G. M. Sheldrick, *SADABS*, University of Göttingen, Germany, **1996**.
- [37] G. Sheldrick, *Acta Crystallogr., Sect. A* **2015**, *71*, 3–8.

Received: March 22, 2020

6.4. Supplementary material



Supporting Information

Traceless Isoprenylation of Aldehydes via N-Boc-N-(1,1-dimethyl-allyl)hydrazones

Desirée Heerdegen, Julia Junker, Sebastian Dittrich, Peter Mayer, and Franz Bracher*

1 Optimisation of reaction conditions (monitoring with GC/MS)

For the optimization of the acid-catalysed rearrangement different temperatures, reaction times and acids/solvents were tested. The reactions were monitored by GC/MS analysis.

1.1 Instrument parameters

Gas chromatography (GC) was performed on a Varian 3800 gas chromatograph coupled to a Saturn 2200 ion trap from Varian (Darmstadt, Germany). The autosampler was from CTC Analytics (Zwingen, Switzerland) and the split/splitless injector was a Varian 1177 (Darmstadt, Germany). Instrument control and data analysis were carried out with Varian Workstation 6.9 SP1 software (Darmstadt, Germany). A Varian VF-5-ms capillary column of 30 m length, 0.25 mm i.d. and 0.25 μm film thickness (Darmstadt, Germany) was used at a constant flow rate of 1.4 mL/min. Carrier gas was helium 99.999% from Air Liquide (Düsseldorf, Germany). The inlet temperature was kept at 300 °C and injection volume was 1 μL with splitless time 1.0 min. The initial column temperature was 50 °C and was held for 1.0 min. Then the temperature was ramped up to 250 °C with 50 °C/min. Then the products were eluted at a rate of 5 °C/min until 310 °C (hold time 3 min). Total run time was 20 min. Transfer line temperature was 300 °C and the ion trap temperature was 150 °C. The ion trap was operated with electron ionization (EI) at 70 eV in scan mode (m/z 50 - 650) with a solvent delay of 6.3 min.

1.2 Experimental procedure

In an oven-dried reaction tube the appropriate catalyst (10 mol %) was dissolved in the appropriate solvent (1.3 mL). A solution of the *N*-Boc-*N*-allylhydrazone **9g** (14.7 mg, 0.050 mmol, 1.0 eq) in dry diglyme was added. Further cholestane in dry diglyme was added as internal standard (IS, final concentration 5 $\mu\text{g}/\text{mL}$ in the test tube) at room temperature. The reaction tube was purged with N_2 , closed and then immediately heated at the corresponding temperature. After 15, 45 and 75 min samples (3 x 60 μL) were taken. The reaction mixture was neutralised with sat. aq. NaHCO_3 solution (60 μL) and water (1.0 mL) was added. The aqueous phase was extracted with methyl *tert*-butyl ether (M*t*BE) (1 x 500 μL). The organic layer was dried with Na_2SO_4 and 300 μL were transferred into an autosampler vial. After dilution with additional 300 μL M*t*BE the solution was analysed by GC/MS.

1.3 Quantification

For the quantification of the reaction product **10g**, a standard curve with five levels (10-100 $\mu\text{g}/\text{mL}$) of product **10g** and a constant level of IS was used ($n = 3$; $R^2 > 0.996$). The corresponding standard curve was measured on the same day the samples were analysed. With this method only the concentration of product **10g** can be measured, but not the

6. Traceless isoprenylation

concentration of any side product, as these may have different ionisation properties. As a result, the complete mass balance of this reaction cannot be determined.

1.4 Optimisation of reaction conditions for temperature and time

To examine the effect of temperature and time on the yield of product **10g** the reactions were carried out at five different temperatures (23 °C, 50 °C, 75 °C, 100 °C and 125 °C) in diglyme with HNTf₂. The yield of **10g** was determined via GC/MS as described above (see chapter 1.1-1.3) after 15, 45 and 75 min (n = 3). The results of this experiment are shown in Figure S1.

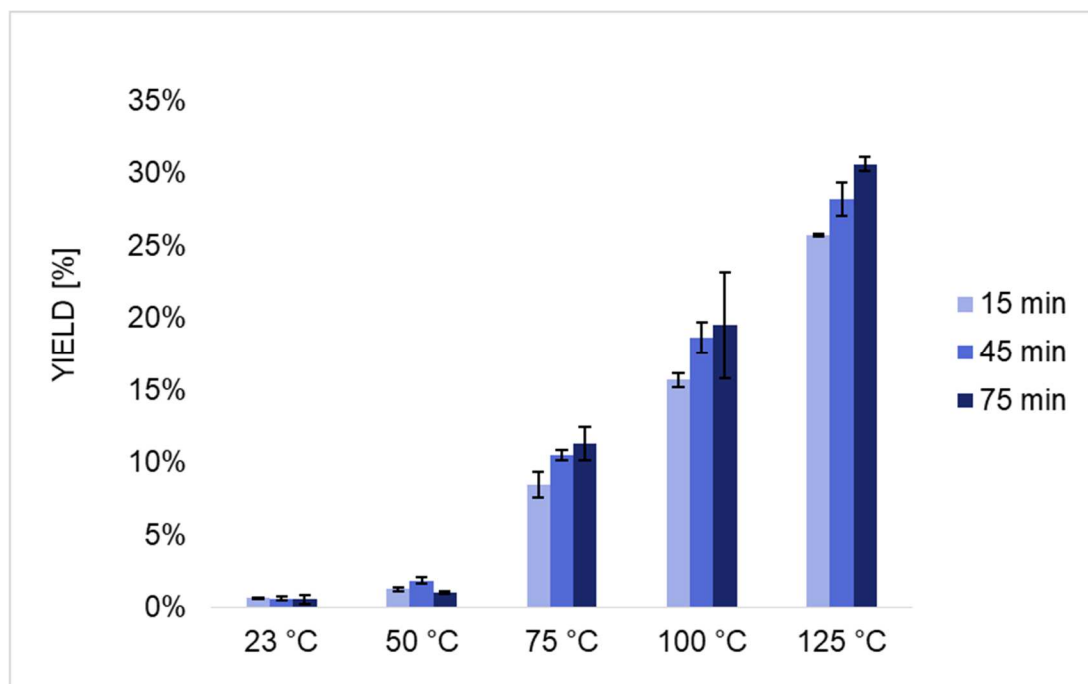


Figure S1. Yields of the optimisation reactions at 23 °C, 50 °C, 75 °C, 100 °C, and 125 °C after different reaction times.

The reaction proceeds best at 125 °C and after 75 min. Under these conditions a yield of 31% was observed. Longer reaction times were not tested, because at this time only Bocdeprotected allylhydrazone was observed, which does not undergo the desired rearrangement. Higher temperatures were not tested, because of a possible decomposition of the final products.

1.5 Optimisation of reaction conditions for different solvents and catalysts

To examine the effect of different solvents and catalysts on the yield of product **10g** the reactions were carried out in THF (70 °C) and diglyme (125 °C). Each solvent was tested with three different catalysts (HNTf₂, TfOH and TFA). The yield of **10g** was determined via GC/MS as described above (see chapter 1.1-1.3) after 15, 45 and 75 min (n = 3). The results of this experiment are shown in Figure S2.

6. Traceless isoprenylation

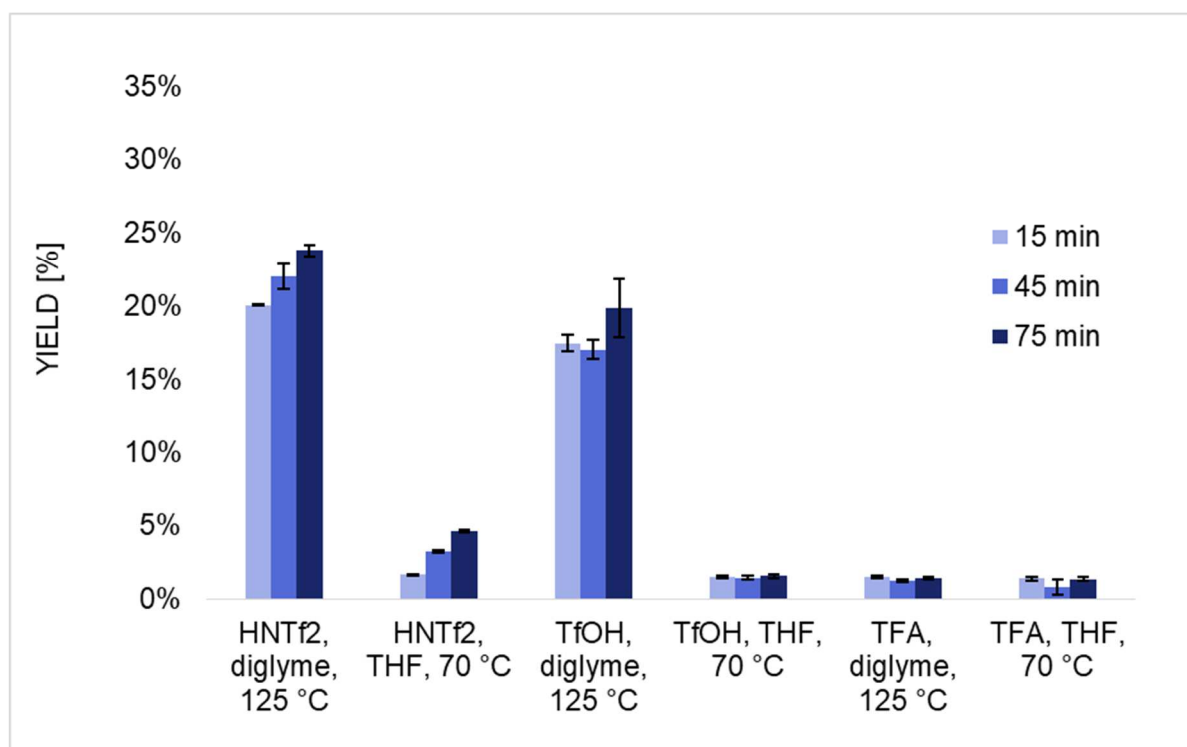


Figure S2. Yields of the optimisation reactions under different conditions after different reaction times. The reaction proceeds best with HNTf₂ in diglyme at 125 °C and after 75 min a yield of 24%, which varies slightly to the value in chapter 1.4, was obtained.

1.6 Optimisation results of reaction conditions

Table S1. Optimisation of reaction conditions for the rearrangement of **9g**^a

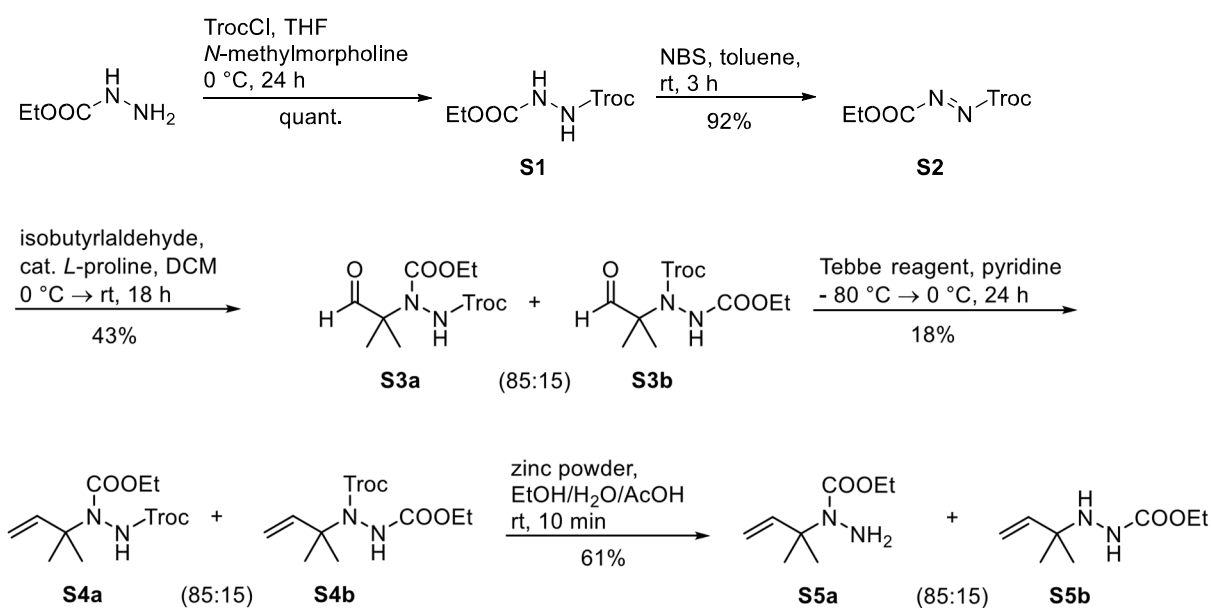
entry ^c	solvent	cat. (10 mol %)	temp [°C]	time [min]	yield 10g [%] ^b
1	diglyme	HNTf ₂	23	15	1
2	diglyme	HNTf ₂	23	45	1
3	diglyme	HNTf ₂	23	75	1
4	diglyme	HNTf ₂	50	15	1
5	diglyme	HNTf ₂	50	45	2
6	diglyme	HNTf ₂	50	75	1
7	diglyme	HNTf ₂	75	15	8
8	diglyme	HNTf ₂	75	45	11
9	diglyme	HNTf ₂	75	75	11
10	diglyme	HNTf ₂	100	15	16
11	diglyme	HNTf ₂	100	45	19
12	diglyme	HNTf ₂	100	75	20
13	diglyme	HNTf ₂	125	15	26
14	diglyme	HNTf ₂	125	45	28
15	diglyme	HNTf ₂	125	75	31
16	diglyme	HNTf ₂	125	15	20

6. Traceless isoprenylation

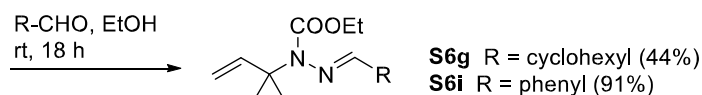
17	diglyme	HNTf ₂	125	45	21
18	diglyme	HNTf ₂	125	75	23
19	THF	HNTf ₂	70	15	2
20	THF	HNTf ₂	70	45	3
21	THF	HNTf ₂	70	75	5
22	diglyme	TfOH	125	15	17
23	diglyme	TfOH	125	45	17
24	diglyme	TfOH	125	75	20
25	THF	TfOH	70	15	1
26	THF	TfOH	70	45	1
27	THF	TfOH	70	75	2
28	diglyme	TFA	125	15	1
29	diglyme	TFA	125	45	1
30	diglyme	TFA	125	75	1
31	THF	TFA	70	15	1
32	THF	TFA	70	45	1
33	THF	TFA	70	75	1

^aThe reactions were performed with 0.05 mmol of **9g**, entries 1-15: HNTf₂ in diglyme with variation of the reaction, entries 16-33: variation of catalyst and solvent. ^bThe yields were determined by GC/MS using cholestane as internal standard (see Supporting Information). ^cEntries 1-15 were performed on the same day as were entries 16-33.

2 Synthesis of the *N*-ethoxycarbonyl-*N*-allylhydrazine building block and two model allylhydrazones

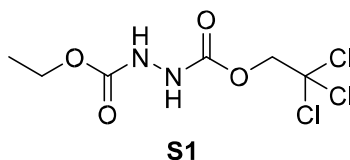


6. Traceless isoprenylation



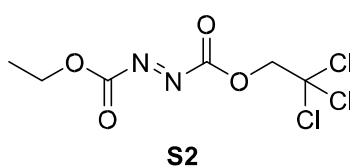
Scheme S1. Synthesis of the *N*-ethoxycarbonyl-*N*-allylhydrazine building block **S5a** and two model allylhydrazones **S6g** and **S6i**

1-Ethyl 2-(2,2,2-trichloroethyl) hydrazine-1,2-dicarboxylate (**S1**)



To a solution of ethyl carbazate (5.2 g, 49 mmol, 1.0 eq) and *N*-methylmorpholine (5.5 mL, 49 mmol, 1.0 eq) in THF, 2,2,2-trichloroethylchloroformate (6.9 mL, 49 mmol, 1.0 eq) was added at 0 °C. The reaction mixture was allowed to warm to room temperature and stirred for 24 h. The suspension was filtered and the filtrate concentrated *in vacuo*. Purification by flash column chromatography (hexanes/EtOAc 7:3) gave hydrazine **S1** (14 g, 49 mmol, quantitative) as a colourless oil: $R_f = 0.28$ (hexanes/EtOAc 7:3); $^1\text{H NMR}$ (400 MHz, chloroform-*d*) $\delta/\text{ppm} = 7.10$ (s, 1H), 6.73 (s, 1H), 4.78 (s, 2H), 4.21 (q, $^3J_{\text{H,H}} = 7.2$ Hz, 2H), 1.27 (t, $^3J_{\text{H,H}} = 7.1$ Hz, 3H); $^{13}\text{C NMR}$ (101 MHz, chloroform-*d*) $\delta/\text{ppm} = 156.6, 155.3, 94.9, 75.2, 62.7, 14.5$; IR (ATR) $\tilde{\nu}/\text{cm}^{-1} = 3258, 1762, 1735, 1697, 1524, 1441, 1367, 1259, 1208, 1095, 1053, 1023, 978, 886, 824, 776, 737, 707$; HRMS (EI): $m/z = \text{calcd for } \text{C}_6\text{H}_9\text{O}_4\text{N}_2\text{Cl}_3 [\text{M}]^+ 277.9622, \text{found } 277.9617$.

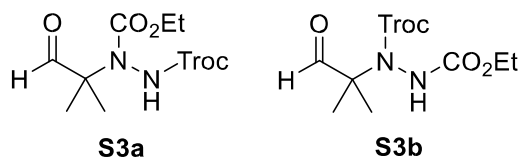
1-Ethyl 2-(2,2,2-trichloroethyl) diazene-1,2-dicarboxylate (**S2**)



Hydrazine **S1** (14.6 g, 52.2 mmol, 1.0 eq) was dissolved in toluene (120 mL), then pyridine (4.22 mL, 52.2 mmol, 1.0 eq) and NBS (9.30 g, 52.2 mmol, 1.0 eq) were added. The reaction mixture was stirred for 3 h at room temperature. The mixture was diluted with toluene (50 mL), washed with water (120 mL), sat. aq. $\text{Na}_2\text{S}_2\text{O}_3$ solution (100 mL), 1M aq. HCl (100 mL), sat. aq. NaHCO_3 solution (100 mL), water (100 mL) and brine (110 mL). The organic layer was dried over Na_2SO_4 , filtered and the solvent was removed *in vacuo*. Azodicarboxylate **S2** (13.4 g, 48.3 mmol, 92%) was obtained as an orange oil and was used without further purification: $R_f = 0.75$ (hexanes/EtOAc 7:3); $^1\text{H NMR}$ (400 MHz, chloroform-*d*) $\delta/\text{ppm} = 5.03$ (s, 2H), 4.54 (q, $^3J_{\text{H,H}} = 7.1$ Hz, 2H), 1.47 (t, $^3J_{\text{H,H}} = 7.1$ Hz, 3H); $^{13}\text{C NMR}$ (101 MHz, chloroform-*d*) $\delta/\text{ppm} = 159.9, 159.0, 93.4, 76.9, 65.9, 14.2$; IR (ATR) $\tilde{\nu}/\text{cm}^{-1} = 1770, 1370, 1200, 1097, 1059, 1015, 854, 801, 718$; HRMS (EI): $m/z \text{ calcd for } \text{C}_6\text{H}_7\text{O}_4\text{N}_2\text{Cl}_3 [\text{M}]^+ 275.9466; \text{found } 275.9458$.

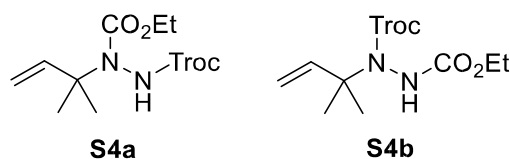
6. Traceless isoprenylation

1-Ethyl 2-(2,2,2-trichloroethyl) 1-(2-methyl-1-oxopropan-2-yl)hydrazine-1,2-dicarboxylate (**S3a**) and 2-ethyl 1-(2,2,2-trichloroethyl) 1-(2-methyl-1-oxopropan-2-yl)hydrazine-1,2-dicarboxylate (**S3b**)



Azodicarboxylate **S2** (6.0 g, 22 mmol, 1.0 eq) and *L*-proline (249 mg, 2.16 mmol, 10 mol %) were dispersed in dry methylene chloride (120 mL) and the suspension was cooled to 0 °C. Isobutyraldehyde (2.96 mL, 32.4 mmol, 1.5 eq) was added and the reaction mixture was allowed to warm to room temperature and stirred for 18 h. The solvent was removed *in vacuo* and the title compound was purified by flash column chromatography (hexanes/EtOAc 7:3). An inseparable mixture of aldehydes **S3a/S3b** (3.23 g, 9.24 mmol, 43%) were obtained as a colourless oil in an isomeric mixture of 85:15 (determined retrospectively via ¹H NMR spectroscopy): *R*_f = 0.75 (hexanes/EtOAc 7:3); ¹H NMR (400 MHz, chloroform-*d*) δ/ppm = 9.51 (s, 1H), 7.02 – 6.57 (m, 1H), 4.78 (d, ²*J*_{H,H} = 31.6 Hz, 2H), 4.20 (dd, ³*J*_{H,H} = 7.1, ²*J*_{H,H} = 2.4 Hz, 2H), 1.47 – 1.20 (m, 9H); ¹³C NMR (101 MHz, chloroform-*d*) δ/ppm = 198.1, 155.6, 155.2, 95.0, 75.1, 67.7, 63.6, 20.4, 14.4; IR (ATR) $\tilde{\nu}/\text{cm}^{-1}$ = 3306, 1733, 1707, 1514, 1469, 1407, 1379, 1342, 1216, 1173, 1096, 1047, 818, 757, 719; HRMS (ESI): *m/z* calcd for C₁₀H₁₆O₅N₂Cl₃ [M+H]⁺ 349.0119; found 349.0123.

1-Ethyl 2-(2,2,2-trichloroethyl) 1-(2-methylbut-3-en-2-yl)hydrazine-1,2-dicarboxylate (**S4a**) and 2-ethyl 1-(2,2,2-trichloroethyl) 1-(2-methylbut-3-en-2-yl)hydrazine-1,2-dicarboxylate (**S4b**)

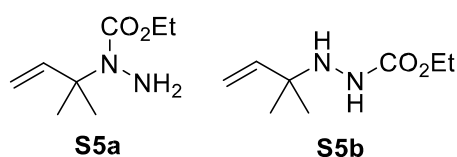


The isomeric mixture of aldehydes **S3a/S3b** (3.1 g, 8.9 mmol, 1.0 eq) and pyridine (1.3 mL, 16 mmol, 1.8 eq) were added to a flame dried flask and cooled to -80 °C. Tebbe reagent (0.5M in toluene, 23.1 mL, 11.5 mmol, 1.3 eq) was added carefully by adding it along the flask. The reaction mixture was allowed to warm up to 0 °C and stirred 24 h. The reaction was quenched with a saturated aqueous NaHCO₃ solution (6 mL) at -80 °C and extracted with methylene chloride (3 x 30 mL). The combined organic layers were dried over MgSO₄, filtered and the solvent was removed *in vacuo*. Purification by flash column chromatography (hexanes/EtOAc 9:1 → 8:2) gave an inseparable mixture of olefines **S4a/S4b** (556 mg, 1.60 mmol, 18%) as a colourless oil in an isomeric mixture of 85:15 (determined retrospectively via ¹H NMR

6. Traceless isoprenylation

spectroscopy): $R_f = 0.39$ (hexanes/EtOAc 8:2); $^1\text{H NMR}$ (400 MHz, chloroform-*d*) $\delta/\text{ppm} = 6.63$ (s, 1H), 6.10 (dd, $^3J_{\text{H,H}} = 17.5, 10.7$ Hz, 1H), 5.10 (dd, $^3J_{\text{H,H}} = 17.9, ^2J_{\text{H,H}} = 6.7$ Hz, 1H), 5.03 (dd, $^3J_{\text{H,H}} = 10.7, ^2J_{\text{H,H}} = 6.7$ Hz, 1H), 4.90 – 4.68 (m, 2H), 4.19 – 4.09 (m, 2H), 1.52 (s, 3H), 1.45 (s, 3H), 1.25 – 1.20 (m, 3H); $^{13}\text{C NMR}$ (101 MHz, chloroform-*d*) $\delta/\text{ppm} = 155.4, 155.2, 143.8, 111.8, 74.9, 63.2, 62.4, 26.3, 26.1, 23.9, 14.5$; IR (ATR) $\tilde{\nu}/\text{cm}^{-1} = 3291, 2985, 1749, 1695, 1517, 1403, 1375, 1338, 1251, 1216, 1181, 1096, 1051, 915, 821, 765, 739, 719$; HRMS (ESI): m/z calcd for $\text{C}_{11}\text{H}_{16}\text{O}_4\text{N}_2\text{Cl}_3$ $[\text{M}-\text{H}]^-$ 345.0181; found 345.0182.

Ethyl 1-(2-methylbut-3-en-2-yl)hydrazine-1-carboxylate (**S5a**) and ethyl 2-(2-methylbut-3-en-2-yl)hydrazine-1-carboxylate (**S5b**)

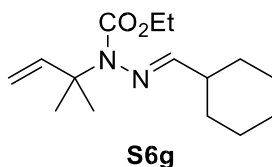


The mixture of olefins **S4a/S4b** (550 mg, 1.58 mmol, 1.0 eq) was dissolved in a mixture of ethanol (1.0 mL), water (1.0 mL) and acetic acid (1.0 mL). Zinc powder (3.62 g, 55.4 mmol, 35.0 eq) was added and the reaction mixture was stirred for 10 min at room temperature. After filtration of the reaction mixture, the filtrate was extracted with methylene chloride (3 x 10 mL).

The combined organic layers were washed with saturated aqueous NaHCO_3 solution (15 mL) and dried over MgSO_4 , filtered and the solvent was removed *in vacuo*. **S5a/S5b** (167 mg, 0.970 mmol, 61%) was obtained as a colourless oil in an isomeric mixture of 85:15 (determined via $^1\text{H NMR}$ spectroscopy). This mixture was used for the next step without purification. $R_f = 0.47$ (hexanes/EtOAc 8:2); $^1\text{H NMR}$ (**S5a**) (500 MHz, chloroform-*d*) $\delta/\text{ppm} = 6.05$ (dd, $^3J_{\text{H,H}} = 17.5, 10.7$ Hz, 1H), 5.01 – 4.92 (m, 2H), 4.13 (q, $^3J_{\text{H,H}} = 7.2$ Hz, 2H), 3.80 (s, 2H), 1.44 (s, 6H), 1.25 (t, $^3J_{\text{H,H}} = 7.1$ Hz, 3H); $^{13}\text{C NMR}$ (**S5a**) (101 MHz, chloroform-*d*) $\delta/\text{ppm} = 157.9, 145.3, 109.9, 61.9, 61.7, 26.5, 14.7$; $^1\text{H NMR}$ (**S5b**) (500 MHz, chloroform-*d*) $\delta/\text{ppm} = 5.97$ (dd, $^3J_{\text{H,H}} = 17.4, 10.7$ Hz, 1H), 5.14 – 5.05 (m, 2H), 4.10 – 4.04 (m, 2H), 1.39 (s, 6H), 1.23 – 1.20 (m, 3H); $^{13}\text{C NMR}$ (**S5b**) (101 MHz, chloroform-*d*) $\delta/\text{ppm} = 155.8, 144.2, 111.8, 61.5, 53.6, 26.5, 14.5$; IR (ATR) $\tilde{\nu}/\text{cm}^{-1} = 2980, 1686, 1465, 1400, 1374, 1318, 1246, 1181, 1081, 1007, 910, 859, 769, 686$; HRMS (ESI): m/z calcd for $\text{C}_8\text{H}_{17}\text{O}_2\text{N}_2$ $[\text{M}+\text{H}]^+$ 173.1285; found 173.1283.

6. Traceless isoprenylation

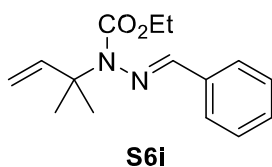
Ethyl 2-(cyclohexylmethylene)-1-(2-methylbut-3-en-2-yl)hydrazine-1-carboxylate (**S6g**)



The mixture of allylhydrazines **S5a/S5b** (200 mg, 1.16 mmol \pm 0.986 mmol of isomer **S5a**, 1.0 eq) was dissolved in absolute EtOH (15 mL) and cyclohexane carboxaldehyde (130 mg, 1.16 mmol, 1.0 eq) was added. The reaction mixture was stirred at room temperature for 18 h. The solvent was removed *in vacuo* and the crude product was purified by flash column chromatography (pentane/Et₂O 9:1). *N*-CO₂Et-*N*-allylhydrazone **S6g** was isolated as colourless oil (115 mg, 0.432 mmol, 44% referred to isomer **S5a**).

R_f = 0.32 (pentane/Et₂O 9:1); ¹H NMR (400 MHz, chloroform-*d*) δ /ppm = 7.60 (d, ³ $J_{H,H}$ = 6.0 Hz, 1H), 6.11 (dd, ³ $J_{H,H}$ = 17.5, 10.8 Hz, 1H), 5.10 – 4.90 (m, 2H), 4.07 (q, ³ $J_{H,H}$ = 7.1 Hz, 2H), 2.42 – 2.32 (m, 1H), 1.89 – 1.62 (m, 6H), 1.41 (s, 6H), 1.37 – 1.28 (m, 4H), 1.20 (t, ³ $J_{H,H}$ = 7.1 Hz, 3H); ¹³C NMR (101 MHz, chloroform-*d*) δ /ppm = 173.9, 154.9, 145.4, 110.1, 61.9, 61.4, 41.4, 29.7, 26.5, 26.1, 25.4, 14.5; IR (ATR) $\tilde{\nu}$ /cm⁻¹ = 2979, 2927, 2853, 1699, 1448, 1369, 1281, 1240, 1177, 1097, 1004, 911, 758, 684; HRMS (EI): m/z calcd for C₁₅H₂₆O₂N₂ [M]⁺ 266.1989; found 266.1989.

Ethyl 2-benzylidene-1-(2-methylbut-3-en-2-yl)hydrazine-1-carboxylate (**S6b**)



The mixture of allylhydrazines **S5a/S5b** (200 mg, 1.16 mmol \pm 0.986 mmol of isomer **S5a**, 1.0 eq) was dissolved in absolute EtOH (15 mL) and benzaldehyde (123 mg, 1.16 mmol, 1.0 eq) was added. The reaction mixture was stirred at room temperature for 17 h. The solvent was removed *in vacuo* and the crude product was purified by flash column chromatography (pentane/Et₂O 9:1). *N*-CO₂Et-*N*-allylhydrazone **S6i** was isolated as colourless oil (234 mg, 0.899 mmol, 91% referred to isomer **S5a**).

R_f = 0.38 (pentane/Et₂O 9:1); ¹H NMR (500 MHz, chloroform-*d*) δ /ppm = 8.60 (s, 1H), 7.74 – 7.70 (m, 2H), 7.44 – 7.38 (m, 3H), 6.18 (dd, ³ $J_{H,H}$ = 17.5, 10.8 Hz, 1H), 5.11 – 4.96 (m, 2H), 4.17 (q, ³ $J_{H,H}$ = 7.1 Hz, 2H), 1.53 (s, 6H), 1.25 (t, ³ $J_{H,H}$ = 7.1 Hz, 3H); ¹³C NMR (101 MHz, chloroform-*d*) δ /ppm = 159.0, 154.6, 145.7, 134.9, 130.5, 128.7, 127.8, 110.0, 63.6, 61.7, 26.9, 14.5; IR (ATR) $\tilde{\nu}$ /cm⁻¹ = 1698, 1597, 1455, 1368, 1282, 1202, 1166, 1098, 1073, 1015, 906, 827, 743, 687; HRMS (ESI): m/z calcd for C₁₅H₂₁O₂N₂ [M+H]⁺ 261.1597; found 261.1596.

3 Crystallographic data

3.1. Sample preparation

To receive crystals out of the oily isomeric mixture of **8a** and **8b**, 80 mg of the neat mixture were placed in a 5 mL round bottom flask and cooled to - 20 °C. After seven days, crystals of **8a** were grown as colourless needles. The crystals are stable at room temperature for one day.

3.2. Crystallographic information of

8a

Table S2. Crystallographic information of **8a**

Compound	8a
	CCDC 1907495
net formula	C ₁₀ H ₂₀ N ₂ O ₂
<i>M</i> /g mol ⁻¹	200.28
crystal size/mm	0.100 × 0.060 × 0.050
<i>T</i> /K	103.(2)
radiation	MoK α
diffractometer	'Bruker D8 Venture TXS'
crystal system	triclinic
space group	'P -1'
<i>a</i> /Å	5.9860(5)
<i>b</i> /Å	9.0630(7)
<i>c</i> /Å	11.4665(9)
α /°	105.616(3)
β /°	99.965(3)
γ /°	97.087(3)
<i>V</i> /Å ³	580.52(8)
<i>Z</i>	2
calc. density/g cm ⁻³	1.146
μ /mm ⁻¹	0.080
absorption correction	Multi-Scan
transmission factor range	0.95–1.00
refls. measured	5785
<i>R</i> _{int}	0.0312
mean $\sigma(I)/I$	0.0416
θ range	3.444–26.370
observed refls.	1982
<i>x</i> , <i>y</i> (weighting scheme)	0.0299, 0.2047
hydrogen refinement	H(C) constr, H(N) refall
refls in refinement	2368
parameters	140
restraints	0
<i>R</i> (<i>F</i> _{obs})	0.0411
<i>R</i> _w (<i>F</i> ²)	0.0961
<i>S</i>	1.072

6. Traceless isoprenylation

shift/error _{max}	0.001
max electron density/e Å ⁻³	0.242 min
electron density/e Å ⁻³	-0.205

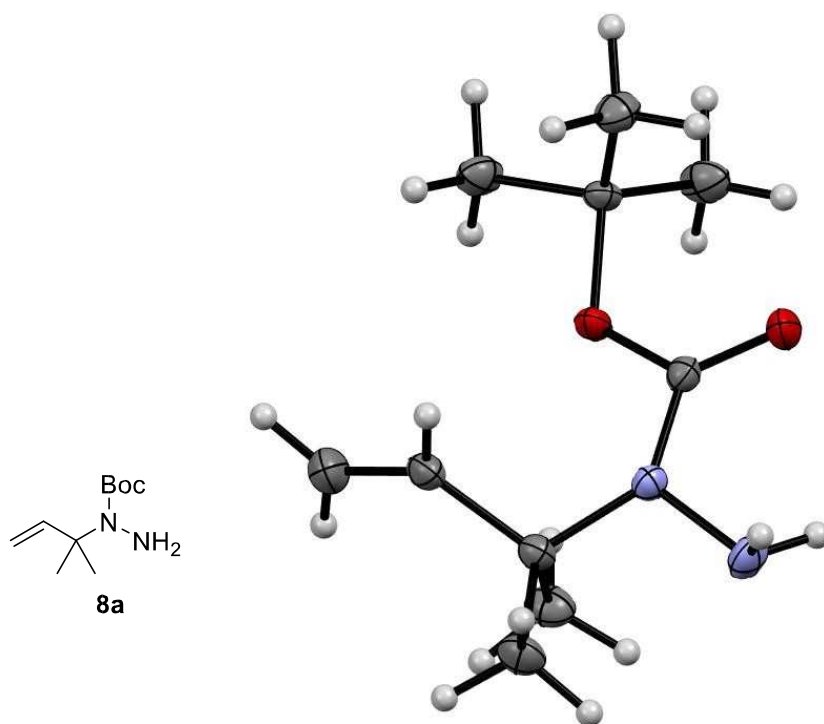


Figure S3. Mercury plot of the solid-state structure of compound **8a** (50% ellipsoid probability level).

6. Traceless isoprenylation

4 NMR spectra

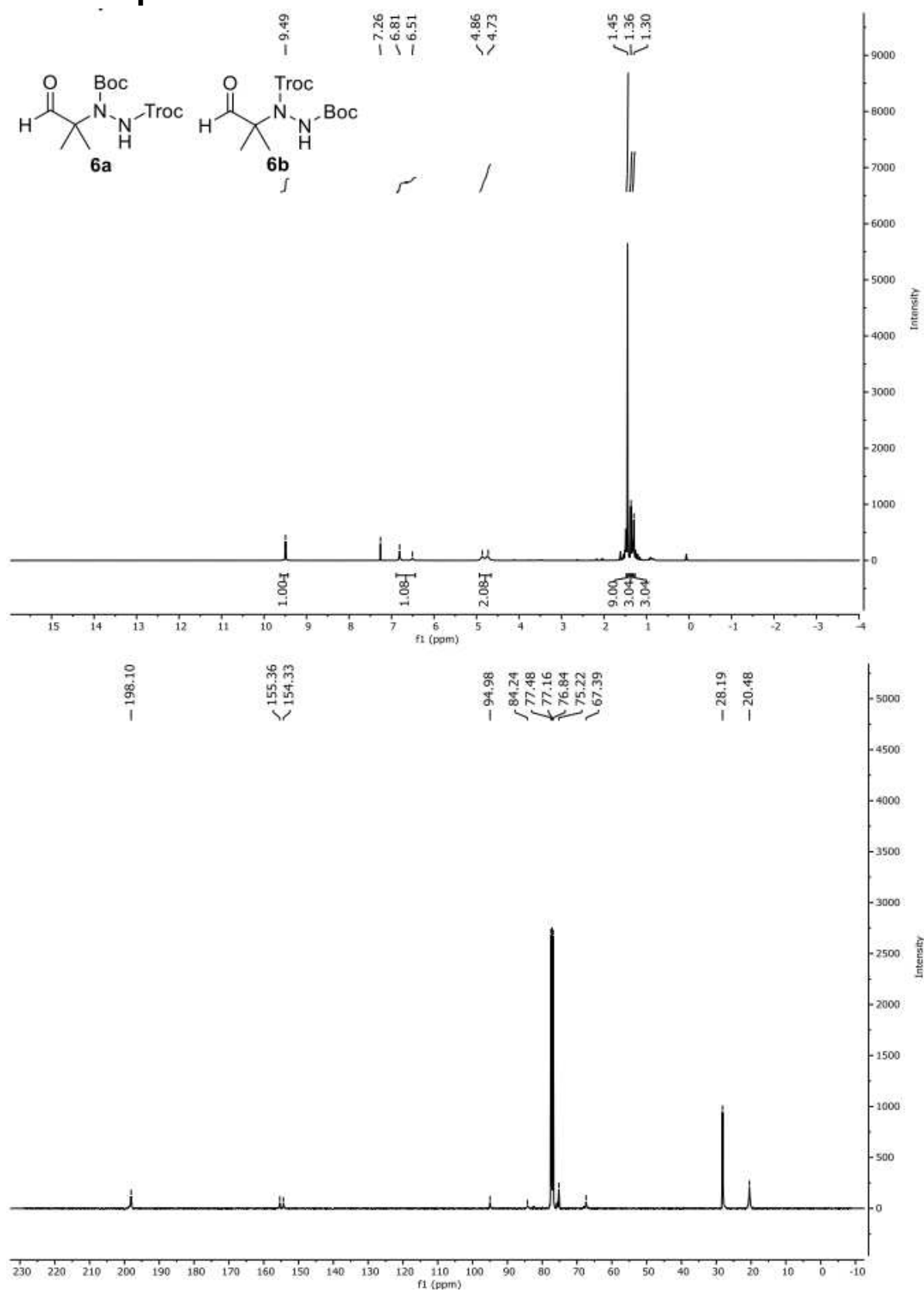


Figure S4. 500 MHz ^1H NMR spectrum (top) and 101 MHz ^{13}C NMR spectrum (bottom) of **6a/6b** in CDCl_3 .

6. Traceless isoprenylation

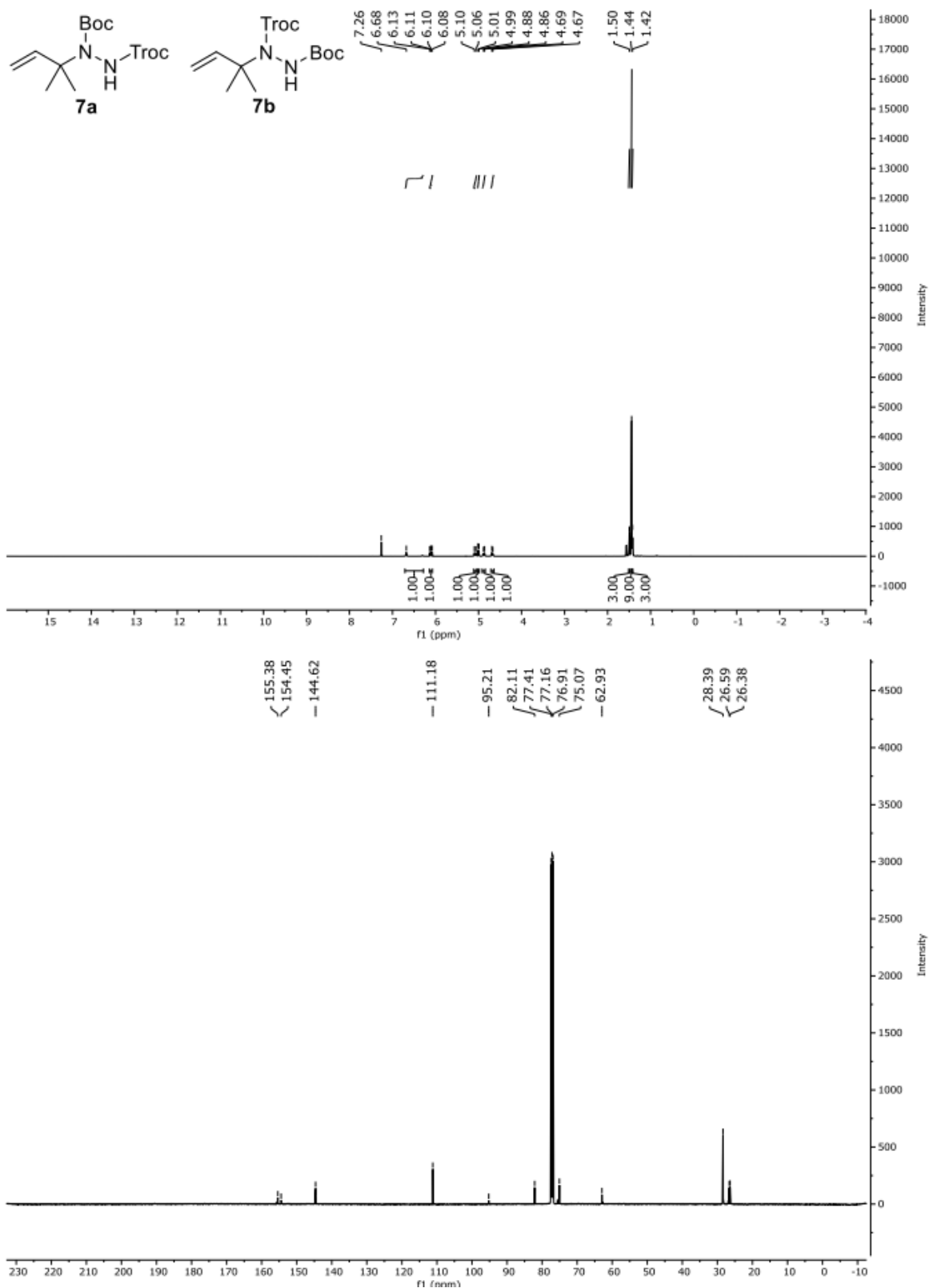


Figure S5. 500 MHz ¹H NMR spectrum (top) and 126 MHz ¹³C NMR spectrum (bottom) of **7a/7b** in CDCl₃.

6. Traceless isoprenylation

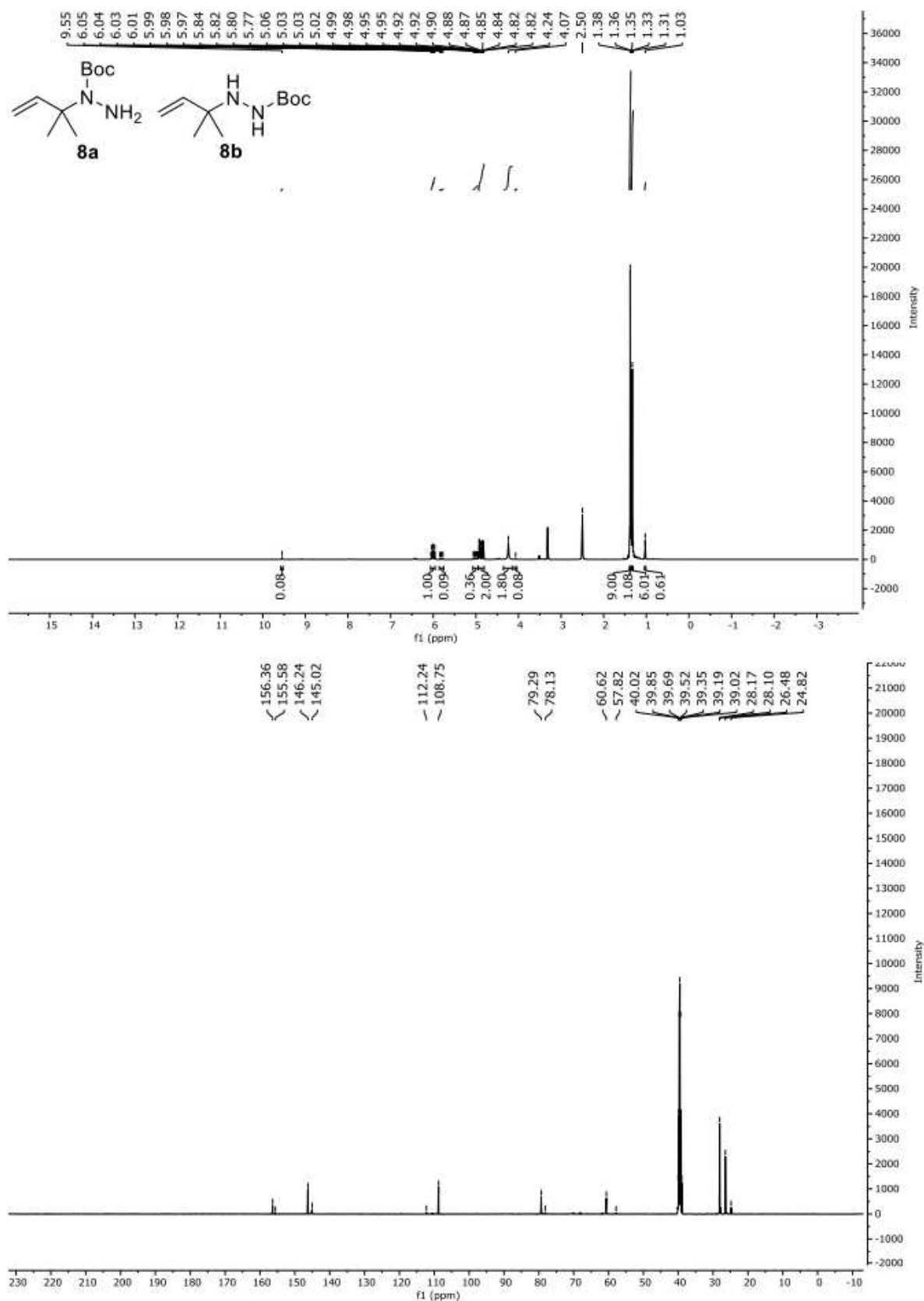


Figure S6. 400 MHz ¹H NMR spectrum (top) and 126 MHz ¹³C NMR spectrum (bottom) of **8a/8b** (ratio 91:9) in DMSO-*d*₆.

6. Traceless isoprenylation

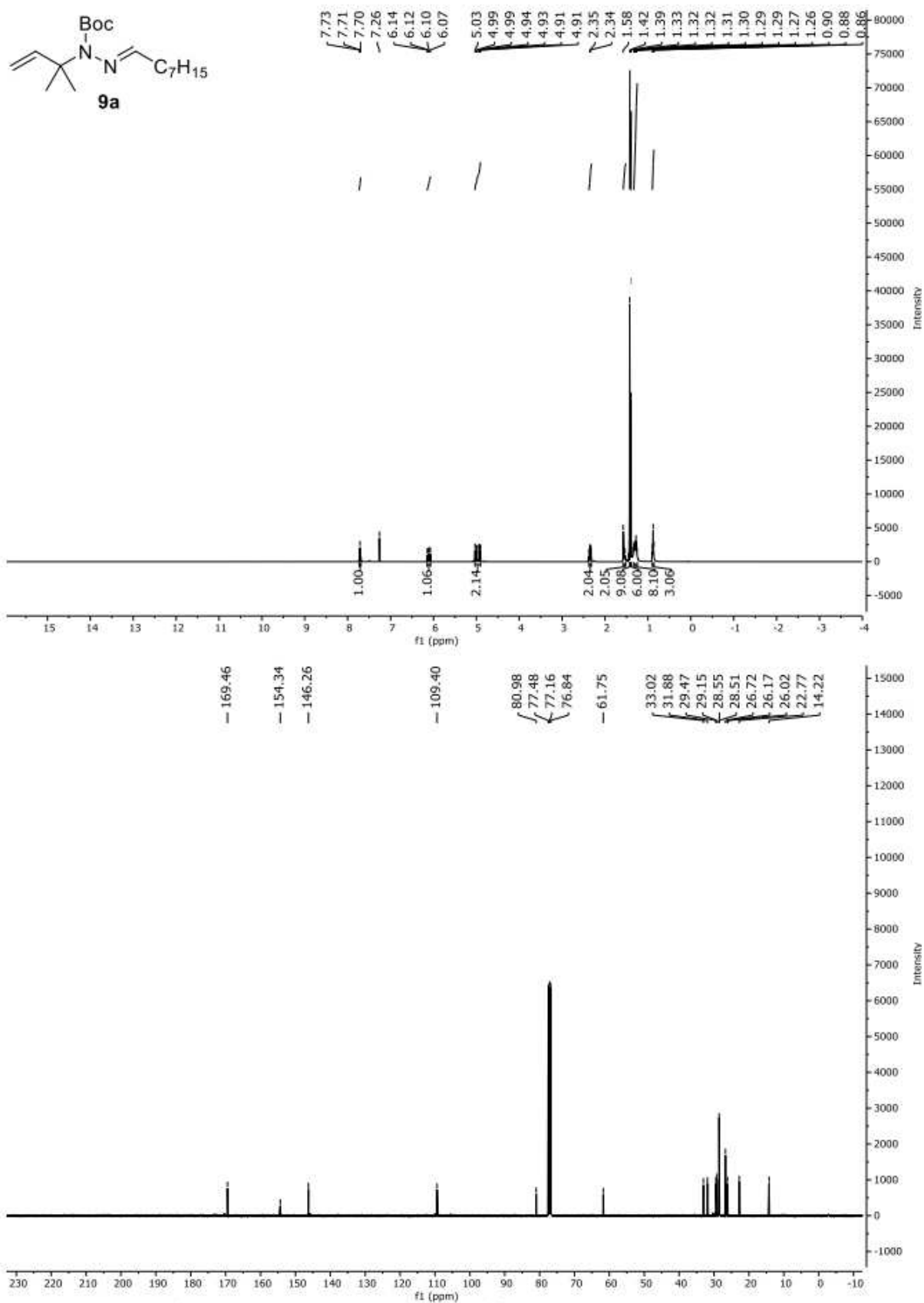


Figure S7. 400 MHz ¹H NMR spectrum (top) and 101 MHz ¹³C NMR spectrum (bottom) of **9a** in CDCl₃.

6. Traceless isoprenylation

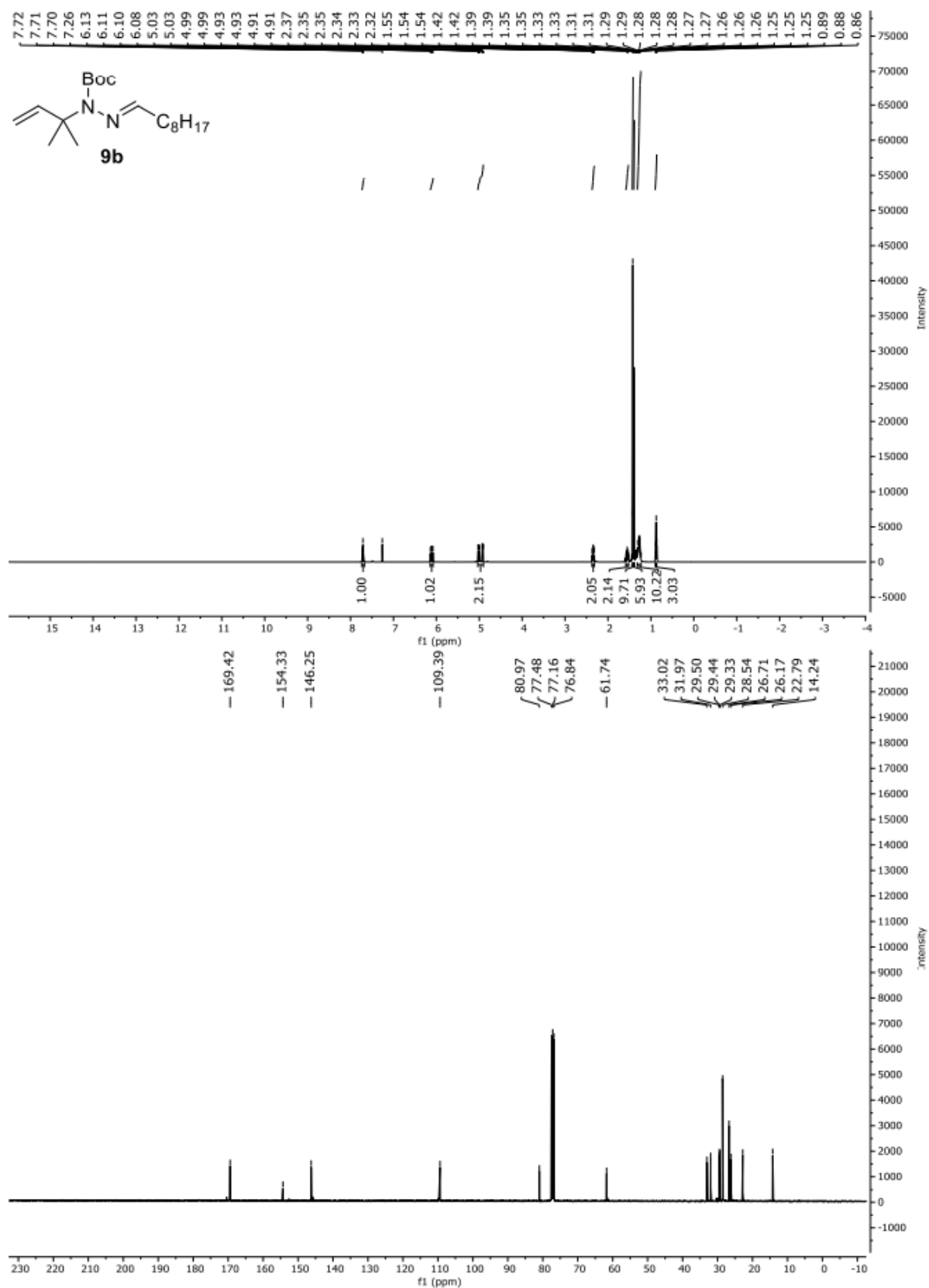


Figure S8. 500 MHz ¹H NMR spectrum (top) and 101 MHz ¹³C NMR spectrum (bottom) of **9b** in CDCl₃.

6. Traceless isoprenylation

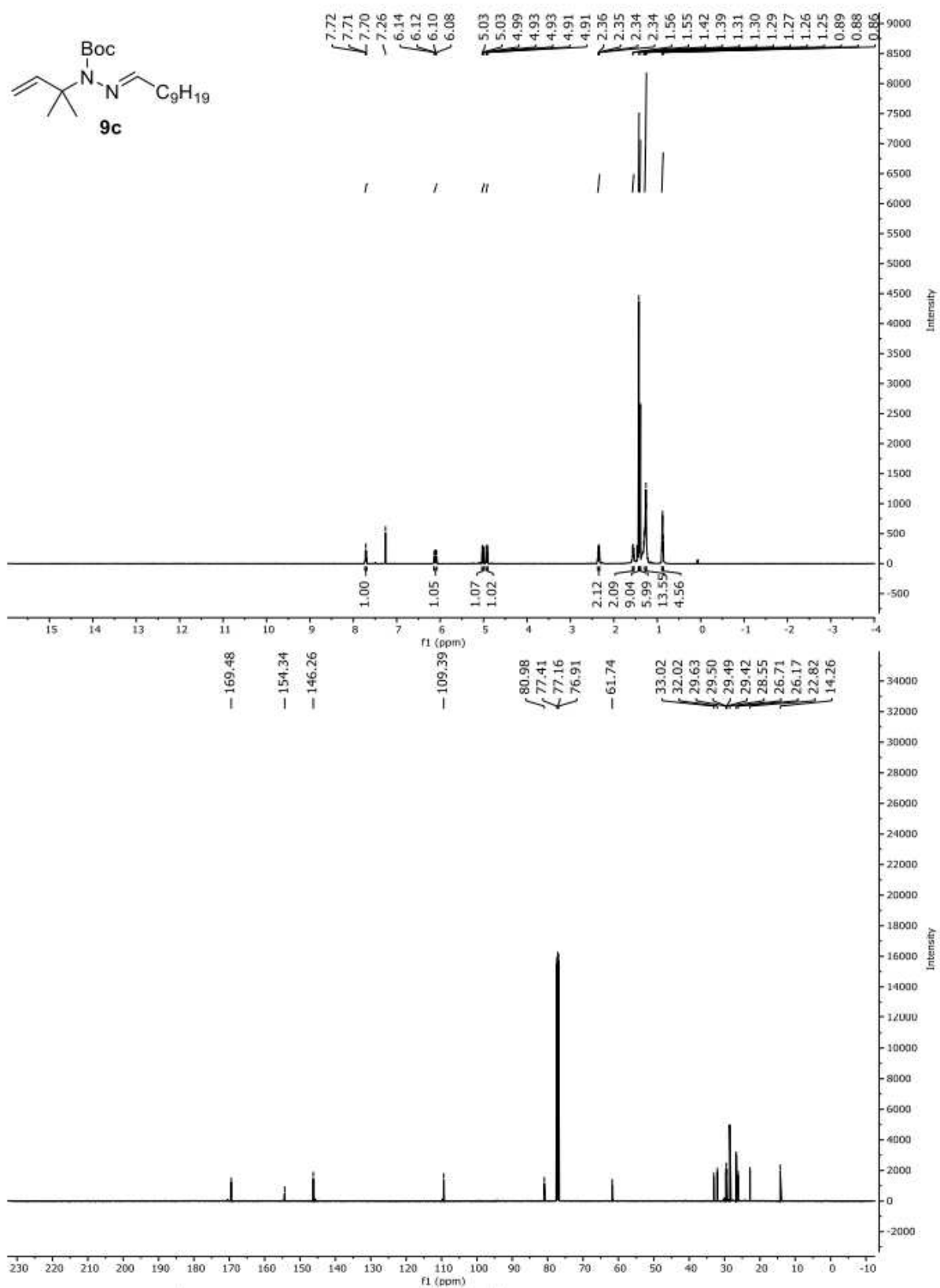


Figure S9. 500 MHz ¹H NMR spectrum (top) and 126 MHz ¹³C NMR spectrum (bottom) of **9c** in CDCl₃.

6. Traceless isoprenylation

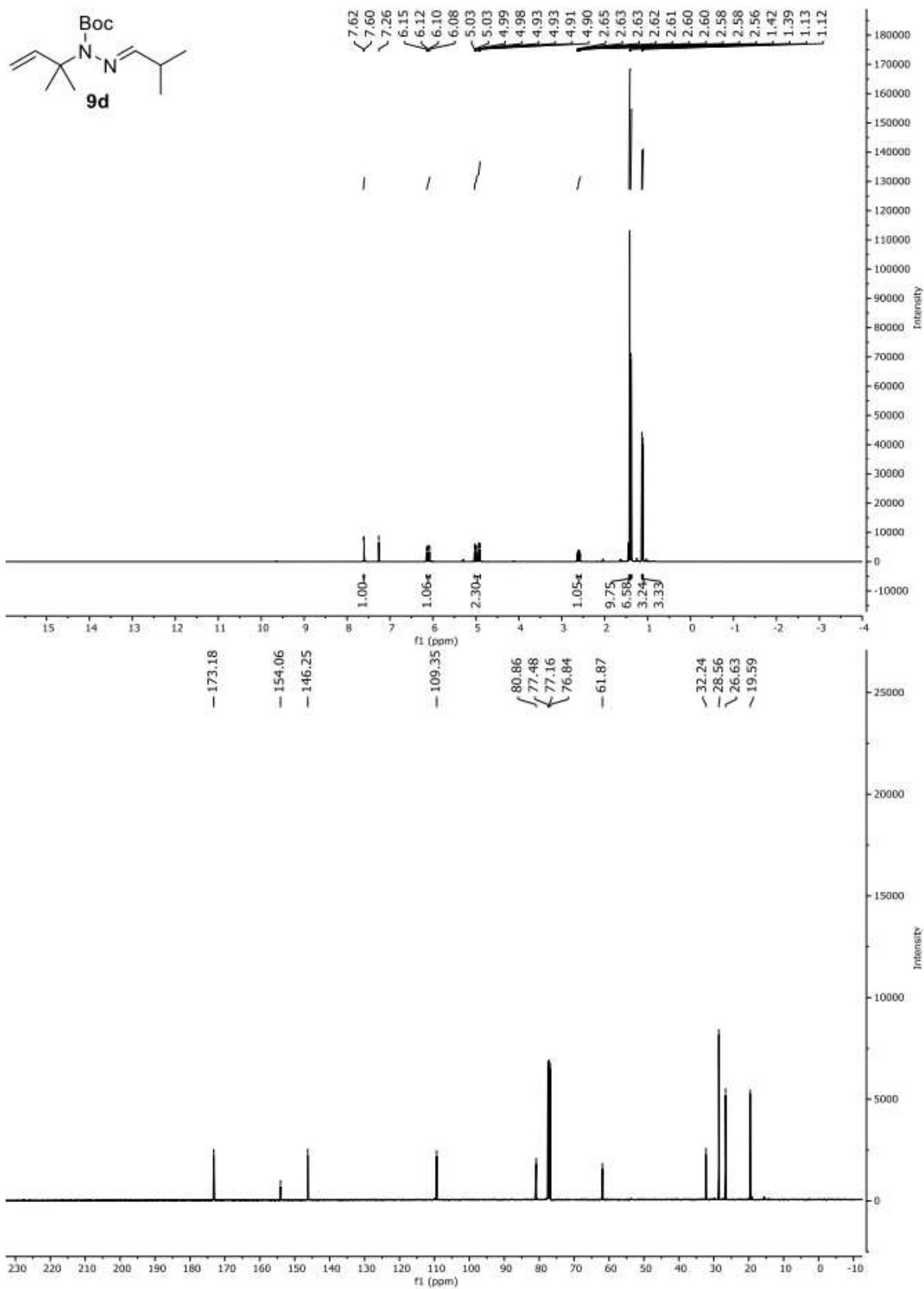


Figure S10. 400 MHz ¹H NMR spectrum (top) and 101 MHz ¹³C NMR spectrum (bottom) of **9d** in CDCl₃.

6. Traceless isoprenylation

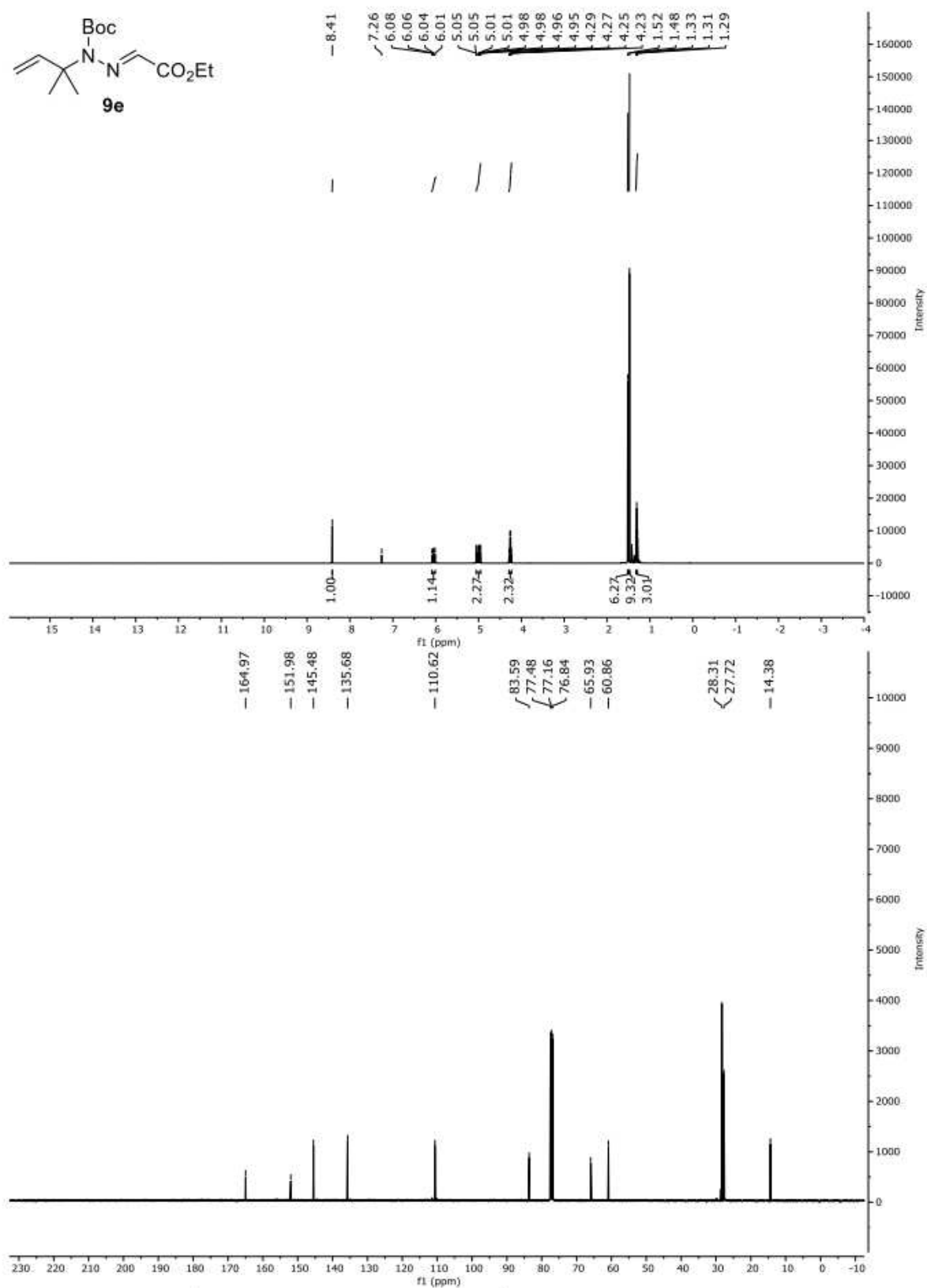


Figure S11. 400 MHz ¹H NMR spectrum (top) and 101 MHz ¹³C NMR spectrum (bottom) of **9e** in CDCl₃

6. Traceless isoprenylation

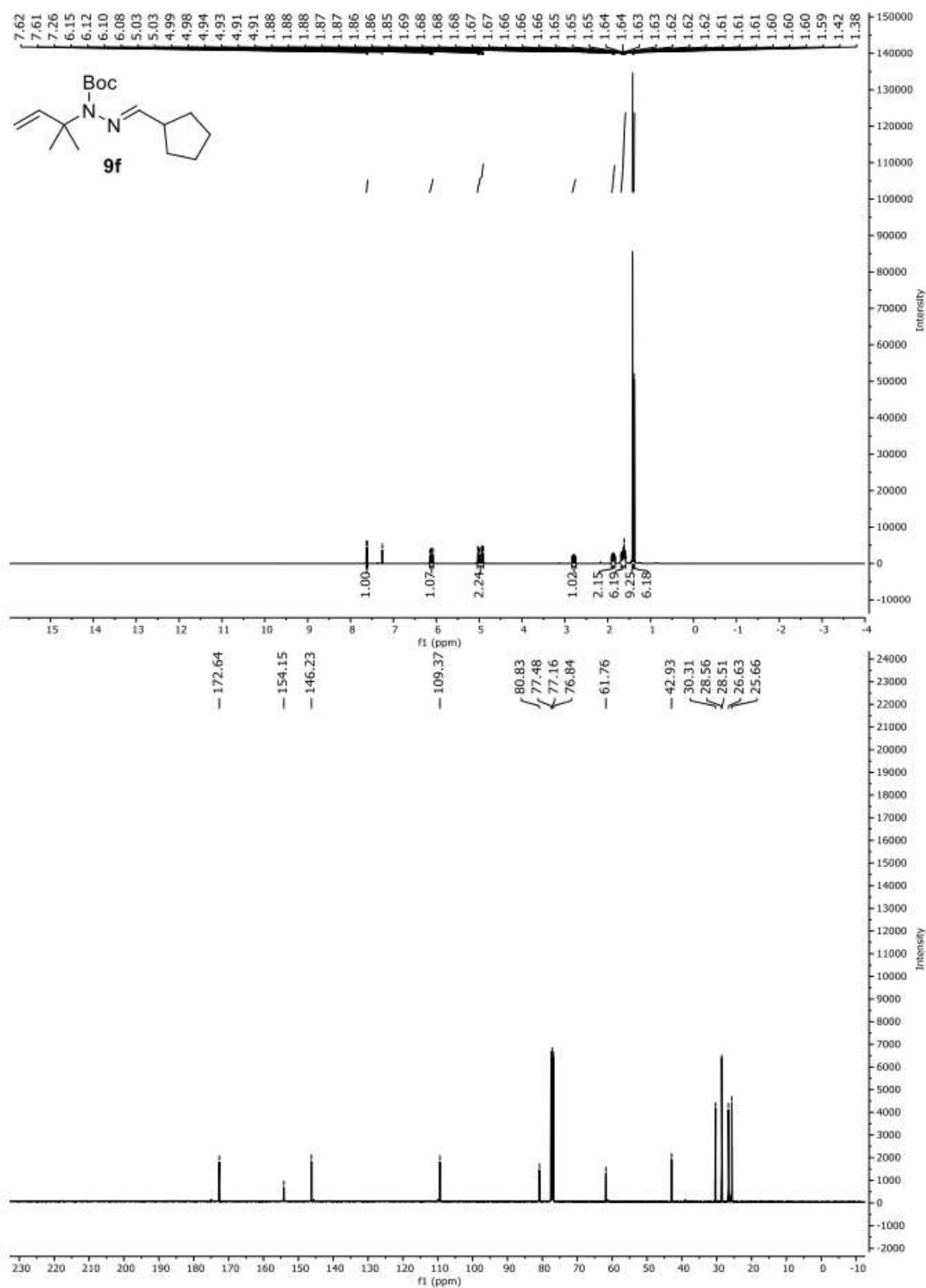


Figure S12. 400 MHz ¹H NMR spectrum (top) and 101 MHz ¹³C NMR spectrum (bottom) of **9f** in CDCl₃

6. Traceless isoprenylation

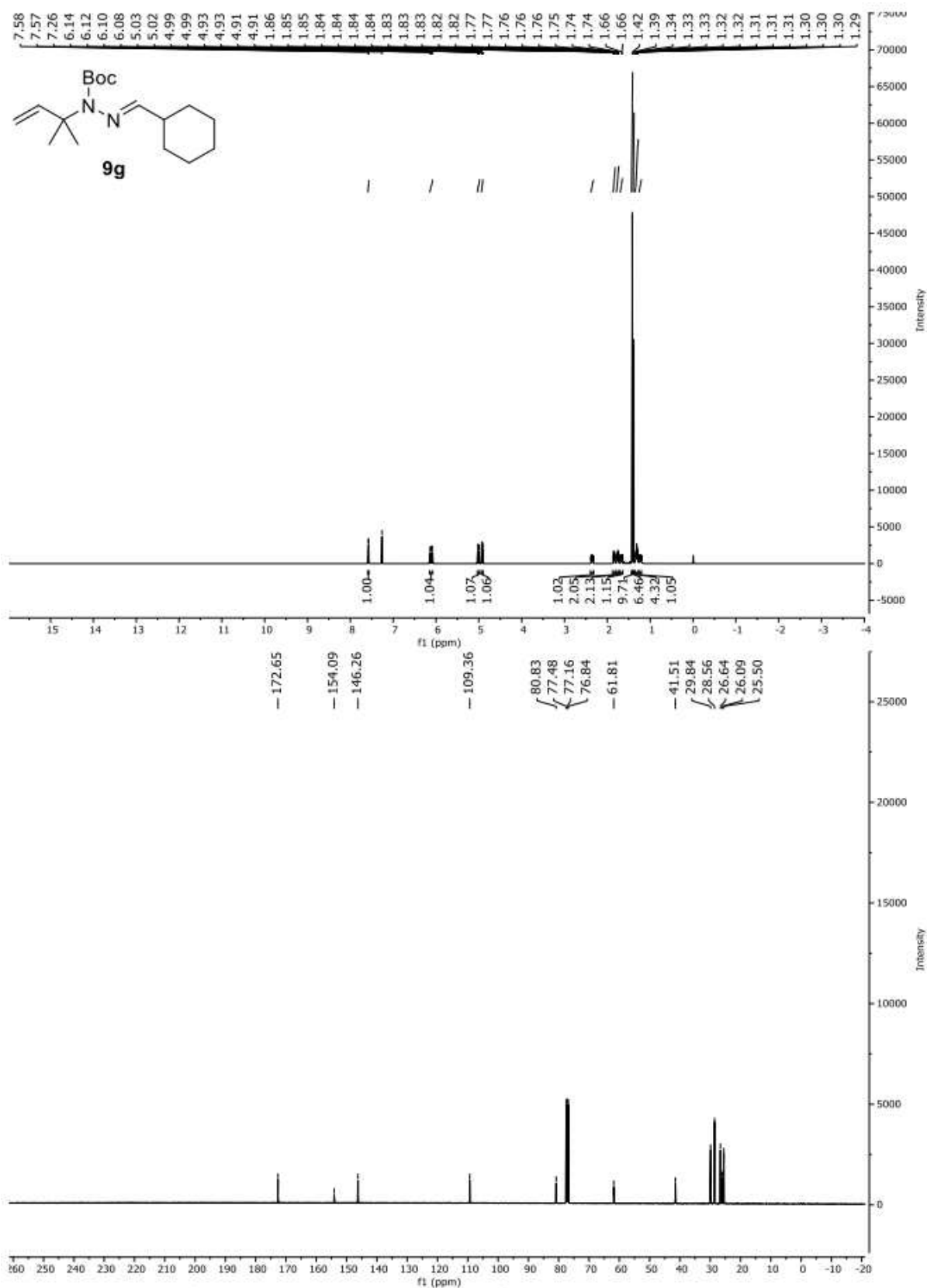


Figure S13. 500 MHz ^1H NMR spectrum (top) and 101 MHz ^{13}C NMR spectrum (bottom) of **9g** in CDCl_3 .

6. Traceless isoprenylation

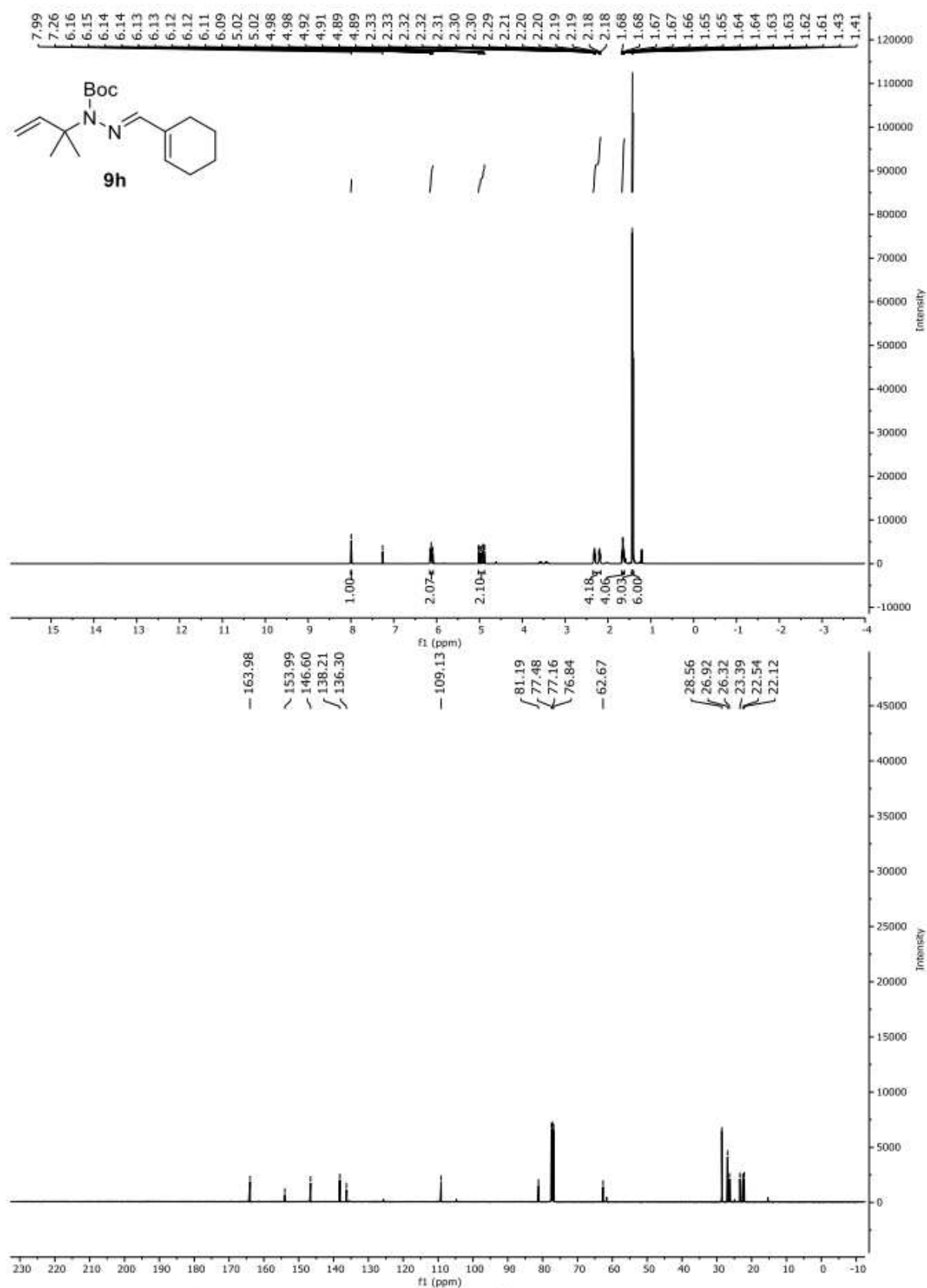


Figure S14. 400 MHz ¹H NMR spectrum (top) and 101 MHz ¹³C NMR spectrum (bottom) of **9h** in CDCl₃.

6. Traceless isoprenylation

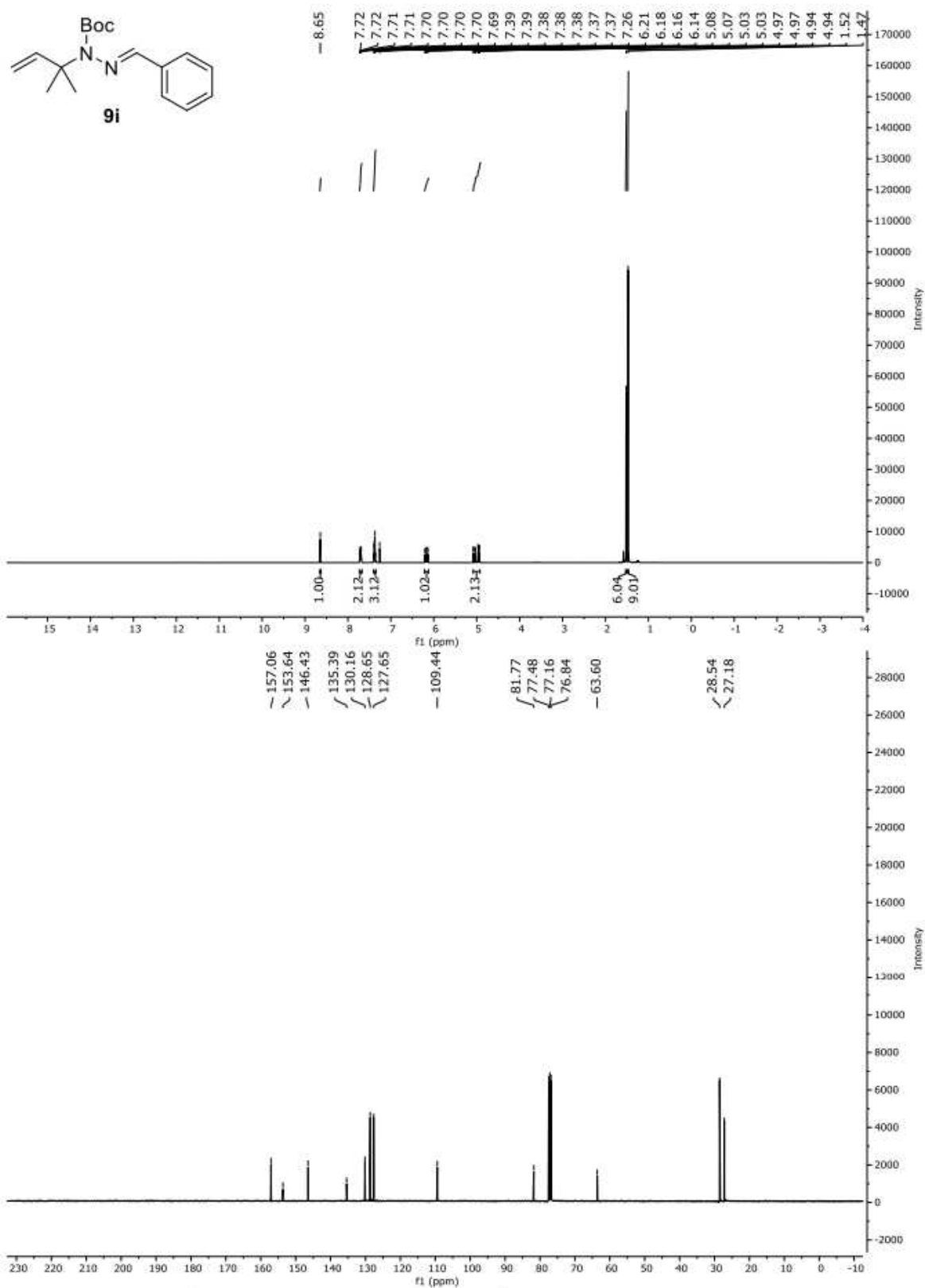


Figure S15. 400 MHz ¹H NMR spectrum (top) and 101 MHz ¹³C NMR spectrum (bottom) of **9i** in CDCl₃.

6. Traceless isoprenylation

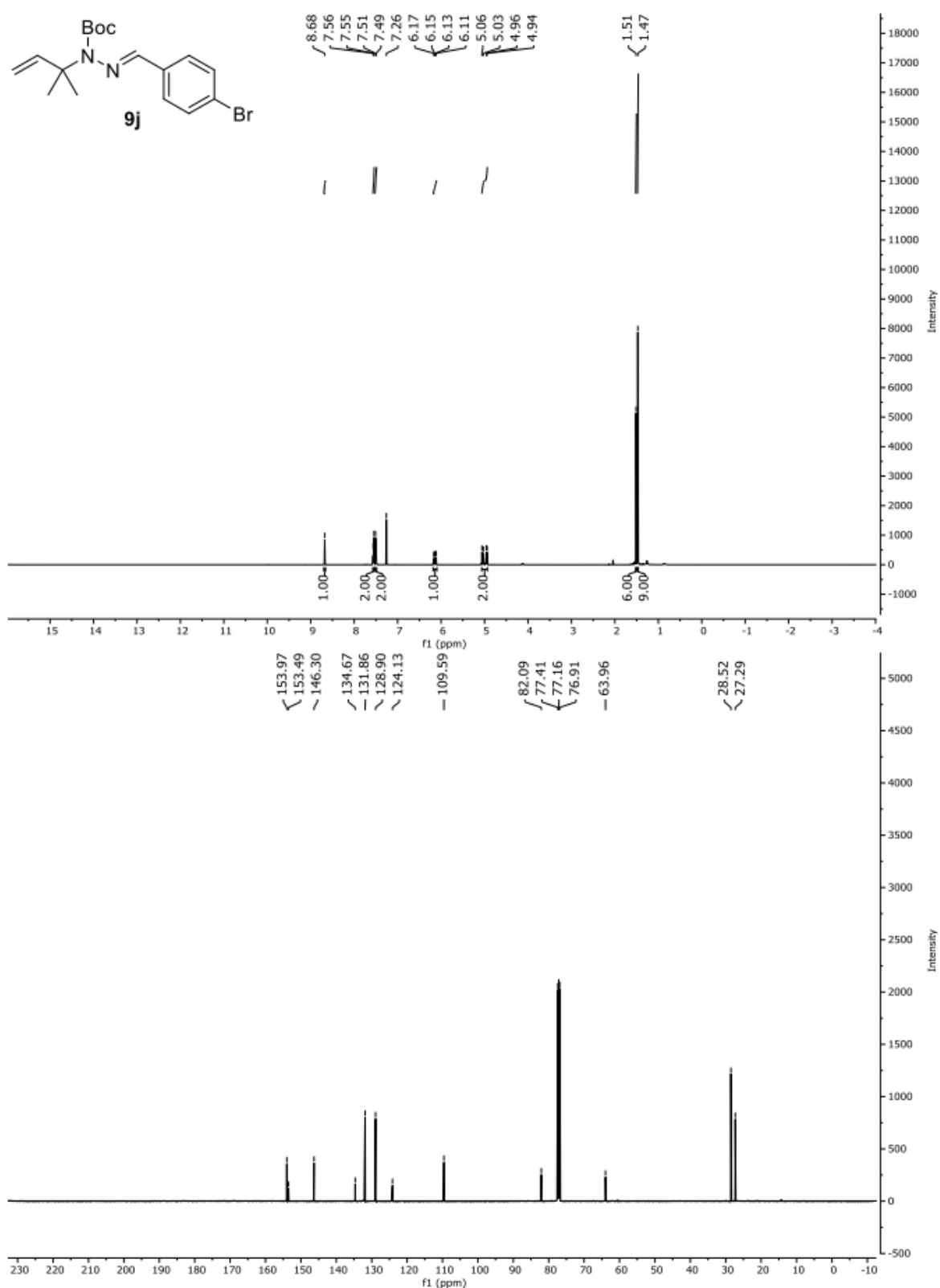


Figure S16. 500 MHz ^1H NMR spectrum (top) and 126 MHz ^{13}C NMR spectrum (bottom) of **9j** in CDCl_3 .

6. Traceless isoprenylation

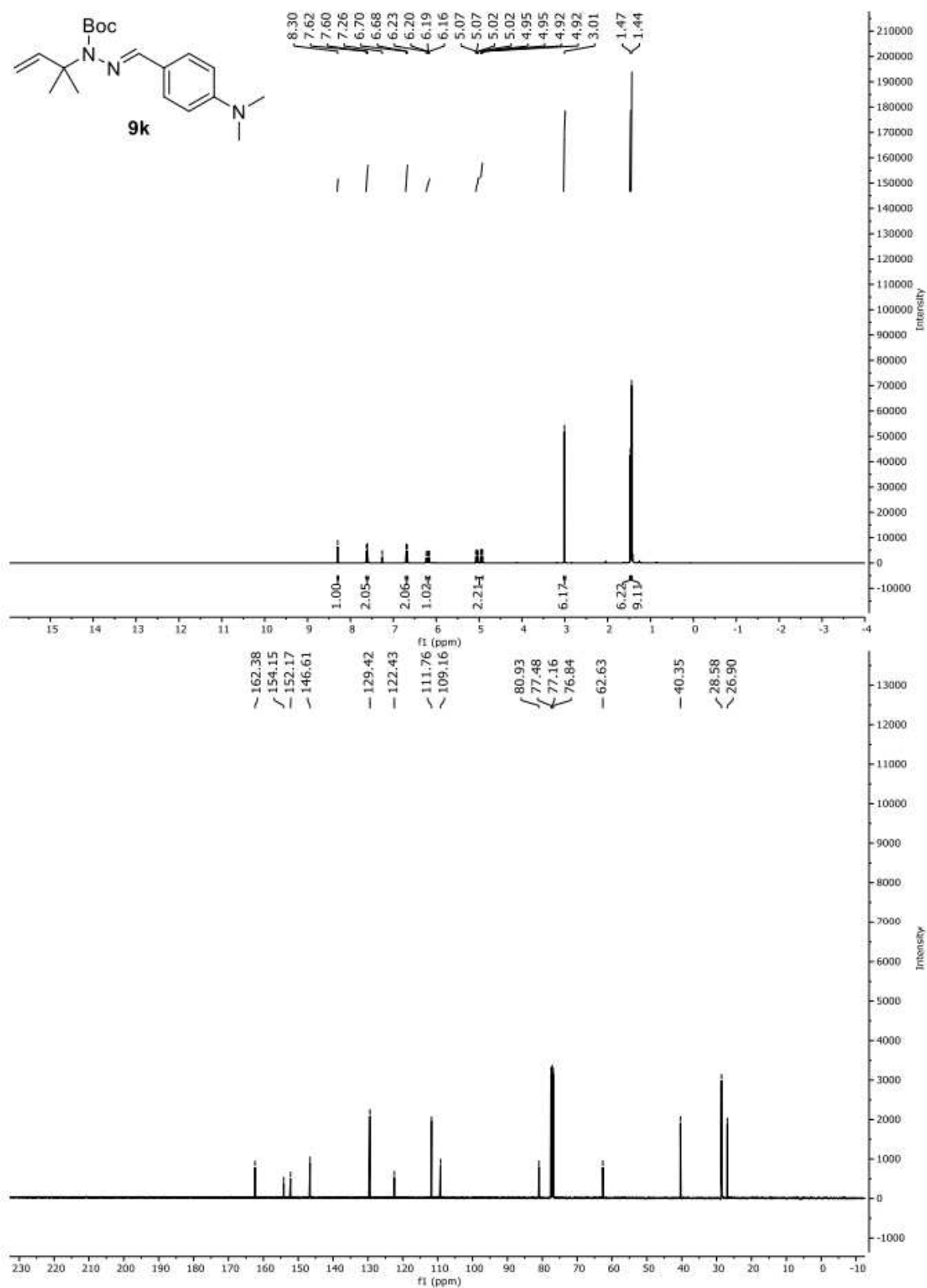


Figure S17. 400 MHz ¹H NMR spectrum (top) and 101 MHz ¹³C NMR spectrum (bottom) of **9k** in CDCl₃.

6. Traceless isoprenylation

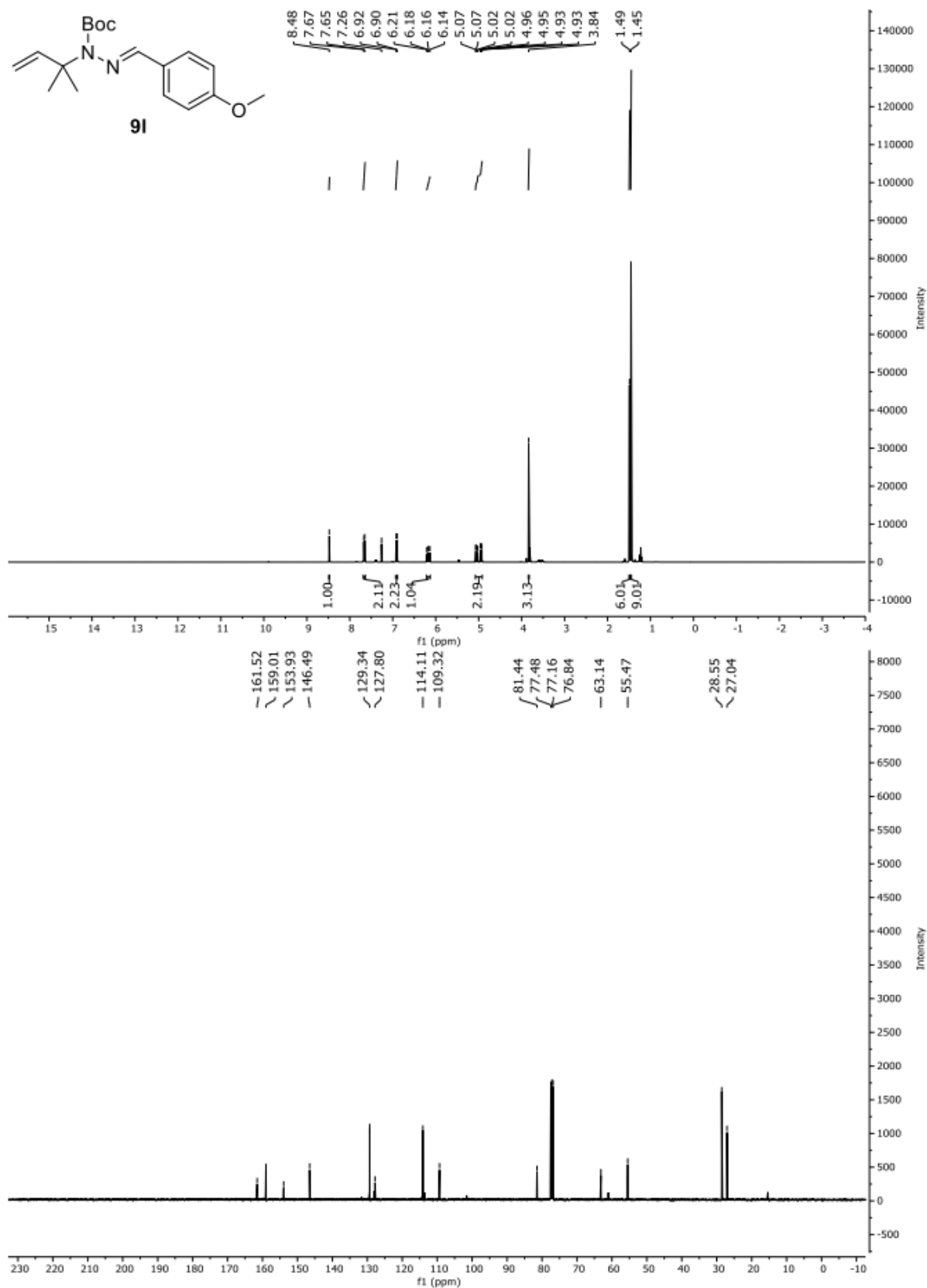


Figure S18. 400 MHz ¹H NMR spectrum (top) and 101 MHz ¹³C NMR spectrum (bottom) of **9I** in CDCl₃.

6. Traceless isoprenylation

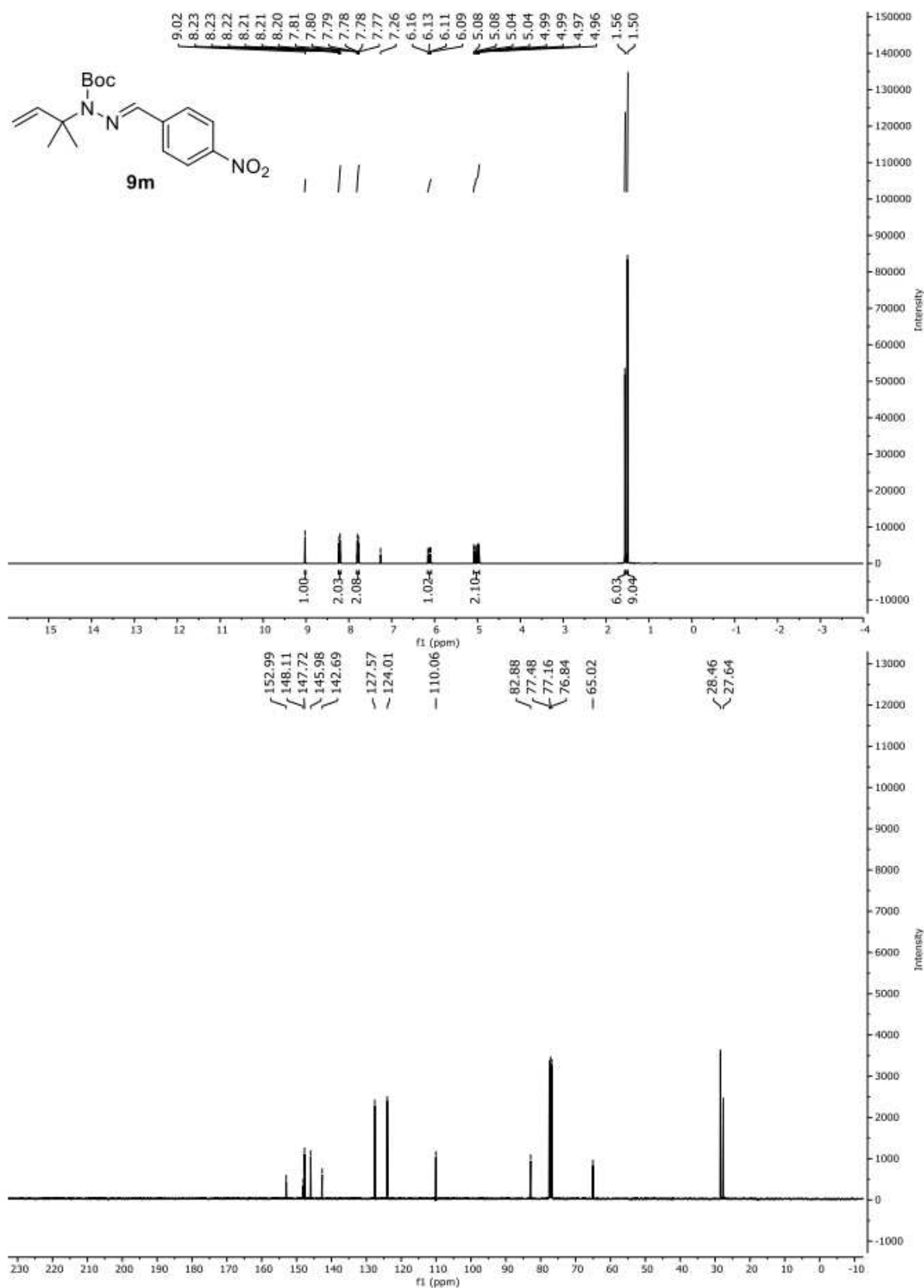


Figure S19. 400 MHz ¹H NMR spectrum (top) and 101 MHz ¹³C NMR spectrum (bottom) of **9m** in CDCl₃.

6. Traceless isoprenylation

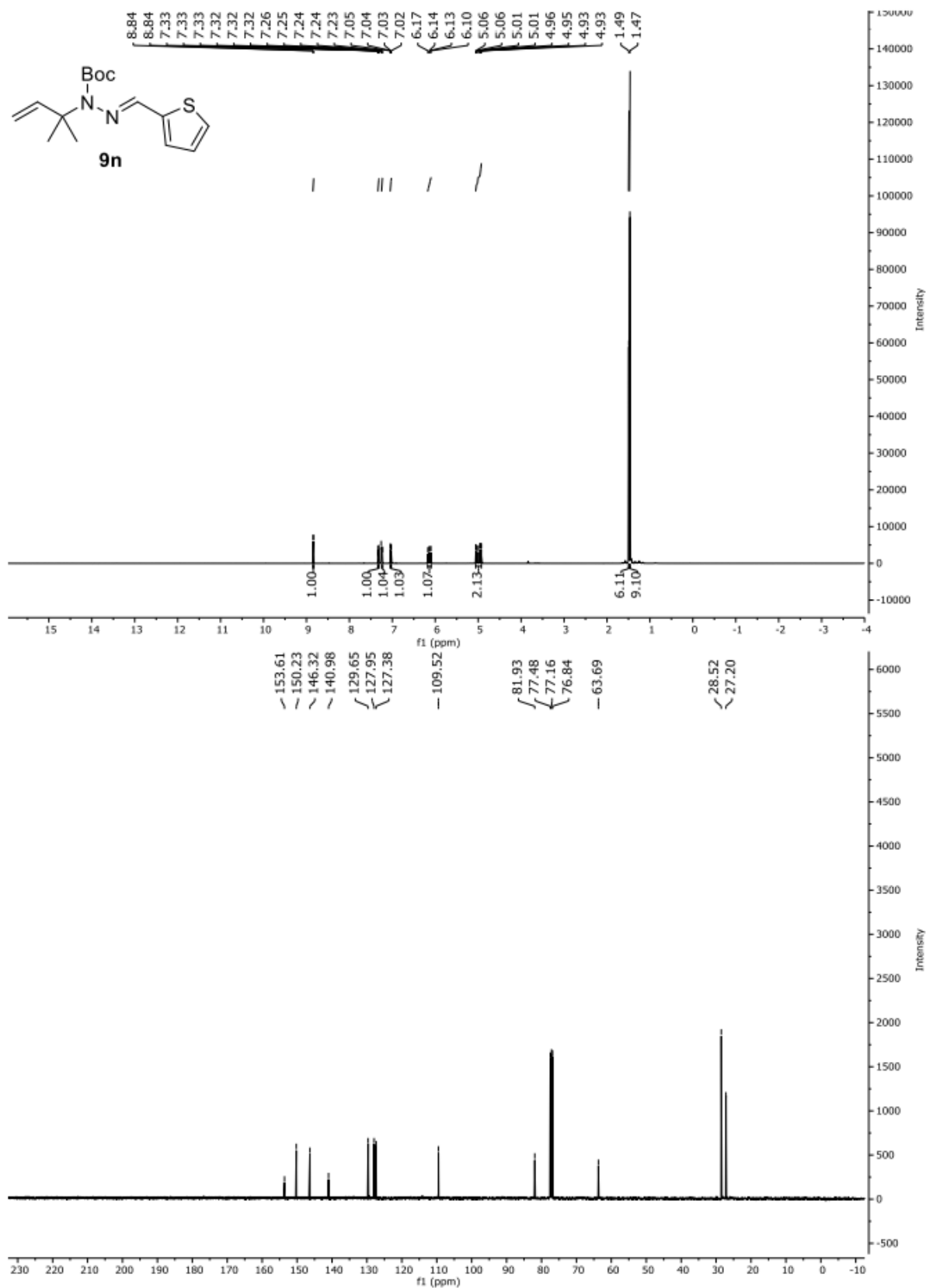


Figure S20. 400 MHz ¹H NMR spectrum (top) and 101 MHz ¹³C NMR spectrum (bottom) of **9n** in CDCl₃.

6. Traceless isoprenylation

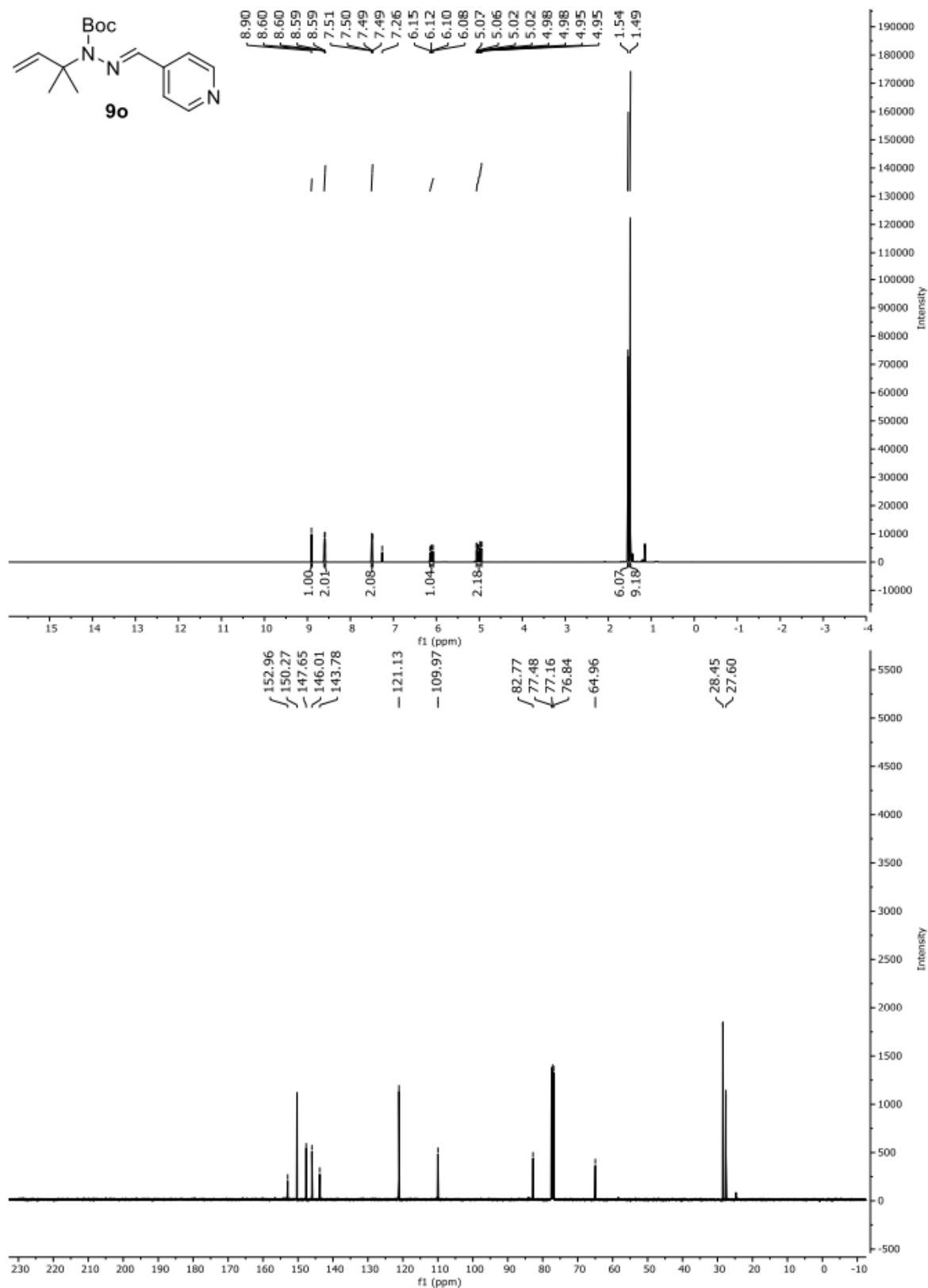


Figure S21. 400 MHz ¹H NMR spectrum (top) and 101 MHz ¹³C NMR spectrum (bottom) of **9o** in CDCl₃.

6. Traceless isoprenylation

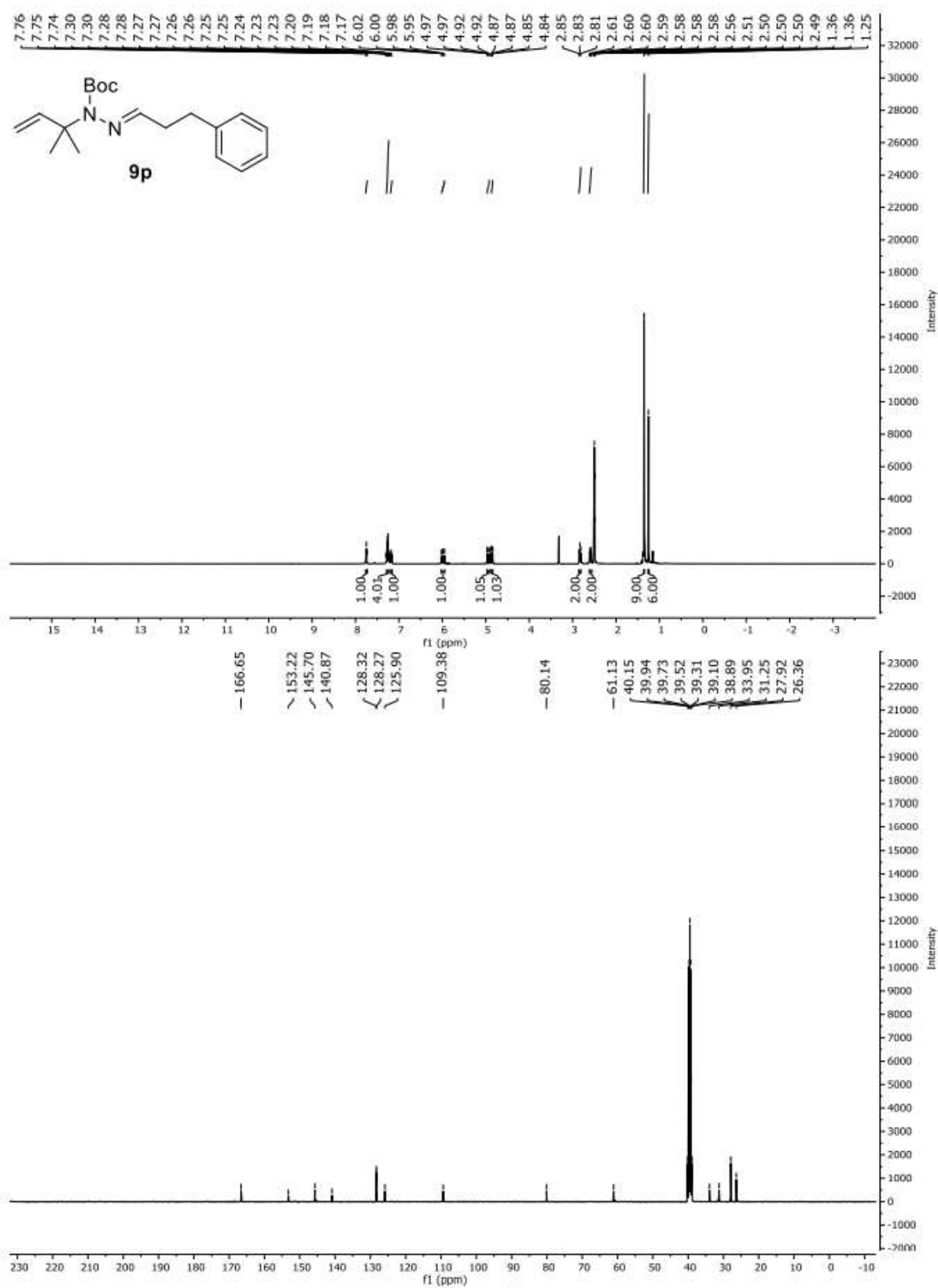


Figure S22. 400 MHz ¹H NMR spectrum (top) and 101 MHz ¹³C NMR spectrum (bottom) of **9p** in DMSO-*d*₆

6. Traceless isoprenylation

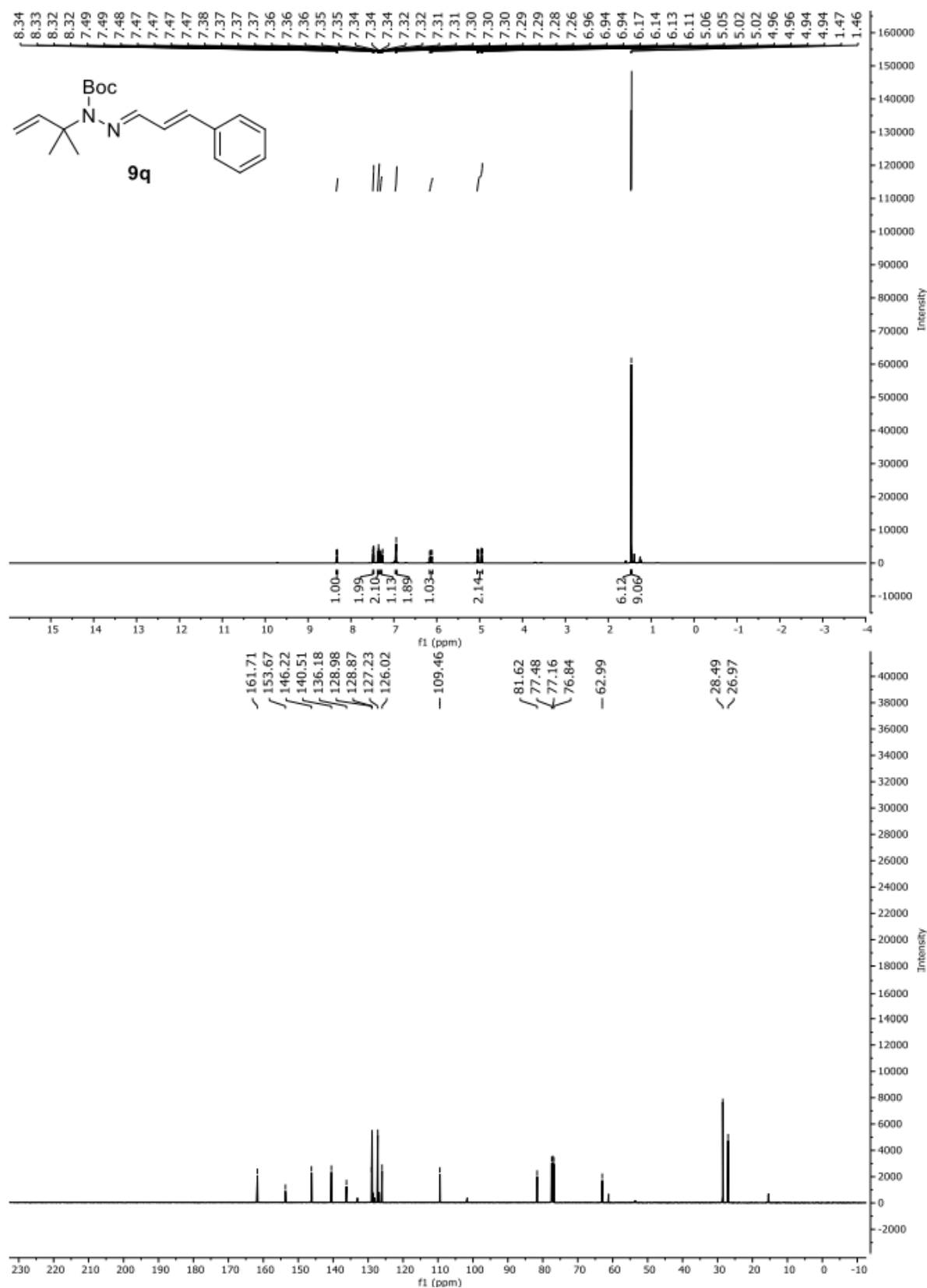


Figure S23. 500 MHz ¹H NMR spectrum (top) and 101 MHz ¹³C NMR spectrum (bottom) of **9q** in CDCl₃

6. Traceless isoprenylation

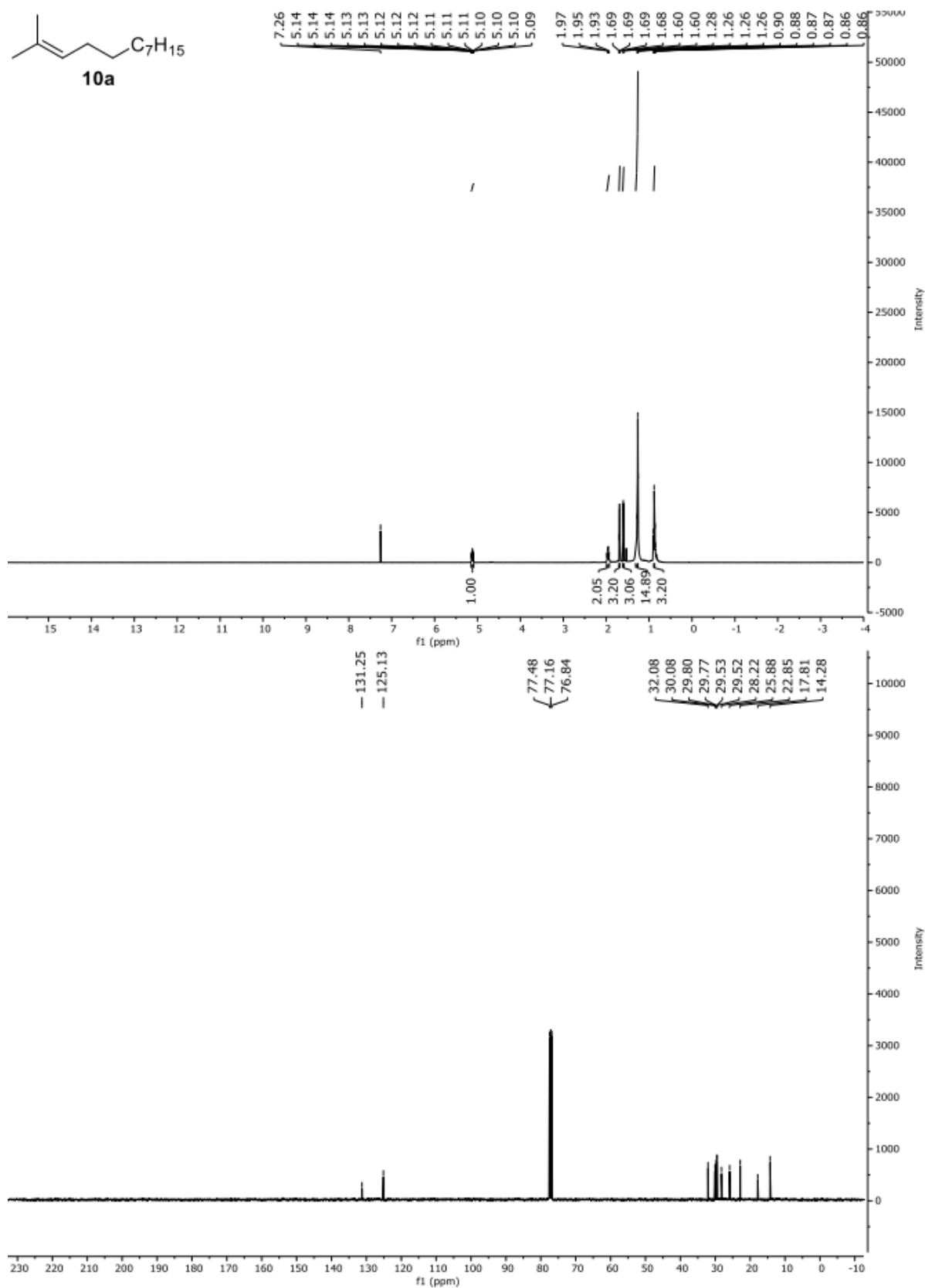


Figure S24. 400 MHz ¹H NMR spectrum (top) and 101 MHz ¹³C NMR spectrum (bottom) of **10a** in CDCl₃.

6. Traceless isoprenylation

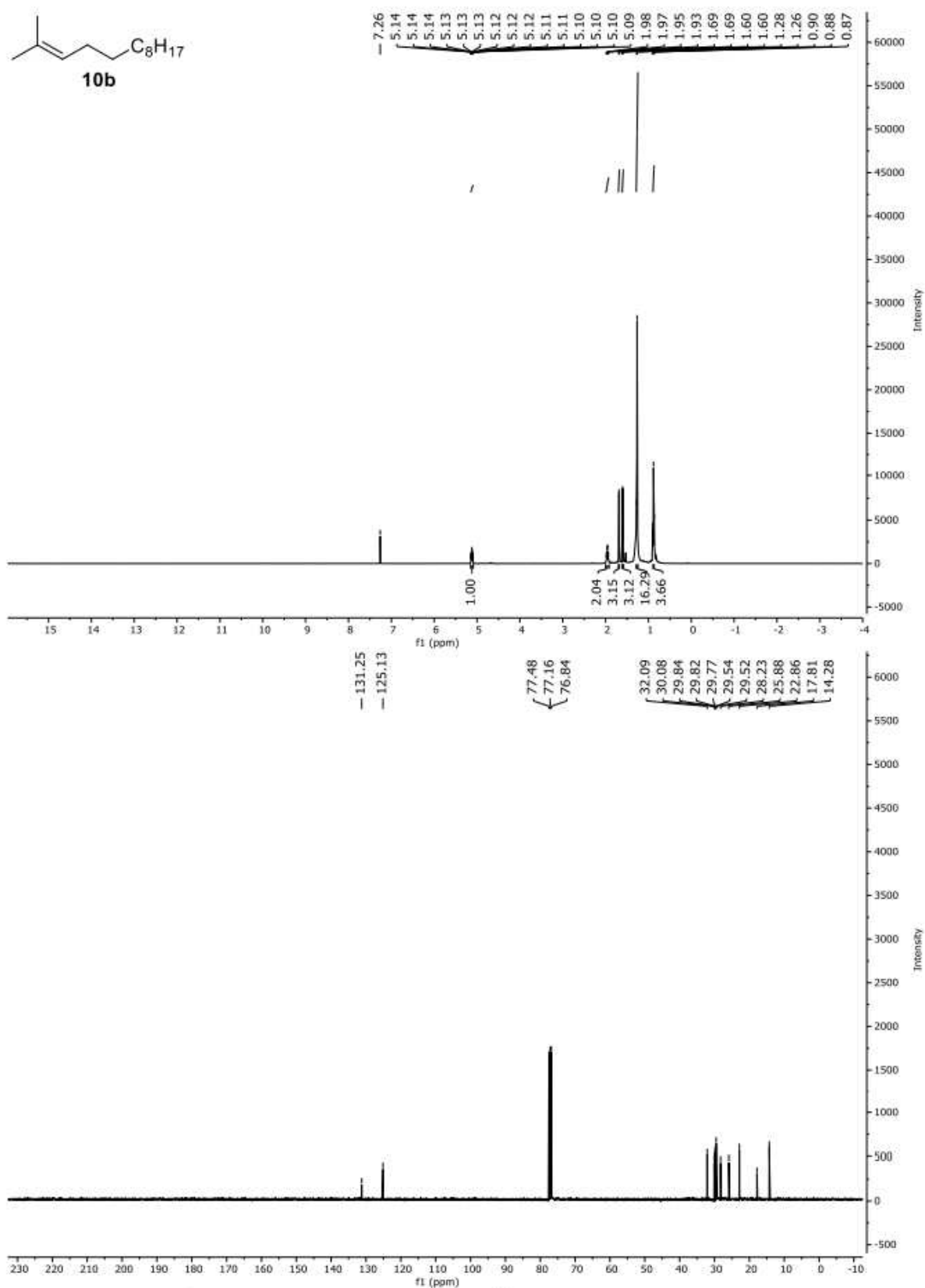


Figure S25. 400 MHz ¹H NMR spectrum (top) and 101 MHz ¹³C NMR spectrum (bottom) of **10b** in CDCl₃.

6. Traceless isoprenylation

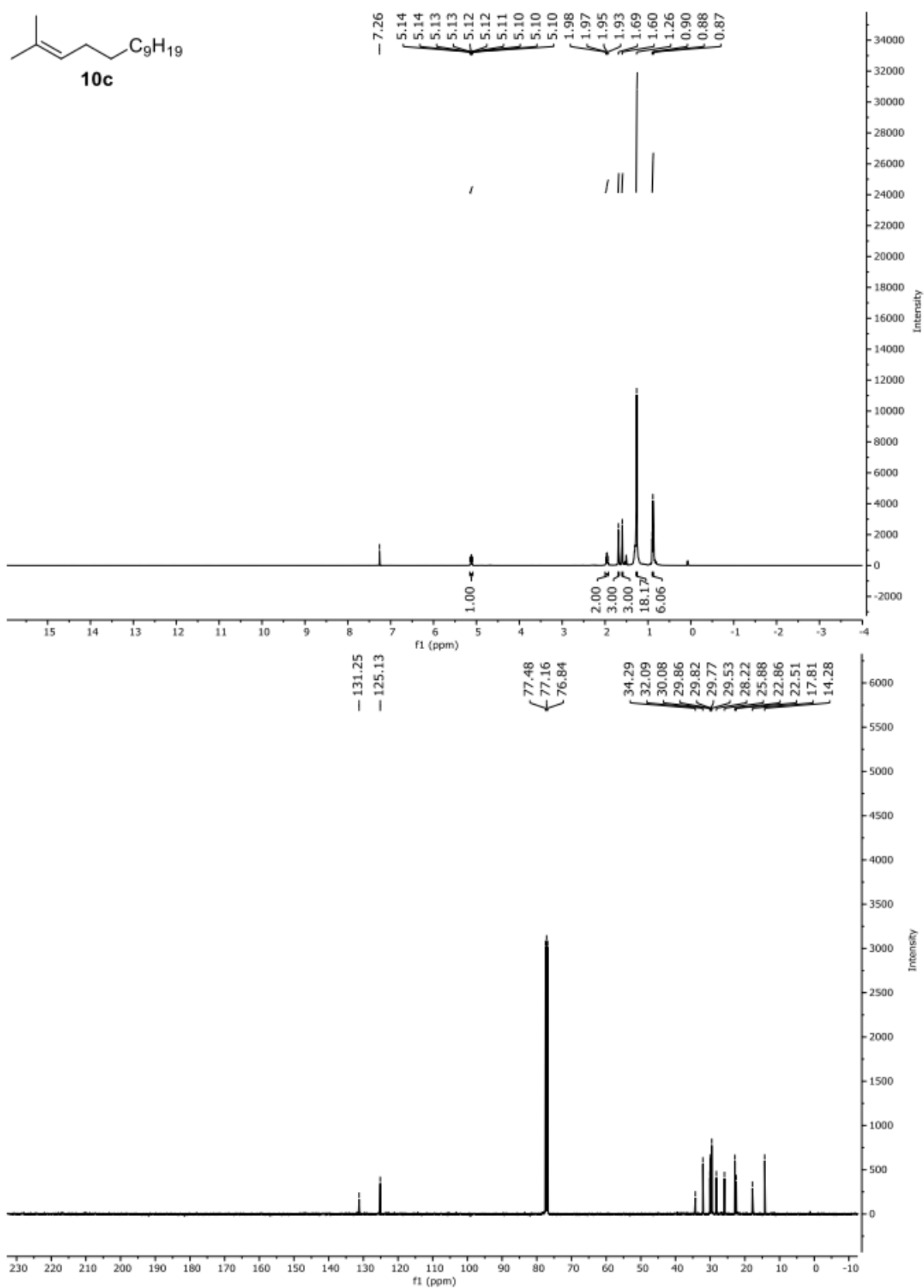


Figure S26. 400 MHz ¹H NMR spectrum (top) and 101 MHz ¹³C NMR spectrum (bottom) of **10c** in CDCl₃.

6. Traceless isoprenylation

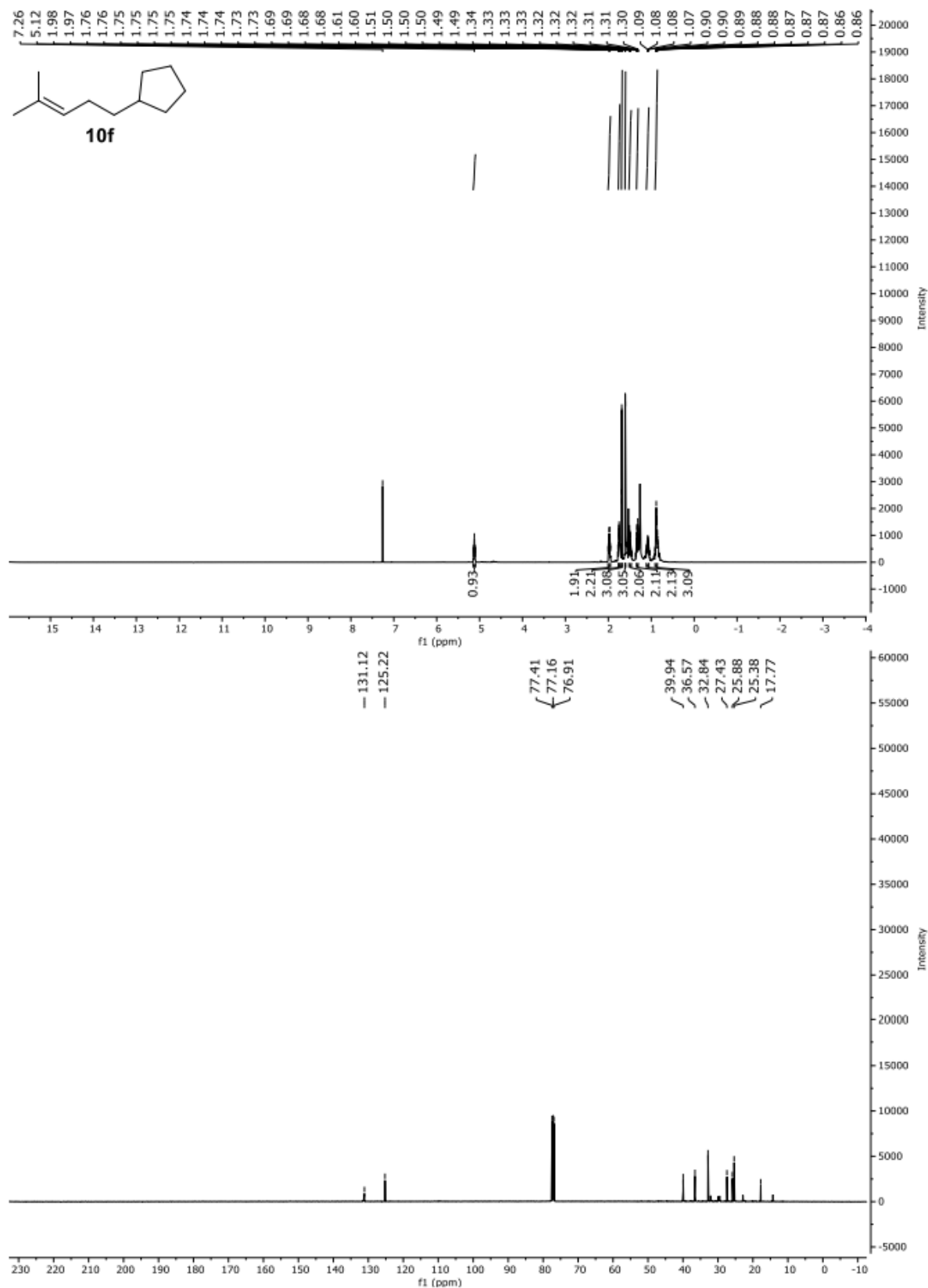


Figure S27. 500 MHz ¹H NMR spectrum (top) and 126 MHz ¹³C NMR spectrum (bottom) of **10f** in CDCl₃.

6. Traceless isoprenylation

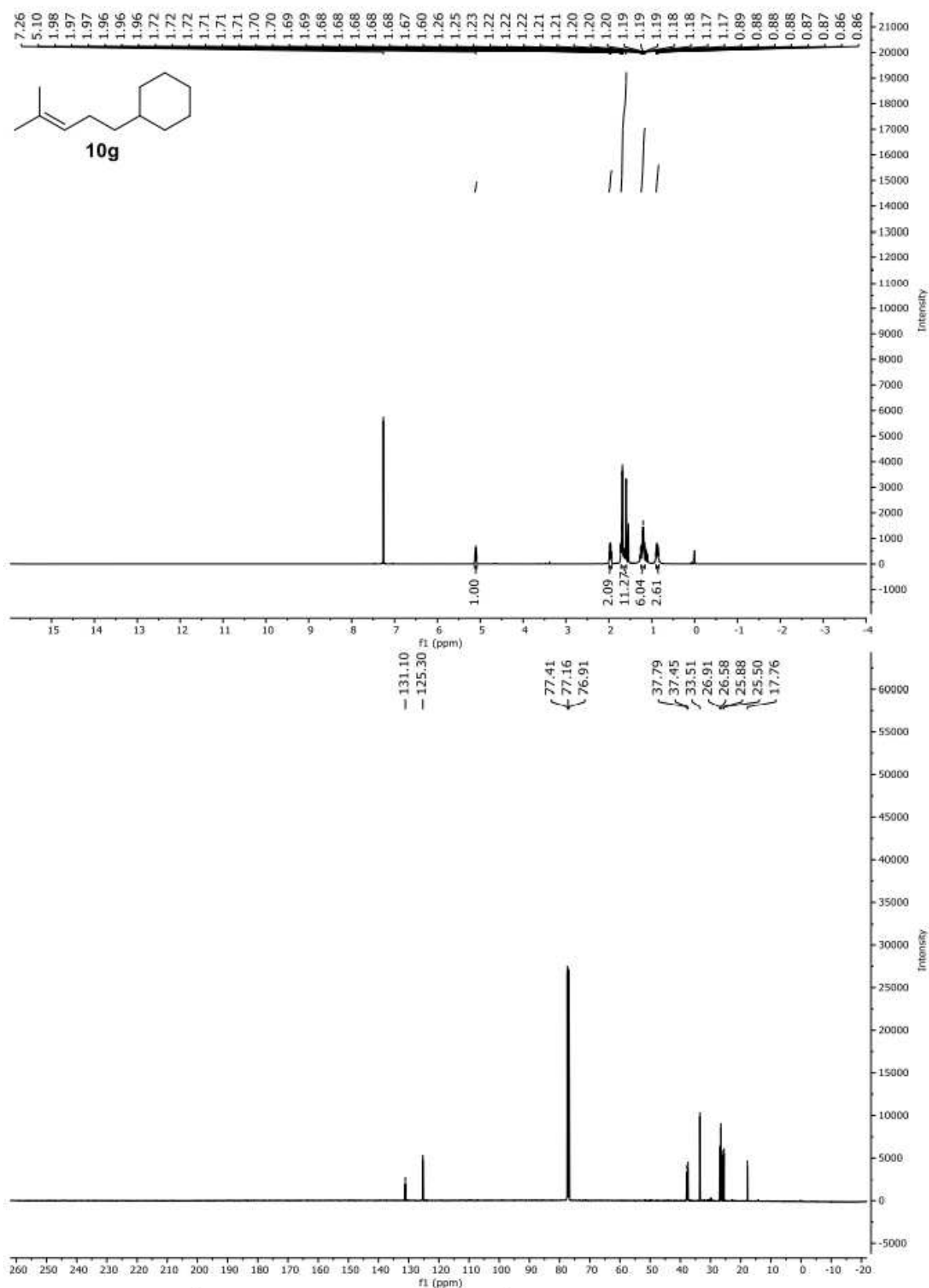


Figure S28. 500 MHz ¹H NMR spectrum (top) and 126 MHz ¹³C NMR spectrum (bottom) of **10g** in CDCl₃.

6. Traceless isoprenylation

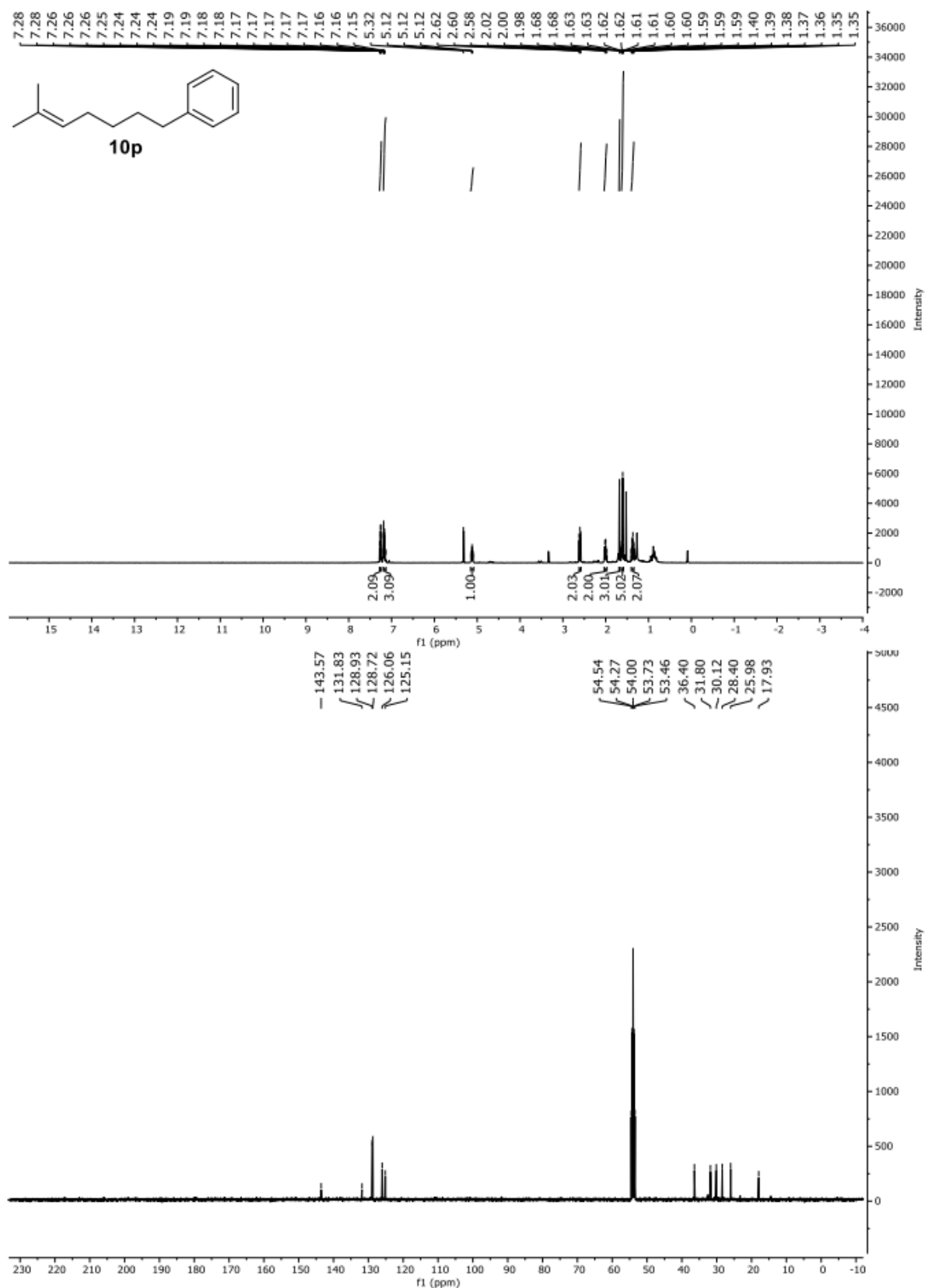


Figure S29. 400 MHz ¹H NMR spectrum (top) and 101 MHz ¹³C NMR spectrum (bottom) of **10p** in CD₂Cl₂.

6. Traceless isoprenylation

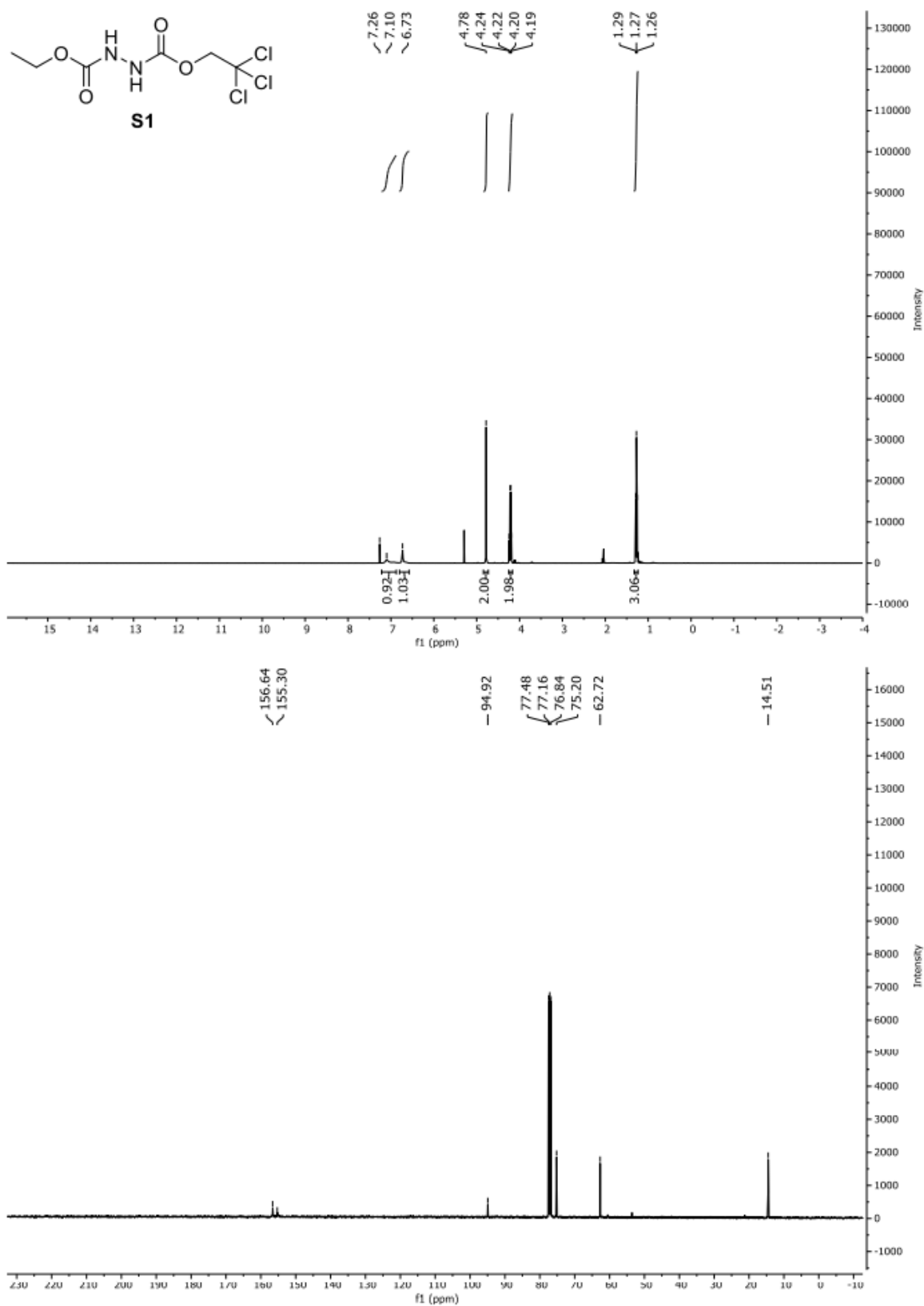


Figure S30. 400 MHz ¹H NMR spectrum (top) and 101 MHz ¹³C NMR spectrum (bottom) of **S1** in CDCl₃.

6. Traceless isoprenylation

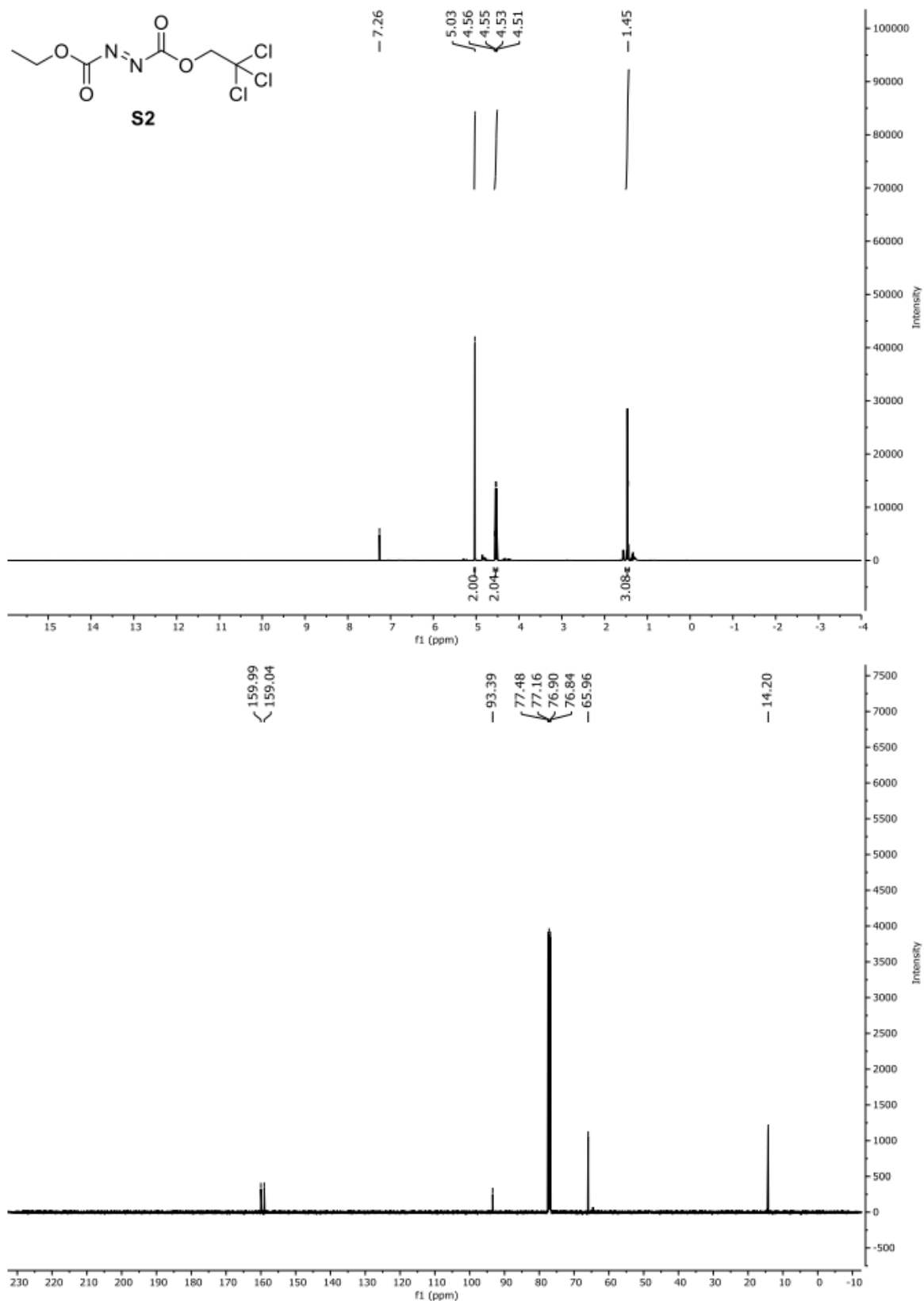


Figure S31. 400 MHz ¹H NMR spectrum (top) and 101 MHz ¹³C NMR spectrum (bottom) of **S2** in CDCl₃.

6. Traceless isoprenylation

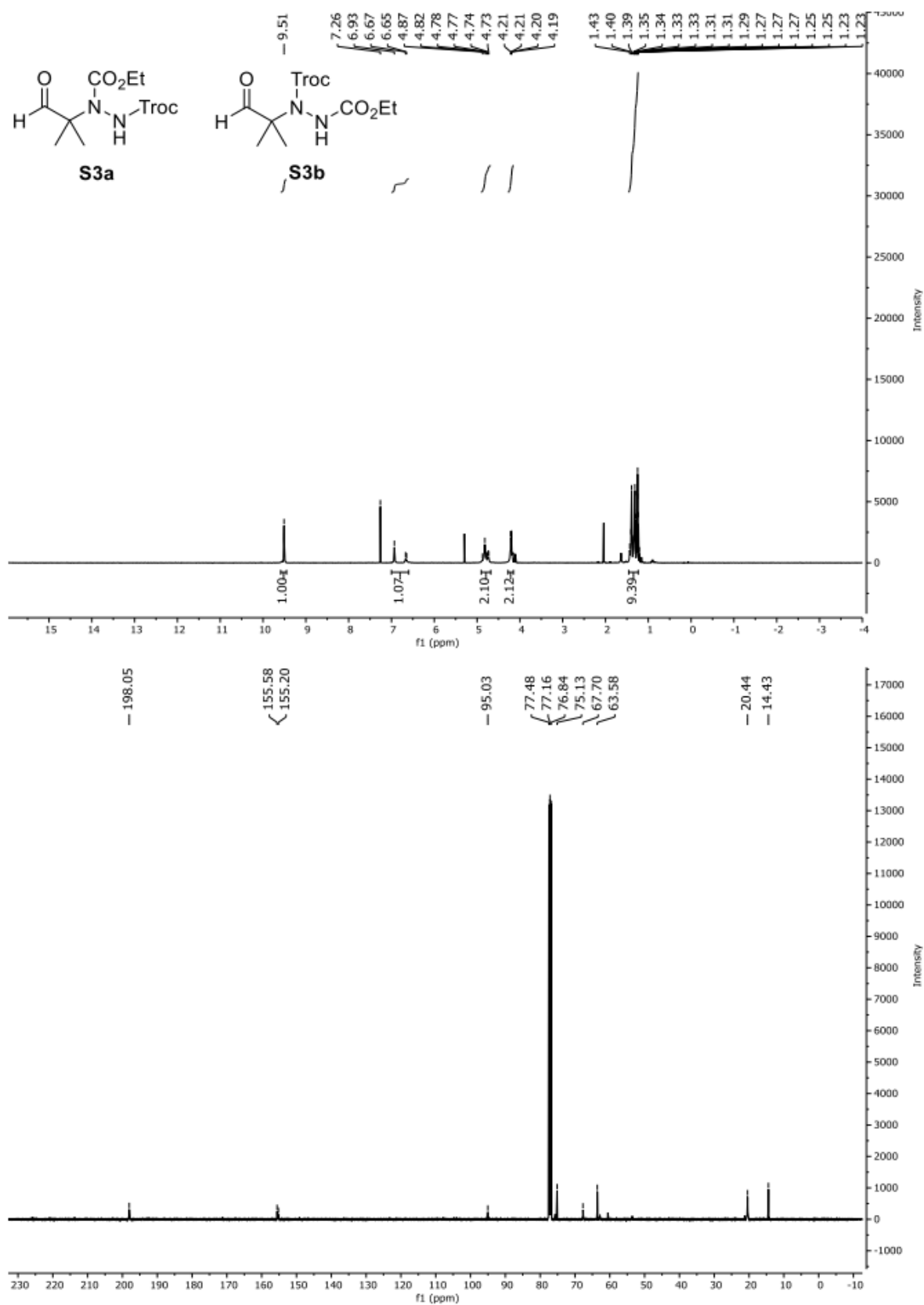


Figure S32. 400 MHz ^1H NMR spectrum (top) and 101 MHz ^{13}C NMR spectrum (bottom) of **S3a/S3b** in CDCl_3 .

6. Traceless isoprenylation

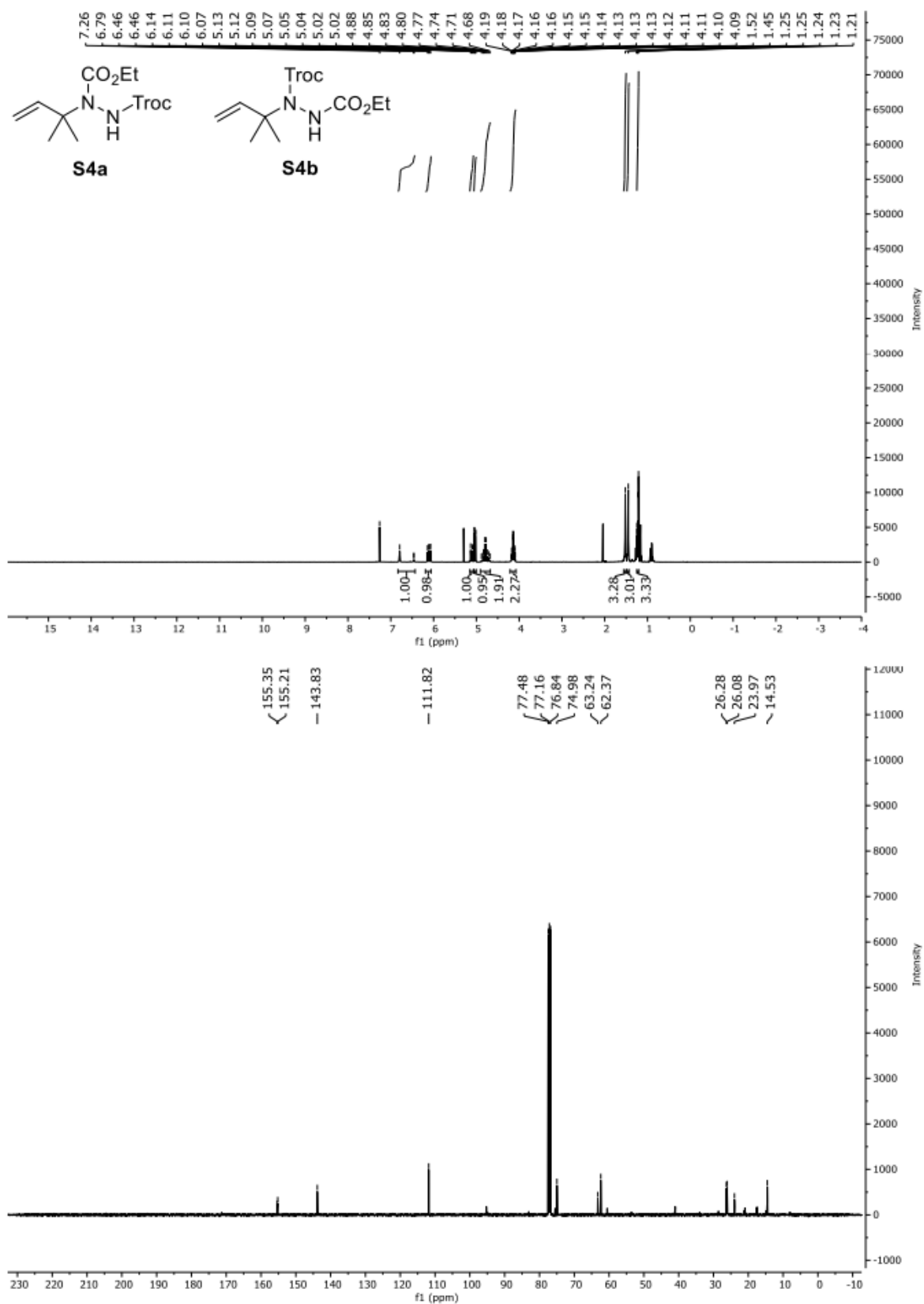


Figure S33. 400 MHz ^1H NMR spectrum (top) and 101 MHz ^{13}C NMR spectrum (bottom) of **S4a/S4b** in CDCl_3 .

6. Traceless isoprenylation

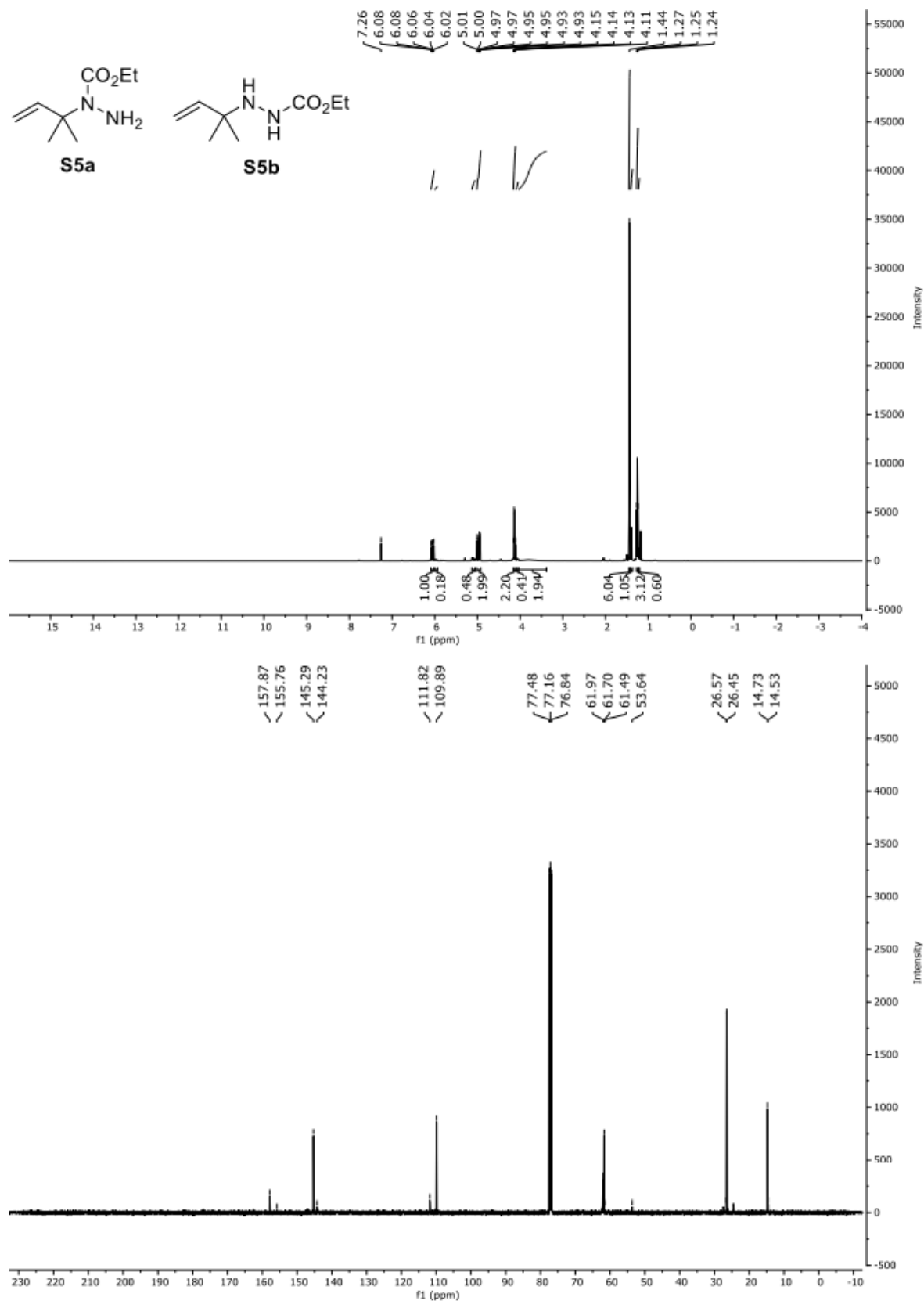


Figure S34. 500 MHz ¹H NMR spectrum (top) and 101 MHz ¹³C NMR spectrum (bottom) of **S5a/S5b** in CDCl₃.

6. Traceless isoprenylation

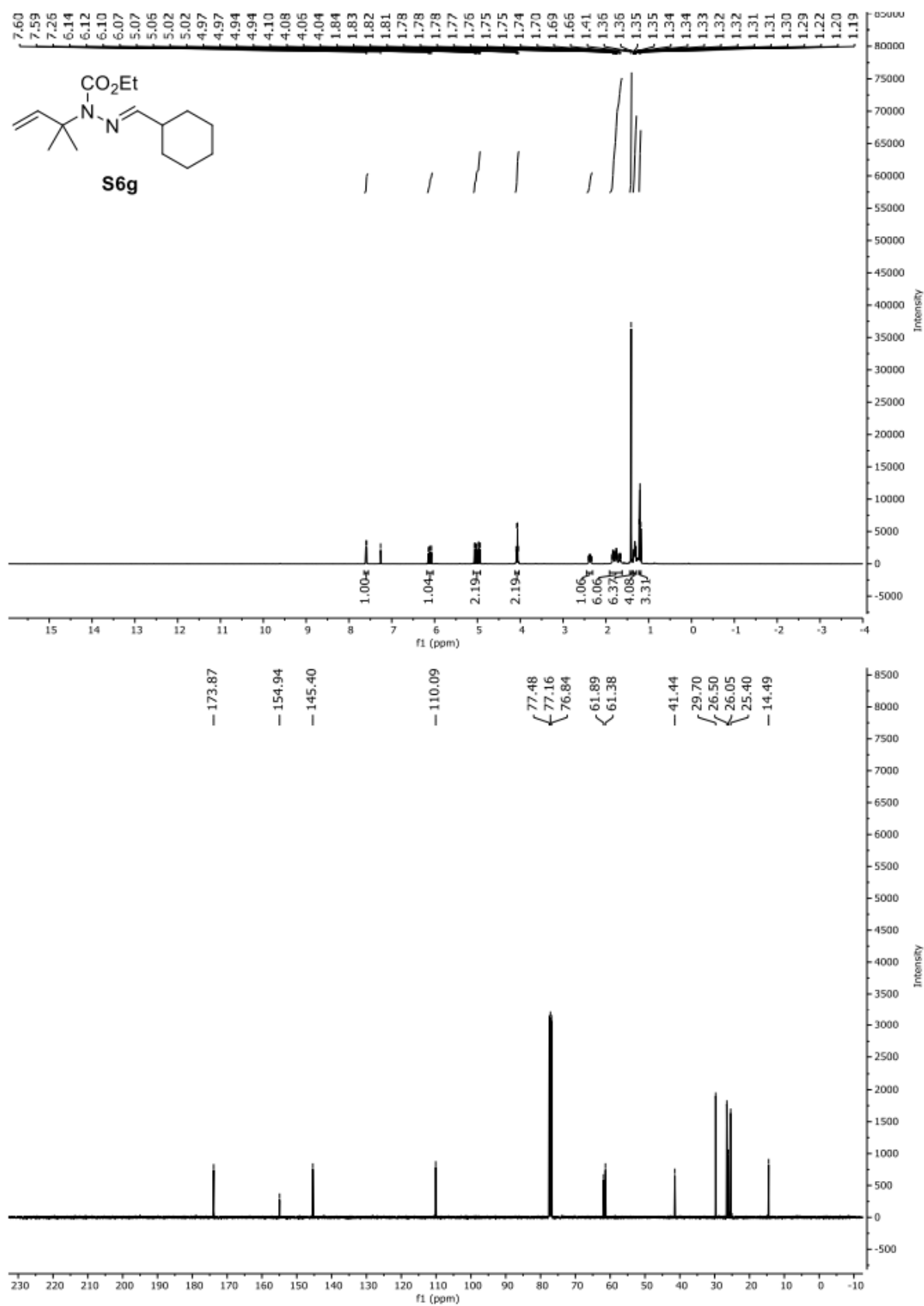


Figure S35. 400 MHz ¹H NMR spectrum (top) and 101 MHz ¹³C NMR spectrum (bottom) of **S6g** in CDCl₃.

6. Traceless isoprenylation

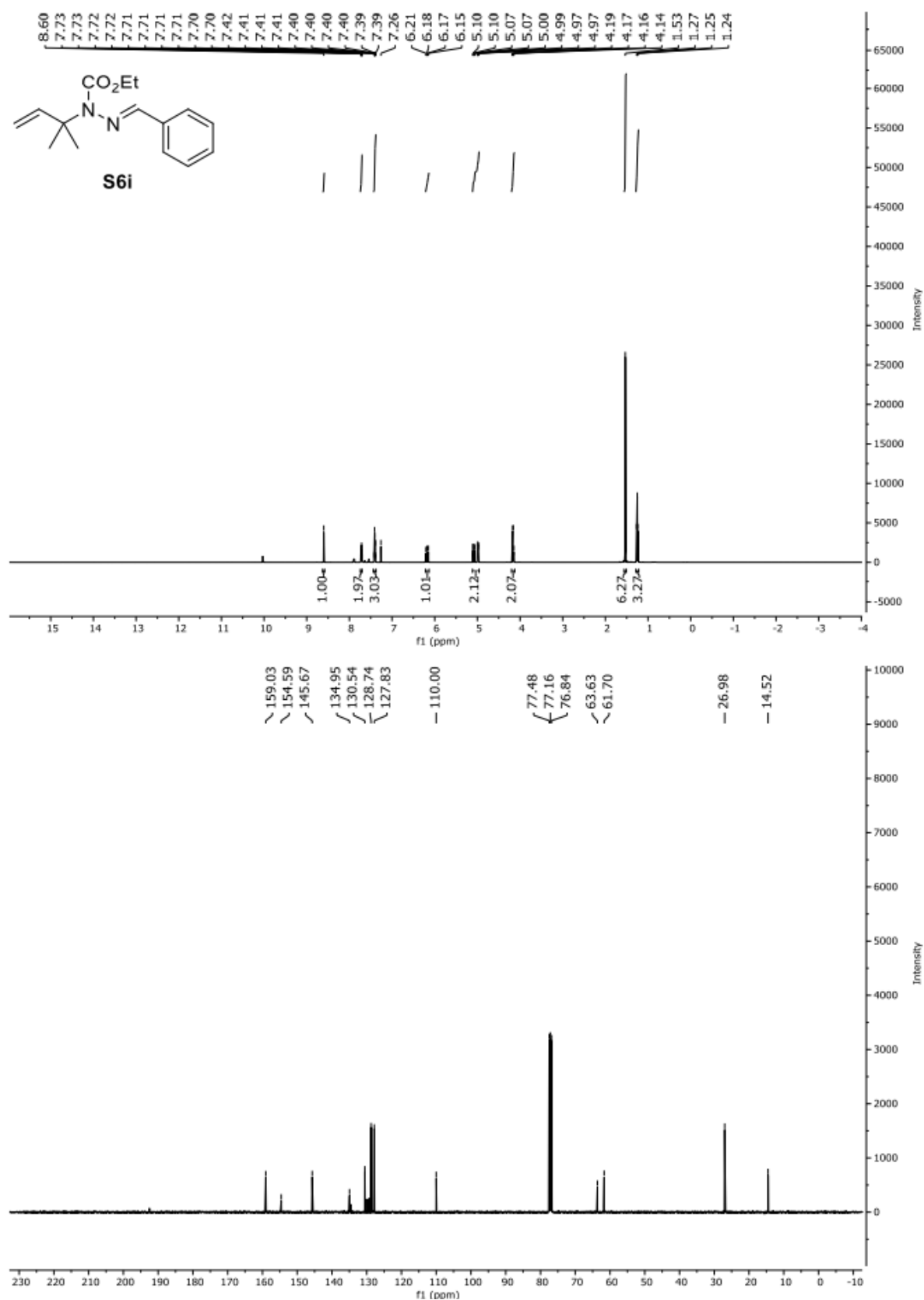


Figure S36. 500 MHz ¹H NMR spectrum (top) and 101 MHz ¹³C NMR spectrum (bottom) of **S6i** in CDCl₃.

7. Summary

Monitoring pathological changes of the steroid profile could lead to a better understanding of the progression of diseases like Alzheimer's disease. So, the aim of this work was the development of a comprehensive analytical method that could provide a wide overview of the sterolome of a specific tissue or cultured cells. In the end, an effective sample preparation protocol was developed and validated for 37 steroidal compounds of five different steroid classes. The scope of this method includes cholesterol precursors, oxysterols, neurosteroids, steroid acids and sterol sulfates. While other published methods focus on one or two of these subgroups, this new method can give an extensive overview of the sterolome. The corresponding article (Chapter 4) was submitted for publication in the Journal of Steroid Biochemistry and Molecular Biology and currently the revised manuscript is under review. In order to achieve this goal, some obstacles had to be overcome. One problem was the GC-MS measurement of sterol sulfates. Especially for this steroid class, several different deconjugation and derivatization procedures were evaluated and finally, a new and straightforward protocol for direct MO-TMS derivatization was found and published (Chapter 3). As sterol sulfates and unconjugated sterols were both measured as unconjugated MO-TMS derivatives, they had to be separated before deconjugation and derivatization. Also, the group of steroid acids needed to be separated due to different derivatization procedures. The necessary steroid group separation was accomplished by a newly developed SPE protocol that was included in the novel sample preparation procedure (Chapter 4). Another difficulty was the partly huge concentration difference of the analytes. Therefore, the processed samples needed to be analyzed on two different GC-MS systems in scan mode and in dMRM mode. This approach allowed untargeted screening as well as highly sensitive analysis of steroids of interest at trace levels. For scan analysis, a mass spectral library was created that contained mainly steroids of interest, defined by the group of Prof. Dr. Harald Steiner at DZNE. Additionally, cholesterol precursors could be integrated. Those had already been part of a previously published assay for cholesterol biosynthesis inhibitors in Nature Protocols, in which I contributed by creating the mass spectral library (Chapter 5). In addition to the creation of the mass spectral library, the transitions and collision energies for analysis in dMRM mode were optimized individually for each compound. This was the first method transfer from an IT-mass spectrometer (scan) to a qQq-mass spectrometer (dMRM) that was performed within our working group. Finally, the method was validated and applied to different biological samples including brain tissue, liver tissue and cultured cells. The levels of several endogenous compounds were measured and compared to literature data wherever possible. Some endogenous concentrations had never been reported before. Beside the analysis of biological samples, I contributed to a chemical synthesis article which demonstrated a new traceless

7. Summary

bond synthesis for isoprenylated products (Chapter 6). In this case I analyzed the synthesis products using GC-MS and in this way supported the necessary optimization experiments.

8. Abbreviations

AD	Alzheimer's disease
APP	Amyloid precursor protein
A β	amyloid β
CHILD	Congenital Hemidysplasia with Ichthyosiform nevus and Limb Defects
CNS	central nervous system
CoA	Coenzyme A
CTX	cerebrotendinous xanthomatosis
dMRM	dynamic multiple reaction monitoring
DZNE	Deutsches Zentrum für neurodegenerative Erkrankungen
GABA _A	γ -aminobutyric acid
GC-MS	gas chromatography-mass spectrometry
HDL	high density lipoprotein
HMG	3-Hydroxy-3-methylglutaryl
IPP	Isopentenyl diphosphate
IT	ion trap
LC-MS	liquid chromatography-mass spectrometry
LDL	low density lipoprotein
LXR	liver X receptor
MO-TMS	methyl oxime-trimethyl silyl
MS	mass spectrometry
MS/MS	tandem MS
MSTFA	<i>N</i> -methyl- <i>N</i> -trimethylsilyl acetamide
MtBE	methyl- <i>tert</i> -butyl ether
NMDA	<i>N</i> -methyl-D-aspartate
NPC	Niemann-Pick type C
QqQ	triple quadrupole
RIA	radioimmunoassays
RRT	relative retention time
SFC-MS	supercritical fluid chromatography- mass spectrometry
SLOS	Smith-Lemli-Opitz syndrome
SPE	solid phase extraction
TFA	trifluoroacetyl
TFAA	trifluoroacetic anhydride
TMS	trimethylsilyl
TRPM	melastatin-like transient receptor potential channels
TSIM	trimethylsilyl imidazole
VLDL	very low density lipoprotein

9. References

- [1] A. Bot, Phytosterols, in: L. Melton, F. Shahidi, P. Varelis (Eds.) Encyclopedia of food chemistry, *Academic Press*, Oxford, **2019**, 225-228.
- [2] IUPAC-IUB Joint Commission on Biochemical Nomenclature (JCBN), The nomenclature of steroids, *European Journal of Biochemistry*, 186, **1989**, 429-458.
- [3] J. Wollam, A. Antebi, Sterol regulation of metabolism, homeostasis, and development, *Annual review of biochemistry*, 80, **2011**, 885-916.
- [4] J.A. Svoboda, M.F. Feldlaufer, Neutral sterol metabolism in insects, *Lipids*, 26, **1991**, 614-618.
- [5] R.E. Summons, A.S. Bradley, L.L. Jahnke, J.R. Waldbauer, Steroids, triterpenoids and molecular oxygen, *Philosophical Transactions of the Royal Society B*, 361, **2006**, 951-968.
- [6] L.-L. Chen, G.-Z. Wang, H.-Y. Zhang, Sterol biosynthesis and prokaryotes-to-eukaryotes evolution, *Biochemical and Biophysical Research Communications*, 363, **2007**, 885-888.
- [7] K.E. Bloch, Speculations on the evolution of sterol structure and function, *CRC Critical Reviews in Biochemistry*, 7, **1979**, 1-5.
- [8] V.M. Olkkonen, R. Hynynen, Interactions of oxysterols with membranes and proteins, *Molecular Aspects of Medicine*, 30, **2009**, 123-133.
- [9] J. Luo, H. Yang, B.-L. Song, Mechanisms and regulation of cholesterol homeostasis, *Nature Reviews Molecular Cell Biology*, 21, **2020**, 225-245.
- [10] G.R. Bayly, Chapter 37 - Lipids and disorders of lipoprotein metabolism, in: W.J. Marshall, M. Lapsley, A.P. Day, R.M. Ayling (Eds.) Clinical Biochemistry: Metabolic and Clinical Aspects (Third Edition), *Churchill Livingstone*, **2014**, 702-736.
- [11] J.M. Dietschy, S.D. Turley, Cholesterol metabolism in the brain, *Current opinion in lipidology*, 12, **2001**, 105-112.
- [12] H.R. Waterham, R.J.A. Wanders, Biochemical and genetic aspects of 7-dehydrocholesterol reductase and Smith-Lemli-Opitz syndrome, *Biochimica et Biophysica Acta (BBA) - Molecular and Cell Biology of Lipids*, 1529, **2000**, 340-356.
- [13] W.D. Nes, Biosynthesis of cholesterol and other sterols, *Chemical Reviews*, 111, **2011**, 6423-6451.

9. References

- [14] C. Müller, J. Junker, F. Bracher, M. Giera, A gas chromatography-mass spectrometry-based whole-cell screening assay for target identification in distal cholesterol biosynthesis, *Nature protocols*, 14, **2019**, 2546-2570.
- [15] D.R. Brady, R.D. Crowder, W.J. Hayes, Mixed function oxidases in sterol metabolism. Source of reducing equivalents, *The Journal of biological chemistry*, 255, **1980**, 10624-10629.
- [16] M.J.M. Nowaczyk, M.B. Irons, Smith–Lemli–Opitz syndrome: Phenotype, natural history, and epidemiology, *American Journal of Medical Genetics Part C (Seminars in Medical Genetics)*, 160C, **2012**, 250-262.
- [17] R.I. Kelley, G.E. Herman, Inborn errors of sterol biosynthesis, *Annual Review of Genomics and Human Genetics*, 2, **2001**, 299-341.
- [18] E. Lloyd-Evans, F.M. Platt, Lipids on trial: The search for the offending metabolite in Niemann-Pick type C disease, *Traffic*, 11, **2010**, 419-428.
- [19] N.B. Javitt, Oxysterols: Novel biologic roles for the 21st century, *Steroids*, 73, **2008**, 149-157.
- [20] E.G. Lund, T.A. Kerr, J. Sakai, W.-P. Li, D.W. Russell, cDNA cloning of mouse and human cholesterol 25-hydroxylases, polytopic membrane proteins that synthesize a potent oxysterol regulator of lipid metabolism, *The Journal of biological chemistry*, 273, **1998**, 34316-34327.
- [21] D.W. Russell, The enzymes, regulation, and genetics of bile acid synthesis, *Annual Review of Biochemistry*, 72, **2003**, 137-174.
- [22] Y. Wang, W.J. Griffiths, Chapter 3 steroids, sterols and the nervous system, in: W.J. Griffiths (Ed.) *Metabolomics, metabonomics and metabolite profiling*, *The Royal Society of Chemistry*, Cambridge, UK, **2008**, 71-115.
- [23] W.J. Griffiths, P.J. Crick, Y. Wang, Methods for oxysterol analysis: Past, present and future, *Biochemical Pharmacology*, 86, **2013**, 3-14.
- [24] X. Fu, J.G. Menke, Y. Chen, G. Zhou, K.L. MacNaul, et al., 27-Hydroxycholesterol is an endogenous ligand for liver X receptor in cholesterol-loaded cells, *The Journal of biological chemistry*, 276, **2001**, 38378-38387.
- [25] S. Hannedouche, J. Zhang, T. Yi, W. Shen, D. Nguyen, et al., Oxysterols direct immune cell migration via EBI2, *Nature*, 475, **2011**, 524-527.
- [26] G. Salen, R. Steiner, Epidemiology, diagnosis, and treatment of cerebrotendinous xanthomatosis (CTX), *The Journal of Inherited Metabolic Disease*, 40, **2017**.
- [27] P.A. Dawson, S.J. Karpen, Intestinal transport and metabolism of bile acids, *Journal of lipid research*, 56, **2015**, 1085-1099.

9. References

- [28] B.S. Kumar, B.C. Chung, Y.-J. Lee, H.J. Yi, B.-H. Lee, et al., Gas chromatography–mass spectrometry-based simultaneous quantitative analytical method for urinary oxysterols and bile acids in rats, *Analytical Biochemistry*, 408, **2011**, 242-252.
- [29] J.I. Jung, A.R. Price, T.B. Ladd, Y. Ran, H.-J. Park, et al., Cholestenoic acid, an endogenous cholesterol metabolite, is a potent γ -secretase modulator, *Molecular Neurodegeneration*, 10, **2015**, 29.
- [30] J. Zhang, Y. Akwa, M. el-Etr, E.E. Baulieu, J. Sjoval, Metabolism of 27-, 25- and 24-hydroxycholesterol in rat glial cells and neurons, *The Biochemical journal*, 322 (Pt 1), **1997**, 175-184.
- [31] M. Vaňková., M. Hill, M. Velíková, J. Včelák., G. Vacínová, et al., Preliminary evidence of altered steroidogenesis in women with Alzheimer's disease: Have the patients "older" adrenal zona reticularis?, *Journal of Steroid Biochemistry and Molecular Biology*, 158, **2016**, 157-177.
- [32] A.R. Stiles, J.G. McDonald, D.R. Bauman, D.W. Russell, CYP7B1: one cytochrome P450, two human genetic diseases, and multiple physiological functions, *The Journal of biological chemistry*, 284, **2009**, 28485-28489.
- [33] J. Teubel, M.K. Parr, Determination of neurosteroids in human cerebrospinal fluid in the 21st century: A review, *Journal of Steroid Biochemistry and Molecular Biology*, 204, **2020**, 105753.
- [34] E.E. Baulieu, Neurosteroids: A novel function of the brain, *Psychoneuroendocrinology*, 23, **1998**, 963-987.
- [35] N.A. Compagnone, S.H. Mellon, Neurosteroids: biosynthesis and function of these novel neuromodulators, *Front. Neuroendocrinol.*, 21, **2000**, 1-56.
- [36] R.P. Baulieu EE., Vatier O., Haug M., Le Goascogne C., Bourreau E. , Neurosteroids: Pregnenolone and Dehydroepiandrosterone in the Brain. , *Springer*, Boston, MA, **1987**.
- [37] M.D. Majewska, Neurosteroids: endogenous bimodal modulators of the GABA_A receptor. Mechanism of action and physiological significance, *Progress in neurobiology*, 38, **1992**, 379-395.
- [38] W.J. Griffiths, Y. Wang, Analysis of neurosterols by GC-MS and LC-MS/MS, *Journal of Chromatography B*, 877, **2009**, 2778-2805.
- [39] S.M. Paul, G. Pinna, A. Guidotti, Allopregnanolone: From molecular pathophysiology to therapeutics. A historical perspective, *Neurobiology of Stress*, 12, **2020**, 100215.
- [40] S. Luchetti, I. Huitinga, D.F. Swaab, Neurosteroid and GABA-A receptor alterations in Alzheimer's disease, Parkinson's disease and multiple sclerosis, *Neuroscience*, 191, **2011**, 6-21.

9. References

- [41] C.A. Strott, Sulfonation and molecular action, *Endocrine reviews*, 23, **2002**, 703-732.
- [42] C.A. Strott, Y. Higashi, Cholesterol sulfate in human physiology: what's it all about?, *Journal of lipid research*, 44, **2003**, 1268-1278.
- [43] X. Li, W.M. Pandak, S.K. Erickson, Y. Ma, L. Yin, et al., Biosynthesis of the regulatory oxysterol, 5-cholesten-3 β ,25-diol 3-sulfate, in hepatocytes, *Journal of lipid research*, 48, **2007**, 2587-2596.
- [44] C.N. Falany, Enzymology of human cytosolic sulfotransferases, *Federation of American Societies for Experimental Biology journal*, 11, **1997**, 206-216.
- [45] D. Papadopoulos, M. Shihan, G. Scheiner-Bobis, Physiological implications of DHEAS-induced non-classical steroid hormone signaling, *Journal of Steroid Biochemistry and Molecular Biology*, 179, **2018**, 73-78.
- [46] C. Harteneck, Pregnenolone sulfate: from steroid metabolite to TRP channel ligand, *Molecules*, 18, **2013**, 12012-12028.
- [47] M.R. Bowlby, Pregnenolone sulfate potentiation of N-methyl-D-aspartate receptor channels in hippocampal neurons, *Molecular pharmacology*, 43, **1993**, 813-819.
- [48] J. Geyer, K. Bakhaus, R. Bernhardt, C. Blaschka, Y. Dezhkam, et al., The role of sulfated steroid hormones in reproductive processes, *Journal of Steroid Biochemistry and Molecular Biology*, 172, **2017**, 207-221.
- [49] M. Vallée, W. Mayo, M. Darnaudéry, C. Corpéchet, J. Young, et al., Neurosteroids: Deficient cognitive performance in aged rats depends on low pregnenolone sulfate levels in the hippocampus, *Proceedings of the National Academy of Sciences of the United States of America*, 94, **1997**, 14865-14870.
- [50] M. Vaňková, M. Hill, M. Velíková, J. Včelák, G. Vacínová, et al., Reduced sulfotransferase SULT2A1 activity in patients with Alzheimer's disease, *Physiological research*, 64 Suppl 2, **2015**, S265-273.
- [51] M. Iwamori, Y. Iwamori, N. Ito, Regulation of the activities of thrombin and plasmin by cholesterol sulfate as a physiological inhibitor in human plasma, *Journal of biochemistry*, 125, **1999**, 594-601.
- [52] S. Krishnaswamy, G. Verdile, D. Groth, L. Kanyenda, R.N. Martins, The structure and function of Alzheimer's gamma secretase enzyme complex, *Critical reviews in clinical laboratory sciences*, 46, **2009**, 282-301.
- [53] J.I. Jung, T.B. Ladd, T. Kukar, A.R. Price, B.D. Moore, et al., Steroids as γ -secretase modulators, *Federation of American Societies for Experimental Biology journal*, 27, **2013**, 3775-3785.

9. References

- [54] M.G. Bursavich, B.A. Harrison, J.F. Blain, Gamma secretase modulators: New Alzheimer's drugs on the horizon?, *Journal of medicinal chemistry*, 59, **2016**, 7389-7409.
- [55] M.P. Burns, G.W. Rebeck, Intracellular cholesterol homeostasis and amyloid precursor protein processing, *Biochimica et biophysica acta*, 1801, **2010**, 853-859.
- [56] H. Kölsch, R. Heun, F. Jessen, J. Popp, F. Hentschel, et al., Alterations of cholesterol precursor levels in Alzheimer's disease, *Biochim. Biophys. Acta*, 1801, **2010**, 945-950.
- [57] T. Wisniewski, K. Newman, N.B. Javitt, Alzheimer's disease: brain desmosterol levels, *Journal of Alzheimer's Disease*, 33, **2013**, 881-888.
- [58] A. Zarrouk, A. Vejux, J. Mackrill, Y. O'Callaghan, M. Hammami, et al., Involvement of oxysterols in age-related diseases and ageing processes, *Ageing Research Reviews*, 18, **2014**, 148-162.
- [59] A.J. Beel, M. Sakakura, P.J. Barrett, C.R. Sanders, Direct binding of cholesterol to the amyloid precursor protein: An important interaction in lipid-Alzheimer's disease relationships?, *Biochimica et biophysica acta*, 1801, **2010**, 975-982.
- [60] E. Winkler, F. Kamp, J. Scheuring, A. Ebke, A. Fukumori, et al., Generation of Alzheimer disease-associated amyloid beta42/43 peptide by gamma-secretase can be inhibited directly by modulation of membrane thickness, *The Journal of biological chemistry*, 287, **2012**, 21326-21334.
- [61] K.S. Vetrivel, G. Thinakaran, Membrane rafts in Alzheimer's disease beta-amyloid production, *Biochimica et biophysica acta*, 1801, **2010**, 860-867.
- [62] N. Krone, B.A. Hughes, G.G. Lavery, P.M. Stewart, W. Arlt, et al., Gas chromatography/mass spectrometry (GC/MS) remains a pre-eminent discovery tool in clinical steroid investigations even in the era of fast liquid chromatography tandem mass spectrometry (LC/MS/MS), *Journal of Steroid Biochemistry and Molecular Biology*, 121, **2010**, 496-504.
- [63] K. Robards, P. Towers, Chromatography as a reference technique for the determination of clinically important steroids, *Biomedical Chromatography*, 4, **1990**, 1-19.
- [64] S.A. Wudy, G. Schuler, A. Sánchez-Guijo, M.F. Hartmann, The art of measuring steroids: Principles and practice of current hormonal steroid analysis, *Journal of Steroid Biochemistry and Molecular Biology*, 179, **2018**, 88-103.
- [65] J. Teubel, B. Wüst, C.G. Schipke, O. Peters, M.K. Parr, Methods in endogenous steroid profiling – A comparison of gas chromatography mass spectrometry (GC–MS) with supercritical fluid chromatography tandem mass spectrometry (SFC-MS/MS), *Journal of Chromatography A*, 1554, **2018**, 101-116.

9. References

- [66] M. Giera, F. Plössl, F. Bracher, Fast and easy in vitro screening assay for cholesterol biosynthesis inhibitors in the post-squalene pathway, *Steroids*, 72, **2007**, 633-642.
- [67] C. Gomez, A. Fabregat, Ó.J. Pozo, J. Marcos, J. Segura, et al., Analytical strategies based on mass spectrometric techniques for the study of steroid metabolism, *Trends in Analytical Chemistry*, 53, **2014**, 106-116.
- [68] J. Marcos, O.J. Pozo, Derivatization of steroids in biological samples for GC–MS and LC–MS analyses, *Bioanalysis*, 7, **2015**, 2515-2536.
- [69] W.J. Griffiths, Y. Wang, Sterolomics in biology, biochemistry, medicine, *Trends in Analytical Chemistry*, 120, **2019**, 115280.
- [70] C. Müller, U. Binder, F. Bracher, M. Giera, Antifungal drug testing by combining minimal inhibitory concentration testing with target identification by gas chromatography-mass spectrometry, *Nature protocols*, 12, **2017**, 947-963.
- [71] C. Müller, S. Hemmers, N. Bartl, A. Plodek, A. Korner, et al., New chemotype of selective and potent inhibitors of human delta 24-dehydrocholesterol reductase, *European journal of medicinal chemistry*, 140, **2017**, 305-320.
- [72] J. Junker, I. Chong, F. Kamp, H. Steiner, M. Giera, et al., Comparison of strategies for the determination of sterol sulfates via GC-MS leading to a novel deconjugation-derivatization protocol, *Molecules*, 24, **2019**, 2353.
- [73] R.F.N. Hutchins, J.N. Kaplanis, Sterol sulfates in an insect, *Steroids*, 13, **1969**, 605-614.
- [74] S. Burstein, S. Lieberman, Hydrolysis of ketosteroid hydrogen sulfates by solvolysis procedures, *Journal of Biological Chemistry*, 233, **1958**, 331-335.
- [75] J. Junker, Methodenentwicklung zur Bestimmung von Neurosteroiden mittels GC-MS, *Martin-Luther-Universität, Halle-Wittenberg*, **2016**.
- [76] G. Testa, E. Staurenghi, C. Zerbinati, S. Gargiulo, L. Iuliano, et al., Changes in brain oxysterols at different stages of Alzheimer's disease: Their involvement in neuroinflammation, *Redox Biol*, 10, **2016**, 24-33.
- [77] M. Ogundare, S. Theofilopoulos, A. Lockhart, L.J. Hall, E. Arenas, et al., Cerebrospinal fluid sterolomics: are bioactive bile acids present in brain?, *Journal of Biological Chemistry*, 285, **2010**, 4666-4679.
- [78] H.D. Ackerman, G.S. Gerhard, Bile acids in neurodegenerative disorders, *Frontiers in Aging Neuroscience* 8,**2016**, 1-13.
- [79] S.M. Grundy, J.I. Cleeman, C.N.B. Merz, H.B. Brewer, L.T. Clark, et al., Implications of Recent Clinical Trials for the National Cholesterol Education Program Adult Treatment Panel III Guidelines, *Circulation*, 110, **2004**, 227-239.

9. References

- [80] T.J. Kirby, Cataracts produced by triparanol. (MER-29), *Transactions of the American Ophthalmological Society*, 65, **1967**, 494-543.
- [81] C. Roux, C. Horvath, R. Dupuis, Teratogenic action and embryo lethality of AY 9944R. Prevention by a hypercholesterolemia-provoking diet, *Teratology*, 19, **1979**, 35-38.
- [82] F. Chevy, F. Illien, C. Wolf, C. Roux, Limb malformations of rat fetuses exposed to a distal inhibitor of cholesterol biosynthesis, *Journal of lipid research*, 43, **2002**, 1192-1200.
- [83] E.J. Zerenturk, L.J. Sharpe, E. Ikonen, A.J. Brown, Desmosterol and DHCR24: unexpected new directions for a terminal step in cholesterol synthesis, *Progress in lipid research*, 52, **2013**, 666-680.
- [84] A. Körner, E. Zhou, C. Müller, Y. Mohammed, S. Herceg, et al., Inhibition of Δ 24-dehydrocholesterol reductase activates pro-resolving lipid mediator biosynthesis and inflammation resolution, *Proceedings of the National Academy of Sciences*, 116, **2019**, 20623.
- [85] Z. Hubler, D. Allimuthu, I. Bederman, M.S. Elitt, M. Madhavan, et al., Accumulation of 8,9-unsaturated sterols drives oligodendrocyte formation and remyelination, *Nature*, 560, **2018**, 372-376.
- [86] M.R. Boland, N.P. Tatonetti, Investigation of 7-dehydrocholesterol reductase pathway to elucidate off-target prenatal effects of pharmaceuticals: a systematic review, *The pharmacogenomics journal*, 16, **2016**, 411-429.
- [87] A. Canfrán-Duque, M.E. Casado, O. Pastor, J. Sánchez-Wandelmer, G. de la Peña, et al., Atypical antipsychotics alter cholesterol and fatty acid metabolism in vitro, *Journal of lipid research*, 54, **2013**, 310-324.
- [88] J. Sánchez-Wandelmer, A.M. Hernández-Pinto, S. Cano, A. Dávalos, G. De La Peña, et al., Effects of the antipsychotic drug haloperidol on the somatostatinergic system in SH-SY5Y neuroblastoma cells, *Journal of Neurochemistry*, 110, **2009**, 631-640.
- [89] M. Giera, Entwicklung neuer Testsysteme zur Charakterisierung von Enzym-Inhibitoren des Post-Squalen-Abschnitts der Cholesterol- und Ergosterol-Biosynthese, *Ludwig-Maximilians-Universität, München*, **2007**.
- [90] M. Giera, C. Müller, F. Bracher, Analysis and experimental inhibition of distal cholesterol biosynthesis, *Chromatographia*, 78, **2015**, 343-358.
- [91] A. Horling, C. Müller, R. Barthel, F. Bracher, P. Imming, A new class of selective and potent 7-dehydrocholesterol reductase inhibitors, *Journal of medicinal chemistry*, 55, **2012**, 7614-7622.

9. References

- [92] W.A. Maltese, Posttranslational modification of proteins by isoprenoids in mammalian cells, *Federation of American Societies for Experimental Biology journal*, 4, **1990**, 3319-3328.
- [93] D.A. Mundal, C.T. Avetta, R.J. Thomson, Triflimide-catalysed sigmatropic rearrangement of N-allylhydrazones as an example of a traceless bond construction, *Nature Chemistry*, 2, **2010**, 294-297.
- [94] S. Dittrich, F. Bracher, Traceless bond construction via rearrangement of N-Boc-N-allylhydrazones giving 1,1-disubstituted olefins, *Tetrahedron*, 71, **2015**, 2530-2539.
- [95] S. Dittrich, F. Bracher, Triflimide-catalysed rearrangement of N-(1-trimethylsilyl)allylhydrazones results in the formation of vinylsilanes and cyclopropanes, *European Journal of Organic Chemistry*, 2015, **2015**, 8024-8033.